INSIGHTS IN CORONARY ARTERY DISEASE: 2021

EDITED BY: Stéphane Cook
PUBLISHED IN: Frontiers in Cardiovascular Medicine

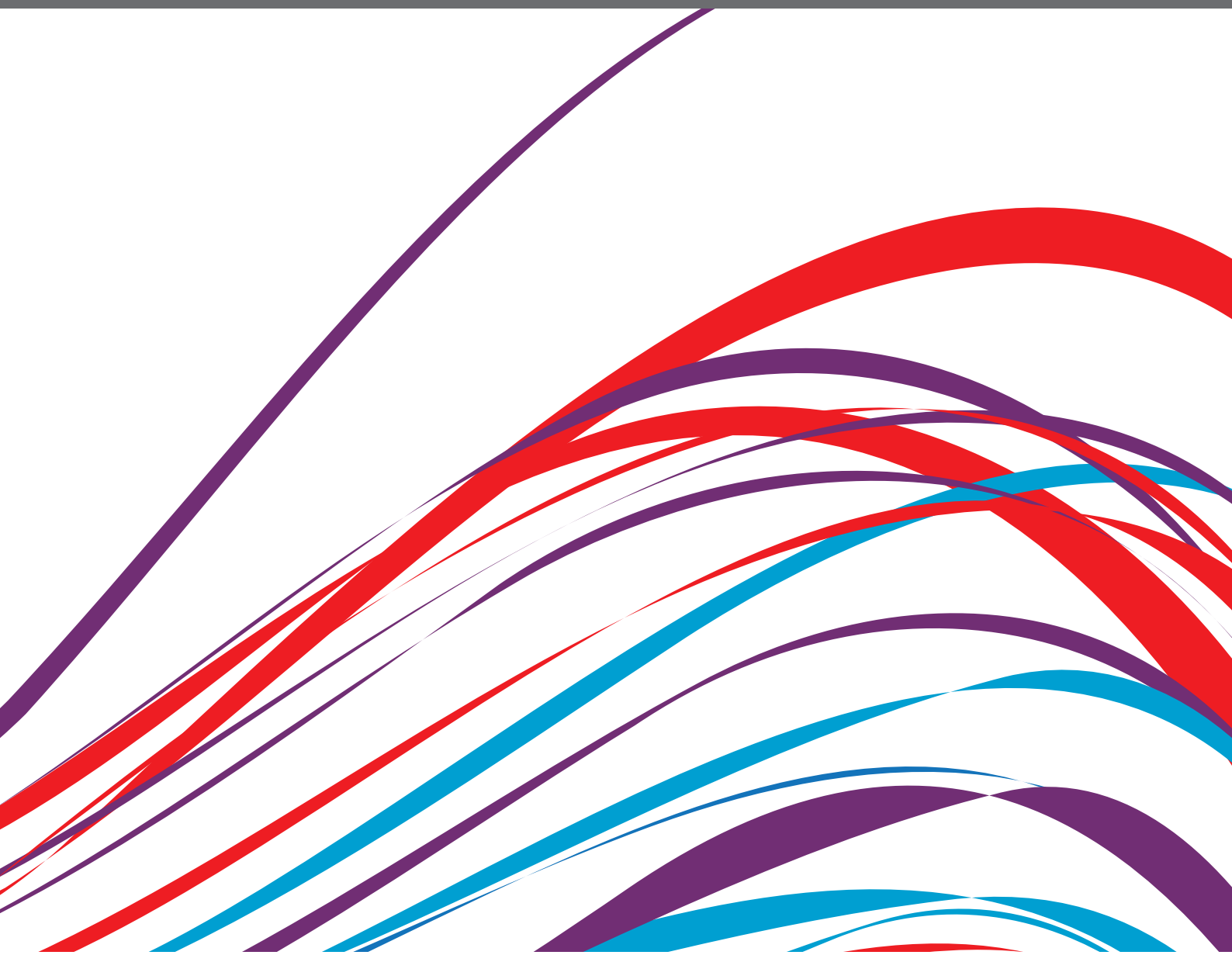

frontiers Research Topics

ISSN 1664-8714
ISBN 978-2-88976-970-4
DOI 10.3389/978-2-88976-970-4

About Frontiers

Frontiers is more than just an open-access publisher of scholarly articles: it is a pioneering approach to the world of academia, radically improving the way scholarly research is managed. The grand vision of Frontiers is a world where all people have an equal opportunity to seek, share and generate knowledge. Frontiers provides immediate and permanent online open access to all its publications, but this alone is not enough to realize our grand goals.

Frontiers Journal Series

The Frontiers Journal Series is a multi-tier and interdisciplinary set of open-access, online journals, promising a paradigm shift from the current review, selection and dissemination processes in academic publishing. All Frontiers journals are driven by researchers for researchers; therefore, they constitute a service to the scholarly community. At the same time, the Frontiers Journal Series operates on a revolutionary invention, the tiered publishing system, initially addressing specific communities of scholars, and gradually climbing up to broader public understanding, thus serving the interests of the lay society, too.

Dedication to Quality

Each Frontiers article is a landmark of the highest quality, thanks to genuinely collaborative interactions between authors and review editors, who include some of the world's best academicians. Research must be certified by peers before entering a stream of knowledge that may eventually reach the public - and shape society; therefore, Frontiers only applies the most rigorous and unbiased reviews.
Frontiers revolutionizes research publishing by freely delivering the most outstanding research, evaluated with no bias from both the academic and social point of view. By applying the most advanced information technologies, Frontiers is catapulting scholarly publishing into a new generation.

What are Frontiers Research Topics?

Frontiers Research Topics are very popular trademarks of the Frontiers Journals Series: they are collections of at least ten articles, all centered on a particular subject. With their unique mix of varied contributions from Original Research to Review Articles, Frontiers Research Topics unify the most influential researchers, the latest key findings and historical advances in a hot research area! Find out more on how to host your own Frontiers Research Topic or contribute to one as an author by contacting the Frontiers Editorial Office: frontiersin.org/about/contact

INSIGHTS IN CORONARY ARTERY DISEASE: 2021

Topic Editor:
Stéphane Cook, Université de Fribourg, Switzerland

Citation: Cook, S., ed. (2022). Insights in Coronary Artery Disease: 2021. Lausanne: Frontiers Media SA. doi: 10.3389/978-2-88976-970-4

Table of Contents

frontiers in Cardiovascular Medicine

ORIGINAL RESEARCH
published: 02 November 2021
doi: 10.3389/fcvm.2021.741890

Circulating Monocyte Subsets Are Associated With Extent of Myocardial Injury but Not With Type of Myocardial Infarction

Noushin Askari[1†], *Christoph Lipps*[1,2,3†], *Sandra Voss*[2,3], *Nora Staubach*[2,3], *Dimitri Grün*[1], *Roland Klingenberg*[2,3], *Beatrice von Jeinsen*[2], *Jan Sebastian Wolter*[2], *Steffen Kriechbaum*[2,3], *Oliver Dörr*[1], *Holger Nef*[1,2,3], *Christoph Liebetrau*[1,2,3,4], *Christian W. Hamm*[1,2,3] *and Till Keller*[1,2,3*]

[1] Department of Internal Medicine I, Cardiology, Justus-Liebig-University Gießen, Giessen, Germany, [2] Department of Cardiology, Kerckhoff Heart and Thorax Center, Bad Nauheim, Germany, [3] German Center for Cardiovascular Research e.V. (DZHK), Partner Site RhineMain, Bad Nauheim, Germany, [4] Cardiovascular Center Bethanien (CCB), Frankfurt, Germany

OPEN ACCESS

Edited by:
Turgay Celik,
VM Medical Park Ankara (Kecioren), Turkey

Reviewed by:
Istvan Szokodi,
University of Pécs, Hungary
Florian Kahles,
University Hospital RWTH Aachen, Germany

***Correspondence:**
Till Keller
till.keller@med.uni-giessen.de

[†] These authors have contributed equally to this work and share first authorship

Specialty section:
This article was submitted to Coronary Artery Disease, a section of the journal Frontiers in Cardiovascular Medicine

Received: 15 July 2021
Accepted: 14 October 2021
Published: 02 November 2021

Citation:
Askari N, Lipps C, Voss S, Staubach N, Grün D, Klingenberg R, von Jeinsen B, Wolter JS, Kriechbaum S, Dörr O, Nef H, Liebetrau C, Hamm CW and Keller T (2021) Circulating Monocyte Subsets Are Associated With Extent of Myocardial Injury but Not With Type of Myocardial Infarction. Front. Cardiovasc. Med. 8:741890. doi: 10.3389/fcvm.2021.741890

Inflammation is a hallmark of the period after a myocardial infarction (MI) that is either promoted or resolved by distinct subtypes of circulating inflammatory cells. The three main monocyte subpopulations play different roles inflammation. This study examined whether the type of MI (type 1 or type 2) or the extent of myocardial injury is associated with differences in monocyte subpopulations. For this purpose, peripheral whole blood from patients with a suspected MI was used for flow cytometric measurements of the monocyte subpopulations, and myocardial injury was classified by cardiac troponin levels in serum. In patients with acute coronary syndrome ($n = 82$, 62.2% male) similar proportions of the monocyte subsets were associated with the two types of MI, whereas total monocyte counts were increased in patients with substantial myocardial injury vs. those with minor injury ($p = 0.045$). This was accompanied by a higher proportion of intermediate ($p = 0.045$) and classical monocytes ($p = 0.059$); no difference was found for non-classical monocytes ($p = 0.772$). In patients with chronic coronary syndrome ($n = 144$, 66.5% male), an independent association with myocardial injury was also observed for classical monocytes ($p = 0.01$) and intermediate monocytes ($p = 0.08$). In conclusion, changes in monocyte subpopulation counts, particularly for classical and intermediate monocytes, were related to the extent of myocardial injury in acute and stable coronary artery disease but not to the type of MI.

Keywords: monocytes, acute coronary syndrome, inflammation, biomarker, troponin, chronic coronary syndrome

INTRODUCTION

Myocardial infarction (MI) is one of the most frequent cardiovascular events and leads to relevant morbidity and mortality. Early inflammatory processes after MI are largely dependent on monocyte-related mechanisms (1, 2). It has been established that following the onset of acute MI, monocytes invade the infarcted area to promote healing of damaged myocardial tissue by removing dead cells and have an important impact on remodeling of myocardial structure (2).

Monocytes represent ∼5% of peripheral blood leucocytes; they constitute an essential component of the immune system linking innate and adaptive immunity and are critical drivers in many inflammatory processes (3). This is also the case in atherosclerosis, in which monocytosis after an MI is associated with impaired recovery and unfavorable prognosis of atherosclerotic disease (4, 5).

Three different monocyte subsets can be distinguished, as delineated by the Nomenclature Committee of the International Union of Immunological Societies in 2010. Thus, monocytes are divided into classical monocytes (CD14++CD16–), representing up to 90% of the blood monocytes, intermediate monocytes (CD14++CD16+), and non-classical monocytes (CD14+CD16++) (6). These three monocyte subsets have distinct phenotypic and functional characteristics and play different roles in inflammation and malignancy. Each subset displays different immune functions, including phagocytic activity, cytokine profile, and regenerative capacity (7). Classical monocytes are characterized by a high expression of genes encoding antimicrobial proteins (7). Non-classical cells display numerous patrolling properties and therefore are thought to be involved in innate surveillance of tissues (7). Intermediate monocytes constitute a transitional population that shares some phenotypic and functional features of both classical and non-classical monocytes (7). It has been suggested that the proportion of the three subpopulations of monocytes can differ with the presence of disease, such as the different characteristics associated with different types of MI (8).

MI can be classified by the universal definition as type 1, caused by a spontaneous coronary plaque rupture, and type 2, resulting from increased oxygen demand or decreased supply (9). MI in general is characterized by cell death due to prolonged ischemia, irrespective of the type of MI. Myocardial cell death as related to the extent of myocardial injury can be quantified by measuring different muscle-associated proteins released into the circulation from the damaged myocytes, including cardiac troponins, that serve as biomarkers with high myocardial specificity (10).

The aim of our study was to evaluate whether the type of MI and the extent of myocardial injury are associated with the inflammatory profile and quantity of circulating monocyte subpopulations.

MATERIALS AND METHODS

Clinical Cohorts

The present analyses are based on two independent multicenter cohorts located at the Kerckhoff Heart Center in Bad Nauheim, Germany, and the University Hospital of the Justus-Liebig-University in Giessen, Germany. The two studies were approved by the local Ethics Committee of the University Giessen (AZ 199/15) and each patient gave written informed consent. The studies were carried out in accordance with the Declaration of Helsinki.

The first cohort, referred to as the acute coronary syndrome (ACS) cohort, utilized data and biomaterial from a prospective, multicenter biomarker registry that enrolled patients presenting with suspected acute MI between August 2011 and October 2016, as described previously (11). Here, the final gold-standard study diagnosis, including type of MI, was made independently by two cardiologists based on the Third Universal Definition of Myocardial Infarction (9) using all available clinical, laboratory, and imaging data. In this ACS cohort, flow cytometry data and troponin I values were available in 101 patients.

For the second cohort, referred to as the chronic coronary syndrome (CCS) cohort, data and biomaterial were used from an ongoing multicenter biomarker registry that enrolled patients with suspected CCS starting in August 2010, as described previously (12). This cohort comprised patients with a clinical indication for invasive coronary angiography due to suspected CCS, including patients with and without previously known coronary artery disease. In this CCS cohort, flow cytometry data and troponin I values were available in 144 patients.

Laboratory Analyses and Definition of Myocardial Injury

Standard laboratory parameters such as cholesterol or creatinine levels were measured directly upon enrollment via the respective central laboratories of the recruiting centers. At study enrollment blood samples were taken, centrifuged, aliquoted and stored at −80°C according to standard operating procedures in both cohorts.

To define myocardial injury (13), troponin I in serum samples was measured batchwise with two commercially available troponin I assays. High-sensitive cardiac troponin I (hs-cTnI) was measured in the ACS cohort using an automated immunoassay (ARCHITECT STAT high-sensitive troponin, Abbott Diagnostics, Abbott Park, IL, USA) with a limit of detection (LOD) of 1.9 ng/L, a limit of quantitation (LOQ) of 10 ng/L, and a 99th percentile concentration of 26.2 ng/L (used to define relevant myocardial injury) according to the manufacturer's specifications. To take into account the potentially smaller amount of myocardial injury in patients without MI, a super-sensitive cardiac troponin I (ss-cTnI) was measured in the CCS cohort using a single-molecule array (Simoa Troponin-I, Quanterix, Billerica, MA, USA) on the Quanterix SR-X system with an LOD of 0.021 pg/mL and an LOQ of 0.122 pg/mL according to the manufacturer's information. As no established threshold is available in the context of CCS, we used the median concentration of 3.0 ng/mL to signify the presence of myocardial injury. In both ACS and CCS cohorts, patients were grouped according to the troponin I levels: those in the "minor" injury group had troponin levels below the respective threshold and those in the "substantial" injury group had levels that were higher.

Flow Cytometry

To determine absolute counts of monocyte subsets, 50 μl of freshly collected EDTA-anticoagulated whole blood were transferred into TruCount Absolute Counting Tubes (BD Biosciences, San Jose, CA, USA) by reverse pipetting and stained immediately with fluorophore-labeled monoclonal antibodies directed against the monocyte key markers CD14 (Clone M5E2), CD16 (Clone 3G8), and CD11b (Clone ICRF44) (BioLegend,

TABLE 1 | Baseline characteristics of the acute coronary syndrome (ACS) cohort.

Acute coronary syndrome (ACS) cohort	Type and unit	Overall ACS cohort	Substantial myocardial injury	Minor myocardial Injury	*p*–value
		***n* = 82**	***n* = 42**	***n* = 40**	
Age	Median (IQR), [years]	69.52 (58.89–78.47)	71.26 (57.56–80.47)	68.61 (63.5–75.43)	0.702
Male sex	*n* (%)	51 (62.2)	26 (61.9)	25 (62.5)	1
Final diagnosis					
Acute myocardial infarction	*n* (%)	48 (58.54)	38 (90.48)	10 (25)	<0.001
Cardiovascular risk factors					
Arterial hypertension	*n* (%)	58 (79.45)	26 (76.47)	32 (82.05)	0.091
Dyslipidemia	*n* (%)	39 (55.71)	19 (55.88)	20 (55.56)	0.825
Diabetes mellitus	*n* (%)	21 (28.77)	9 (26.47)	12 (30.77)	0.452
Smoking	*n* (%)	29 (50.88)	14 (53.85)	15 (48.39)	0.818
Family history	*n* (%)	15 (28.3)	7 (26.92)	8 (29.63)	0.779
History					
Known coronary artery disease	*n* (%)	30 (50.85)	11 (44)	19 (55.88)	0.066
Laboratory analyses					
eGRF	median (IQR), [ml/min/1.73 m^2]	86.17 (58.28–104.84)	87.13 (55.52–104.45)	83.12 (66.54–103.66)	0.612
Creatinine	median (IQR), [mg/dl]	0.87 (0.75–1.11)	0.86 (0.73–1.12)	0.87 (0.78–1.07)	0.545
hs-cTnI	median (IQR), [pg/mL]	28.2 (4–531.35)	525.6 (214.03–2,986.82)	4 (2.55–7.25)	<0.001
Cholesterol	mean ± SD, [mg/dl]	201.91 ± 45.52	211 ± 45.93	184.88 ± 42.25	0.19
C-reactive protein	median (IQR), [mg/dl]	0.3 (0.2–1.4)	0.4 (0.18–1.52)	0.3 (0.2–1)	0.82

Data are shown stratified according to the extent of myocardial injury defined by high sensitivity cardiac troponin I values (99th percentile cut-off).
Data are presented as percentage, mean, or median as appropriate. eGFR denotes estimated glomerular filtration rate, hs-cTnI denotes high sensitivity cardiac troponin I.

San Diego, CA, USA) as well as a granulocyte marker (CD66b, Clone G10F5, BioLegend). Erythrocytes were lysed using Pharm Lyse Buffer (BD Biosciences) before acquiring specimen data on a FACSVerse flow cytometer (BD Biosciences). Instrument performance was tracked daily with BD FACSuite CS&T Beads (BD Biosciences), and assay-specific settings were updated daily to ensure proper assay reproducibility.

The resulting FCS files were exported in FCS 3.0 format and analyzed using FACSDiva software (Version 6.3.1, BD Biosciences). An exemplary dataset taken from the ACS cohort is shown in **Supplementary Figure 1**. Absolute counting beads were identified as highly fluorescent events with low forward scatter. All events outside the bead region were displayed in a two-dimensional dot plot to exclude events with low forward scatter and low side scatter from the analysis. Granulocytes, defined as events with high side scatter and high CD66b staining intensity, were excluded in the next step. Monocytes were identified in the remaining events as a population with intermediate side scatter and high CD11b expression, excluding lymphocytes from the analysis. Events in the monocyte gate were further divided into the three monocyte subsets according to their CD14 and CD16 staining intensity: CD14++ CD16- classical monocytes, CD14++ CD16+ intermediate monocytes, and CD14+ CD16++ non-classical monocytes. Cell counts were calculated according to the manufacturer's protocol.

Statistical Analyses

Data are presented as mean with standard deviation (SD) for normally distributed variables and as median with interquartile range (IQR) for skewed continuous variables. For dichotomous variables data are given as absolute number and percentage. Fischer's exact test, Student's *t*-test, or the Mann-Whitney *U*-test were applied, as appropriate, to test for differences between groups. Spearman correlations were calculated between monocytes subsets and peak creatine kinase (CK) values as marker for peak myocardial injury during the individual ACS time course. Further, the potential independent associations of troponin as marker for myocardial injury with monocyte subsets were checked in the ACS and the CCS cohort by using multivariate regression analysis. Not normally distributed variables were logarithmic transformed in the evaluation. All calculated and presented *P*-values should be viewed as descriptive. All statistical analyses were carried out using the R 3.6.1 software package (R Foundation for Statistical Computing, Vienna, Austria).

RESULTS

Type of MI and Extent of Myocardial Injury in the Acute Coronary Syndrome Cohort

The ACS cohort comprised 101 patients with suspected acute MI. Of those, 62 patients (69% male, age 59–78 years) experienced an MI, whereas in 39 patients (59% male, age 59–76 years) an MI could be excluded. MI patients were further classified according to the final diagnosis of MI type: MI type 1, the prototypical acute MI (T1MI, $n = 52$, 73% male, age: 59–78 years) or MI type 2, an MI based on ischemia due to an oxygen demand/supply mismatch (T2MI, $n = 10$, 50% male, age: 61–81 years). T1MI and

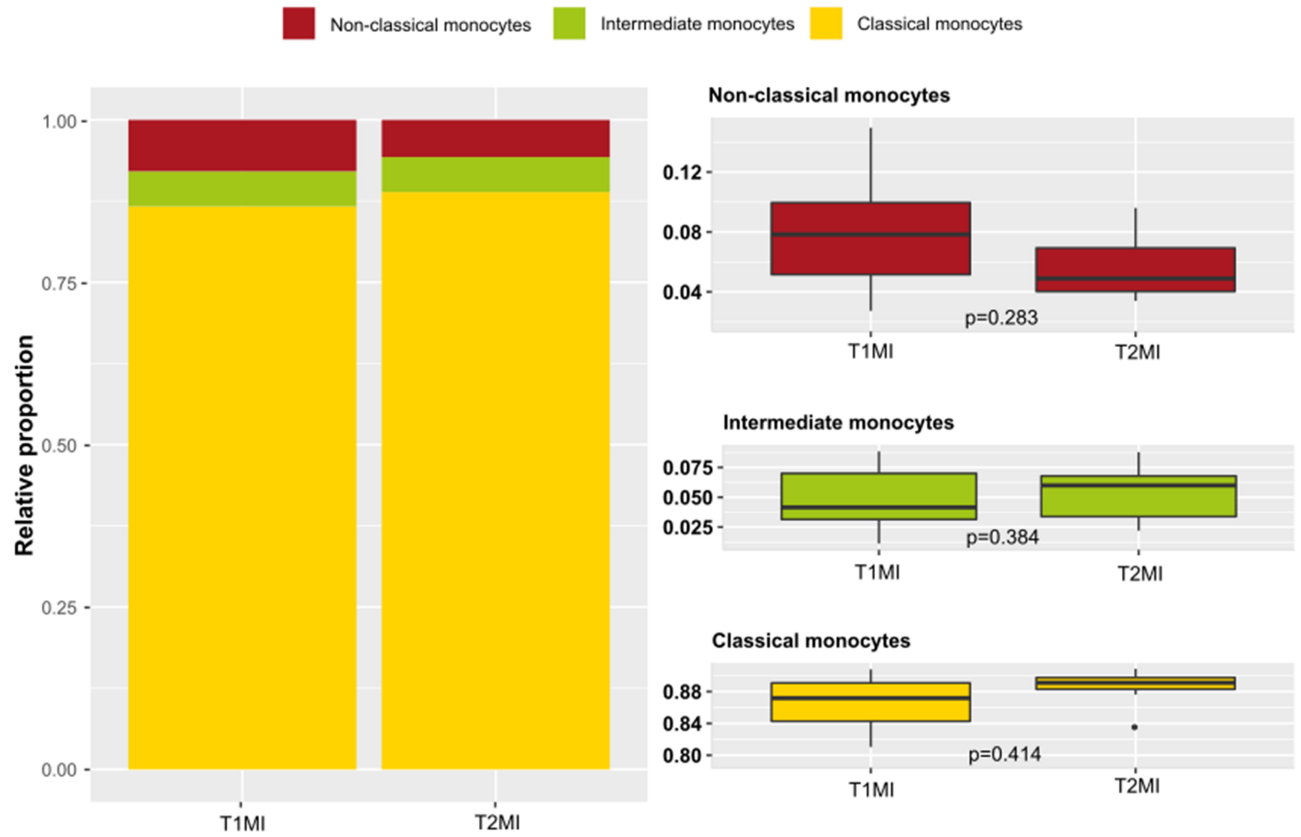

FIGURE 1 | Monocyte subsets in myocardial infarction (MI) type 1 vs. type 2. Presented are data from the ACS cohort ($n = 101$) including patients suffering MI type 1 ($n = 52$) and type 2 ($n = 10$). **Left:** proportions of monocyte subsets in peripheral blood of patients with an MI type 1 or type 2. **Right:** box-and-whiskers plot of the distribution of the specific monocyte subsets in type 1 and type 2 MI (whiskers represent the interquartile range).

T2MI patients did not differ regarding their cardiovascular risk profile. The baseline characteristics of the ACS cohort stratified by MI type are provided in **Supplementary Table 1**.

To evaluate the influence of the extent of myocardial damage irrespective of the final diagnosis given, patients of the entire ACS cohort were classified as having minor or substantial myocardial injury based on the troponin I level. Troponin I data were available in 82 patients. In 42 patients substantial myocardial damage was present (61.9% male, age: 58–81 years), whereas 40 patients showed only minor myocardial injury (62.5% male, age: 64–75 years). In the group of patients with minor myocardial damage, a higher proportion (55.9%) tended to have previously known coronary artery disease compared to patients with substantial injury (44%, $p = 0.066$). Baseline characteristics of the ACS cohort stratified according to extent of myocardial injury are provided in **Table 1**.

Monocyte Subpopulations in Different Types of MI

Figure 1 shows the distribution of different monocyte subpopulations (classical, non-classical and intermediate) in T1MI and T2MI patients. Visually, there was a slight shift from classical to non-classical in T1MI compared with T2MI (classical median (IQR) 510 (402–687) vs. 758 (426–916); non-classical median (IQR) 48 (33–58) vs. 35 (31–44)); however, none of the differences in subpopulations reached a p-value below 0.05 (see also **Supplementary Table 2** for detailed information on the absolute and relative counts of the specific monocyte populations).

Monocyte Subpopulations in Acute Myocardial Injury

A potential relationship between the extent of myocardial injury, irrespective of the final diagnosis, and the distribution of monocyte subsets was investigated (**Figure 2**). There was a higher proportion of intermediate monocytes in patients with substantial myocardial injury compared to patients with minor injury ($p = 0.045$). Patients with substantial injury showed only a tendency to have a lower proportion of non-classical monocytes ($p = 0.772$). To investigate this apparent difference in detail, absolute monocyte counts were further evaluated (**Figure 3**). In general, the total monocyte count was higher in patients with substantial injury compared with those with minor injury ($p = 0.045$). Regarding the different monocyte subset counts, the most relevant difference with respect to the extent of myocardial injury was observed in intermediate monocytes

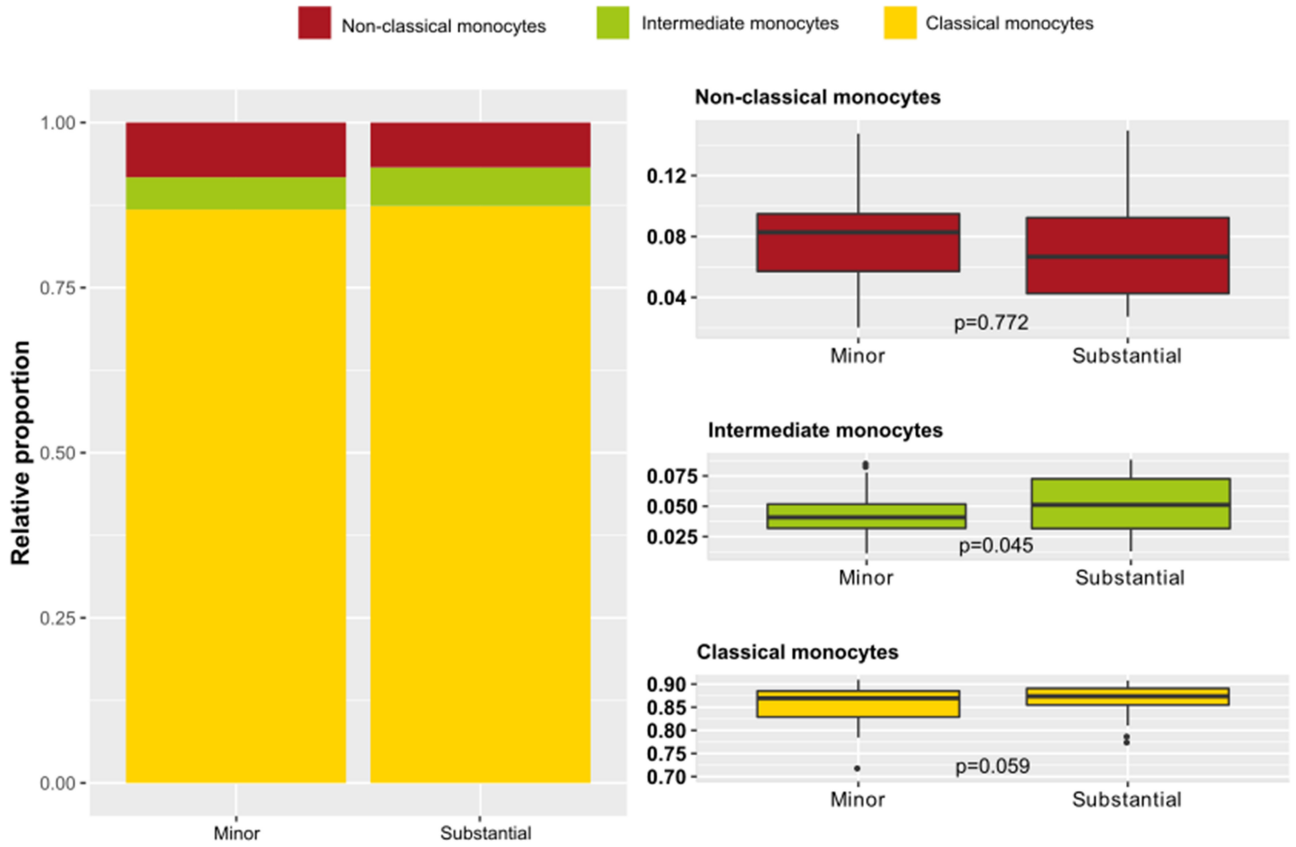

FIGURE 2 | Monocyte subset proportions according to extent of myocardial injury in acute coronary syndrome (ACS) patients. Presented are data from the ACS cohort ($n = 82$) including patients with substantial ($n = 42$) and with minor myocardial injury ($n = 40$). ACS patients were stratified as having minor or substantial myocardial injury defined by high sensitivity cardiac troponin I values (99th percentile cut-off). **Left:** proportions of monocyte subsets in ACS patients with minor vs. substantial myocardial injury. **Right:** distribution of the specific monocyte subsets in relation to the extent of myocardial injury.

($p = 0.045$), a subset that only accounts for 4.9 or 5.8% of total monocytes in patients with minor or substantial injury, respectively. The absolute counts in classical monocytes differed slightly in relation to myocardial injury, with higher counts in patients with substantial injury ($p = 0.059$). A multivariate analysis did not show relevant independent predictors of classical monocytes (see also **Supplementary Table 4**).

We further used the maximum CK value during the individual ACS time course as marker for peak injury. Here we observed a weak correlation with intermediate monocytes (rho $= -0.273$, $p = 0.01$), whereas no correlation was seen with classical (rho $= -0.172$, $p = 0.112$) or non-classical (rho $= -0.102$, $p = 0.347$) monocytes.

Monocyte Subpopulations in Chronic Myocardial Injury

The non-ACS cohort of patients with suspected CCS was investigated to determine whether there was an association of monocyte subsets with extent of myocardial injury in patients without MI. Baseline characteristics of the CCS cohort are provided in **Table 2**. In comparison with patients showing no myocardial injury, patients showing substantial myocardial injury in this cohort were older (72.7 vs. 63.4 years, $p < 0.001$), more often male (78.4 vs. 54.3%, $p = 0.003$), and had a higher percentage of known diabetes mellitus (25.7 vs. 9.0%, $p = 0.008$), previously known coronary artery disease (54.1 vs. 34.8%, $p = 0.02$) and poorer renal function (creatinine 0.79 vs. 0.94 mg/dl, $p = 0.001$).

As in the ACS cohort, the total monocyte count was higher in patients of the CCS cohort presenting with substantial myocardial injury than in patients with minor injury ($p = 0.01$; **Figure 4**). Regarding the specific monocyte subsets in these non-acute patients, the presence of greater myocardial injury was associated with higher counts of classical monocytes ($p = 0.01$) and a tendency for higher counts of intermediate monocytes ($p = 0.08$).

The results of the groups with minor or substantial damage in the CCS cohort were analyzed by multivariate regression. The regression focused on the classical monocyte subpopulation: a 1% increase in troponin I caused a 0.062% increase in classical monocytes ($p < 0.05$). The other evaluated parameters (diabetes mellitus, known coronary artery disease, creatinine, eGFR, age, and sex) showed no relevant relationship to the amount of classical monocytes (**Supplementary Table 5**).

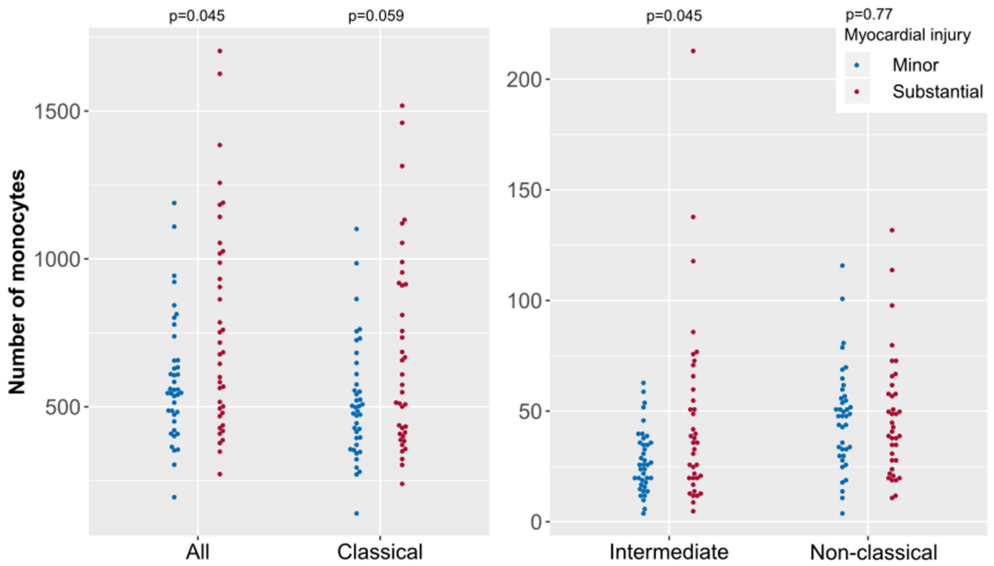

FIGURE 3 | Absolute monocyte counts of specific subsets according to extent of myocardial injury in acute coronary syndrome (ACS). Presented are data from the ACS cohort ($n = 82$) including patients with substantial ($n = 42$) and with minor myocardial injury ($n = 40$). ACS patients were stratified as having minor or substantial myocardial injury defined by high sensitivity cardiac troponin I values (99th percentile cut-off). Each point represents the monocyte count of one patient.

TABLE 2 | Baseline characteristics of the chronic coronary syndrome (CCS) cohort.

Chronic coronary syndrome (CCS) cohort	Type and unit	Overall CCS cohort	Substantial myocardial injury	Minor myocardial injury	*p*–value
		***n* = 144**	***n* = 74**	***n* = 70**	
Age	Median (IQR), [years]	66.84 (59.79–75.31)	72.7 (63.61–77.6)	63.44 (54.22–70.9)	<0.001
Male sex	*n* (%)	96 (66.67)	58 (78.38)	38 (54.29)	0.003
Cardiovascular risk factors					
Arterial hypertension	*n* (%)	121 (87.05)	66 (92.96)	55 (80.88)	0.111
Hypercholesterolemia	*n* (%)	100 (72.46)	54 (76.06)	46 (68.66)	0.37
Diabetes mellitus	*n* (%)	25 (17.73)	19 (25.68)	6 (8.96)	0.008
Smoking	*n* (%)	30 (27.27)	13 (21.31)	17 (34.69)	0.412
History					
Known coronary artery disease	*n* (%)	64 (44.76)	40 (54.05)	24 (34.78)	0.02
Laboratory analyses					
eGRF	Median (IQR), [ml/min/1.73 m^2]	87.33 ± 26.62	82.12 ± 28.51	92.62 ± 23.59	0.02
Creatinine	Median (IQR), [mg/dl]	0.85 (0.73–1.02)	0.94 (0.74–1.23)	0.79 (0.69–0.92)	0.001
ss-cTnI	Median (IQR), [pg/mL]	3.06 (1.28–5.34)	5.28 (3.77–12.35)	1.24 (0.92–1.83)	<0.001
Cholesterol	Median (IQR), [mg/dl]	196 (164–229)	195 (167–222)	197 (163.5–237)	0.595
C-reactive protein	Median (IQR), [mg/dl]	0.2 (0.1–0.4)	0.2 (0.1–0.4)	0.2 (0.1–0.32)	0.91

Data are shown stratified according to the extent of myocardial injury defined by super sensitivity cardiac troponin I values.
Data are presented as percentage, mean, or median as appropriate. eGFR denotes estimated glomerular filtration rate, ss-cTnI denotes super sensitivity cardiac troponin I.

DISCUSSION

The inflammatory response component of MI is currently of great interest, as recent studies have documented that post-MI modulation of inflammation via medication reduces the occurrence of atherothrombotic events (14) and ischemic cardiovascular events (15). The early inflammatory response after MI is dominated by inflammatory cells such as monocytes, which are the initial protagonists of the complement cascade that migrate to the site of the event (2). However, the specific role of individual monocyte subsets in this context is still not fully understood.

This study presents data derived from two independent cohorts. In the first cohort of analyzed patients, that enrolled individuals with suspected ACS, a potential association of monocyte subsets with the type of MI and with the extent of myocardial damage was investigated. An association with the extent of myocardial damage was also evaluated in a second

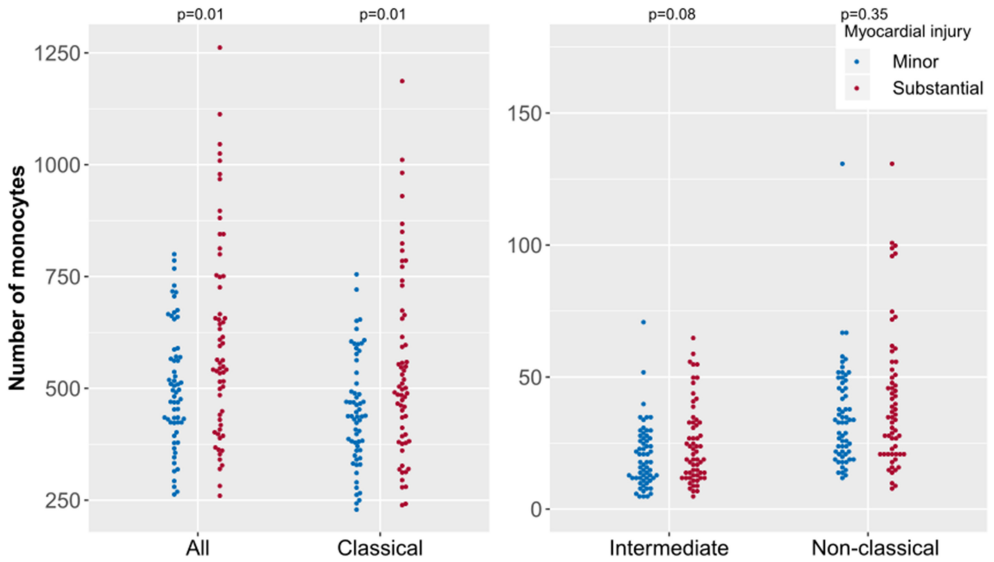

FIGURE 4 | Absolute monocyte counts of specific subsets according to extent of myocardial injury in chronic coronary syndrome (CCS). Presented are data from the CCS cohort ($n = 144$) including patients with substantial ($n = 74$) and with minor myocardial injury ($n = 70$). CCS patients were stratified as having minor or substantial myocardial injury defined by super sensitivity cardiac troponin I values. Each point represents the monocyte count of one patient.

cohort comprising stable patients with suspected CCS having less myocardial injury.

The most important findings are: (i) type 1 as well as type 2 MI are associated with comparable proportions of the three monocyte subsets; (ii) monocyte subsets vary according to the extent of myocardial injury, irrespective of the presence of a diagnosed MI; (iii) even a small degree of myocardial injury, as observed in CCS patients, independently affects the distribution of monocyte subsets; (iv) this shift in monocyte subsets is mainly based on a change in intermediate and classical monocyte counts in ACS and CCS patients.

Given the difference in the pathophysiological background of T1MI and T2MI, one would expect a difference in monocyte subpopulations according to the type of MI. It has been shown that, in fact, inflammatory markers play a crucial role in the determination of the type of MI. For example, the type of MI can be differentiated with the help of a combination of the biomarkers MRP 8/14 and troponin I (11). Interestingly, in the present cohort no relevant relationship between the type of MI and monocyte subsets was observed. It must be emphasized that the diagnosis T1MI as well as the respective therapeutic regimen is clearly defined in the literature (16), whereas the group of patients diagnosed with T2MI is much more heterogeneous.

Previous research has shown that there is a difference in the monocyte subpopulations with respect to MI, in particular for patients with ST-elevation MI (STEMI) vs. non-STEMI (NSTEMI) (17). It is a common understanding that the electrocardiogram of STEMI patients is more often associated with a transmural infarction than that of NSTEMI patients. Hence, besides the pathophysiological differences, STEMI is associated with greater myocardial damage compared with NSTEMI. In the present study, cardiac troponins were used as indicators of the extent of damage to the heart due to their role as the current gold-standard biomarkers in MI (16) as well as their association with infarct size (18). Importantly, while previous study cohorts have often been limited to patients with a definite diagnosis of MI (4, 7, 17), our first analyzed patient cohort, named ACS cohort, comprised the whole spectrum of the working diagnoses of "suspected ACS" used in the emergency room, ranging from non-coronary origin of the clinical symptoms or unstable angina to a STEMI with total vessel occlusion.

In the ACS cohort, there was a shift in monocyte subsets according to the extent of myocardial injury, irrespective of the presence of an MI. Previous studies have also shown such a shift in monocyte subsets after a cardiac event, especially in the intermediate monocyte population (15, 19). Greater myocardial damage was associated with a higher monocyte count. This suggests that the observed shift in monocytes is at least in part dependent on the nature of the myocardial damage rather than on the specific cause of damage. To examine this idea further, monocyte subsets were evaluated in stable patients with suspected CCS. Even though the absolute troponin levels were markedly lower in the CCS cohort than in the ACS cohort, reflecting the smaller amount of myocardial injury overall, there was a clear shift in the monocyte subsets according to the degree of myocardial damage. The subset of intermediate monocytes in particular showed a relevant shift between patients with and without myocardial damage in both cohorts evaluated, suggesting an ACS-independent mechanism.

As expected, confounding factors such as age, sex, diabetes mellitus, previously known coronary artery disease, and renal

function differed between patients with and without myocardial injury in the CCS cohort. However, multivariate regression analysis showed that the observed association of the amount of myocardial injury and the monocyte count was independent of these factors.

The predictive value of monocyte subsets regarding cardiovascular events occurring within 2 years after an invasively treated MI has been described, which underlines the relevance of changes in these subsets (20). Previous data suggest that changes in monocyte subsets are associated with pathophysiological aspects of ACS. For example, increased intermediate monocyte subsets were reported to be an independent predictor of thin-cap fibroatheroma (21), which itself is a precursor of plaque rupture (22) in ACS scenarios (23). The site of the culprit lesion may be a factor in promoting a shift in subsets (24). Differences in monocyte subsets have also been described between stable patients with coronary artery disease and controls (25). Further, monocyte subsets seem to be associated with prognosis in stable conditions, and it has been observed that the absolute counts of classical monocytes are predictive of major adverse cardiac events in patients with coronary artery disease. Intermediate monocytes express receptors that are crucial for angiogenesis and tissue repair (7). As such, they are predominantly involved in post-AMI healing process, whereas an enrichment of intermediate monocytes has been observed in the circulation of CCS patients and subjects with high risk plaques (26). This highlights the importance of CD14++ monocytes in cardiovascular diseases (27, 28). This upregulation of intermediate monocytes in patients with ACS and CCS might at least partly reflect accelerated mobilization from bone marrow (29). To fully understand the complex role of monocyte subsets in pathophysiological mechanisms further studies need to be performed and additional characterization features have to be considered. Recently, NFAT activating protein with ITAM motif 1 (NFAM1), which is associated with monocyte recruitment, has been identified as novel mediator affecting pathobiological progression of coronary artery disease. NFAM1 was highly elevated in ACS and CCS patients. NFAM1 is significantly higher expressed in classical and intermediate monocytes compared to non-classical monocytes (30). This might be an important link to our results, where a change in classical and intermediate monocyte subsets cell count but not in the non-classical monocyte subpopulation was observed in both ACS and CCS.

Limitations

The present analysis has several limitations. First, due to the small numbers of patients, data from the analysis of each individual monocyte subpopulation could not be related to the final specific diagnoses in the ACS cohort. Second, the transferability to other cohorts with a different ethnicity is limited, as only patients from central Europe were enrolled in the two cohorts. Third, due to limited data availability on information between symptom onset and blood withdrawal in the ACS cohort it was not possible to evaluate a potential influence of differences in the time from symptom onset to measurement of monocyte subsets with adequate validity.

Conclusion

The shift in monocyte subset counts after an MI is related to the severity of myocardial injury rather than the specific type of MI leading to that injury. This association of changes in monocyte subsets with myocardial injury applies to both acute and chronic coronary disease.

DATA AVAILABILITY STATEMENT

The raw data supporting the conclusions of this article will be made available by the authors, without undue reservation.

ETHICS STATEMENT

The studies involving human participants were reviewed and approved by Local Ethics Committee of the Justus-Liebig-University Giessen. The patients/participants provided their written informed consent to participate in this study.

AUTHOR CONTRIBUTIONS

NA, CLip, and TK contributed to conception and design of the study and wrote the first draft of the manuscript. TK organized the database and supervised the project. NS, NA, and CLip performed data acquisition. NS, NA, CLip, DG, SV, and TK performed data analysis. NA and DG performed the statistical analysis. RK, BJ, JW, SK, OD, HN, CLie, and CH supported conduction of clinical study. All authors contributed to the interpretation of the results and contributed manuscript revision, read, and approved the submitted version.

FUNDING

The present analysis is based on two cohorts that are part of the Kerckhoff Biomarker Registry (BioReg) that was financially supported by the Kerckhoff Heart Research Institute (KHFI) and the German Center for Cardiovascular Research (DZHK). The sponsors had no influence on the study design, statistical analyses, or draft of the paper.

ACKNOWLEDGMENTS

We thank F. Z. Kabelitz for proofreading the article and Elizabeth Martinson of the KHFI Editorial Office for editorial assistance. The present analyses include data from the doctoral thesis of NA.

SUPPLEMENTARY MATERIAL

The Supplementary Material for this article can be found online at: https://www.frontiersin.org/articles/10.3389/fcvm.2021.741890/full#supplementary-material

REFERENCES

1. Libby P, Hansson GK. Taming immune and inflammatory responses to treat atherosclerosis. *J Am Coll Cardiol.* (2018) 71:173–6. doi: 10.1016/j.jacc.2017.10.081
2. Andreadou I, Cabrera-Fuentes HA, Devaux Y, Frangogiannis NG, Frantz S, Guzik T, et al. Immune cells as targets for cardioprotection: new players and novel therapeutic opportunities. *Cardiovasc Res.* (2019) 115:1117–30. doi: 10.1093/cvr/cvz050
3. Shi C, Pamer EG. Monocyte recruitment during infection and inflammation. *Nat Rev Immunol.* (2011) 11:762–74. doi: 10.1038/nri3070
4. Tapp LD, Shantsila E, Wrigley BJ, Pamukcu B, Lip GYH. The CD14++CD16+ monocyte subset and monocyte-platelet interactions in patients with ST-elevation myocardial infarction. *J Thromb Haemost.* (2012) 10:1231–41. doi: 10.1111/j.1538-7836.2011.04603.x
5. Takano K, Hibi K, Konishi M, Matsuzawa Y, Ebina T, Kosuge M, et al. Monocytosis after myocardial infarction accelerates atherosclerosis: results of a five-year follow-up study. *J Am Coll Cardiol.* (2013) 61:E198. doi: 10.1016/S0735-1097(13)60199-0
6. Ziegler-Heitbrock L, Ancuta P, Crowe S, Dalod M, Grau V, Hart DN, et al. Nomenclature of monocytes and dendritic cells in blood. *Blood.* (2010) 116:e74–80. doi: 10.1182/blood-2010-02-258558
7. Idzkowska E, Eljaszewicz A, Miklasz P, Musial WJ, Tycinska AM, Moniuszko M. The role of different monocyte subsets in the pathogenesis of atherosclerosis and acute coronary syndromes. *Scand J Immunol.* (2015) 82:163–73. doi: 10.1111/sji.12314
8. Arslan U, Kocaoglu I, Balci MM, Gülkan B, Falay MY, Temizhan A. Monocyte heterogeneity in myocardial infarction with and without ST elevation and its association with angiographic findings. *Coron Artery Dis.* (2013) 24:404–11. doi: 10.1097/MCA.0b013e328361a98c
9. Thygesen K, Alpert JS, White HD. Universal definition of myocardial infarction. *Eur Heart J.* (2007) 28:2525–38. doi: 10.1093/eurheartj/ehm355
10. Jaffe AS, Ravkilde J, Roberts R, Naslund U, Apple FS, Galvani M, et al. It's time for a change to a troponin standard. *Circulation.* (2000) 102:1216–20. doi: 10.1161/01.CIR.102.11.1216
11. Bormann J, Psyrakis DA, von Jeinsen B, Grün D, Elsner LK, Wolter JS, et al. Myeloid-related protein 8/14 and high-sensitivity cardiac troponin I to differentiate type 2 myocardial infarction. *Int J Cardiol.* (2020) 304:144–7. doi: 10.1016/j.ijcard.2020.01.043
12. Elsner LK, Jeinsen B von, Grün D, Wolter JS, Weferling M, Diouf K, et al. Prognostic performance of the ESC SCORE and its German recalibrated versions in primary and secondary prevention. *Eur J Prev Cardiol.* (2019). 27:2166–2169 doi: 10.1177/2047487319868034
13. Thygesen K, Alpert JS, Jaffe AS, Chaitman BR, Bax JJ, Morrow DA, et al. Fourth universal definition of myocardial infarction. *J Am Coll Cardiol.* (2018) 72:2231–64. doi: 10.1016/j.jacc.2018.08.1038
14. Everett BM, MacFadyen JG, Thuren T, Libby P, Glynn RJ, Ridker PM. Inhibition of interleukin-1β and reduction in atherothrombotic cardiovascular events in the CANTOS trial. *J Am Coll Cardiol.* (2020) 76:1660–70. doi: 10.1016/j.jacc.2020.08.011
15. Bouabdallaoui N, Tardif JC, Waters DD, Pinto FJ, Maggioni AP, Diaz R, et al. Time-to-treatment initiation of colchicine and cardiovascular outcomes after myocardial infarction in the colchicine cardiovascular outcomes trial (COLCOT). *Eur Heart J.* (2020) 7:4092–9. doi: 10.1093/eurheartj/ehaa659
16. Terkelsen CJ, Pinto DS, Thiele H, Clemmensen P, Nikus K, Lassen JF, et al. 2012 ESC STEMI guidelines and reperfusion therapy. *Heart*. (2013) 99:1154–6. doi: 10.1136/heartjnl-2013-304117
17. Kamińska J, Lisowska A, Koper-Lenkiewicz O, Miklasz P, Grubczak K, Moniuszko M, et al. Differences in monocyte subsets and monocyte-platelet aggregates in acute myocardial infarction—preliminary results. *Am J Med Sci.* (2019) 357:421–34. doi: 10.1016/j.amjms.2019.02.010
18. Wu KC, Zerhouni EA, Judd RM, Lugo-Olivieri CH, Barouch LA, Schulman SP, et al. Prognostic significance of microvascular obstruction by magnetic resonance imaging in patients with acute myocardial infarction. *Circulation.* (1998) 97:765–72. doi: 10.1161/01.CIR.97.8.765
19. Nahrendorf M, Pittet MJ, Swirksi FK. Monocytes: protagonists of infarct inflammation and repair after myocardial infarction. *Circulation.* (2010) 121:2437–45. doi: 10.1161/CIRCULATIONAHA.109.916346
20. Zhou X, Liu XL, Ji WJ, Liu JX, Guo ZZ, Ren D, et al. The kinetics of circulating monocyte subsets and monocyte-platelet aggregates in the acute phase of ST-elevation myocardial infarction associations with 2-year cardiovascular events. *Medicine.* (2016) 95:e3466. doi: 10.1097/MD.0000000000003466
21. Yamamoto H, Yoshida N, Shinke T, Otake H, Kuroda M, Sakaguchi K, et al. Impact of CD14(++)CD16(+) monocytes on coronary plaque vulnerability assessed by optical coherence tomography in coronary artery disease patients. *Atherosclerosis.* (2018) 269:245–51. doi: 10.1016/j.atherosclerosis.2018.01.010
22. Drakopoulou M, Tousoulis D, Toutouzas K. Subsets of monocytes: a driving force of coronary plaque instability? *Hell J Cardiol.* (2020) 62:182–3. doi: 10.1016/j.hjc.2020.05.001
23. Iannaccone M, Quadri G, Taha S, D'Ascenzo F, Montefusco A, Omede' P, et al. Prevalence and predictors of culprit plaque rupture at OCT in patients with coronary artery disease: a meta-analysis. *Eur Hear J Cardiovasc Imaging.* (2016) 17:1128–37. doi: 10.1093/ehjci/jev283
24. Mangold A, Hofbauer TM, Ondracek AS, Artner T, Scherz T, Speidl WS, et al. Neutrophil extracellular traps and monocyte subsets at the culprit lesion site of myocardial infarction patients. *Sci Rep.* (2019) 9:16304. doi: 10.1038/s41598-019-52671-y
25. Schlitt A, Heine G, Blankenberg S, Espinola-Klein C, Dopheide J, Bickel C, et al. CD14+CD16+ monocytes in coronary artery disease and their relationship to serum TNF-α levels. *Thromb Haemost.* (2004) 92:419–24. doi: 10.1160/TH04-02-0095
26. Moroni F, Ammirati E, Norata GD, Magnoni M, Camici PG. The role of monocytes and macrophages in human atherosclerosis, plaque neoangiogenesis, and atherothrombosis. *Med Inflamm.* (2019) 2019:7434376. doi: 10.1155/2019/7434376
27. Höpfner F, Jacob M, Ulrich C, Russ M, Simm A, Silber RE, et al. Subgroups of monocytes predict cardiovascular events in patients with coronary heart disease. The PHAMOS trial (prospective halle monocytes study). *Hell J Cardiol.* (2019) 60:311–21. doi: 10.1016/j.hjc.2019.04.012
28. Berg KE, Ljungcrantz I, Andersson L, Bryngelsson C, Hedblad B, Fredrikson GN, et al. Elevated CD14++CD16– monocytes predict cardiovascular events. *Circ Cardiovasc Genet.* (2012) 5:122–31. doi: 10.1161/CIRCGENETICS.111.960385
29. Weber C, Shantsila E, Hristov M, Caligiuri G, Guzik T, Heine GH, et al. Role and analysis of monocyte subsets in cardiovascular disease. Joint consensus document of the European society of cardiology (ESC) working groups "atherosclerosis & vascular biology" and "thrombosis". *Thromb Haemost.* (2016) 116:626–37. doi: 10.1160/TH16-02-0091
30. Long J, Chen J, Wang Q, Gao F, Lian M, Zhang P, et al. NFAT activating protein with ITAM motif 1 (NFAM1) is upregulated on circulating monocytes in coronary artery disease and potentially correlated with monocyte chemotaxis. *Atherosclerosis.* (2020) 307:39–51. doi: 10.1016/j.atherosclerosis.2020.06.001

Conflict of Interest: The authors declare that the research was conducted in the absence of any commercial or financial relationships that could be construed as a potential conflict of interest.

Publisher's Note: All claims expressed in this article are solely those of the authors and do not necessarily represent those of their affiliated organizations, or those of the publisher, the editors and the reviewers. Any product that may be evaluated in this article, or claim that may be made by its manufacturer, is not guaranteed or endorsed by the publisher.

frontiers in Cardiovascular Medicine

ORIGINAL RESEARCH
published: 12 November 2021
doi: 10.3389/fcvm.2021.754826

Myocardial Viability, Functional Status, and Collaterals of Patients With Chronically Occluded Coronary Arteries

Xueyao Yang[1†], Jinfan Tian[1†], Lijun Zhang[2], Wei Dong[3], Hongzhi Mi[3], Jianan Li[1], Jiahui Li[1], Ye Han[4], Huijuan Zuo[5], Jing An[6], Yi He[4] and Xiantao Song[1*]*

[1] Department of Cardiology, Beijing Anzhen Hospital, Capital Medical University, Beijing, China, [2] Department of Radiology, Beijing Anzhen Hospital, Capital Medical University, Beijing, China, [3] Department of Nuclear Medicine, Beijing Anzhen Hospital, Capital Medical University, Beijing, China, [4] Department of Radiology, Beijing Friendship Hospital, Capital Medical University, Beijing, China, [5] Department of Community Health Research, Beijing Institute of Heart, Lung and Blood Vessel Disease, Beijing Anzhen Hospital, Capital Medical University, Beijing, China, [6] Siemens Shenzhen Magnetic Resonance Ltd., Shenzhen, China

OPEN ACCESS

Edited by:
Minjie Lu,
Chinese Academy of Medical Sciences and Peking Union Medical College, China

Reviewed by:
Hsin-jung Yang,
Cedars Sinai Medical Center, United States
Chiara Martini,
University Hospital of Parma, Italy
Heng Ma,
Yantai Yuhuangding Hospital, China

***Correspondence:**
Xiantao Song
songxiantao0929@qq.com
Yi He
heyi139@sina.com

[†] These authors have contributed equally to this work

Specialty section:
This article was submitted to Coronary Artery Disease, a section of the journal Frontiers in Cardiovascular Medicine

Received: 07 August 2021
Accepted: 11 October 2021
Published: 12 November 2021

Citation:
Yang X, Tian J, Zhang L, Dong W, Mi H, Li J, Li J, Han Y, Zuo H, An J, He Y and Song X (2021) Myocardial Viability, Functional Status, and Collaterals of Patients With Chronically Occluded Coronary Arteries. Front. Cardiovasc. Med. 8:754826. doi: 10.3389/fcvm.2021.754826

Objective: Viability and functional assessments are recommended for indication and intervention for chronic coronary total occlusion (CTO). We aimed to evaluate myocardial viability and left ventricular (LV) functional status by using cardiovascular magnetic resonance (CMR) and to investigate the relationship between them and collaterals in patients with CTO.

Materials and Methods: We enrolled 194 patients with one CTO artery as detected by coronary angiography. Patients were scheduled for CMR within 1 week after coronary angiography.

Results: A total of 128 CTO territories (66%) showed scar based on late gadolinium enhancement (LGE) imaging. There were 1,112 segments in CTO territory, while only 198 segments (18%) subtended by the CTO artery showed transmural scar (i.e., >50% extent on LGE). Patients with viable myocardium had higher LV ejection fraction (LVEF) (56.7 ± 13.5% vs. 48.3 ± 15.4%, $p < 0.001$) than those with transmural scar. Angiographically, well-developed collaterals were found in 164 patients (85%). There was no significant correlation between collaterals and the presence of myocardial scar ($p = 0.680$) or between collaterals and LVEF ($p = 0.191$). Nevertheless, more segments with transmural scar were observed in patients with poorly-developed collaterals than in those with well-developed collaterals (25 vs. 17%, $p = 0.010$).

Conclusion: Myocardial infarction detected by CMR is widespread among patients with CTO, yet only a bit of transmural myocardial scar was observed within CTO territory. Limited number of segments with transmural scar is associated with preserved LV function. Well-developed collaterals are not related to the prevalence of myocardial scar or systolic functioning, but could be related to reduce number of non-viable segments subtended by the CTO artery.

Keywords: chronic total occlusion, myocardial viability, coronary artery disease, cardiovascular magnetic resonance, cardiac function

INTRODUCTION

Coronary chronic total occlusions (CTOs) are detected in ∼15–25% of patients who undergo coronary angiography (1–4). Beneficial effects of CTO revascularization include angina relief, decreased ischemia, and improved functional status (5–7). However, while better outcomes have been shown in non-randomized studies (5–7), evidence from randomized trials suggests that CTO percutaneous coronary intervention (PCI) treatment is not superior to conservative treatment with regard to functional status and long-term outcomes (8–10). Thus, an appropriate indication of CTO intervention is crucial when considering potential benefits, challenges, and risks. Therefore, baseline characteristics of patients with CTO need to be recorded in detail. Current guidelines recommend evaluation of symptoms and ischemia burden, but myocardial viability is also recommended as it is a newly recognized potential predictor of functional recovery following successful CTO PCI (11). In this study, we assessed the myocardial viability and functional status in CTO territories by using cardiovascular magnetic resonance (CMR) imaging and investigated the relationship between them and collaterals.

MATERIALS AND METHODS

Patients

A total of 254 patients who underwent coronary angiography due to suspected angina or ischemic evidence between December 2014 and March 2020 were verified to have CTO in only one major epicardial coronary artery and were considered for inclusion in this study. The study protocol was approved by the Ethics Board of Beijing Anzhen Hospital, Capital Medical University. Patients with acute myocardial infarction within 3 months, patients with coagulation disorders, and patients who refused or were unable to undergo CMR ($n = 46$) were excluded from the study. Patients were scheduled for CMR within 1 week after coronary angiography. A total of 14 patients with poor CMR images or failed procedures were also excluded, leaving a final total of 194 eligible patients that were enrolled in the study. **Figure 1** shows a schematic diagram describing the study cohort. All the patients were treated with optimal medical therapy (OMT) (medical therapy formulated by clinicians in full consideration of risk factor modification and permanent lifestyle changes) (12), regardless if the revascularization procedure succeeded or not. Written informed consent was obtained from all the patients and the study protocol conformed to the ethical guidelines of the 1975 Declaration of Helsinki.

Coronary Angiography and Collateral Assessment

Coronary angiography was performed by using the standard method. CTO was defined as 100% stenosis with the thrombolysis in myocardial infarction (TIMI) grade 0 flow in a major epicardial coronary artery (≥2.5 mm) for at least 3 months (13). Significant non-CTO coronary disease was diagnosed if there was ≥70% lumen stenosis in a major epicardial coronary artery (≥2.5 mm), except for the left main (LM) artery or ≥50% lumen stenosis in the LM artery. The presence and state of collaterals supplying the totally occluded vessel from the contralateral artery were graded by using the Rentrop classification system (14): Grade 0 referred to no collateral circulation, grade 1 referred to collateral circulation that only supplied the occluded vessel branch, grade 2 referred to collateral circulation that partially supplied the occluded vessel trunk, and grade 3 referred to collateral circulation that completely filled the occluded vessel trunk. Patients were classified as having poorly-developed collaterals (Rentrop scores of 0 and 1) or well-developed collaterals (Rentrop scores of 2 and 3). Collateral circulation scores were independently assessed by two experienced interventional cardiologists.

Cardiovascular Magnetic Resonance Data Acquisition and Processing

Cardiovascular magnetic resonance was performed with the Siemens 3.0-T Whole-body Scanner (MAGNETOM Verio, Tim System; Siemens Healthcare, Erlangen, Germany, UK). The CMR protocol included cine images and late gadolinium enhancement (LGE) imaging. As described in our previous study (15), 8-mm sections with no intersection gaps were obtained in the short-axis plane (from the base to the apex) and the long-axis plane of the left ventricle (LV) to perform cine cardiac MR and LGE imaging. Postprocessing analyses were performed by using the Siemens–Argus software.

Two experienced radiologists performed a visual analysis of all the images based on the American Heart Association 17-segment model of LV. Discrepancies were resolved by a discussion involving the presence of another senior investigator. Segments 1, 2, 7, 8, 13, 14, and 17 were considered left anterior descending (LAD) artery territory. Segments 5, 6, 11, 12, and 16 were considered left circumflex (LCX) artery territory. Segments 3, 4, 9, 10, and 15 were considered right coronary artery (RCA) territory (16). Taking coronary dominance into account, the inferoseptal segments, inferior segments, and inferolateral segments could be reassigned (17). The wall motion and extent of LGE were graded. The wall motion of each myocardial segment was scored on a scale of 1–4: 1 = normal, 2 = hypokinesia, 3 = akinesia, and 4 = dyskinesia. The extent of segmental wall enhancement was graded on a five-point scale: 1 = no hyperenhancement, 2 = hyperenhancement of 1–25% of tissue, 3 = hyperenhancement of 26–50% of tissue, 4 = hyperenhancement of 51–75% of tissue, and 5 = hyperenhancement of 76–100% of tissue (18, 19). LGE > 50% was considered to be a transmural scar, LGE between 1 and 50% was considered to be an endocardial scar with viable myocardium, and no LGE was considered to be absent of myocardial scar. Viable myocardium was defined as one with either no LGE or 1–50% LGE. Patients with left ventricular ejection fraction (LVEF) < 50% were defined as having left ventricular dysfunction.

Statistical Analysis

Statistical analysis was performed by using the Statistical Package for the Social Sciences (SPSS) 26.0 software (IBM Corp., Armonk, NY, USA). Normally distributed data were expressed as mean

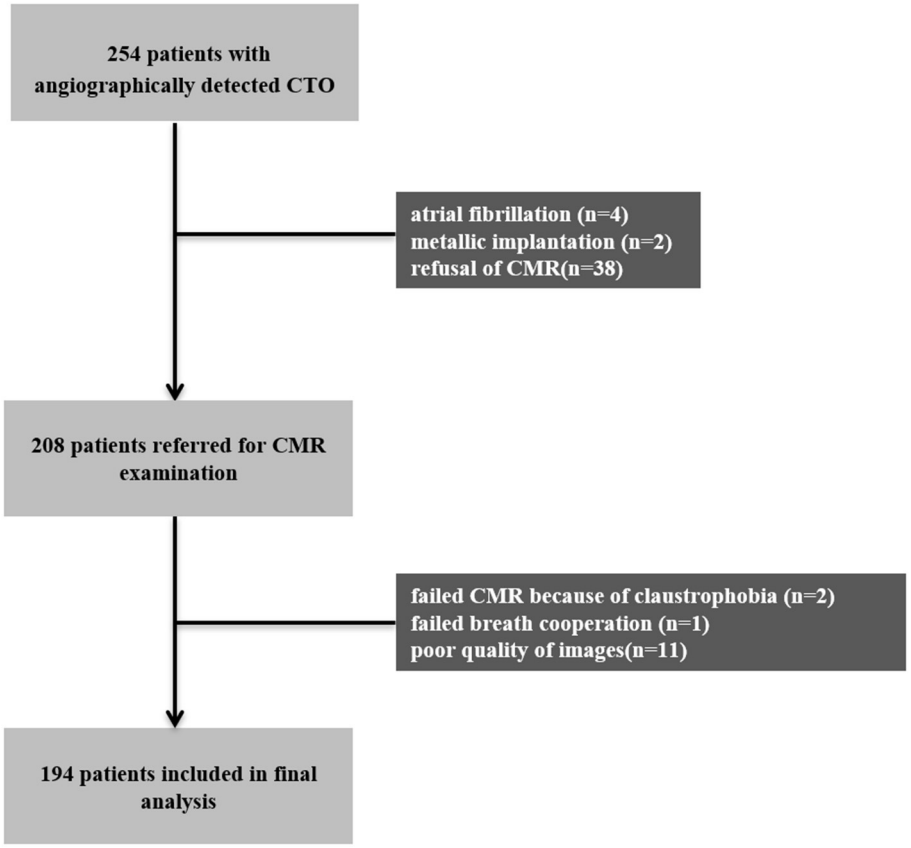

FIGURE 1 | Patient and imaging flowchart. CMR, cardiovascular magnetic resonance; CTO, chronic total occlusion.

± SD. Non-normally distributed data were expressed as median (interquartile range). Continuous variables were compared by using the *t*-test or the Mann–Whitney *U* test and categorical variables were compared by using the $\chi 2$ test or the Spearman's rank correlation test. Interobserver and intraobserver agreement were tested by using the Cohen's kappa. The correlation between wall motion score and extent of LGE was evaluated by using the Spearman's rank correlation test. A two-tailed $p < 0.05$ was considered to be statistically significant.

RESULTS

Baseline Characteristics

Baseline clinical and angiographic characteristics are presented in **Table 1** and are ordered according to myocardial scar formation in CTO territories. Statistical analyses demonstrated that patients with myocardial scar were likely to be males and smokers and were more likely to have hypertension. The prevalence of myocardial scar in CTO territory detected by CMR (66%) was strikingly higher than traditional clinical evidence that would suggest, as only 11% of included study patients showed pathological Q waves on ECG. Angiographically, 79 patients (41%) showed at least one concomitant main artery with severe stenosis.

Myocardial Viability and Functional Status

Of the 194 patients included in this study, a total of 128 patients (66%) had myocardial scar in CTO territory detected by CMR, while 66 patients (34%) did not have myocardial scar in CTO territory detected by CMR.

Late gadolinium enhancement imaging demonstrated myocardial scar in 417 segments (37%) out of 1,112 total segments. Over 50% LGE was observed in 198 (18%) CTO-related segments, while no scar was observed in 695 (63%) CTO-related segments (see **Table 2**). A total of 780 segments (70%) in CTO territory showed normal wall motion (score = 1). The Spearman's rank correlation test showed a significantly positive correlation between wall motion scores and LGE scores ($r = 0.488$, $p < 0.001$).

Left ventricular dysfunction was observed in 67 enrolled patients (35%) with an average LVEF of 36.4 ± 9.4%. Over 50% LGE was observed in 27% (103/381) of segments in CTO territory of patients with reduced LVEF (<50%), but only in 13% (95/731) of segments in CTO territory of those patients with normal systolic function (≥50%, $p < 0.001$). Patients with viable myocardia (LGE 0–50%) had higher LVEF (56.7 ± 13.5% vs. 48.3 ± 15.4%, $p < 0.001$, **Figure 2A**) and lower LV end-diastolic volume (LVEDV) (97.3 ± 33.8 ml vs. 121.7 ± 54.4 ml, $p = 0.003$, **Figure 2B**) and LV end-systolic volume (LVESV) (43.3

TABLE 1 | Baseline characteristics.

	All patients ($n = 194$)	No scar in CTO territory on CMR ($n = 66$)	Scar detected in CTO territory by CMR ($n = 128$)	*P*
Age	57 ± 10	56 ± 10	58 ± 10	0.067
Male	160 (82%)	46 (70%)	114 (89%)	<0.0001
Smoking	102 (53%)	25 (38%)	77 (60%)	0.004
Hypertension	115 (59%)	29 (44%)	86 (67%)	0.002
Diabetes	60 (31%)	21 (32%)	39 (30%)	0.871
Hyperlipemia	80 (41%)	28 (42%)	52 (41%)	0.878
Prior PCI	52 (27%)	11 (17%)	37 (29%)	0.079
Previous MI	45 (23%)	9 (14%)	36 (28%)	0.031
Q wave	22 (11%)	1 (2%)	21 (16%)	0.001
Angiographic presentation				
CTO location				
LAD	71 (37%)	31 (46%)	40 (31%)	–
LCX	21 (11%)	6 (12%)	15 (12%)	–
RCA	102 (53%)	29 (42%)	73 (57%)	–
Successful CTO revascularization	126 (65%)	49 (71%)	77 (60%)	0.058
Concomitant non-CTO lesion	79 (41%)	28 (38%)	51 (40%)	0.759
CMR characteristics				
Scar on CMR in CTO territory	128 (66%)	–	–	–
Wall motion abnormality in CTO territory	101 (52%)	13 (20%)	88 (75%)	<0.0001
LVEF (%)	53.3 ± 14.9	58.3 ± 12.7	50.7 ± 15.2	0.001
LVEDV (mL)	107.1 ± 44.8	90.0 ± 32.4	115.9 ± 47.8	<0.0001
LVESV (mL)	53.5 ± 37.8	38.7 ± 20.1	61.1 ± 42.4	<0.0001

CTO, chronic total occlusion; CMR, cardiovascular magnetic resonance imaging; LAD, left anterior descending coronary artery; LCX, left circumflex coronary artery; LVEF, left ventricular ejection fraction; LVESV, left ventricular end-systolic volume; LVEDV, left ventricular end-diastolic volume; PCI, percutaneous coronary intervention; RCA, right coronary artery.

TABLE 2 | Distribution of myocardial segments in CTO territory according to scar formation.

	0%	1–25%	26–50%	51–75%	>75%	Total
Distribution of the myocardial segments with different extent of myocardial scar						
LAD ($n = 71$)	336 (68%)	34 (7%)	32 (6%)	49 (10%)	46 (9%)	497
LCX ($n = 21$)	63 (60%)	9 (9%)	15 (14%)	8 (8%)	10 (10%)	105
RCA ($n = 102$)	296 (58%)	51 (10%)	78 (15%)	44 (9%)	41 (8%)	510
Total	695 (63%)	94 (8%)	125 (11%)	101 (9%)	97 (9%)	1,112

CTO, chronic total occlusion; LAD, left anterior descending; LCX, left circumflex; RCA, right coronary artery.

± 24.4 ml vs. 68.6 ± 48.1 ml, $p < 0.001$, **Figure 2C**) than those with transmural scar.

Myocardial Viability, LV Function, and Collateral Status

Poorly-developed angiographic collaterals were observed in 30 patients (15%), while well-developed collaterals were found in 164 patients (85%). Interobserver and intraobserver agreement for the Rentrop grading of collaterals in 50 (26%) randomly selected patients was high (intraobserver agreement = 90%; the Cohen's kappa = 0.62, 95% CI: 0.32–0.92).

Of the patients with poorly-developed collaterals, a total of 21 (70%) patients had a myocardial scar in CTO territory, while 65% of patients with well-developed collaterals (107/164) showed scar in CTO territory. There was no significant correlation between the presence of myocardial scar and collateral status ($p = 0.680$). Nevertheless, 25% of segments subtended to CTO arteries showed over 50% LGE in patients with poorly-developed collaterals, while only 17% of segments subtended to CTO arteries showed over 50% LGE in those patients with well-developed collaterals ($p = 0.010$; **Figure 3**). Additionally, more viable CTO-related segments were found in the presence of well-developed collaterals than in the presence of poorly-developed collaterals, despite the non-statistically significant difference [591 out of 934 (63%) vs. 104 out of 178 (58%) segments, $p = 0.237$].

There were no significant differences between mean LVEF and ventricular volume in patients with poorly-developed collaterals when compared with those with well-developed collaterals (*p*-values: LVEF = 0.191, LVEDV = 0.360, LVESV = 0.300, **Figures 2D–F**). Typical case scenarios displaying patients with

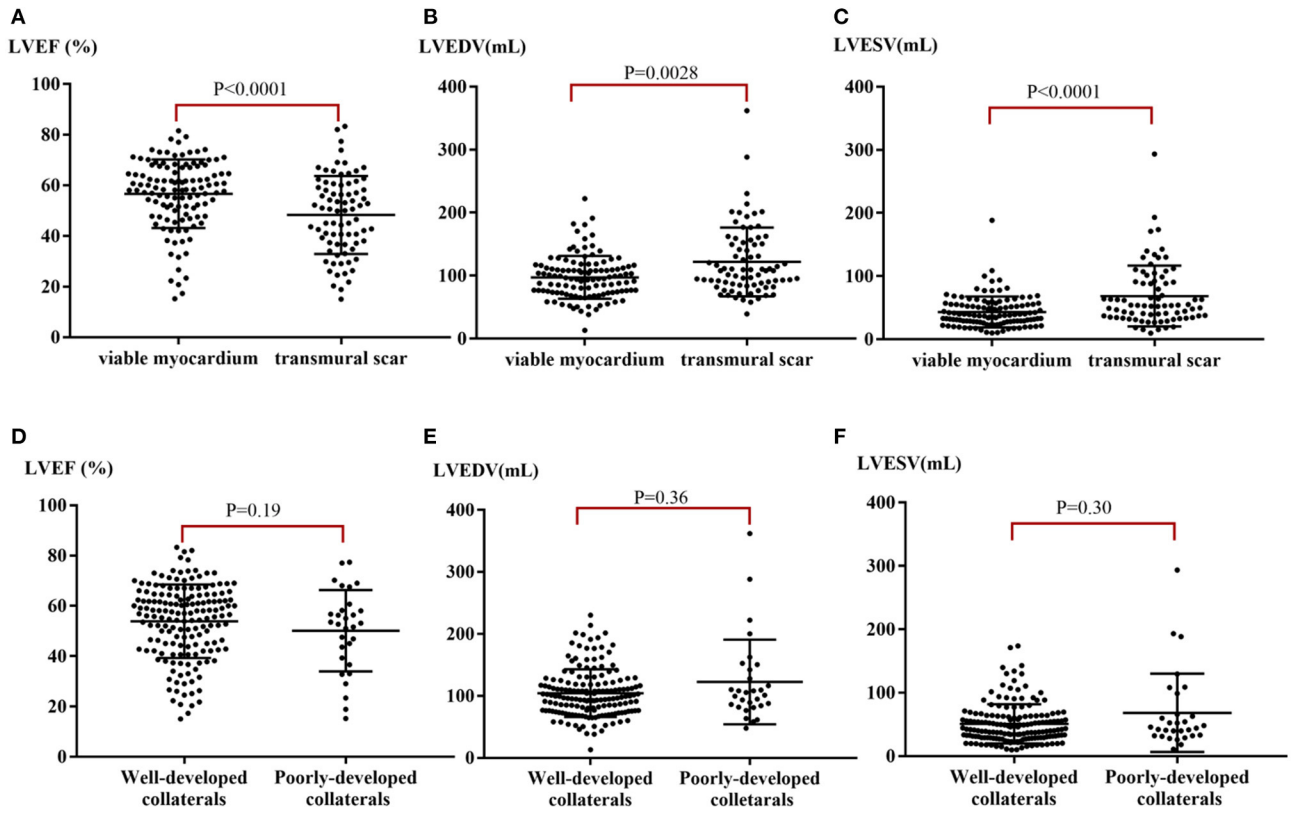

FIGURE 2 | LV function stratified by myocardial viability and collaterals. **(A)** Median LVEF stratified by the extent of myocardial scar. **(B)** Median LVEDV stratified by the extent of myocardial scar. **(C)** Median LVESV stratified by the extent of myocardial scar. **(D)** Median LVEF stratified by well- or poorly-developed collaterals. **(E)** Median LVEDV stratified by well- or poorly-developed collaterals. **(F)** Median LVESV stratified by well- or poorly-developed collaterals. LVEF, left ventricular ejection fraction; LVEDV, left ventricular end-diastolic volume; LVESV, left ventricular end-systolic volume.

well- or poorly-developed collaterals and patients with different extents of myocardial scar are shown in **Figure 4**.

DISCUSSION

In this study, we assessed the myocardial viability and functional status in CTO territory by using CMR and investigated the correlation between the prevalence of myocardial viability, LV systolic function, and collateral status. The prevalence of myocardial scar in CTO territory was >50%, while only 18% of segments had transmural scar. Patients with transmural scar had worse systolic functioning. Although collateral status was not related to the presence of myocardial scar or to LV function, well-developed collaterals reduced the number of segments with transmural scar in CTO territory.

Assessment of Myocardial Viability to Predict the Value of CTO PCI

We reported a higher prevalence of myocardial scar detected by CMR than traditional clinical evidence in this study. However, this finding was consistent with previous work (20). We attribute this to the high sensitivity of CMR for recognizing endocardial scar, while the occurrence of myocardial infarction symptoms or Q waves on ECG relates more to transmural necrosis. Despite the considerable prevalence of myocardial scar, less than one-fifth of the segments showed transmural scar, suggesting that severe ischemic injury is limited in CTO territory. However, since the benefits of revascularization for CTO are still controversial, many researchers pay more attention to factors that predict better outcomes following CTO PCI. Studies have shown that myocardial viability is an important outcome predictor, as confined endocardial scar or absolute viability has been associated with functional recovery (21, 22). Schumacher et al. previously reported that 76% of patients had evidence of LGE and that only 5% of CTO segments demonstrated transmural scar tissue that could be detected by CMR (23). The notion that the ischemic myocardial scar is common but most limited within the endocardium would be consistent with our results. Particularly, an evident extensive myocardial scar was observed beyond CTO territories in a few patients, despite adjustment according to the dominance of coronary artery. Indeed, the complexity of vascular variability made it difficult to assign the 17 segments of LV to specific coronary arteries. As previously reported (17), the most specific segments including anterior, anteroseptal segments correspond to LAD, but no segments can

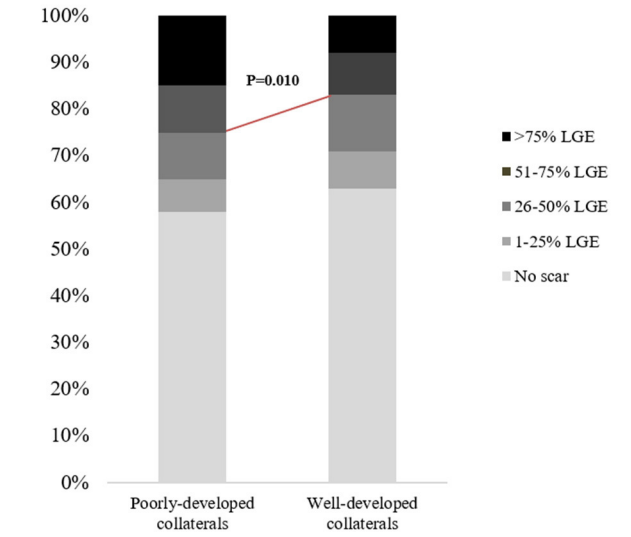

FIGURE 3 | Distribution of myocardial segments subtended by CTO arteries according to scar formation. CTO, chronic total occlusion; LGE, late gadolinium enhancement.

be exclusively attributed to RCA or LCX. Additionally, Yajima et al. (24) also reported myocardial scar in territories adjacent or remote to CTO territories in a chronic myocardial infarction (MI) adult porcine model and explained it by endothelium swelling and microvasculature disruption. Therefore, the variable vascular territories and extensive microvasculature injury could account for the bias of myocardial viability analysis.

Functional Status and Recovery

Ischemia is estimated to be responsible for around two-thirds of heart failure cases (25). In patients with ischemic ventricular dysfunction, the presence of CTO is associated with higher morbidity and poor prognosis (26). In this study, we reported that 35% of patients had impaired systolic functioning and that patients with transmural scar had worse functional statuses. A few observational studies investigating the outcomes of CTO PCI among patients with LV dysfunction have shown substantial LVEF improvement and decreased cardiac mortality, especially in those with severely impaired systolic functions (27–30). Interventional procedures are more challenging in these complicated patients. A study demonstrated that PCI was a safe strategy in patients with low LVEF ($\leq$35%), as the angiographic success rate was high and similar to that in patients with LVEF $>$ 35% without more periprocedural complications (31). However, these outcomes are still limited in non-randomized controlled trials (RCTs). The REVASC trial (A Randomized Trial to Assess Regional Left Ventricular Function After Stent Implantation in Chronic Total Occlusion) did not show any benefits related to CTO PCI. Therefore, experts recommend both the viability and functional assessment in patients with ischemic cardiomyopathy for CTO PCI (32).

Collaterals, Myocardial Viability, and Functional Status

There was no significant difference in the prevalence of myocardial scar or systolic functioning in patients with well- or poorly-developed collaterals and there were fewer non-viable segments in the CTO territory supplied by well-developed collaterals. The presence of well-developed collaterals may not directly predict myocardial viability, but could protect the myocardium from severe ischemic injury to some extent. In fact, whether collaterals could have protective effects on myocardial viability and contractility have long been a matter of debate. In a recent study, patients with well-developed collaterals showed less myocardial scar as assessed by quantitative CMR analysis and more retained systolic function in CTO territory (23). Previously, a few studies reported that collaterals had lower sensitivity for predicting myocardial viability (33, 34). The blood supply from collaterals to the totally occluded territory could be limited, especially when myocardial oxygen consumption increases. Additionally, myocardial viability and contractility could be affected by many concomitant factors including multiple-vessel stenosis and microvascular dysfunction. In the subgroup analysis of the EXPLORE (Evaluating Xience and Left Ventricular Function in Percutaneous Coronary Intervention on Occlusions After ST-Elevation Myocardial Infarction) trial, the presence of well-developed collaterals was shown to correlate with better outcomes. However, well-developed collaterals did not translate into better clinical outcomes. A recent meta-analysis showed that the presence of well-developed collaterals is not well-related to lower rates of acute MI (AMI) or mortality, but does increase the likelihood of successful CTO PCI (35, 36). These results indicated that well-developed collaterals should not be the only factor that affects prognosis.

Limitations

There are several limitations inherent in this study. First, it was a single-center and observational study with a small sample size that enrolled patients with a range of LVEF—meaning the population with impaired LVEF accounted for a minority of patients. This does, however, reflect a real-world trend. Second, the LGE images were analyzed by using a semi-quantitative visual method rather than a quantitative method. However, the utility of quantitative CMR analysis by using commercial software is still limited and thresholds for signal intensity are not unified. Third, stress perfusion imaging was not performed on our patients, meaning that we lacked analysis of ischemic burden in CTO territory. Finally, collateral circulation was only assessed by using visualized angiography and functional intravascular evaluations were not employed.

CONCLUSION

This study demonstrates that myocardial injuries in CTO territory are common, but those non-viable myocardia only account for a minority. Further, transmural myocardial scar appears to be associated with worse functional outcomes. Finally, well-developed collaterals are not related to the prevalence of myocardial scar or systolic functioning, but can reduce the

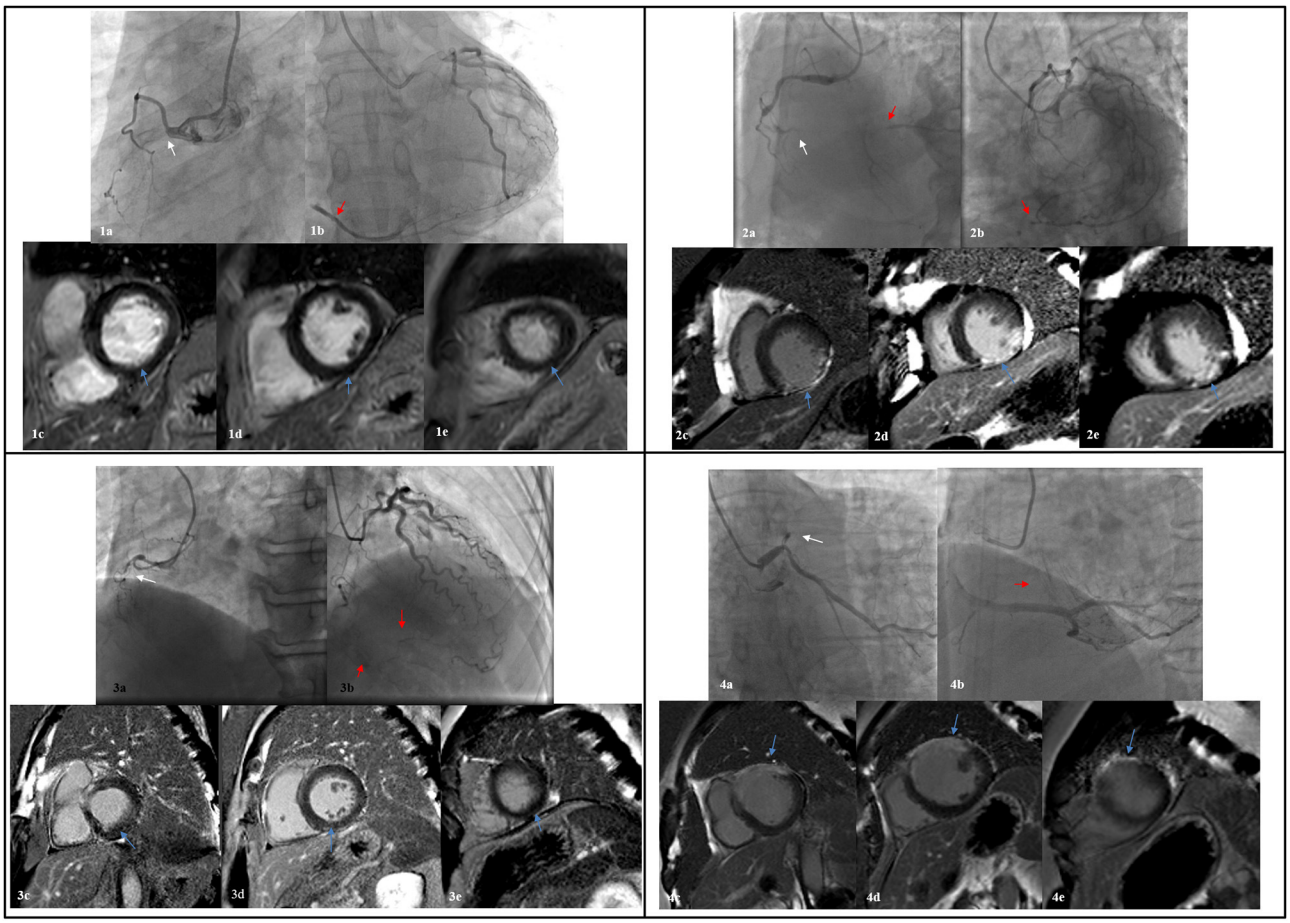

FIGURE 4 | Four typical case scenarios displaying patients with well- or poorly-developed collaterals and different extent of myocardial scar. 1: a, CTO in proximal RCA (white arrow); b, a well-developed epicardial collateral from LCX (red arrow); c-e, no myocardial scar of the inferior wall was observed from basal, intermediate, and to apex level. 2: a, CTO in distal RCA (white arrow); b, well-developed collaterals from LCX and septum branches (red arrow); c-e, transmural scar of the inferior wall was observed from basal, intermediate, and to apex level. 3: a, CTO in proximal RCA (white arrow); b, poorly-developed collaterals from septum branches (red arrow); c-e, no myocardial scar of the inferior wall was observed from basal, intermediate, and to apex level. 4: a, CTO in proximal LAD (white arrow); b, poorly-developed collaterals from septum branches (red arrow); c-e, transmural myocardial scar of the anterior wall was observed from basal, intermediate, and to apex level. CTO, chronic total occlusion; RCA, right coronary artery; LCX, left circumflex; LAD, left anterior descending.

number of segments with non-viable scar that are subtended by CTO arteries.

DATA AVAILABILITY STATEMENT

The raw data supporting the conclusions of this article will be made available by the authors, without undue reservation.

ETHICS STATEMENT

The studies involving human participants were reviewed and approved by Beijing Anzhen Hospital. The patients/participants provided their written informed consent to participate in this study.

AUTHOR CONTRIBUTIONS

XY, JT, LZ, WD, HM, JianL, JiahL, YHa, HZ, JA, YHe, and XS: conceptualization. JT and JianL: data curation. XY and JT: formal analysis. JT and XS: funding acquisition. XY, JT, and JianL: investigation. LZ, WD, HM, HZ, YHe, and XS: methodology. XY, JT, JianL, and XS: project administration. XS: resources. LZ, WD, HM, and YHe: software. YHe and XS: supervision, validation, and visualization. XY and JT: writing—original draft. LZ, YHe, and XS: writing—review and editing. All authors contributed to the article and approved the submitted version.

FUNDING

This work was supported by Capital Health Development Research Project (No. 2018-2-2063), National Natural Science Foundation of China (Nos. 81971569, 81670324, and 81671650), Beijing Lab for Cardiovascular Precision Medicine (PXM2018_014226_000013), Beijing Municipal Science and Technology Project (Z161100000516139), 2018 Beijing Excellent Talent Fund (NO. 2018000021469G241).

REFERENCES

1. Råmunddal T, Hoebers LP, Henriques JP, Dworeck C, Angerås O, Odenstedt J, et al. Chronic total occlusions in Sweden–a report from the Swedish Coronary Angiography and Angioplasty Registry (SCAAR). *PLoS ONE.* (2014) 9:e103850. doi: 10.1371/journal.pone.0103850
2. Fefer P, Knudtson ML, Cheema AN, Galbraith PD, Osherov AB, Yalonetsky S, et al. Current perspectives on coronary chronic total occlusions: the Canadian Multicenter Chronic Total Occlusions Registry. *J Am Coll Cardiol.* (2012) 59:991–7. doi: 10.1016/j.jacc.2011.12.007
3. Tomasello SD, Boukhris M, Giubilato S, Marzà F, Garbo R, Contegiacomo G, et al. Management strategies in patients affected by chronic total occlusions: results from the Italian Registry of Chronic Total Occlusions. *Eur Heart J.* (2015) 36:3189–98. doi: 10.1093/eurheartj/ehv450
4. Azzalini L, Jolicoeur EM, Pighi M, Millán X, Picard F, Tadros VX, et al. Epidemiology, management strategies, and outcomes of patients with chronic total coronary occlusion. *Am J Cardiol.* (2016) 118:1128–35. doi: 10.1016/j.amjcard.2016.07.023
5. Grantham JA, Jones PG, Cannon L, Spertus JA. Quantifying the early health status benefits of successful chronic total occlusion recanalization: results from the FlowCardia's Approach to Chronic Total Occlusion Recanalization (FACTOR) trial. *Circ Cardiovasc Qual Outcomes.* (2010) 3:284–90. doi: 10.1161/CIRCOUTCOMES.108.825760
6. Stuijfzand WJ, Biesbroek PS, Raijmakers PG, Driessen RS, Schumacher SP, van Diemen P, et al. Effects of successful percutaneous coronary intervention of chronic total occlusions on myocardial perfusion and left ventricular function. *Eurointervention.* (2017) 13:345–54. doi: 10.4244/EIJ-D-16-01014
7. Roth C, Goliasch G, Aschauer S, Gangl C, Ayoub M, Distelmaier K, et al. Impact of treatment strategies on long-term outcome of CTO patients. *Eur J Intern Med.* (2020) 77:97–104. doi: 10.1016/j.ejim.2020.03.008
8. Lee SW, Lee PH, Ahn JM, Park DW, Yun SC, Han S, et al. Randomized trial evaluating percutaneous coronary intervention for the treatment of chronic total occlusion. *Circulation.* (2019) 139:1674–83. doi: 10.1161/CIRCULATIONAHA.118.031313
9. Werner GS, Martin-Yuste V, Hildick-Smith D, Boudou N, Sianos G, Gelev V, et al. A randomized multicentre trial to compare revascularization with optimal medical therapy for the treatment of chronic total coronary occlusions. *Eur Heart J.* (2018) 39:2484–93. doi: 10.1093/eurheartj/ehy220
10. Henriques JP, Hoebers LP, Råmunddal T, Laanmets P, Eriksen E, Bax M, et al. Percutaneous intervention for concurrent chronic total occlusions in patients with STEMI: the EXPLORE trial. *J Am Coll Cardiol.* (2016) 68:1622–32. doi: 10.1016/j.jacc.2016.07.744
11. Neumann FJ, Sousa-Uva M, Ahlsson A, Alfonso F, Banning AP, Benedetto U, et al. 2018 ESC/EACTS Guidelines on myocardial revascularization. *Eur Heart J.* (2019) 40:87–165. doi: 10.1093/eurheartj/ehy855
12. Piepoli MF, Hoes AW, Agewall S, Albus C, Brotons C, Catapano AL, et al. 2016 European Guidelines on cardiovascular disease prevention in clinical practice: the Sixth Joint Task Force of the European Society of Cardiology and Other Societies on Cardiovascular Disease Prevention in Clinical Practice (constituted by representatives of 10 societies and by invited experts) developed with the special contribution of the European Association for Cardiovascular Prevention & Rehabilitation (EACPR). *Eur Heart J.* (2016). 37:2315–81. doi: 10.1093/eurheartj/ehw106
13. Di Mario C, Werner GS, Sianos G, Galassi AR, Büttner J, Dudek D, et al. European perspective in the recanalisation of Chronic Total Occlusions (CTO): consensus document from the EuroCTO Club. *Eurointervention.* (2007) 3:30–43.
14. Rentrop KP, Cohen M, Blanke H, Phillips RA. Changes in collateral channel filling immediately after controlled coronary artery occlusion by an angioplasty balloon in human subjects. *J Am Coll Cardiol.* (1985) 5:587–92. doi: 10.1016/S0735-1097(85)80380-6
15. Li JN, He Y, Dong W, Zhang LJ, Mi HZ, Zhang DF, et al. Comparison of cardiac MRI with PET for assessment of myocardial viability in patients with coronary chronic total occlusion. *Clin Radiol.* (2019) 74:410.e411-19. doi: 10.1016/j.crad.2019.01.021
16. Cerqueira MD, Weissman NJ, Dilsizian V, Jacobs AK, Kaul S, Laskey WK, et al. Standardized myocardial segmentation and nomenclature for tomographic imaging of the heart. A statement for healthcare professionals from the Cardiac Imaging Committee of the Council on Clinical Cardiology of the American Heart Association. *Int J Cardiovasc Imaging.* (2002) 18:539–542. doi: 10.1161/hc0402.102975
17. Pereztol-Valdés O, Candell-Riera J, Santana-Boado C, Angel J, Aguadé-Bruix S, Castell-Conesa J et al. Correspondence between left ventricular 17 myocardial segments and coronary arteries. *Eur Heart J.* (2005) 26:2637–43. doi: 10.1093/eurheartj/ehi496
18. Kim RJ, Wu E, Rafael A, Chen EL, Parker MA, Simonetti O, et al. The use of contrast-enhanced magnetic resonance imaging to identify reversible myocardial dysfunction. *N Engl J Med.* (2000) 343:1445–53. doi: 10.1056/NEJM200011163432003
19. Thiele H, Kappl MJ, Conradi S, Niebauer J, Hambrecht R, Schuler G. Reproducibility of chronic and acute infarct size measurement by delayed enhancement-magnetic resonance imaging. *J Am Coll Cardiol.* (2006) 47:1641–5. doi: 10.1016/j.jacc.2005.11.065
20. Choi JH, Chang SA, Choi JO, Song YB, Hahn JY, Choi SH, et al. Frequency of myocardial infarction and its relationship to angiographic collateral flow in territories supplied by chronically occluded coronary arteries. *Circulation.* (2013) 127:703–9. doi: 10.1161/CIRCULATIONAHA.112.092353
21. Nandalur KR, Dwamena BA, Choudhri AF, Nandalur MR, Carlos RC. Diagnostic performance of stress cardiac magnetic resonance imaging in the detection of coronary artery disease: a meta-analysis. *J Am Coll Cardiol.* (2007) 50:1343–53. doi: 10.1016/j.jacc.2007.06.030
22. Baks T, van Geuns RJ, Duncker DJ, Cademartiri F, Mollet NR, Krestin GP, et al. Prediction of left ventricular function after drug-eluting stent implantation for chronic total coronary occlusions. *J Am Coll Cardiol.* (2006) 47:721–5. doi: 10.1016/j.jacc.2005.10.042
23. Schumacher SP, Everaars H, Stuijfzand WJ, Huynh JW, van Diemen PA, Bom MJ, et al. Coronary collaterals and myocardial viability in patients with chronic total occlusions. *Eurointervention.* (2020) 16:e453–61. doi: 10.4244/EIJ-D-19-01006
24. Yajima S, Miyagawa S, Fukushima S, Isohashi K, Watabe T, Ikeda H, et al. Microvascular dysfunction related to progressive left ventricular remodeling due to chronic occlusion of the left anterior descending artery in an adult porcine heart. *Int Heart J.* (2019) 60:715–27. doi: 10.1536/ihj.18-346
25. Bui AL, Horwich TB, Fonarow GC. Epidemiology and risk profile of heart failure. *Nat Rev Cardiol.* (2011) 8:30–41. doi: 10.1038/nrcardio.2010.165
26. Tajstra M, Pyka Ł, Gorol J, Pres D, Gierlotka M, Gadula-Gacek E, et al. Impact of chronic total occlusion of the coronary artery on long-term prognosis in patients with ischemic systolic heart failure: insights from the COMMIT-HF registry. *JACC Cardiovasc Interv.* (2016) 9:1790–7. doi: 10.1016/j.jcin.2016.06.007
27. Cardona M, Martín V, Prat-Gonzalez S, Ortiz JT, Perea RJ, de Caralt TM, et al. Benefits of chronic total coronary occlusion percutaneous intervention in patients with heart failure and reduced ejection fraction: insights from a cardiovascular magnetic resonance study. *J Cardiovasc Magn Reson.* (2016) 18:78. doi: 10.1186/s12968-016-0287-5
28. Samy M, El Awady WS, Al-Daydamony MM, Abd El Samei MM, Shokry K. Echocardiographic assessment of left ventricular function recovery post percutaneous coronary intervention of chronic total occlusions in patients with low and mid-range left ventricular ejection fractions. *Echocardiography.* (2020) 37:239–246. doi: 10.1111/echo.14582
29. Chadid P, Markovic S, Bernhardt P, Hombach V, Rottbauer W, Wöhrle J. Improvement of regional and global left ventricular function in magnetic resonance imaging after recanalization of true coronary chronic total occlusions. *Cardiovasc Revasc Med.* (2015) 16:228–32. doi: 10.1016/j.carrev.2015.03.003
30. Toma A, Stähli BE, Gick M, Gebhard C, Kaufmann BA, Mashayekhi K, et al. Comparison of benefit of successful percutaneous coronary intervention for chronic total occlusion in patients with versus without reduced (≤40%) left ventricular ejection fraction. *Am J Cardiol.* (2017) 120:1780–6. doi: 10.1016/j.amjcard.2017.07.088
31. Galassi AR, Boukhris M, Toma A, Elhadj Z, Laroussi L, Gaemperli O, et al. Percutaneous coronary intervention of chronic total occlusions in patients

with low left ventricular ejection fraction. *JACC Cardiovasc Interv.* (2017) 10:2158–70. doi: 10.1016/j.jcin.2017.06.058

32. Brilakis ES, Mashayekhi K, Tsuchikane E, Abi Rafeh N, Alaswad K, Araya M, et al. Guiding principles for chronic total occlusion percutaneous coronary intervention. *Circulation.* (2019) 140:420–33. doi: 10.1161/CIRCULATIONAHA.119.039797
33. Dong W, Li J, Mi H, Song X, Jiao J, Li Q. Relationship between collateral circulation and myocardial viability of (18)F-FDG PET/CT subtended by chronic total occluded coronary arteries. *Ann Nucl Med.* (2018) 32:197–205. doi: 10.1007/s12149-018-1234-3
34. Wang L, Lu MJ, Feng L, Wang J, Fang W, He ZX, et al. Relationship of myocardial hibernation, scar, and angiographic collateral flow in ischemic cardiomyopathy with coronary chronic total occlusion. *J Nucl Cardiol.* (2019) 26:1720–30. doi: 10.1007/s12350-018-1241-8
35. van Dongen IM, Elias J, van Houwelingen KG, Agostoni P, Claessen B, Hoebers LP, et al. Impact of collateralisation to a concomitant chronic total occlusion in patients with ST-elevation myocardial infarction: a subanalysis of the EXPLORE randomised controlled trial. *Open Heart.* (2018) 5:e000810. doi: 10.1136/openhrt-2018-000810
36. Allahwala UK, Nour D, Bhatia K, Ward MR, Lo S, Weaver JC, et al. Prognostic impact of collaterals in patients with a coronary chronic total occlusion: a meta-analysis of over 3,000 patients. *Catheter Cardiovasc Interv.* (2020) 98:217–22. doi: 10.1002/ccd.29348

Conflict of Interest: JA was employed by the company Siemens Shenzhen Magnetic Resonance Ltd.

The remaining authors declare that the research was conducted in the absence of any commercial or financial relationships that could be construed as a potential conflict of interest.

Publisher's Note: All claims expressed in this article are solely those of the authors and do not necessarily represent those of their affiliated organizations, or those of the publisher, the editors and the reviewers. Any product that may be evaluated in this article, or claim that may be made by its manufacturer, is not guaranteed or endorsed by the publisher.

frontiers in Cardiovascular Medicine

REVIEW
published: 01 December 2021
doi: 10.3389/fcvm.2021.762391

Duration of Dual Antiplatelet Therapy After Implantation of Drug-Coated Balloon

Yuxuan Zhang[1†], *Xinyi Zhang*[1†], *Qichao Dong*[1], *Delong Chen*[1], *Yi Xu*[2] *and Jun Jiang*[1*]

[1] *Department of Cardiology, Second Affiliated Hospital, School of Medicine, Zhejiang University, Hangzhou, China,*
[2] *Department of Cardiology, Ningbo First Hospital, Ningbo, China*

The drug-coated balloon (DCB) is an emerging percutaneous coronary intervention (PCI) device with theoretical advantages and promising results. Recent clinical observations have demonstrated that DCB tends to have both good efficacy and a good safety profile in the treatment of in-stent restenosis (ISR) for both bare-metal and drug-eluting stents (DES), *de novo* coronary artery disease (CAD), and other situation, such as high bleeding risk, chronic total occlusion, and acute coronary syndrome (ACS). Dual antiplatelet therapy (DAPT) has become an essential medication in daily clinical practice, but the optimal duration of DAPT after the implantation of a DCB remains unknown. At the time of the first *in vivo* implantation of paclitaxel-DCB for the treatment of ISR in 2006, the protocol-defined DAPT duration was only 1 month. Subsequently, DAPT duration ranging from 1 to 12 months has been recommended by various trials. However, there have been no randomized controlled trials (RCTs) on the optimal duration of DAPT after DCB angioplasty. Current clinical guidelines normally recommend the duration of DAPT after DCB-only angioplasty based on data from RCTs on the optimal duration of DAPT after stenting. In this review, we summarized current clinical trials on DCB-only angioplasty for different types of CADs and their stipulated durations of DAPT, and compared their clinical results such as restenosis, target lesion revascularization (TLR) and stent thrombosis event. We hope this review can assist clinicians in making reasonable decisions about the duration of DAPT after DCB implantation.

Keywords: drug-coated balloon, dual antiplatelet therapy, in-stent restenosis, *de novo* coronary artery disease, percutaneous coronary intervention

OPEN ACCESS

Edited by:
Gianluca Caiazzo,
Azienda Sanitaria Locale Caserta, Italy

Reviewed by:
Arturo Cesaro,
University of Campania Luigi Vanvitelli, Italy
Enrico Fabris,
University of Trieste, Italy

***Correspondence:**
Jun Jiang
jiang-jun@zju.edu.cn

[†] *These authors have contributed equally to this work and share first authorship*

Specialty section:
This article was submitted to Coronary Artery Disease, a section of the journal Frontiers in Cardiovascular Medicine

Received: *21 August 2021*
Accepted: *08 November 2021*
Published: *01 December 2021*

Citation:
Zhang Y, Zhang X, Dong Q, Chen D, Xu Y and Jiang J (2021) Duration of Dual Antiplatelet Therapy After Implantation of Drug-Coated Balloon. Front. Cardiovasc. Med. 8:762391. doi: 10.3389/fcvm.2021.762391

INTRODUCTION

Drug-coated balloon (DCB) technology is a combined therapy that involves a balloon and drug to treat coronary lesions, eliminating stent thrombosis, and reducing the rate of restenosis by leaving no metal behind (1). Since 2001, the DCB has been tested experimentally (1), and was later clinically validated in small-randomized controlled trials (RCTs) on coronary in-stent restenosis (ISR) (2) and peripheral stenosis (3). This technology has played an increasingly important role in the field of percutaneous coronary intervention (PCI), and a variety of products have been developed (**Table 1**). Drug-coated balloon technology has demonstrated safety and efficacy in the treatment of ISR and is recommended by guidelines as Class 1 indication for the treatment of ISR (5–8). Meanwhile, an increasing number of clinical studies using DCB have shown promising results for the treatment of both small and large vessel *de novo* coronary artery disease (CAD), bifurcation lesions, and other variable disease subsets.

TABLE 1 | Major current drug-coated balloon available in the market (4).

Name	Manufacturer	Type	Dosage	Coating method	Release characteristics
SeQuent please	B. Braun Melsungen AG, Berlin, Germany	Paclitaxel	3 $\mu g/mm^2$	Matrix coating: paclitaxel + hydrophilic spacer (iopromide)	Inflate for at least 40 s to allow enough drug to be released into the vessel wall (4.5% of the drug remains on the balloon)
DIOR-II	Eurocor GmbH, Bonn, Germany	Paclitaxel	3 $\mu g/mm^2$	1:1 mixture of aleuritic and shellolic acid with paclitaxel (shellac® coating)	Drug delivery by simple diffusion, inflate 20–30 s at normal pressure
Elutax	Aachen Resonance GmbH, Aachen, Germany	Paclitaxel	2 $\mu g/mm^2$	Two layers of paclitaxel (the first on the inflated balloon and the second as a crystal power), without any excipient	10% of the drug remains on the balloon after an inflation of 30–60 s
RESTORE DCB	Cardionovum, Bonn, Germany	Paclitaxel	3 $\mu g/mm^2$	Shellac	A short-term balloon-to-vessel wall contact time of 45 s is enough
Pantera Lux	Biotronik, Bulach, Switzerland	Paclitaxel	3 $\mu g/mm^2$	Paclitaxel + butyryl-trihexyl citrate	Minimum inflation time is 30 s to allow enough drug to be released into the vessel wall
Danubio	Minvasys, Gennevilliers, France	Paclitaxel	2.5 $\mu g/mm^2$	Paclitaxel + butyryl-trihexyl citrate	Minimum inflation time is 30 s to allow enough drug to be released into the vessel wall
Protégé and Protégé NC	Blue Medical, Helmond, Netherlands	Paclitaxel	3 $\mu g/mm^2$	Drug component encapsulated in wings using Wing Seal Technology	Load secured to achieve the therapeutic window within 30 s inflation time, also available with non-compliant balloon
MagicTouch	Concept Medical, Surat, India	Sirolimus	1.27 $\mu g/mm^2$	Sirolimus is encapsulated in a phospholipid bi-layer as drug carrier and in Nanocarriers configuration	Inflate for at least 45 s if clinically tolerated
IN.PACT Falcon	Medtronic, Inc., Santa Rosa, California, USA	Paclitaxel	3 $\mu g/mm^2$	Crystalline coating: paclitaxel + urea (FreePac®)	Inflate 30–60 s at normal pressure to allow enough drug release into the vessel wall (4.7% of the drug remains on the balloon)
Agent	Boston Scientific, Natick, MA, USA	Paclitaxel	2 $\mu g/mm^2$	Balanced hydrophobic and hydrophilic properties of TransPax, Fewer particulates are lost distally during the procedure	Inflate for at least 30 s to allow enough drug to be released into the vessel wall
AngiosculptX	Spectranetics, Colorado Springs, Colorado, USA	Paclitaxel	3 $\mu g/mm^2$	Nordihydroguaiaretic acid excipient to facilitate drug transfer to tissue	Inflate for at least 30 s, Improved dilatation in calcified or resistant lesion using a scoring balloon
Chocolate touch	QT Vascular	Paclitaxel	3 $\mu g/mm^2$	Crystalline paclitaxel coating with hydrophilic excipient	The pillows and grooves of the inflated Chocolate Touch balloon result in 20% more drug-coated surface compared to conventional balloons of the same size
Essential	Ivascular	Paclitaxel	3 $\mu g/mm^2$	Microcrystalline coating	Inflation process must last from 30 s to 1 min

Dual antiplatelet therapy (DAPT) has become an essential medication in daily clinical practice; it combines aspirin and a $P2Y_{12}$-receptor inhibitor following PCI and is needed for the primary prevention of stent thrombosis and the secondary prevention of ischemic thrombotic event. With the "leave nothing behind" strategy, based on the shorter period of inflammatory response without a metallic scaffold, this strategy offers the theoretical advantage of virtually eliminating the threat of thrombosis over both the short and long term. Therefore, one possible benefit for many patients using DCB-only angioplasty is a short duration of DAPT, in some cases only 4 weeks, such as in patients with a high bleeding risk (9).

However, it must be pointed out that all previous studies have not adequately addressed questions about the optimal duration of DAPT after DCB implantation. The purpose of this review is to outline different DAPT strategies and trials with the use of DCB for ISR, *de novo* lesions, and other specific situations and to explore the appropriate DAPT duration to assist clinical practice.

CURRENT GUIDANCE

As first recommended by the German Consensus Group (10), DAPT is necessary for 4 weeks if the DCB is used as a stand-alone procedure, and 6–12 months of DAPT is recommended in combination with bare metal stent (BMS). Then, they formulated more detailed recommendations regarding DAPT duration. In cases of the treatment of an ISR, the patient should receive

aspirin 100 mg in the long-term and additional clopidogrel 75 mg for 4 weeks after PCI in BMS and at least 4 weeks or the duration defined by the drug-eluting stent (DES) implantation date. After treatment of small vessel *de novo* coronary lesions, aspirin 100 mg should be given long-term and clopidogrel 75 mg is recommended for 4 weeks after PCI with DCB alone and for 3 months after DCB with additional spot BMS. Dual antiplatelet therapy is recommended for 4 weeks if only DCB without stenting is used for the treatment of a bifurcation lesion and 6–12 months in case stents are used before or after the DCB procedure. To treat acute coronary syndromes (ACS), the recommended duration of DAPT is 12 months regardless of the use of a BMS, DES, or DCB (11). The Italian Position Group gave similar recommendations regarding a DAPT duration of at least 1 month in the case of DCB-only treatment and 3 months in cases of the implantation of a BMS (12).

However, the European Society of Cardiology Guidelines on DAPT gave more conservative recommendations. In patients with stable CAD treated with DCB, DAPT for 6 months should be considered. Dual antiplatelet therapy for 3 months should be considered if patients with stable CAD are considered a high bleeding risk. In patients with stable CAD in whom 3-months DAPT poses safety concerns, DAPT for 1 month may be considered. As in patients with ACS treated with coronary stent implantation, DAPT with a $P2Y_{12}$ inhibitor on top of aspirin is recommended for 12 months unless contraindicated. In cases of patients who are at high risk of bleeding, discontinuation of $P2Y_{12}$ inhibitor therapy after 6 months should be considered (13).

Recently, the Asia-Pacific Consensus Group updated the DCB treatment protocols for CAD and gave their recommendations regarding optimal medical treatment. For the treatment of BMS-ISR and DES-ISR, patients should maintain a lifelong therapy with aspirin 100 mg and take clopidogrel 75 mg for at least 1–3 months. For the treatment of *de novo* coronary disease except ACS with DCB only, patients should receive DAPT for at least 1 month and then receive aspirin 100 mg for life. Moreover, in cases of *de novo* stable coronary disease with DCB plus bail-out BMS, DAPT is recommended for at least 3–6 months. For the treatment of bifurcation disease, if the DCB-only method without stenting is used, the duration of DAPT should be the same as other *de novo* coronary disease. In the case of the DCB method plus stenting, the recommended DAPT duration is at least 6–12 months. For patients with ACS, similar to other guidelines, DAPT is recommended for at least 12 months regardless of the use of BMS, DCB, or DES (7).

PHARMACOLOGY OF ANTIPLATELETS

The goal of antiplatelet therapy after PCI is to maximize protection against short- and long-term postoperative stent or vessel thrombosis by blocking platelet activation while limiting bleeding risk. **Figure 1** illustrates the main mechanisms of platelet activation and the sites of action of antiplatelet agents. Platelet adhesion is mediated by the interaction between platelet receptors and ligands exposed at the sites of vascular injury, e.g., the glycoprotein (GP) Ib/V/IX receptor complex with the von Willebrand factor and GPVI and GPla proteins with collagen (15–17). Then the local platelet activating factors, such as adenosine diphosphate (ADP), thromboxane A_2 (TXA_2), serotonin, and thrombin, promote and amplify the platelet activation by interacting with specific platelet membrane receptors [such as P2Y purinoceptor 12 ($P2Y_{12}$), 5-hydroxytryptamine 2A receptor, TXA_2 receptor isoform-α, and proteinase-activated receptors (PARs)] (15–17). Antiplatelet drugs block platelet activation through different phases: (1) Acetylsalicylic acid, commonly known as aspirin, is an irreversible cyclooxygenase 1 (COX1) inhibitor that diminishes platelet activation and aggregation promoted by TXA_2 by blocking TXA_2 production during pathological thrombus formation: (2) $P2Y_{12}$ ADP receptor antagonists, which include clopidogrel, prasugrel, and ticagrelor, exert their clinical benefit by inhibiting the activation of $P2Y_{12}$-mediated platelet activation during pathological thrombosis (when the occlusive platelet-rich thrombus is formed); (3) Glycoprotein IIb/IIIa inhibitors, including eptifibatide and tirofiban, are currently only for ACS patients undergoing PCI, and interfere with platelet cross-linking and clot formation by competing with fibrinogen and vWF for GP IIb/IIIa binding; (4) Vorapaxar, as a PAR-1 inhibitor, blocks the binding of thrombin to PAR-1, thus inhibiting thrombin-induced activation, and the aggregation of platelets; (5) Cilostazol is an inhibitor of phosphodiesterase type III, which possesses both antiplatelet and vasodilatory effects (15–17).

DAPT DURATION IN MULTIPLE DISEASES

In-stent Restenosis

In-stent restenosis remains the primary cause of PCI failure, though the development of DESs generations has improved anti-restenosis performance (18). A recent report showed that approximately 20% of patients required target lesion revascularization (TLR) at the 10-year follow-up (19). Several therapies for ISR of BMS or DES have been tested in clinical trials (20), and DCB and repeated stenting with DES have become the most effective therapeutic options, which have been recommended as class IA by guidance (5). A recent meta-analysis of 10 RCTs showed that DCB and DES were similarly effective and safe in the treatment of BMS-ISR, whereas DES had higher efficacy than DCB in the treatment of DES-ISR (21).

As the first trial demonstrated that paclitaxel-DCB angioplasty was superior to plain old balloon angioplasty (POBA) alone in BMS-ISR, the PACCOCATH ISR trial recommended DAPT for 1 month followed by treatment with aspirin alone (2). At 6 months, the primary endpoint late lumen loss (LLL) in-segment was lower in the DCB group than in the POBA group (0.03 ± 0.48 mm vs. 0.74 ± 0.86 mm, $P = 0.002$). Restenosis occurred in 10 of 23 patients (43%) in the POBA group, compared to only 1 of 22 patients (5%) in the DCB group ($P = 0.002$). Patents who required TLR were significantly fewer in the DCB group than in the POBA group (0 vs. 6%, $P = 0.02$). At 5 years, TLR rates were still significantly lower in the DCB group than in the POBA group (38.9 vs. 9.3%, $P = 0.004$) (22). No stent thrombosis was found

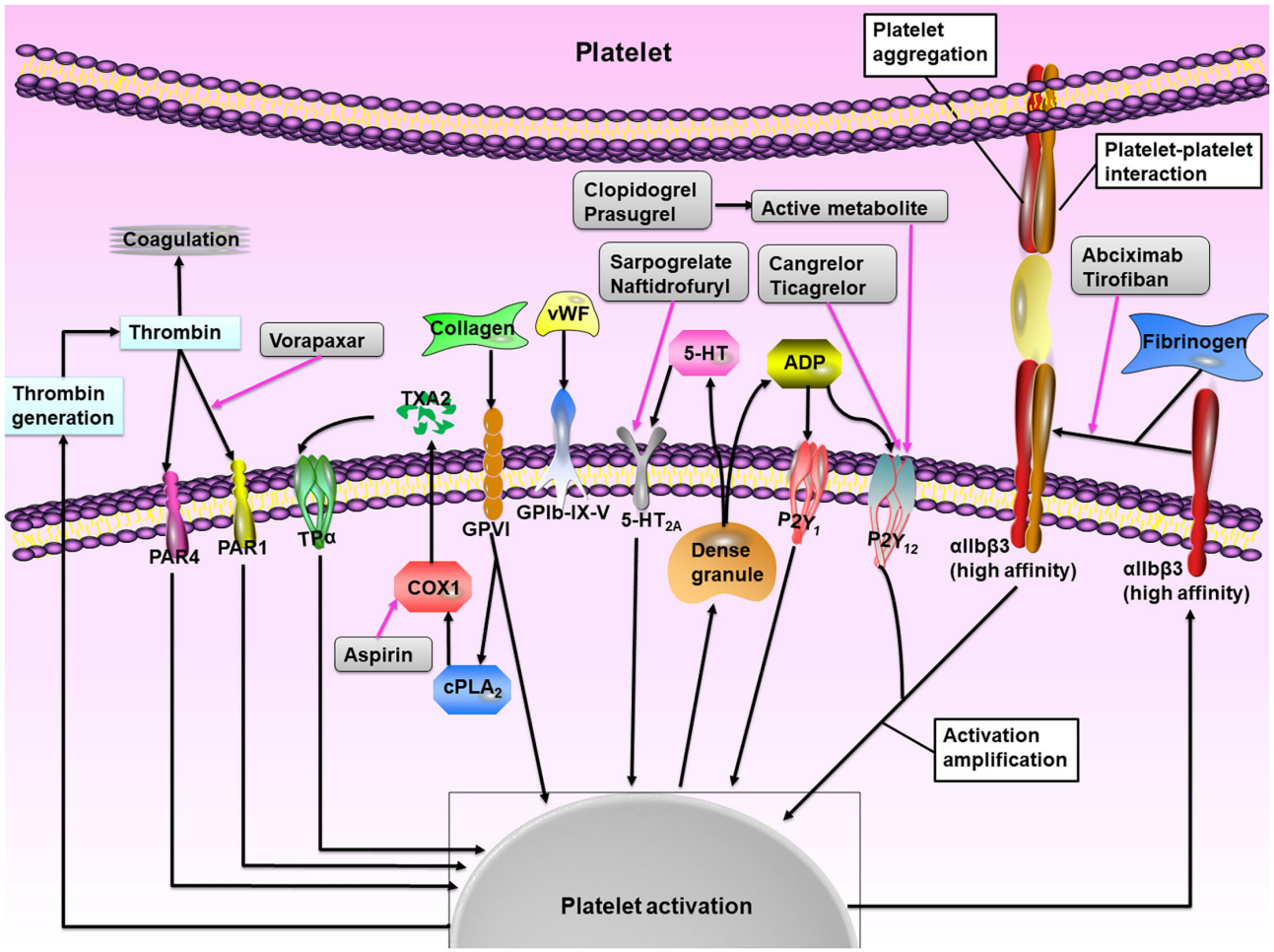

FIGURE 1 | The role of platelet activation. At the site of vascular injury, platelet adherence to the endothelium through the combination of glycoprotein (GP) receptors with exposed extracellular matrix proteins (particularly collagen and von Willebrand factor, vWF). Platelet activation occurs through complex intracellular signaling processes and leads to the release of various agonists, including thromboxane A_2 (TXA_2), ADP, and 5-hydroxytryptamine (5-HT), which act by binding to their respective G protein-coupled receptors and mediate paracrine and autocrine platelet activation. The receptor P2Y purinoceptor 12 ($P2Y_{12}$) has a major role in the amplification of platelet activation, which is also supported by outside-in signaling via αIIbβ3 integrin (the glycoprotein IIb/IIIa receptor). The main platelet integrin GPIIb/IIIa mediates platelet aggregation through conformational shape changes and binding to fibrinogen and vWF, thereby mediating the final common step of platelet activation. The net result of these interactions is thrombus formation mediated by the interaction of platelet aggregate with fibrin and thrombin. The available drugs (gray boxes) blockade different pathways of platelet activation and show additive inhibitory effects when used in combination. PAR, proteinase-activated receptor; TPα, TXA_2 receptor isoform-α; COX1, cyclooxygenase 1. Adapted from Varga-Szabo et al. (14).

during the entire follower-up trial, which suggests that short-term DAPT may be feasible and safe for patients who undergo DCB angioplasty.

In most trials on BMS-ISR treatment, DAPT with aspirin 100 mg per day and clopidogrel was recommended for 3 months (23–26) (**Table 2**). Among these trials, only two cases of stent thrombosis were found during the follow-up (24, 25). It is worth mentioning that one patient in the DCB group experienced stent thrombosis due to clopidogrel discontinuation before late angiography in the RIBS V trial. The PEPCAD II ISR study showed that 19 of 66 (28.8%) patients in the DCB group and 42 of 65 (64.4%) patients in the DES group were still using clopidogrel ($P < 0.0001$) at 6 months, whereas after 12 months, the usage declined to 12 of 66 (18.1%) and 27 of 65 (41.5%), respective ($P <$ 0.01) (23). However, there was no significance difference between the treatment groups with DAPT at 1 and 3 years ($P = 0.80$ and 0.47, respectively) (35).

However, the duration of DAPT varied from 3 to 12 months in trials for DES-ISR treatment (**Table 2**). In the RIBS IV randomized clinical trial, which showed DCB had lower efficacy compared to EES in patients presenting with DES-ISR, DAPT was prescribed for only 3 months after DCB angioplasty, and then aspirin monotherapy was maintained (30, 36). The TLR rates were significantly reduced in the EES group both at 1-year (4.5 vs. 13.0%, $P = 0.007$) and 3-years (7.1 vs. 15.6%, $P = 0.015$) follow-up, but the need for "late" (>1 year) TLR (2.6 vs. 4%) was similar in the two groups. Stent thrombosis (both definitive and probable) occurred in three patients (two in the DCB group and

TABLE 2 | Characteristics of randomized trials of DCB for treatment of ISR.

Trial (year)	Patients, N	Design	DAPT duration (months)	Primary endpoint (follow-up, months)	Binary restenosis rate, %	TLR, % (follow-up, months)	ST, *N* (follow-up, months)
BMS-ISR							
PACCOCATH ISR (2006) (2)	52	DCB vs. POBA	1 in both groups	LLL: 0.03 ± 0.48 mm vs. 0.74 ± 0.86 mm* (6)	5 vs. 43%*	0 vs. 23%** (12)	0 vs. 0 (12)
PEPCAD II isr (2009) (23)	131	DCB vs. PES	3 in DCB vs. 6 in PES	LLL: 0.17 ± 0.42 mm vs. 0.38 ± 0.61 mm (6)	7 vs. 20%	6.3 vs. 15.4% (36)	0 vs. 0 (36)
ribs V (2014) (24)	189	DCB vs. EES	3 in DCB vs. 12 in EES	MLD: 2.01 ± 0.6 mm vs. 2.36 ± 0.6 mm* (9)	9.5 vs. 4.7%	6 vs. 1% (12) 8 vs. 2%** (36)	1 vs. 0 (36)
PATENE-C (2016) (25)	61	PCSB vs. USB	3 in both	LLL: 0.17 ± 0.40 mm vs. 0.48 ± 0.51 mm* (6)	7 vs. 41%*	3 vs. 32%* (12)	0 vs. 0 (12)
Pleva et al. (2016) (26)	136	DCB vs. EES	3 in DCB vs. 6-12 in EES	LLL: 0.09 ± 0.73 mm vs. 0.44 ± 0.73 mm* (12)	8.7 vs. 19.12%	7.35 vs. 16.18% (12)	1 VS. 0 (12)
DES-ISR							
PEPCAD-DES (2012) (27)	110	DCB vs. POBA	6 in both groups	LLL: 0.43 ± 0.61 mm vs. 1.03±0.77 mm* (6)	17.2 vs. 58.1%*	15.3 vs. 36.6%* (6) 19.4 vs. 36.8%** (36)	1 vs. 4** (36)
ISAR-DESIRE 3(2013) (28)	402	DCB vs. PES vs. POBA	6 in all groups	DS: 38.0% in DCB vs. 37.4% in PES vs. 54.1% in POBA (6–8)	NA	22.1% in DCB vs. 13.5% in PES vs. 43.5% in POBA (12) 33.3% in DCB vs. 24.2% in PES vs. 50.8% in POBA (36)	1 vs. 1 vs. 0 (12) 1 vs. 2 vs. 0 (36)
Pepcad China ISR (2014) (29)	220	DCB vs. PES	12 in both groups	LLL: 0.46 ± 0.51 mm vs. 0.55 ± 0.61 mm (9)	18.6 vs. 23.8%	15.6 vs. 12.3% (12) 15.9 vs. 13.7% (24)	1 vs. 2 (12) 1 vs. 3 (24)
Ribs IV (2015) (30)	309	DCB vs. EES	3 in DCB vs. 12 in EES	MLD: 1.80 ± 0.6 mm vs. 2.03 ± 0.7 mm* (6–9)	19 vs. 11%	13.0 vs. 4.5%* (12) 15.6 vs. 7.1%** (36)	3 vs. 2 (12) 4 vs. 2 (36)
ISAR-DESIRE 4 (2017) (31)	252	DCB vs. SB-DCB	6 in both groups	DS: 40.4 ± 21.4 vs. 35 ± 16.8%** (6–8)	32.0 vs. 18.5%**	21.8 vs. 16.2% (12)	0 vs. 0 (12)
Restore (2018) (32)	172	DCB vs. EES	6 in both groups	LLL: 0.15 ± 0.49 mm vs. 0.19 ± 0.41 mm (9)	19.5 vs. 5.6%	5.8 vs. 1.2% (12)	0 vs. 0 (12)
Both BMS-ISR and DES-ISR							
DARE (2018) (33)	278	DCB vs. EES	12 in both groups	MLD: 1.71 ± 0.51 vs. 1.74 ± 0.61 (6)	18.1 vs. 20.9%	8.8 vs. 7.1% (12)	0 vs. 0 (12)
Blolux (2018) (34)	229	DCB vs. SES	Given as per local standard	LLL: 0.03 ± 0.40 mm vs. 0.20 ± 0.70 (6)	NA	13.5 vs. 11.6% (18)	1 vs. 2 (18)

DAPT, dual anti-platelet therapy; TLR, target lesion revascularization; ST, stent thrombosis including definite and possible; DCB, drug-coated balloon; POBA, plain old balloon angioplasty; LLL, late lumen loss; PES, paclitaxel-eluting stent; EES, everolimus-eluting stent; MLD, minimal lumen diameter; PCSB, paclitaxel-coated scoring balloon; USB, uncoated scoring balloon; DS, diameter restenosis; SB-DCB, scoring balloon before drug-coated balloon; SES, sirolimus-eluting stent.

**P < 0.01 vs. non-DCB group.*

***P < 0.05 vs. non-DCB group.*

one in the EES group) at 1 year and after that another two cases of stent thrombosis occurred in the DCB group at 3 years (36). However, during the actual follow-up for the trial, 84% of patients in the DCB group were still receiving DAPT at 9 months, and 64% were still receiving DAPT at 1 year, of which 52% suffered from unstable angina at the time of recruitment. For most trials, DAPT was administered for 6 months after DCB dilatation (27, 28, 31, 32). In these trials, DCB showed higher efficacy than POBA with DES-ISR treatment, which showed similar efficacy to DES. Two stent thrombosis cases were found in the DCB group during the follow-up, one in the PEPCAD-DES trial (37) and another in the ISAR-DESIRE trial (28). The PEPCAD China ISR trial also demonstrated that angioplasty with DCB was non-inferior to PES implantation when used to treat DES-ISR (29, 38). In this trial, all patients, irrespective of treatment allocation, were prescribed DAPT for 12 months. There was one late stent thrombosis occurred in the DCB group and two in the PES group at the 1-year follow-up, and another very late stent thrombosis occurred in the PES group at the 2-year follow-up (38).

Small Vessel *de novo* Coronary Artery Disease

It remains challenging to treat coronary small-vessel disease, which is usually defined as lesions in vessels <3.0 or ≤2.75 mm, because it is significantly and directly associated with an increased risk of clinical events (39). Though DES has been found to be equally effective in small and large vessels, the resulting LLL occupies a higher percentage of the respective vessel diameter, leading to a higher incidence of ISR and other clinical events (40).

TABLE 3 | Characteristics of randomized control trials of DCB for treatment of small vessel *de novo* coronary artery disease.

Trial (year)	Patients, *N*	Design	DAPT duration (months)	Primary endpoint (follow-up, months)	Binary restenosis rate, %	TLR, % (follow-up, months)	ST, N (follow-up, months)
PICCOLETO (2010) (42)	57	DCB vs. DES	1 in SAP and alone DCB use vs. 3 in DCB + stent implantation vs. 12 in UAP or DES	DS: 43.6 vs. 24.3%** (6)	32.1 vs. 10.3%**	32.1 vs. 10.3% (9)	0 vs. 0 (9)
Bello (2012) (43)	182	DCB vs. PES	1 in DCB only vs. 3 in DCB + BMS vs. 12 in PES	LLL: 0.08 ± 0.38 mm vs. 0.29 ± 0.44 mm* (6)	8.9 vs. 14.1%	4.4 vs. 7.6% (6) 6.7 vs. 13% (36)	0 vs. 0 (36)
Funatsu et al. (2017) (44)	135	DCB vs. POBA	3 in both groups	TVF: 3.4 vs. 10.3% (6)	13.3 vs. 42.5%*	2.3 vs. 10.3% (6)	0 vs. 0 (6)
BASKET-SMALL 2 (2018) (45)	758	DCB vs. nDES	1 in SAP and DCB only vs. 6 in SAP and DES vs. 12 in ACS vs. 3 in DCB + BMS vs. 6 in DCB + DES	MACE: 7.3 vs. 7.5% (12) MACE: 15 vs. 15% (36)	NA	3.4 vs. 4.5% (12) 9 vs. 9% (36)	2 vs. 4 (13) 2 vs. 6 (36)
Angiographic analysis from the BASKET-SMALL 2 (2020) (46)	111	ditto	ditto	DS: 35.8 vs. 29.0%** (median 5.7)	20.4 vs. 21.5%	NA	NA
Restore SVD China (2018) (47)	230	DCB vs. nDES	At least 6 in both groups	DS: 29.6 ± 2.0 vs. 24.1 ± 2.0% (9)	11.0 vs. 8.6%	4.4 vs. 2.6% (12) 5.2 vs. 2.8% (24)	0 vs. 0 (24)
PICCOLETO II (2020) (48)	232	DCB vs. EES	1 in SAP and DCB vs. 6 in EES vs. 12 in ACS	LLL: 0.04 ± 0.28 mm vs. 0.17 ± 0.39 mm** (6)	6.3 vs. 6.5%	5.6 vs. 5.6% (12)	0 vs. 2 (12)

DAPT, dual anti-platelet therapy; TLR, target lesion revascularization; ST, stent thrombosis including definite and possible; DCB, drug-coated balloon; DES, drug-eluting stent; SAP, stable angina pectoris; UAP, unstable angina pectoris; DS, diameter restenosis; PES, paclitaxel-eluting stent; BMS, bare-metal stent; POBA, plain old balloon angioplasty; TVF, target vessel failure; nDES, new-generation drug-eluting stent; ACS, acute coronary syndrome; MACE, major adverse cardiac events; EES, everolimus-eluting stent.

*$P < 0.01$ vs. non-DCB group.

**$P < 0.05$ vs. non-DCB group.

Drug-coated balloon angioplasty has the theoretical advantage of providing immediate and homogenous drug uptake, leaving no metal in the coronary artery and respecting the vessel anatomy, thus forming a "leave nothing behind" strategy in the treatment of *do novo* CAD (41). Many notable RCTs involving small vessel disease have used this strategy and all studies have shown the benefits of DCB except the PICCOLETO (42) (**Table 3**), which may be explained as the limitations of the first-generation Dior DCB (49). A recent meta-analysis showed that the use of DCB in the treatment of *do novo* CAD was associated with comparable clinical outcomes regardless of the indication or comparator device (50). However, there is still no clear conclusion regarding the duration of DAPT against small-vessel disease treated by DCB.

At present, the widely used postoperative DAPT strategy from clinical trials for the DCB treatment of small-vessel disease is the following: (1) DAPT duration in stable patients using DCB is 4 weeks; (2) DAPT duration in stable patients using DES is 6 months; (3) DAPT duration in patients with ACS is 12 months; and (4) DAPT duration in patients treated with a combination of DCB and BMS is 3 months, and in patients with DCB and DES is 6 months. Notable trials that used this strategy include PICCOLETO (42), BELLO (43), BASKET-SMALL 2 (45), and PICCOLETO II (48). Among these trials, the binary restenosis rates and TLR rates were comparable between the DCB and DES groups and were all low-probability events. It is important to acknowledge that patients treated with DCB and without stenting did not experience any thrombotic events in these trials, whereas only two stent thrombosis events were found in the BASKET-SMALL 2 trial during the 3-year follow-up (45). These results suggest that DCB may provide significant advantages over DES in treating small vessel disease, such as a lower risk of stent thrombosis, a shorter duration and less dependence on DAPT (43).

The RESTORE SVD China trial also demonstrated that the Restore DCB was non-inferior to the second-generation RESOLUTE Integrity DES (47, 51). However, DAPT was prescribed for at least 6 months after discharge from the hospital. During the 12-month follow-up, no significant difference was observed in the comparison of DAPT duration between the DCB and DES groups (91.4 vs. 94.7%), which was partly due to the high proportion of unstable angina in this study and the high incidence of MACE in small vessels.

Large Vessel *de novo* Coronary Artery Disease

Many interventional cardiologists had doubts about the safety of DCB alone for large vessel *de novo* CAD because large coronary

TABLE 4 | Characteristics of prospective trials of DCB for treatment of *de novo* coronary artery disease including large vessels.

Trial (year)	Patients, *N*	Design	DAPT duration (months)	RVD, mm	Primary endpoint (follow-up, months)	TLR, % (follow-up, months)	ST, N (follow-up, months)
Randomized control trial Nishiyama et al. (2016) (53)	60	DCB vs. EES	8 in both groups	2.88 ± 0.57 mm vs. 2.72 ± 0.64 mm	LLL: 0.25 ± 0.25 mm vs. 0.37 ± 0.40 mm (8)	0.0 vs. 6.1% (8)	NA
Gobić et al. (2017) (54)	75	DCB vs. SES	12 in both groups	2.61 ± 0.49 mm vs. 3.04 ± 0.46 mm	LLL: −0.09 ± 0.08 mm vs. 0.10 ± 0.19 mm** (6)	0.0 vs. 5.4% (6)	0 vs. 2 (6)
REVELATION (2019) (55)	120	DCB vs. DES	9 in both groups	3.28 ± 0.52 mm vs. 3.20 ± 0.48 mm	FFR: 0.92 ± 0.05 vs. 0.91 ± 0.06 (9)	3 vs. 2% (9)	1 vs. 0 (9)
DEBUT (2019) (9)	220	DCB vs. BMS	1 in both groups	NA	MACE: 1 vs. 14%* (9) MACE: 4 vs. 14%** (12)	0 vs. 6%* (9) 2 vs. 6% (12)	0 vs. 2 (12)
Prospective study Cortese et al. (2015) (56)	156	DCB	1 in DCB only vs. 6 in DCB and stent implantation	2.83 (2.12–3.01) mm	Complete vessel healing rate: 93.8% (6)	6.2% in dissection cohort vs. 5.3% in ALL DCB	NA
Shin et al. (2016) (57)	66	DCB vs. nDES	1.5 in DCB vs. 12 in DES vs. 6 in BMS	2.69 ± 0.45 mm vs. 2.92 ± 0.31 mm	LLL: 0.05 ± 0.27 mm vs. 0.40 ± 0.54 mm** (9)	0.0 vs. 4.5% (12)	0 vs. 0 (12)
Ann et al. (2016) (58)	27	DCB	1.5	2.58 ± 0.45 mm	LLL: 0.02 ± 0.27 mm (9)	0.0% (9)	NA
Lu et al. (2019) (59)	92	DCB	6	3.32 ± 0.46	LLL: −0.02 ± 0.49 mm (9)	4.3% (12)	NA
Rosenberg et al. (2019) (60)	686	DCB	1 in DCB vs. 6 in DCB + stent implantation	2.31 ± 0.26 mm in small vessels vs. 3.16 ± 0.26 mm in large vessels	TLR: 2.4% in small vessels vs. 1.8% in large vessels (9)	TLR: 2.4% in small vessels vs. 1.8% in large vessels (9)	1 in small vessels vs. 1 in large vessels (9)

DAPT, dual anti-platelet therapy; RVD, reference vessel diameter; TLR, target lesion revascularization; ST, stent thrombosis including definite and possible; DCB, drug-coated balloon; EES, everolimus-eluting stent; LLL, late lumen loss; DES, drug-eluting stent; FFR, fractional flow reserve; SES, sirolimus-eluting stent; BMS, bare-metal stent; MACE, major adverse cardiac events.

$P < 0.01$ vs. non-DCB group.

**$P < 0.05$ vs. non-DCB group.*

arteries have more smooth muscle fibers than small vessel arteries and are more prone to recoil and dissection, which may lead to acute occlusion or restenosis of blood vessels (52). Although randomized data for comparing DCB and DES in the treatment of large vessels are still lacking, there are variable proportions of large vessels that were treated using the DCB-only approach in studies, which creates growing evidence for the safety and efficacy of the DCB-only strategy for the treatment of large coronary arteries. The durations of DAPT in these trials ranged from 1 to 12 months (**Table 4**).

A recent prospective large-scale multicenter trial demonstrated that DCB as a stand-alone-therapy showed similar efficacy on large and small vessels (60, 61). In this trial, standard DAPT duration was recommended for 1 month in DCB-only treatment and a minimum of 6 months when additional stents were implanted. During the follow-up, in the large vessel group, the DAPT duration was 2.7 ± 1.6 months, whereas in the small vessel group, the DAPT duration was 2.8 ± 1.6 months ($p = 0.583$). Meanwhile, this trial observed that around half of each group had a recommendation for 4 weeks of DAPT (>2.75 mm: 53.3% vs. ≤2.75 mm: 48.1%, p = ns). Only one case of stent thrombosis occurred in each group. The DEBUT trial which showed DCB-only coronary intervention was superior to BMS in patients at bleeding risk, was also administered 1-month of DAPT for all patients (9). In patients assigned to DCB, 64% were treated with a DCB that was 3 mm or larger diameter, and stent thrombosis occurred in none of them. A short duration of DAPT after DCB angioplasty was recommended in the other three trials without any stent thrombosis found and low risk rates of clinical events (56–58). These results indicate that short-term DAPT may be feasible and safe. On the contrary, some trials recommended DAPT for 6 months or longer, and they also did not find stent thrombosis during follow-up (53–55). These trials chose a longer DAPT duration because most patients in these trials were admitted to the hospital for ACS.

Other Clinical Situations

Chronic Total Occlusions

Chronic Total Occlusions (CTOs) of the coronary arteries remain one of interventional cardiologists' biggest challenges and some scholars have also attempted to apply the DCB-only strategy to

CTO (62, 63). A prospective trial led by Köln et al. showed that the DCB-only strategy as a treatment option for CTO was feasible and well-tolerated (63). Most patients received DAPT for at least 4 weeks and 4 of 34 patients had contraindications for DAPT who received only lifelong aspirin in this trial. Restenosis occurred in 11.8% of all patients, re-occlusion in 5.9%, TLR in 17.6%, and no stent thrombosis was found.

High Bleeding Risk

An all-comers retrospective study that contained 52% high-bleeding-risk patients showed the safety and feasibility of short-term DAPT after DCB angioplasty for both stable CAD and ACS (64). The median and mean durations of DAPT were 1 and 2.8 months in the stable CAD population and 1 and 3.3 months in the ACS population. The MACE rate was 9.8 and 14.8% at 12 and 24 months with 2.1 and 3.1% TLR rates, respectively. Recently, the DEBUT trial demonstrated that DCB was superior to BMS for the treatment of *de novo* coronary artery lesions in patients with high bleeding risk (9). The duration of DAPT was 1 month in patients with stable CAD and ACS in both groups. For ACS patients receiving anticoagulation therapy, the duration of aspirin was 6 months. At 9 months, the MACE and TLR rates were 1 and 0% in the DCB group and 14 and 6% in the BMS group, respectively. One case of stent thrombosis occurred in each group.

Duration in ACS

Although receiving second-generation DES is the most common option for the treatment of patients with ACS and is generally considered the optimal strategy (65), some small sample size clinical trials have attempted to use the DCB-only strategy in primary percutaneous coronary intervention (PPCI) (54, 55, 66–68). Nicola et al. conducted the first study of a DCB-only strategy in the setting of PPCI, and DPAT was scheduled to be continued for 12 months (66). This study showed good 1-year clinical results with only five MACEs occurring, including three TLR and one acute stent thrombosis, but additional stenting was performed in half of the patients. Recently, the REVELATION study shown that DCB was non-inferior to the second-generation DES in the treatment of ST-segment elevated myocardial infarction patients (55). All patients were on DAPT and/or combined with oral anticoagulation for at least 1 year. Up to the 9-month follow-up, only three patients required TLR (one in the DES group and two in the DCB group) and only one thrombotic event was found in the DCB group. The 1-year duration of DAPT seemed to be a reasonable option based on the guideline recommendations and the results of existing clinical trials.

However, it remains a question whether DAPT duration for ACS patients is worth reducing or prolonging. A recent meta-analysis of the duration of DAPT after PCI with DES demonstrated that short-term DAPT presented similar efficacy and safety to standard-term DAPT for patients with ACS (69).

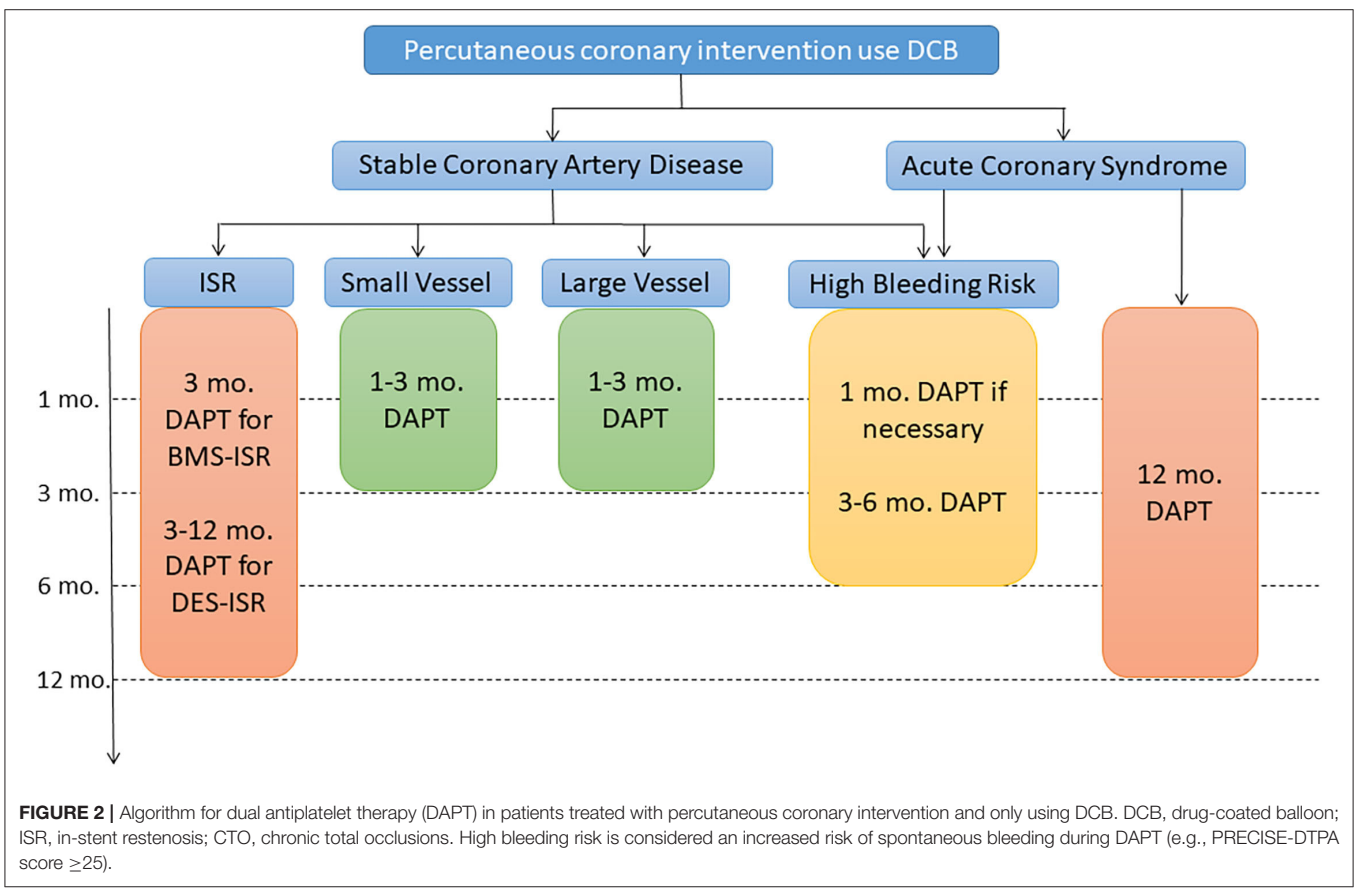

FIGURE 2 | Algorithm for dual antiplatelet therapy (DAPT) in patients treated with percutaneous coronary intervention and only using DCB. DCB, drug-coated balloon; ISR, in-stent restenosis; CTO, chronic total occlusions. High bleeding risk is considered an increased risk of spontaneous bleeding during DAPT (e.g., PRECISE-DTPA score ≥25).

In the DEBUT trial, 46% of patients treated with DCB only were diagnosed with ACS (9). All patients in this trial were recommended to undergo only a 1-month duration of DAPT, and the results showed low MACE rates with no TLR event at 9 months. Meanwhile, no stent thrombosis event occurred during the follow-up. In another retrospective study which contained 55% of ACS patients showed a 12% MACE rate and 2.8% TLR rate at 12 months (64). The median and mean durations of DAPT were 1 and 3.3 months in the ACS population. Of note, half of the patients had at least one risk factor for bleeding. Furthermore, about 4% of patients did not receive any ADP receptor blockers at all during or after PCI due to a contraindication for DAPT. Meanwhile, the European Society of Cardiology Guidelines also suggest that patients at high or moderate ischemic risk who have well-tolerated DAPT within the first year after myocardial infarction may benefit from more intense antithrombotic therapy beyond 12 months from the acute event (70). For this kind of patients (e.g., age ≥65 years and multivessel coronary disease), aspirin 75–100 mg with ticagrelor 60 mg twice daily or rivaroxaban 2.5 mg twice daily may be administered, which would reduce the ischemic risk with no major bleeding events and infrequent minor/minimal bleeding (71, 72). Whether prolonging or reducing the duration of DAPT, it is important to tailor the treatment to each patient to get the best benefits of DAPT.

Duration for New-Generation Sirolimus DCB

Thus far, paclitaxel, as a cytotoxic agent, is the preferred drug for balloon coating and has been widely cited in cardiovascular interventional therapies. With the growing clinical research evidence of sirolimus-coated balloon (SCB), their clinical feasibility and safety are being increasingly recognized. The SABRE trial showed excellent procedural success for the Virtue sirolimus-eluting angioplasty balloon in the treatment of ISR (73). In this trial, DAPT was continued for at least 3 months and the MACE rate was 14.3% at 12 months, with a 12.2% TLR rate. Soon after that, an RCT that compared a crystalline coating SCB with paclitaxel-coated balloon (PCB) demonstrated similar angiographic outcomes in the treatment of coronary DES-ISR (74). Interestingly, DAPT was recommended for 1 months in stable patients and 12 months in cases of ACS. The MACE and TLR rates were similar between the two groups, and only one stent thrombosis occurred in the PCB group. Two other large prospective trials that enrolled a real-world, all-comer patient population also showed the safety and efficacy of SCB, both in patients with ISR or *de novo* lesions (75, 76). The Nanolutè study evaluated the clinical performance of a novel SCB (Concept Medical Research Private Limited, India) for the treatment of ISR and *de novo* coronary lesions. Dual antiplatelet therapy was recommended for 3–12 months in this trial (75). The MACE rate was 4.2% with 3.2% TLR at 2 years. The EASTBOURNE registry also evaluated this kind of SCB and obtained similar results as the Nanolutè study (76). In this trial, DAPT duration was prescribed for a minimum of 1 and 6 months in the case of additional stent implantation. As for ACS patients, DAPT duration was prescribed according to the current guidelines.

CONCLUSIONS AND PERSPECTIVE

As DCB technology is playing an increasingly important role in PCI, standardizing postoperative drug treatment is essential. Defining the optimal duration of DAPT after DCB-only angioplasty remains an interesting question but the currently available evidence is limited. Here, we give a simple summary with suggestions for DAPT duration in the different clinical scenarios based on current evidence (**Figure 2**).

For a decade, we have been passionate about defining the optimal duration of DAPT after stenting and have conducted many RCTs. Now, it is time to focus on the optimal duration of DAPT after DCB-only angioplasty. Meanwhile, with the advancement of DCB technology and the discovery of potent antiplatelet drugs, the DAPT approach may shift to a new paradigm of single antiplatelet therapy. It is necessary to explore the feasibility of single antiplatelet therapy after DCB-only angioplasty.

AUTHOR CONTRIBUTIONS

All authors contributed to the manuscript production and in the final revision. YZ, QD, DC, and YX structured the manuscript giving contribute to table, figures, and text editing. JJ, XZ, and YZ revisited the article implementing the final manuscript form.

FUNDING

JJ was supported by grant from the National Natural Science Foundation of China (No. 82170332) and Key Research and Development Program of Zhejiang Province (No. 2020C03016). XZ was supported by grant from the National Natural Science Foundation for young scientists of China (No. 82100346).

REFERENCES

1. Scheller B, Speck U, Abramjuk C, Bernhardt U, Bohm M, Nickenig G. Paclitaxel balloon coating, a novel method for prevention and therapy of restenosis. *Circulation.* (2004) 110:810–4. doi: 10.1161/01.CIR.0000138929.71660.E0
2. Scheller B, Hehrlein C, Bocksch W, Rutsch W, Haghi D, Dietz U, et al. Treatment of coronary in-stent restenosis with a paclitaxel-coated balloon catheter. *N Engl J Med.* (2006) 355:2113–24. doi: 10.1056/NEJMoa061254
3. Tepe G, Zeller T, Albrecht T, Heller S, Schwarzwalder U, Beregi JP, et al. Local delivery of paclitaxel to inhibit restenosis during angioplasty of the leg. *N Engl J Med.* (2008) 358:689–99. doi: 10.1056/NEJMoa0706356
4. Nestelberger T, Kaiser C, Jeger R. Drug-coated balloons in cardiovascular disease: benefits, challenges, and clinical applications. *Expert Opin Drug Deliv.* (2020) 17:201–11. doi: 10.1080/17425247.2020.1714590
5. Neumann FJ, Sousa-Uva M, Ahlsson A, Alfonso F, Banning AP, Benedetto U, et al. 2018 ESC/EACTS Guidelines on myocardial revascularization. *Eur Heart J.* (2019) 40:87–165. doi: 10.1093/eurheartj/ehy855

6. Jeger RV, Eccleshall S, Wan Ahmad WA, Ge J, Poerner TC, Shin ES, et al. Drug-coated balloons for coronary artery disease: third report of the international DCB consensus group. *JACC Cardiovasc Interv.* (2020) 13:1391–402. doi: 10.1016/j.jcin.2020.02.043
7. Her AY, Shin ES, Bang LH, Nuruddin AA, Tang Q, Hsieh IC, et al. Drug-coated balloon treatment in coronary artery disease: recommendations from an asia-pacific consensus group. *Cardiol J.* (2021) 28:136–49. doi: 10.5603/CJ.a2019.0093
8. Levine GN, Bates ER, Bittl JA, Brindis RG, Fihn SD, Fleisher LA, et al. 2016 ACC/AHA Guideline Focused Update on Duration of Dual Antiplatelet Therapy in Patients With Coronary Artery Disease: A Report of the American College of Cardiology/American Heart Association Task Force on Clinical Practice Guidelines: An Update of the 2011 ACCF/AHA/SCAI Guideline for Percutaneous Coronary Intervention, 2011 ACCF/AHA Guideline for Coronary Artery Bypass Graft Surgery, 2012 ACC/AHA/ACP/AATS/PCNA/SCAI/STS Guideline for the Diagnosis and Management of Patients With Stable Ischemic Heart Disease, 2013 ACCF/AHA Guideline for the Management of ST-Elevation Myocardial Infarction, 2014 AHA/ACC Guideline for the Management of Patients With Non-ST-Elevation Acute Coronary Syndromes, and 2014 ACC/AHA Guideline on Perioperative Cardiovascular Evaluation and Management of Patients Undergoing Noncardiac Surgery. *Circulation.* (2016) 134:e123–55. doi: 10.1161/CIR.0000000000000404
9. Rissanen TT, Uskela S, Eränen J, Mäntylä, P, Olli A, Romppanen H, et al. Drug-coated balloon for treatment of de-novo coronary artery lesions in patients with high bleeding risk (DEBUT): a single-blind, randomised, non-inferiority trial. *Lancet.* (2019) 394:230–9. doi: 10.1016/S0140-6736(19)31126-2
10. Kleber F, Mathey D, Rittger H, Scheller B. How to use the drug-eluting balloon: recommendations by the German consensus group. *EuroIntervention.* (2011) 7:K125–8. doi: 10.4244/EIJV7SKA21
11. Kleber FX, Rittger H, Bonaventura K, Zeymer U, Wöhrle J, Jeger R, et al. Drug-coated balloons for treatment of coronary artery disease: updated recommendations from a consensus group. *Clin Res Cardiol.* (2013) 102:785–97. doi: 10.1007/s00392-013-0609-7
12. Cortese B, Berti S, Biondi-Zoccai G, Colombo A, Limbruno U, Bedogni F, et al. Drug-coated balloon treatment of coronary artery disease: a position paper of the Italian Society of Interventional Cardiology. *Catheter Cardiovasc Interv.* (2014) 83:427–35. doi: 10.1002/ccd.25149
13. Valgimigli M, Bueno H, Byrne RA, Collet JP, Costa F, Jeppsson A, et al. 2017 ESC focused update on dual antiplatelet therapy in coronary artery disease developed in collaboration with EACTS: the Task Force for dual antiplatelet therapy in coronary artery disease of the European Society of Cardiology (ESC) and of the European Association for Cardio-Thoracic Surgery (EACTS). *Eur Heart J.* (2018) 39:213–60. doi: 10.1093/eurheartj/ehx419
14. Varga-Szabo D, Pleines I, Nieswandt B. Cell adhesion mechanisms in platelets. *Arterioscler Thromb Vasc Biol.* (2008) 28:403–12. doi: 10.1161/ATVBAHA.107.150474
15. Angiolillo DJ, Ueno M, Goto S. Basic principles of platelet biology and clinical implications. *Circ J.* (2010) 74:597–607. doi: 10.1253/circj.CJ-09-0982
16. Angiolillo DJ, Capodanno D, Goto S. Platelet thrombin receptor antagonism and atherothrombosis. *Eur Heart J.* (2010) 31:17–28. doi: 10.1093/eurheartj/ehp504
17. Ueno M, Kodali M, Tello-Montoliu A, Angiolillo DJ. Role of platelets and antiplatelet therapy in cardiovascular disease. *J Atheroscler Thromb.* (2011) 18:431–42. doi: 10.5551/jat.7633
18. Byrne RA, Joner M, Kastrati A. Stent thrombosis and restenosis: what have we learned and where are we going? The Andreas Gruntzig lecture ESC 2014. *Eur Heart J.* (2015) 36:3320–31. doi: 10.1093/eurheartj/ehv511
19. Kufner S, Joner M, Thannheimer A, Hoppmann P, Ibrahim T, Mayer K, et al. Ten-year clinical outcomes from a trial of three limus-eluting stents with different polymer coatings in patients with coronary artery disease: results from the ISAR-TEST 4 randomized trial. *Circulation.* (2019) 139:325–33. doi: 10.1161/CIRCULATIONAHA.118.038065
20. Alfonso F, Byrne RA, Rivero F, Kastrati A. Current treatment of in-stent restenosis. *J Am Coll Cardiol.* (2014) 63:2659–73. doi: 10.1016/j.jacc.2014.02.545
21. Giacoppo D, Alfonso F, Xu B, Claessen B, Adriaenssens T, Jensen C, et al. Drug-coated balloon angioplasty versus drug-eluting stent implantation in patients with coronary stent restenosis. *J Am Coll Cardiol.* (2020) 75:2664–78. doi: 10.1016/j.jacc.2020.04.006
22. Scheller B, Clever YP, Kelsch B, Hehrlein C, Bocksch W, Rutsch W, et al. Long-term follow-up after treatment of coronary in-stent restenosis with a paclitaxel-coated balloon catheter. *JACC Cardiovasc Interv.* (2012) 5:323–30. doi: 10.1016/j.jcin.2012.01.008
23. Unverdorben M, Vallbracht C, Cremers B, Heuer H, Hengstenberg C, Maikowski C, et al. Paclitaxel-coated balloon catheter versus paclitaxel-coated stent for the treatment of coronary in-stent restenosis. *Circulation.* (2009) 119:2986–94. doi: 10.1161/CIRCULATIONAHA.108.839282
24. Alfonso F, Perez-Vizcayno MJ, Cardenas AB, Garcia Del Blanco, Seidelberger B, Iniguez A, et al. A randomized comparison of drug-eluting balloon versus everolimus-eluting stent in patients with bare-metal stent-in-stent restenosis: the RIBS V clinical trial (restenosis intra-stent of bare metal stents: paclitaxel-eluting balloon vs everolimus-eluting stent). *J Am Coll Cardiol.* (2014) 63:1378–86. doi: 10.1016/j.jacc.2013.12.006
25. Scheller B, Fontaine T, Mangner N, Hoffmann S, Bonaventura K, Clever YP, et al. A novel drug-coated scoring balloon for the treatment of coronary in-stent restenosis: results from the multi-center randomized controlled PATENT-C first in human trial. *Catheter Cardiovasc Interv.* (2016) 88:51–9. doi: 10.1002/ccd.26216
26. Pleva L, Kukla P, Kusnierova P, Zapletalova J, Hlinomaz O. Comparison of the efficacy of paclitaxel-eluting balloon catheters and everolimus-eluting stents in the treatment of coronary in-stent restenosis: the treatment of in-stent restenosis study. *Circ Cardiovasc Interv.* (2016) 9:e003316. doi: 10.1161/CIRCINTERVENTIONS.115.003316
27. Rittger H, Brachmann J, Sinha AM, Waliszewski M, Ohlow M, Brugger A, et al. A randomized, multicenter, single-blinded trial comparing paclitaxel-coated balloon angioplasty with plain balloon angioplasty in drug-eluting stent restenosis: the PEPCAD-DES study. *J Am Coll Cardiol.* (2012) 59:1377–82. doi: 10.1016/j.jacc.2012.01.015
28. Byrne RA, Neumann F-J, Mehilli J, Pinieck S, Wolff B, Tiroch K, et al. Paclitaxel-eluting balloons, paclitaxel-eluting stents, and balloon angioplasty in patients with restenosis after implantation of a drug-eluting stent (ISAR-DESIRE 3): a randomised, open-label trial. *Lancet.* (2013) 381:461–7. doi: 10.1016/S0140-6736(12)61964-3
29. Xu B, Gao R, Wang J, Yang Y, Chen S, Liu B, et al. A prospective, multicenter, randomized trial of paclitaxel-coated balloon versus paclitaxel-eluting stent for the treatment of drug-eluting stent in-stent restenosis: results from the PEPCAD China ISR trial. *JACC Cardiovasc Interv.* (2014) 7:204–11. doi: 10.1016/j.jcin.2013.08.011
30. Alfonso F, Perez-Vizcayno MJ, Cardenas A, Garcia del Blanco B, Garcia-Touchard A, Lopez-Minguez JR, et al. A prospective randomized trial of drug-eluting balloons versus everolimus-eluting stents in patients with in-stent restenosis of drug-eluting stents: the RIBS IV randomized clinical trial. *J Am Coll Cardiol.* (2015) 66:23–33. doi: 10.1016/j.jacc.2015.04.063
31. Kufner S, Joner M, Schneider S, Tolg R, Zrenner B, Repp J, et al. Neointimal modification with scoring balloon and efficacy of drug-coated balloon therapy in patients with restenosis in drug-eluting coronary stents: a randomized controlled trial. *JACC Cardiovasc Interv.* (2017) 10:1332–40. doi: 10.1016/j.jcin,0.2017.04.024
32. Wong YTA, Kang D-Y, Lee JB, Rha S-W, Hong YJ, Shin E-S, et al. Comparison of drug-eluting stents and drug-coated balloon for the treatment of drug-eluting coronary stent restenosis: a randomized RESTORE trial. *Am Heart J.* (2018) 197:35–42. doi: 10.1016/j.ahj.2017.11.008
33. Baan J Jr, Claessen BE, Dijk KB, Vendrik J, van der Schaaf RJ, Meuwissen M, et al. A randomized comparison of paclitaxel-eluting balloon versus everolimus-eluting stent for the treatment of any in-stent restenosis: the DARE trial. *JACC Cardiovasc Interv.* (2018) 11:275–83. doi: 10.1016/j.jcin.2017.10.024
34. Jensen CJ, Richardt G, Tolg R, Erglis A, Skurk C, Jung W, et al. Angiographic and clinical performance of a paclitaxel-coated balloon compared to a second-generation sirolimus-eluting stent in patients with in-stent restenosis: the BIOLUX randomised controlled trial. *EuroIntervention.* (2018) 14:1096–103. doi: 10.4244/EIJ-D-17-01079

35. Unverdorben M, Vallbracht C, Cremers B, Heuer H, Hengstenberg C, Maikowski C, et al. Paclitaxel-coated balloon catheter versus paclitaxel-coated stent for the treatment of coronary in-stent restenosis: the three-year results of the PEPCAD II ISR study. *EuroIntervention.* (2015) 11:926–34. doi: 10.4244/EIJY14M08_12
36. Alfonso F, Perez-Vizcayno MJ, Cuesta J, Garcia Del Blanco B, Garcia-Touchard A, Lopez-Minguez JR, et al. 3-year clinical follow-up of the ribs IV clinical trial: a prospective randomized study of drug-eluting balloons versus everolimus-eluting stents in patients with in-stent restenosis in coronary arteries previously treated with drug-eluting stents. *JACC Cardiovasc Interv.* (2018) 11:981–91. doi: 10.1016/j.jcin.2018.02.037
37. Rittger H, Waliszewski M, Brachmann J, Hohenforst-Schmidt W, Ohlow M, Brugger A, et al. Long-term outcomes after treatment with a paclitaxel-coated balloon versus balloon angioplasty: insights from the pepcad-des study (treatment of drug-eluting stent [DES] in-stent restenosis with sequent please paclitaxel-coated percutaneous transluminal coronary angioplasty [PTCA] catheter). *JACC Cardiovasc Interv.* (2015) 8:1695–700. doi: 10.1016/j.jcin.2015.07.023
38. Xu B, Qian J, Ge J, Wang J, Chen F, Chen J, et al. Two-year results and subgroup analyses of the PEPCAD China in-stent restenosis trial: a prospective, multicenter, randomized trial for the treatment of drug-eluting stent in-stent restenosis. *Catheter Cardiovasc Interv.* (2016) 87(Suppl 1):624–9. doi: 10.1002/ccd.26401
39. Akiyama T, Moussa I, Reimers B, Ferraro M, Kobayashi Y, Blengino S, et al. Angiographic and clinical outcome following coronary stenting of small vessels: a comparison with coronary stenting of large vessels. *J Am Coll Cardiol.* (1998) 32:1610–8. doi: 10.1016/S0735-1097(98)00444-6
40. Biondi-Zoccai G, Moretti C, Abbate A, Sheiban I. Percutaneous coronary intervention for small vessel coronary artery disease. *Cardiovasc Revasc Med.* (2010) 11:189–98. doi: 10.1016/j.carrev.2009.04.007
41. Yerasi C, Case BC, Forrestal BJ, Torguson R, Weintraub WS, Garcia-Garcia HM, et al. Drug-coated balloon for *de novo* coronary artery disease: JACC state-of-the-art review. *J Am Coll Cardiol.* (2020) 75:1061–73. doi: 10.1016/j.jacc.2019.12.046
42. Cortese B, Micheli A, Picchi A, Coppolaro A, Bandinelli L, Severi S, et al. Paclitaxel-coated balloon versus drug-eluting stent during PCI of small coronary vessels, a prospective randomised clinical trial. The PICCOLETO study. Heart. (2010) 96:1291–6. doi: 10.1136/hrt.2010.195057
43. Latib A, Colombo A, Castriota F, Micari A, Cremonesi A, De Felice F, et al. A randomized multicenter study comparing a paclitaxel drug-eluting balloon with a paclitaxel-eluting stent in small coronary vessels: the BELLO (balloon elution and late loss optimization) study. *J Am Coll Cardiol.* (2012) 60:2473–80. doi: 10.1016/j.jacc.2012.09.020
44. Funatsu A, Nakamura S, Inoue N, Nanto S, Nakamura M, Iwabuchi M, et al. A multicenter randomized comparison of paclitaxel-coated balloon with plain balloon angioplasty in patients with small vessel disease. *Clin Res Cardiol.* (2017) 106:824–32. doi: 10.1007/s00392-017-1126-x
45. Jeger RV, Farah A, Ohlow MA, Mangner N, Möbius-Winkler S, Leibundgut G, et al. (2018). Drug-coated balloons for small coronary artery disease (BASKET-SMALL 2): an open-label randomised non-inferiority trial. *Lancet* 392:849–56. doi: 10.1016/S0140-6736(18)31719-7
46. Fahrni G, Scheller B, Coslovsky M, Gilgen N, Farah A, Ohlow MA, et al. Drug-coated balloon versus drug-eluting stent in small coronary artery lesions: angiographic analysis from the BASKET-SMALL 2 trial. *Clin Res Cardiol.* (2020) 109:1114–24. doi: 10.1007/s00392-020-01603-2
47. Tang Y, Qiao S, Su X, Chen Y, Jin Z, Chen H, et al. Drug-coated balloon versus drug-eluting stent for small-vessel disease: the RESTORE SVD China randomized trial. *JACC Cardiovasc Interv.* (2018) 11:2381–92. doi: 10.1016/j.jcin.2018.09.009
48. Cortese B, Di Palma G, Guimaraes MG, Piraino D, Orrego PS, Buccheri D, et al. Drug-coated balloon versus drug-eluting stent for small coronary vessel disease: PICCOLETO II randomized clinical trial. *JACC Cardiovasc Interv.* (2020) 13:2840–9. doi: 10.1016/j.jcin.2020.08.035
49. Cortese, B. The PICCOLETO study and beyond. *EuroIntervention.* (2011) 7(Suppl K):K53–6. doi: 10.4244/EIJV7SKA9
50. Elgendy IY, Gad MM, Elgendy AY, Mahmoud A, Mahmoud AN, Cuesta J, et al. Clinical and angiographic outcomes with drug-coated balloons for *de novo* coronary lesions: a meta-analysis of randomized clinical trials. *J Am Heart Assoc.* (2020) 9:e016224. doi: 10.1161/JAHA.120.016224
51. Tian J, Tang YD, Qiao S, Su X, Chen Y, Jin Z, et al. Two-year follow-up of a randomized multicenter study comparing a drug-coated balloon with a drug-eluting stent in native small coronary vessels: the RESTORE small vessel disease China trial. *Catheter Cardiovasc Interv.* (2020) 95(Suppl 1):587–97. doi: 10.1002/ccd.28705
52. Yu X, Ji F, Xu F, Zhang W, Wang X, Lu D, et al. Treatment of large *de novo* coronary lesions with paclitaxel-coated balloon only: results from a Chinese Institute. *Clin Res Cardiol.* (2019) 108:234–43. doi: 10.1007/s00392-018-1346-8
53. Nishiyama N, Komatsu T, Kuroyanagi T, Fujikake A, Komatsu S, Nakamura H, et al. Clinical value of drug-coated balloon angioplasty for *de novo* lesions in patients with coronary artery disease. *Int J Cardiol.* (2016) 222:113–8. doi: 10.1016/j.ijcard.2016.07.156
54. Gobic D, Tomulic V, Lulic D, Zidan D, Brusich S, Jakljevic T, et al. Drug-coated balloon versus drug-eluting stent in primary percutaneous coronary intervention: a feasibility study. *Am J Med Sci.* (2017) 354:553–60. doi: 10.1016/j.amjms.2017.07.005
55. Vos NS, Fagel ND, Amoroso G, Herrman JR, Patterson MS, Piers LH, et al. Paclitaxel-coated balloon angioplasty versus drug-eluting stent in acute myocardial infarction: the REVELATION randomized trial. *JACC Cardiovasc Interv.* (2019) 12:1691–9. doi: 10.1016/j.jcin.2019.04.016
56. Cortese B, Silva Orrego P, Agostoni P, Buccheri D, Piraino D, Andolina G, et al. Effect of drug-coated balloons in native coronary artery disease left with a dissection. *JACC Cardiovasc Interv.* (2015) 8:2003–9. doi: 10.1016/j.jcin.2015.08.029
57. Shin ES, Ann SH, Balbir Singh G, Lim KH, Kleber FX, Koo BK. Fractional flow reserve-guided paclitaxel-coated balloon treatment for *de novo* coronary lesions. *Catheter Cardiovasc Interv.* (2016) 88:193–200. doi: 10.1002/ccd.26257
58. Ann SH, Balbir Singh G, Lim KH, Koo BK, Shin ES. Anatomical and physiological changes after paclitaxel-coated balloon for atherosclerotic *de novo* coronary lesions: serial IVUS-VH and FFR study. *PLoS ONE.* (2016) 11:e0147057. doi: 10.1371/journal.pone.0147057
59. Lu W, Zhu Y, Han Z, Sun G, Qin X, Wang Z, et al. Short-term outcomes from drug-coated balloon for coronary *de novo* lesions in large vessels. *J Cardiol.* (2019) 73:151–5. doi: 10.1016/j.jjcc.2018.07.008
60. Rosenberg M, Waliszewski M, Krackhardt F, Chin K, Wan Ahmad WA, Caramanno G, et al. Drug coated balloon-only strategy in *de novo* lesions of large coronary vessels. *J Interv Cardiol.* (2019) 2019:6548696. doi: 10.1155/2019/6548696
61. Rosenberg M, Waliszewski M, Chin KW, Ahmad AW, Caramanno G, Milazzo D, et al. Prospective, large-scale multicenter trial for the use of drug-coated balloons in coronary lesions: the DCB-only all-comers registry. *Catheter Cardiovasc Interv.* (2019) 93:181–8. doi: 10.1002/ccd.27724
62. Cortese B, Buccheri D, Piraino D, Silva-Orrego P. Drug-coated balloon without stent implantation for chronic total occlusion of coronary arteries: description of a new strategy with an optical coherence tomography assistance. *Int J Cardiol.* (2015) 191:75–6. doi: 10.1016/j.ijcard.2015.04.278
63. Koln PJ, Scheller B, Liew HB, Rissanen TT, Ahmad WA, Weser R, et al. Treatment of chronic total occlusions in native coronary arteries by drug-coated balloons without stenting - a feasibility and safety study. *Int J Cardiol.* (2016) 225:262–7. doi: 10.1016/j.ijcard.2016.09.105
64. Uskela S, Karkkainen JM, Eranen J, Siljander A, Mantyla P, Mustonen J, et al. Percutaneous coronary intervention with drug-coated balloon-only strategy in stable coronary artery disease and in acute coronary syndromes: an all-comers registry study. *Catheter Cardiovasc Interv.* (2019) 93:893–900. doi: 10.1002/ccd.27950
65. Boersma EG. Primary coronary angioplasty vs. thrombolysis, does time matter? A pooled analysis of randomized clinical trials comparing primary percutaneous coronary intervention and in-hospital fibrinolysis in acute myocardial infarction patients. *Eur Heart J.* (2006) 27:779–88. doi: 10.1093/eurheartj/ehi810
66. Vos NS, Dirksen MT, Vink MA, van Nooijen FC, Amoroso G, Herrman JP, et al. Safety and feasibility of a PAclitaxel-eluting balloon angioplasty in

primary percutaneous coronary intervention in Amsterdam (PAPPA): one-year clinical outcome of a pilot study. *EuroIntervention.* (2014) 10:584–90. doi: 10.4244/EIJV10I5A101

67. Scheller B, Ohlow MA, Ewen S, Kische S, Rudolph TK, Clever YP, et al. Bare metal or drug-eluting stent versus drug-coated balloon in non-ST-elevation myocardial infarction: the randomised PEPCAD NSTEMI trial. *EuroIntervention.* (2020) 15:1527–33. doi: 10.4244/EIJ-D-19-00723
68. Harima A, Sairaku A, Inoue I, Nishioka K, Oka T, Nakama Y, et al. Real-life experience of a stent-less revascularization strategy using a combination of excimer laser and drug-coated balloon for patients with acute coronary syndrome. *J Interv Cardiol.* (2018) 31:284–92. doi: 10.1111/joic.12495
69. Yin SH, Xu P, Wang B, Lu Y, Wu QY, Zhou ML, et al. Duration of dual antiplatelet therapy after percutaneous coronary intervention with drug-eluting stent: systematic review and network meta-analysis. *BMJ.* (2019) 365:l2222. doi: 10.1136/bmj.l2222
70. Knuuti J, Wijns W, Saraste A, Capodanno D, Barbato E, Funck-Brentano C, et al. 2019 ESC guidelines for the diagnosis and management of chronic coronary syndromes. *Eur Heart J.* (2020) 41:407–77. doi: 10.1093/eurheartj/ehz425
71. Cesaro A, Taglialatela V, Gragnano F, Moscarella E, Fimiani F, Conte M, et al. Low-dose ticagrelor in patients with high ischemic risk and previous myocardial infarction: a multicenter prospective real-world observational study. *J Cardiovasc Pharmacol.* (2020) 76:173–80. doi: 10.1097/FJC.0000000000000856
72. Cesaro A, Gragnano F, Calabro P, Moscarella E, Santelli F, Fimiani F, et al. Prevalence and clinical implications of eligibility criteria for prolonged dual antithrombotic therapy in patients with PEGASUS and COMPASS phenotypes: insights from the START-ANTIPLATELET registry. *Int J Cardiol.* (2021) 345:7–13. doi: 10.1016/j.ijcard.2021.10.138
73. Verheye S, Vrolix M, Kumsars I, Erglis A, Sondore D, Agostoni P, et al. The SABRE trial (sirolimus angioplasty balloon for coronary in-stent restenosis): angiographic results and 1-year clinical outcomes. *JACC Cardiovasc Interv.* (2017) 10:2029–37. doi: 10.1016/j.jcin.2017.06.021
74. Ali RM, Abdul Kader M, Wan Ahmad WA, Ong TK, Liew HB, Omar AF, et al. Treatment of coronary drug-eluting stent restenosis by a sirolimus- or paclitaxel-coated balloon. *JACC Cardiovasc Interv.* (2019) 12:558–66. doi: 10.1016/j.jcin.2018.11.040
75. El-Mokdad R, di Palma G, Cortese B. Long-term follow-up after sirolimus-coated balloon use for coronary artery disease. Final results of the Nanolute study. *Catheter Cardiovasc Interv.* (2020) 96:E496–500. doi: 10.1002/ccd.28863
76. Cortese B, Testa L, Di Palma G, Heang TM, Bossi I, Nuruddin AA, et al. Clinical performance of a novel sirolimus-coated balloon in coronary artery disease: EASTBOURNE registry. *J Cardiovasc Med (Hagerstown).* (2021) 22:94–100. doi: 10.2459/JCM.0000000000001070

Conflict of Interest: The authors declare that the research was conducted in the absence of any commercial or financial relationships that could be construed as a potential conflict of interest.

Publisher's Note: All claims expressed in this article are solely those of the authors and do not necessarily represent those of their affiliated organizations, or those of the publisher, the editors and the reviewers. Any product that may be evaluated in this article, or claim that may be made by its manufacturer, is not guaranteed or endorsed by the publisher.

frontiers in Cardiovascular Medicine

ORIGINAL RESEARCH
published: 09 December 2021
doi: 10.3389/fcvm.2021.751525

Single-Cell RNA Sequencing of the Rat Carotid Arteries Uncovers Potential Cellular Targets of Neointimal Hyperplasia

Xiao-Fei Gao[1,2†], Ai-Qun Chen[1†], Zhi-Mei Wang[1†], Feng Wang[1], Shuai Luo[1], Si-Yu Chen[1], Yue Gu[1], Xiang-Quan Kong[1], Guang-Feng Zuo[1], Yan Chen[3], Zhen Ge[1], Jun-Jie Zhang[1,2] and Shao-Liang Chen[1,2]*

[1] Department of Cardiology, Nanjing First Hospital, Nanjing Medical University, Nanjing, China, [2] Department of Cardiology, Nanjing Heart Centre, Nanjing, China, [3] Department of Neurology, Medical School, Affiliated Drum Tower Hospital of Nanjing University, Nanjing, China

OPEN ACCESS

Edited by:
Jian Yang,
The First People's Hospital of Yichang, China

Reviewed by:
Jing Chen,
Renmin Hospital of Wuhan University, China
Chengzhi Lu,
Tianjin First Central Hospital, China

***Correspondence:**
Jun-Jie Zhang
jameszll@163.com

[†] These authors have contributed equally to this work

Specialty section:
This article was submitted to Coronary Artery Disease, a section of the journal Frontiers in Cardiovascular Medicine

Received: 01 August 2021
Accepted: 18 November 2021
Published: 09 December 2021

Citation:
Gao X-F, Chen A-Q, Wang Z-M, Wang F, Luo S, Chen S-Y, Gu Y, Kong X-Q, Zuo G-F, Chen Y, Ge Z, Zhang J-J and Chen S-L (2021) Single-Cell RNA Sequencing of the Rat Carotid Arteries Uncovers Potential Cellular Targets of Neointimal Hyperplasia. Front. Cardiovasc. Med. 8:751525. doi: 10.3389/fcvm.2021.751525

Aims: In-stent restenosis (ISR) remains an Achilles heel of drug-eluting stents despite technical advances in devices and procedural techniques. Neointimal hyperplasia (NIH) is the most important pathophysiological process of ISR. The present study mapped normal arteries and stenotic arteries to uncover potential cellular targets of neointimal hyperplasia.

Methods and Results: By comparing the left (control) and right (balloon injury) carotid arteries of rats, we mapped 11 clusters in normal arteries and 11 mutual clusters in both the control and experimental groups. Different clusters were categorized into 6 cell types, including vascular smooth muscle cells (VSMCs), fibroblasts, endothelial cells (ECs), macrophages, unknown cells and others. An abnormal cell type expressing both VSMC and fibroblast markers at the same time was termed a transitional cell *via* pseudotime analysis. Due to the high proportion of VSMCs, we divided them into 6 clusters and analyzed their relationship with VSMC phenotype switching. Moreover, N-myristoyltransferase 1 (NMT1) was verified as a credible VSMC synthetic phenotype marker. Finally, we proposed several novel target genes by disease susceptibility gene analysis, such as Cyp7a1 and Cdk4, which should be validated in future studies.

Conclusion: Maps of the heterogeneous cellular landscape in the carotid artery were defined by single-cell RNA sequencing and revealed several cell types with their internal relations in the ISR model. This study highlights the crucial role of VSMC phenotype switching in the progression of neointimal hyperplasia and provides clues regarding the underlying mechanism of NIH.

Keywords: in-stent restenosis, single-cell sequencing, vascular smooth muscle cell, transitional-cell, neointimal hyperplasia

INTRODUCTION

It has been more than 30 years since the first stent implantation, and currently, percutaneous coronary intervention (PCI) has been widely adopted for most ischemic heart diseases. Despite technical advances in devices and procedural techniques, along with more intensive drug treatment, in-stent restenosis (ISR) following repeat coronary revascularization remains an Achilles heel

of drug-eluting stents (DESs) (1–3). ISR is classically defined as luminal stenosis with more than 50% diameter narrowing of a stented coronary segment or within 5 mm of a stent edge. Traditionally, several biological factors, such as local inflammation, vascular smooth muscle cell (VSMC) phenotype switching, and delayed healing, are considered the main causes of ISR (4). The general view is that a normal artery consists of endothelial cells (ECs), VSMCs, fibroblasts, immune cells, and neurocytes (5, 6). The proportion of cell types inside the coronary artery changes after the development of atherosclerotic plaque and stent implantation due to the adaptive defense of blood vessels in response to internal and external stimuli. It is important to determine the changes in the proportion and status of these cells in the coronary artery after ISR, which could help us understand the underlying mechanisms of ISR. According to previous studies, neointimal hyperplasia (NIH) with VSMC migration and proliferation remains the most essential pathophysiological mechanism of ISR (7–9). However, there is no optimal method for in-depth analysis of cell types, composition, and properties in restenotic tissues. Thus, use of a novel methodology to investigate the mechanism of NIH is warranted. Therefore, the present study was designed to map the full view of normal arteries and stenotic arteries with an established rat carotid artery balloon injury model to further explore the underlying mechanism of NIH by using advanced single-cell technologies.

METHODS

Expanded methods are provided in the **Supplementary Materials** online.

Animal

Eight-week-old mature male Sprague-Dawley (SD, Hsd, Harlan) rats from the Animal Core Facility of Nanjing Medical University (Nanjing, China) were used in our experiment. Rats were housed in a temperature-controlled room with a 12 h light/dark cycle and free access to fresh water and food. All animal procedures were approved by the Experimental Animal Care and Use Committee of Nanjing Medical University.

Rat Carotid Artery Balloon Injury Model

The rat carotid artery balloon injury model is the most common *in vivo* model widely used to study ISR. This approach consists of isolating a segment from the right common carotid artery in SD rats under general anesthesia (pentobarbital sodium, 60 mg/kg, i.p.), creating an arteriotomy incision in the external carotid branch followed by inserting a balloon catheter (Fogarty, 12A0602F, 0.67 mm, Edwards Lifesciences) into the common carotid artery, repeated balloon inflation and pulling back five times to imitate percutaneous transluminal coronary angioplasty (PTCA), and finally removal of the catheter with external carotid ligation (10). The rats were sacrificed with an overdose of pentobarbital sodium (200 mg/kg, iv) at 28 days after the procedure, and their left (control group) and right (case group) carotid arteries (**Supplementary Figure 1A**) were subsequently collected for further study. We used HE staining to identify the success of the model (**Supplementary Figure 1B**).

Collecting Cells and Single-Cell RNA Sequencing

To avoid data variation incurred by sex differences, only two male SD rats were selected for the study. To capture single cells, the common carotid arteries were washed with PBS twice and stored in MACS tissue storage solution (Cat#: 130-100-008). Tissues were digested by 0.25% Trypsin-EDTA (1*, Gibco) and 0.1% collagenase (1*, Gibco). Single-cell RNA sequencing with the 10x Genomics platform was performed by a commercial service (Shanghai OE Biotech Co., Ltd., China; **Figure 1A**). Briefly, it uses microfluidic technology to wrap the beads and single cells with Cell Barcodes in droplets, lyses the cells in the droplets to connect the mRNA in the cells to the Cell Barcodes on beads, and finally forms single-cell GEMs. Reverse transcription was performed with the droplets to construct a cDNA library. The sample source of the target sequence is distinguished by the sample index on the library sequence.

RESULTS

Single-Cell RNA-Seq of Normal Rat Carotid Artery Cells

We first concentrated the normal carotid artery (control group), which has never been mapped previously. The two whole left carotid arteries were enzymatically digested, and then scRNA-seq libraries were built with the 10x Genomics platform.

A total of 2,445 cells were captured by quality control and visualized in t-SNE dimensionality reduction plots within 11 clusters (**Supplementary Table 1**, **Supplementary Figure 2**, **Figure 1B**). To classify these 11 clusters into known cell types, we filtered out their highly expressed genes and labeled them based on known marker genes (**Figure 1C**). We also examined recognized cell-type markers, such as VSMCs (Acta2, Tagln, Cald1, Myl9), fibroblasts (Col1a1, Col3a1, Dcn, Pdfra), ECs (Cdh5, Cldn5, Sox17), and macrophages (Cd68, Ncf4) (**Figure 1D**). The differentially expressed genes of cluster 11 (only 19 cells) were not specific and could not match the existing recognized cell types; thus, we performed our analysis after excluding cluster 11. A new t-SNE dimension reduction plot of 5 cell types showed the different proportions of cell types, including ECs, VSMCs, fibroblasts, macrophages and unknown cells (**Figure 1E**). Notably, VSMCs and fibroblasts were the major cell types in the normal carotid artery (**Figure 1F**).

Transitional Cells Between VSMCs and Fibroblasts

We found that cells in cluster 7 highly expressed marker genes from both VSMCs and fibroblasts at the same time (**Figure 1D**), but these cells in cluster 7 also had their own specific markers (Adm, Olr1, Thbd, Gfp2, **Figures 2A,B**). Previous studies have reported that the VSMC phenotype might switch to a fibroblast phenotype in some situations (11, 12). Therefore, we tried to

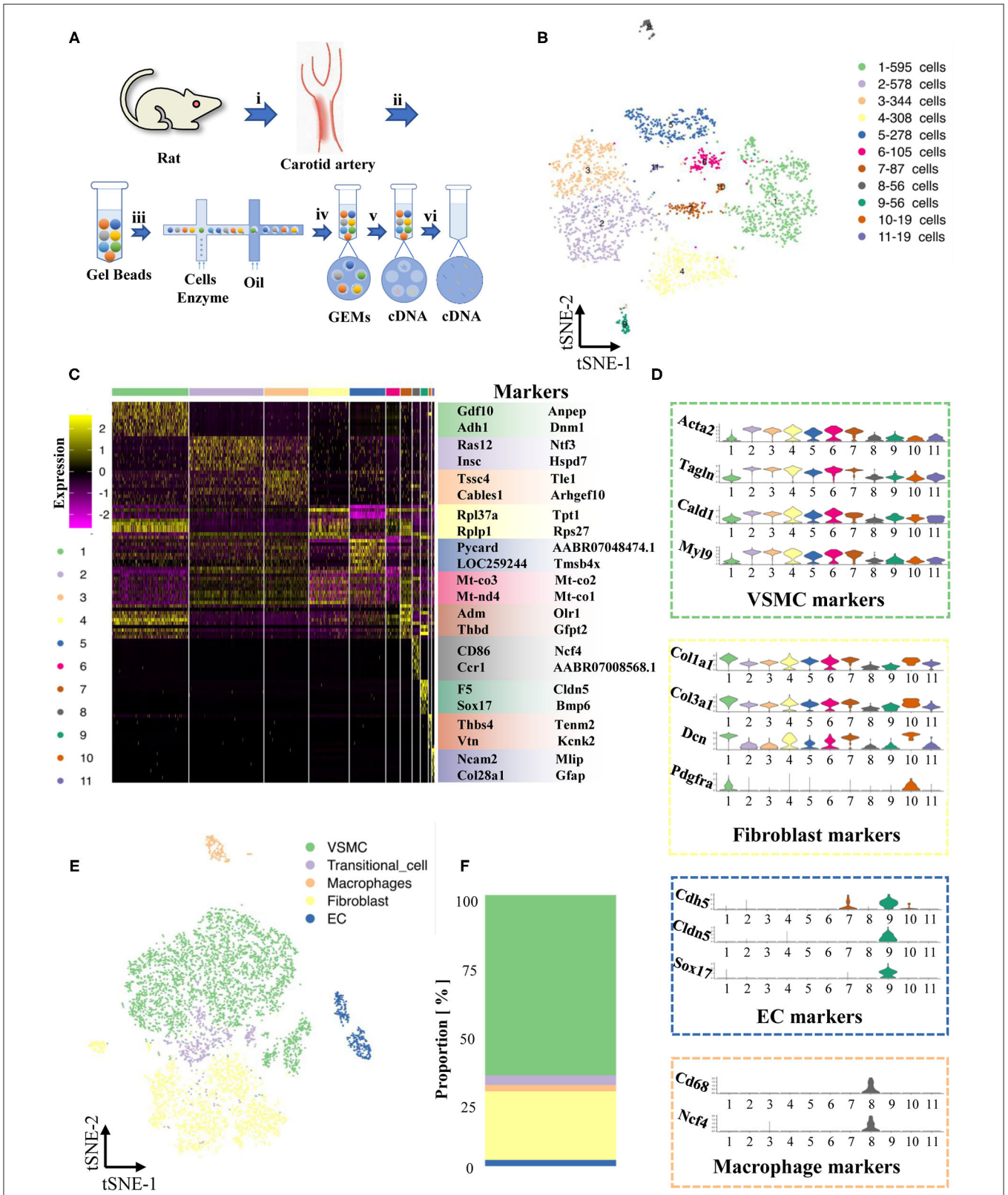

FIGURE 1 | Maps of single-cells in normal cartoid arteries. **(A)** (i). A surgery performed on rats and separated cartoid arteries. (ii). Prepared 10x barcoded gel beads. (iii). Wrapped the beads and cells with cell barcode in droplets, collected the droplets with cells, and then lysed the cells in the droplets.

(Continued)

FIGURE 1 | (iv). Collected single cell GEMs. (v). RT-PCR. (vi). Pool removed oil. **(B)** TSNE of single cells in normal cartoid arteries. **(C)** Differentially expressed genes (Top 10) of 11 clusters. **(D)** Expression of classical markers (VSMC, fibroblast, EC and macrophage) in 11 clusters. **(E)** Classification of 11 clusters into 5 cell types (VSMC, fibroblast, EC, transitional-cell, macrophage). **(F)** Proportion of each cell type in tSNE.

investigate the roles of cluster 7 during the process of VSMC phenotype switching *via* the current model.

We performed pseudotime analysis on VSMCs, fibroblasts, and unknown cells consisting of clusters 1-7 and 10. According to the degree of differentiation, cells were classified into three trajectories (states 1, 2, and 3) in pseudotime analysis (**Figures 2C–F**). Obviously, VSMCs were mainly distributed in state 1 and state 2, while fibroblasts were distributed in state 2. Previous evidence demonstrated that VSMCs had two important phenotypes in the vessel wall, including a contractile phenotype and a synthetic phenotype (13, 14). Fully differentiated/contractile VSMCs, responsible for vascular tone regulation, could be transformed into dedifferentiated/synthetic VSMCs to acquire proliferation, migration and synthesis abilities after vascular injury (13). According to the marker gene analysis, VSMCs in state 2 were considered contractile VSMCs, and VSMCs in state 1 could be regarded as synthetic VSMCs. The unknown cells in cluster 7 were scattered in states 2 and 3 by pseudotime analysis, indicating that these cells could play crucial roles in phenotype switching between contractile VSMCs and fibroblasts. Finally, cells in cluster 7 were termed transitional cells due to the co-expression of cell-type markers of VSMCs and fibroblasts. Moreover, we selected and analyzed the top 10 genes of VSMCs, fibroblasts, and transitional cells through pseudotime analysis, as summarized in **Figure 2G**.

Maps of Cells in Stenotic Arteries

A total of 4,674 cells in the stenotic carotid artery (case group) were acquired after removing unqualified cells from 5,656 cells by quality control. Specific genes from a total of 11 clusters were identified and used to construct a heatmap (**Supplementary Figure 2**, **Figures 3A,B**). We classified all of these cells into five cell types according to recognized markers of VSMCs, fibroblasts, ECs and macrophages (**Figure 3C**). We used the abovementioned strategy to verify the transitional cells and found a similar result. Obviously, the proportion of different cell types changed considerably between the normal artery and stenotic artery. The proportion of fibroblasts, ECs, and macrophages increased in the stenotic artery compared to the normal artery, while the proportion of VSMCs and transitional cells decreased in the stenotic artery (**Figures 3D,E**).

Pseudotime analysis of VSMCs, fibroblasts and transitional cells (**Supplementary Figures 3A,B**) showed that these cells could be classified into 5 states: state 1, 2, and 3 fibroblasts; state 4 synthetic VSMCs; and state 5 contractile VSMCs (**Supplementary Figures 3C,D, 4**). Interestingly, transitional cells in the stenotic artery were distributed in state 4 (synthetic VSMCs), which was different from their co-expression with markers of VSMCs and fibroblasts in the normal artery. This novel finding indicated that contractile VSMCs could switch to both a fibroblast-like phenotype and a synthetic VSMC phenotype in the stenotic artery after balloon injury. Pseudotime analysis and heatmaps of differentially expressed genes in VSMCs, fibroblasts and transitional cells are shown in **Supplementary Figures 5–11**.

Differences in VSMCs Between Normal and Stenotic Arteries

Contractile VSMCs, the major cell type in the artery (**Figure 3E**), are important for vessel contraction/dilation and regulating hemodynamics (14, 15). Thus, the differences in VSMCs between normal and stenotic arteries were analyzed in depth to explore the mechanism of ISR. VSMCs were isolated and then divided into 6 distinct clusters (**Figures 4A,B**) based on gene enrichment analysis. From **Figures 4C,D**, we found that the proportion of VSMCs in these 6 clusters varied greatly, and then several differentially expressed genes were selected to identify these 6 different clusters. Markers of cluster 1 (Hes1, Ccn1), cluster 2 (Notch1, Tmem140), cluster 3 (Rpa3, Ap3s2), cluster 4 (Pycard, Ep400), cluster 5 (Igfbp4, Gpx3), and cluster 6 (Tnfaip6, Mt-cyb) are summarized as dot plots (**Figures 4E,F**). GO and KEGG analyses were also performed to dig deeper into the functions and interactions of VSMCs (**Supplementary Figures 12–19**).

Phenotype Switching Among 6 Clusters of VSMCs

Contractile VSMCs could switch into a synthetic phenotype through dedifferentiation in response to vascular injury, and they could also regain the contractile property *via* differentiation under certain conditions (13, 14). We assigned each cluster to two phenotypes based on recognized contractile (Acta2, Tagln, **Figure 5A**) or synthetic VSMC markers (S100A4, **Figure 5B**). We also discovered an extra novel gene, N-myristoyltransferase 1 (Nmt1), after comparing our data with classical markers, which was previously reported to participate in the development of cancers (16). Higher expression of Nmt1 was found in the stenotic artery, indicating that it might be a new marker in our ISR model (**Figure 5C**) but also in general synthetic VSMCs. To verify the findings above, we used platelet-derived growth factor BB [PDGF-BB, a classical cytokine promoting VSMCs dedifferentiated into the synthetic phenotype (17)] to treat mouse aortic vascular smooth muscle cells (MOVAS) at 20 ng/ml and found that MOVAS expressed a higher level of NMT1 after PDGF-BB treatment (**Figure 5D**).

Pseudotime analysis found that VSMCs in different clusters were separated and distributed in various routes, which were linked *via* three nodes (**Figures 5E,F**). Six clusters of VSMCs (**Figure 5G**) indicated that they were distributed at different stages: clusters 4, 5, and 6 might pause at advanced differentiation

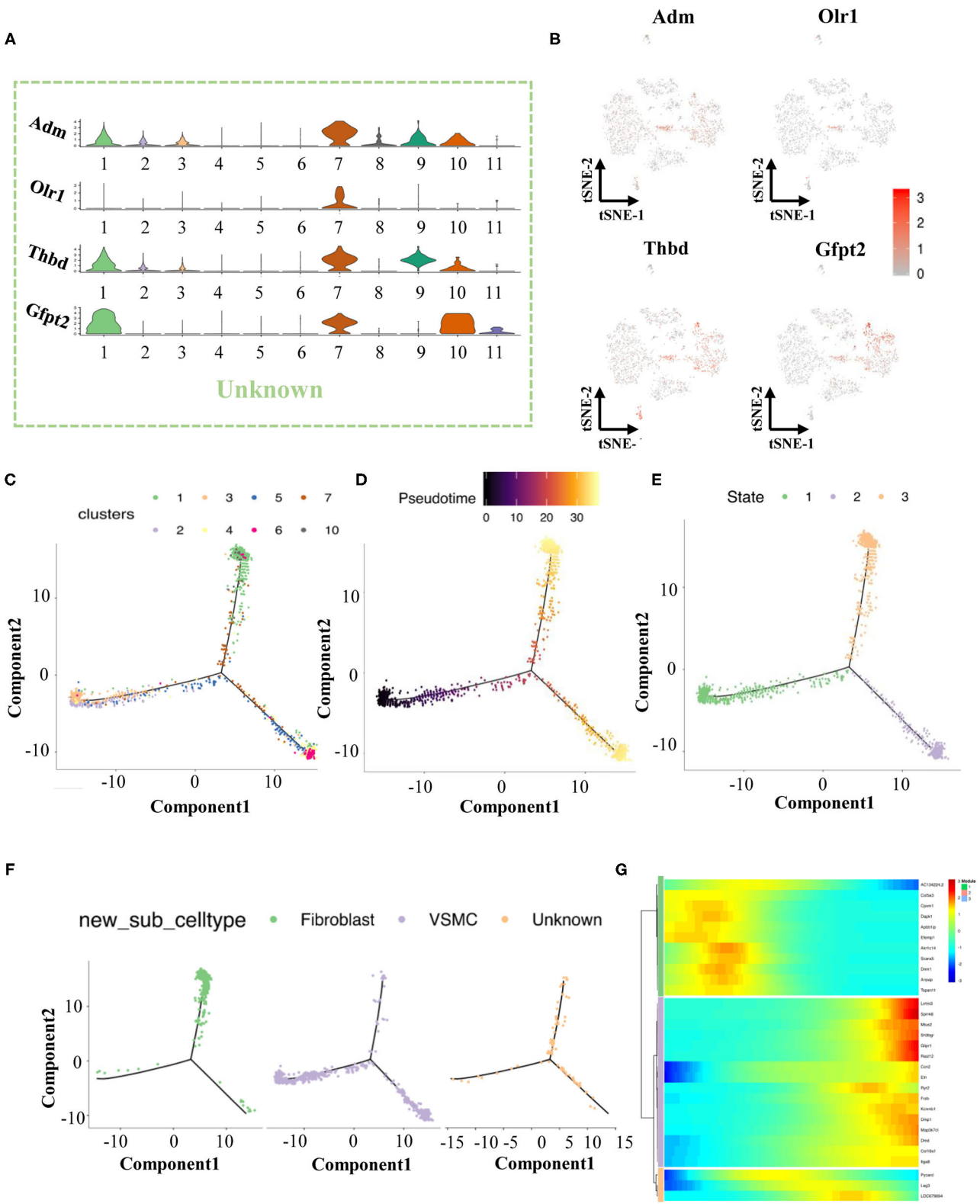

FIGURE 2 | The finding of transitional-cells. **(A)** Violin illustrations showed differentially expressed genes (Top 4) in transitional-cells. **(B)** Scatter plot showed enrichment of differentially expressed genes in transitional-cells. **(C)** Pseudotime analysis of VSMCs, fibroblasts and transitional-cells. **(D)** Coloring for differentiation time. **(E)** Coloring for the state of differentiation. **(F)** Split the branches. **(G)** Heat map of gene expression in cells of different differentiation states.

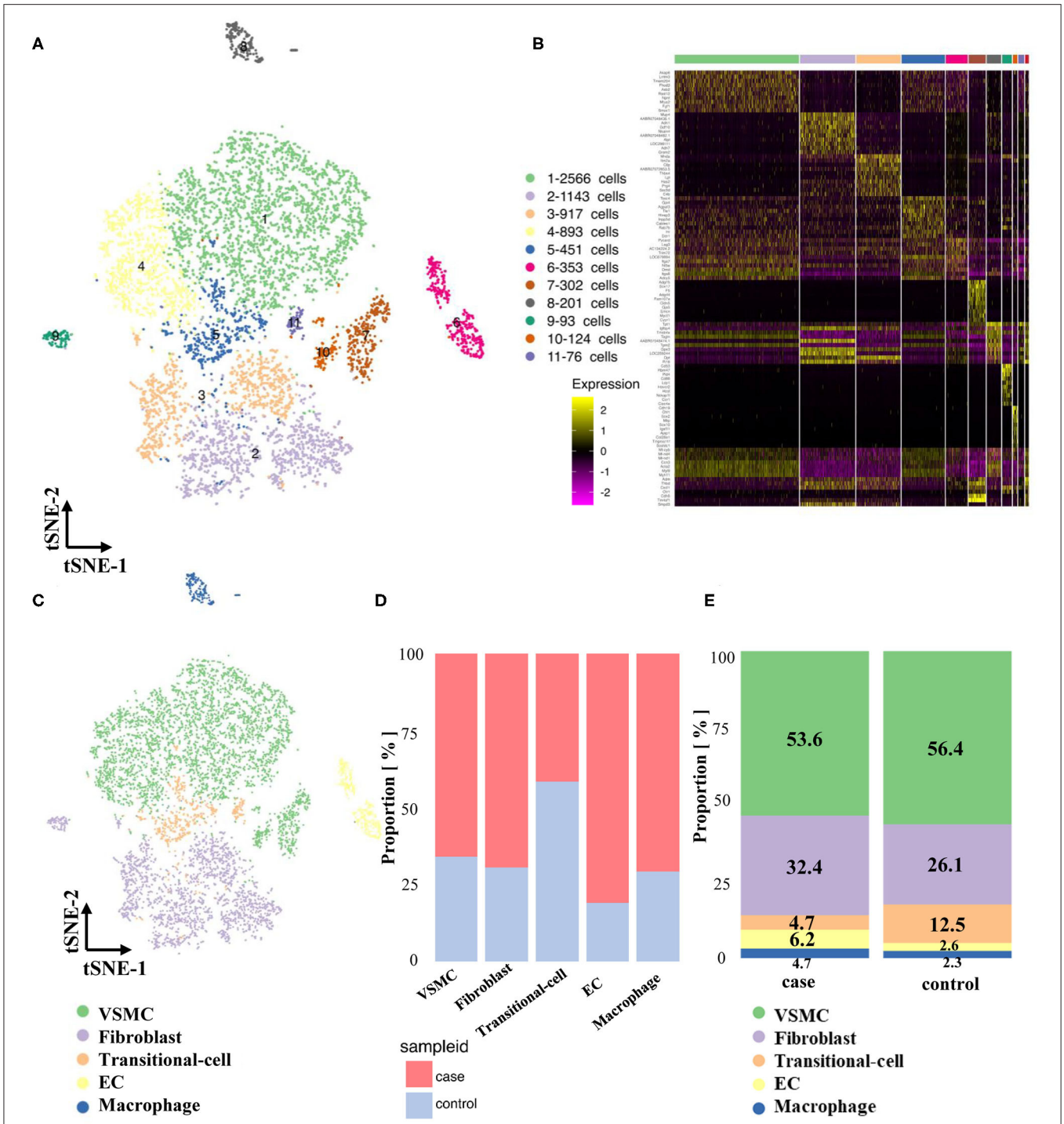

FIGURE 3 | Maps of single-cells in both normal and experimental carotid arteries. **(A)** TSNE of single cells in normal and experimental cartoid arteries. **(B)** Differentially expressed genes (Top 10) of 11 clusters. **(C)** Classification of 11 clusters into 5 cell types (VSMC, fibroblast, EC, transitional-cell, macrophage). **(D)** Comparison of proportion in different cell types. **(E)** Comparison of proportion in case and control groups.

stages; clusters 1, 2, and 3 might pause at early stages. Meanwhile, we found that VSMCs in the case group showed a more extreme distribution in pseudotime routes but a disseminated distribution in the control group (**Figure 5H**). Finally, we identified cluster 4, 5, and 6 cells as contractile VSMCs and cluster 1, 2, and 3 cells as synthetic VSMCs (**Figure 5J**).

It has been reported that the Notch-Hes1 pathway, a pro-differentiation pathway, plays an essential role in the

differentiation of many cell types (18). Notch1 increases after vascular injury, and inactivation of Notch1 might reduce neointimal hyperplasia (19). In our study, Notch1 and Hes1 were highly expressed in synthetic clusters 1 and 2 (**Figure 4E**), indicating that these two genes might be synthetic VSMC-related genes.

Differences in Fibroblasts and ECs Between Normal and Stenotic Arteries

Our data demonstrated that fibroblasts, mainly distributed in the adventitia of blood vessels, could proliferate greatly during the progression of neointimal hyperplasia (**Supplementary Figure 20**). A heatmap could help us identify specific markers of these proliferous fibroblasts and provide a new strategy to distinguish fibroblasts in the normal position or the neointima (**Supplementary Figure 21**). Pseudotime analysis demonstrated that cells in cluster 3 might be proliferous fibroblasts in the case group (**Supplementary Figures 22–25**). In addition, GO terms and KEGG terms reminded us of the relationship between differentially expressed and specific functions (**Supplementary Figures 26–33**).

Originally, our model indicated damaged endothelial cells and VSMCs cause intimal hyperplasia. The increase in ECs might be caused by the appearance of EC-like VSMCs or re-endothelialization (20). Total ECs were clustered, indicating that cells in cluster 2 acted as EC-like VSMCs and that cells in cluster 1 could be related to re-endothelialization (**Supplementary Figures 34–37**). GO terms and KEGG terms also reminded us of the functional changes between the case and control groups (**Supplementary Figures 38–45**).

Disease Susceptibility Gene

To verify the similarity between our model and real-world disease, we compared four sets of independent human disease susceptibility genes from GeneCards (https://www.genecards.org/) (ISR-related genes, VSMC phenotype switching-related genes, atherosclerosis-related genes, neointima proliferation-related genes) with our data to determine the expression abundance of previously recognized disease susceptibility genes (**Figures 6A–D**).

When analyzing ISR-related genes, the Ace, Selp, Nos3, Serpine1, and Sele genes were highly expressed in ECs; the Plat, Il6, Vegfa, F3, and Cdkn2a genes were highly expressed in fibroblasts; the P2ry12, Ccl2, Cdkn1a, and Hmox1 genes were highly expressed in macrophages; the Spp1 gene was highly expressed in transitional cells; and the Crp and Spp1 genes were highly expressed in VSMCs (**Figure 6A**). When analyzing atherosclerosis-related genes, we screened out high expression of the Olr1 and Sele genes in ECs; the Lpl, Ccl2, and Vegfa genes in fibroblasts; the Apoe, Abca1, Pparg, and Ccl2 genes in macrophages; the Ldlr and Eln genes in transitional cells; and the Ldlr, Lmna, Apoa2 and Crp genes in VSMCs (**Figure 6B**). Afterwards, we focused on VSMCs and found that the Lmna, Myh11, Mylk, Cacna1c, and Ptpn11 genes were intensely related to VSMC phenotype switching; the Pdgfb and Mtor genes were closely related to neointimal proliferation.

The matrix metallopeptidase (Mmp) gene family related to ISR was highly expressed in the stenotic artery but expressed at low levels in the control group (Mmp3 in fibroblasts; Mmp9 in macrophages; Mmp3 in transitional cells; **Figure 6A**). Meanwhile, several genes related to ISR exhibited high expression in the case group and low expression in the control group, such as Serpinc1 in ECs, Crp in fibroblasts, and Serpinc1 and Serpind1 in transitional cells (**Figure 6A**). When compared with the control group, several genes related to atherosclerosis were differentially expressed in the case group (Up: Apob in fibroblasts; Cyp7a1 in VSMCs; Down: Pcsk9, Apoa2, Crp, Cyp7a1 in fibroblasts; Apoa1 in macrophages; Alb in transitional cells, **Figure 6C**). We also found that the expression of several VSMC genes related to neointimal proliferation changed considerably with the progression of disease (Up: Pcna; Down: Akt1, Cdk4, and Rb1).

By comparing the susceptibility gene databases with our sequencing data, we obtained some results similar to previous studies and verified them in an *in vivo* study. Moreover, we discovered several novel genes based on the current model, such as Cyp7a1 and Cdk4, which should be further validated.

Cell-to-Cell Communication: Receptor Ligand Analysis

We performed receptor ligand analysis in the normal artery and stenotic artery (**Figure 7A**, **Supplementary Figure 46**). In the normal artery, Fn1, especially Fn1/α8β1 integrin, was enriched in ECs. Col1a1 and Col3a1, whose ligands are α1β1 integrin and α11β1 integrin, were enriched in fibroblasts. Moreover, macrophages were associated with the high expression of Cd74, Cd44/Copa, App, and Hbegf. Col1a1/α1β1 integrin and Col1a1/α11β1 integrin were also enriched in transitional cells. However, the gene expression of ligands in VSMCs was low.

Of note, the expression levels of receptors and ligands in the stenotic artery changed considerably compared with those in the normal artery (**Supplementary Figure 15**). Fn1/α8β1 integrin, Fn1/α5β1 integrin, Fn1/αVβ1 integrin, and Fn1/αVβ5 integrin were all enriched in ECs. Fn1, Col3a1, and Cd44 (ligands) and αVβ1, αVβ5, α8β1, α5β1, α1β1 integrin, SPP1, and Hbegf (receptors) were enriched in fibroblasts. Nrp2/Vegfa, Cd74/Copa, Cd74/App, and Cd74/Hbegf were enriched in macrophages. Moreover, transitional cells seemed to have high enrichment levels of Col18a1/α1β1 integrin and Cd44/Hbegf. The ligand and receptor circuit diagram suggested decreased communication between VSMCs and ECs (**Figures 7B,C**). In addition, ligands from fibroblasts decreased relative to the control group.

DISCUSSION

To the best of our knowledge, this is the first study to investigate the mechanisms of ISR by single-cell RNA sequencing. There are several main findings in our study. First, we found traditional

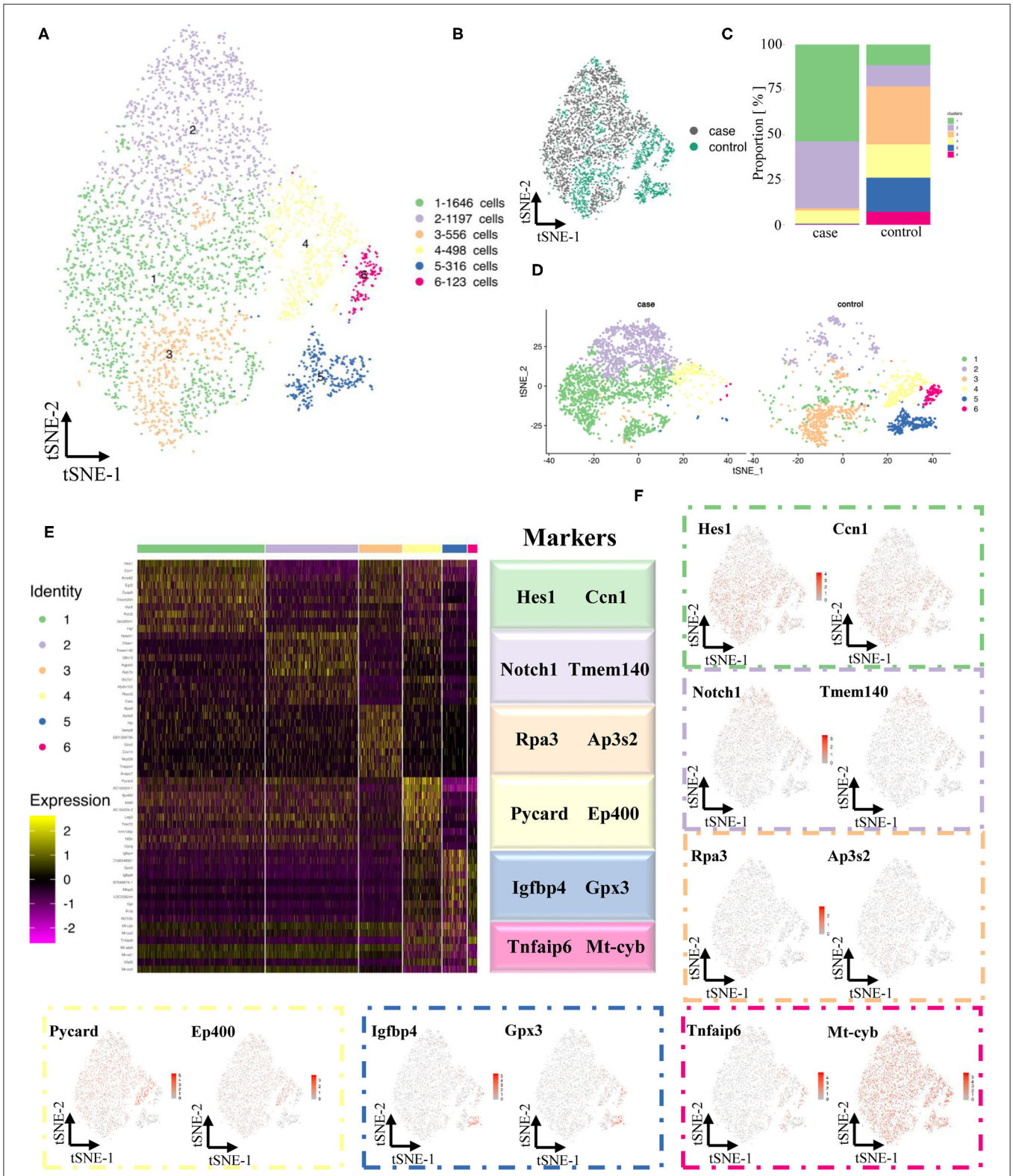

FIGURE 4 | Maps of VSMCs in both normal and experimental carotid arteries. **(A)** TSNE of sing cells of VSMCs. **(B)** Distribution of case and control groups in tSNE. **(C)** Comparison of proportion in case and control groups. **(D)** Comparison of sing cells of case and control groups in tSNE. **(E)** Differentially expressed genes (Top 10) of 6 clusters. **(F)** Expression of classical markers (VSMC, fibroblast, EC and macrophage) in 11 clusters.

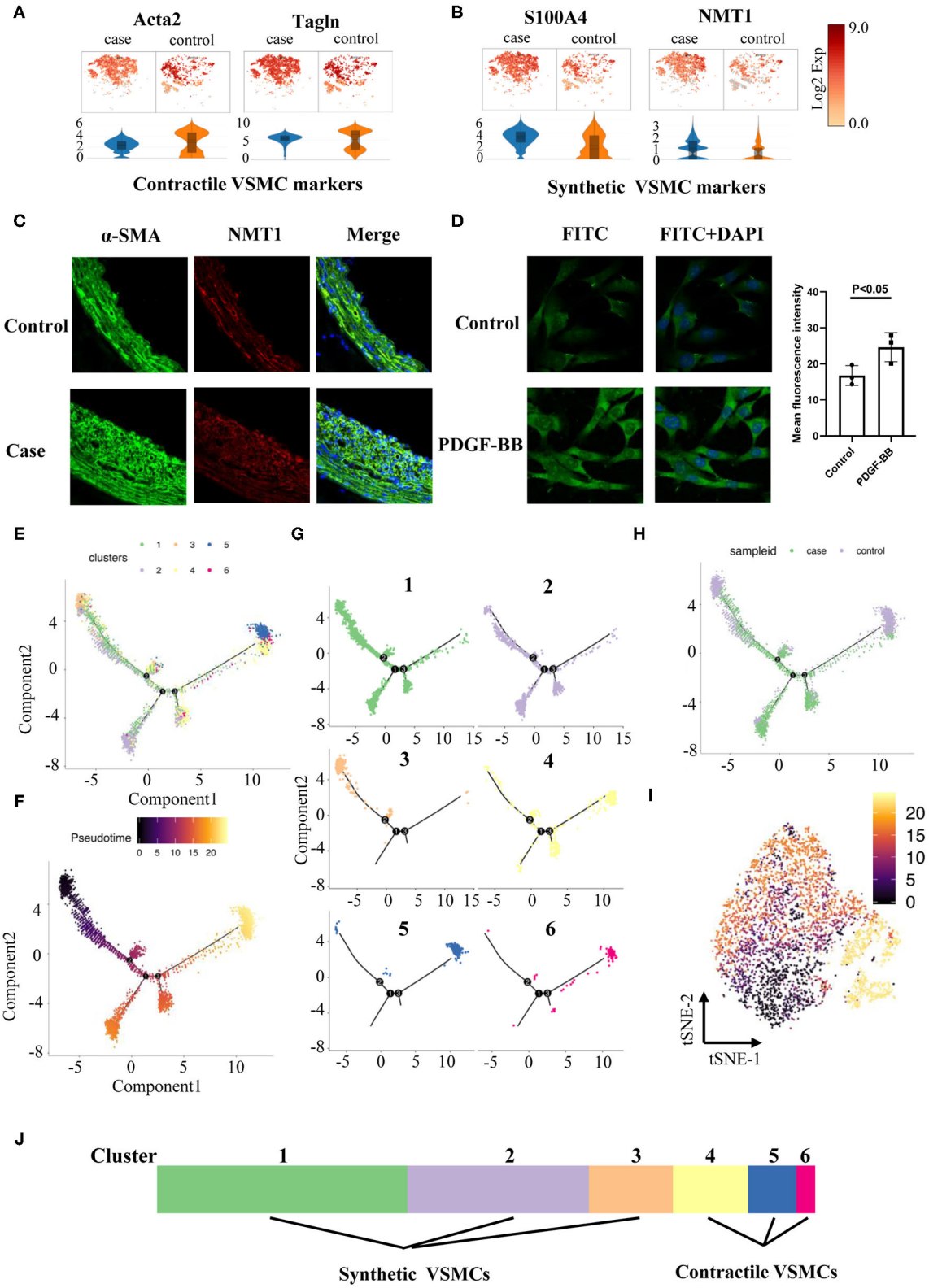

FIGURE 5 | Phenotype switching in VSMCs. **(A)** Dot plots and violin illustrations of contractile makers of VSMC. **(B)** Dot plots and violin illustrations of synthetic makers of VSMC. **(C)** Immunofluorescence images of slices of rats' cartoid arteries in case and control groups. **(D)** Immunofluorescence images of moves under pretreatment (PDGF-BB) and control groups. **(E)** Pseudotime analysis of VSMCs. **(F)** Coloring for differentiation time. **(G)** Split the branches. **(H)** Coloring for case and control groups. **I.** Coloring for differentiation time in tSNE. **(J)** Classified 6 clusters into contractile VSMCs and synthetic VSMCs.

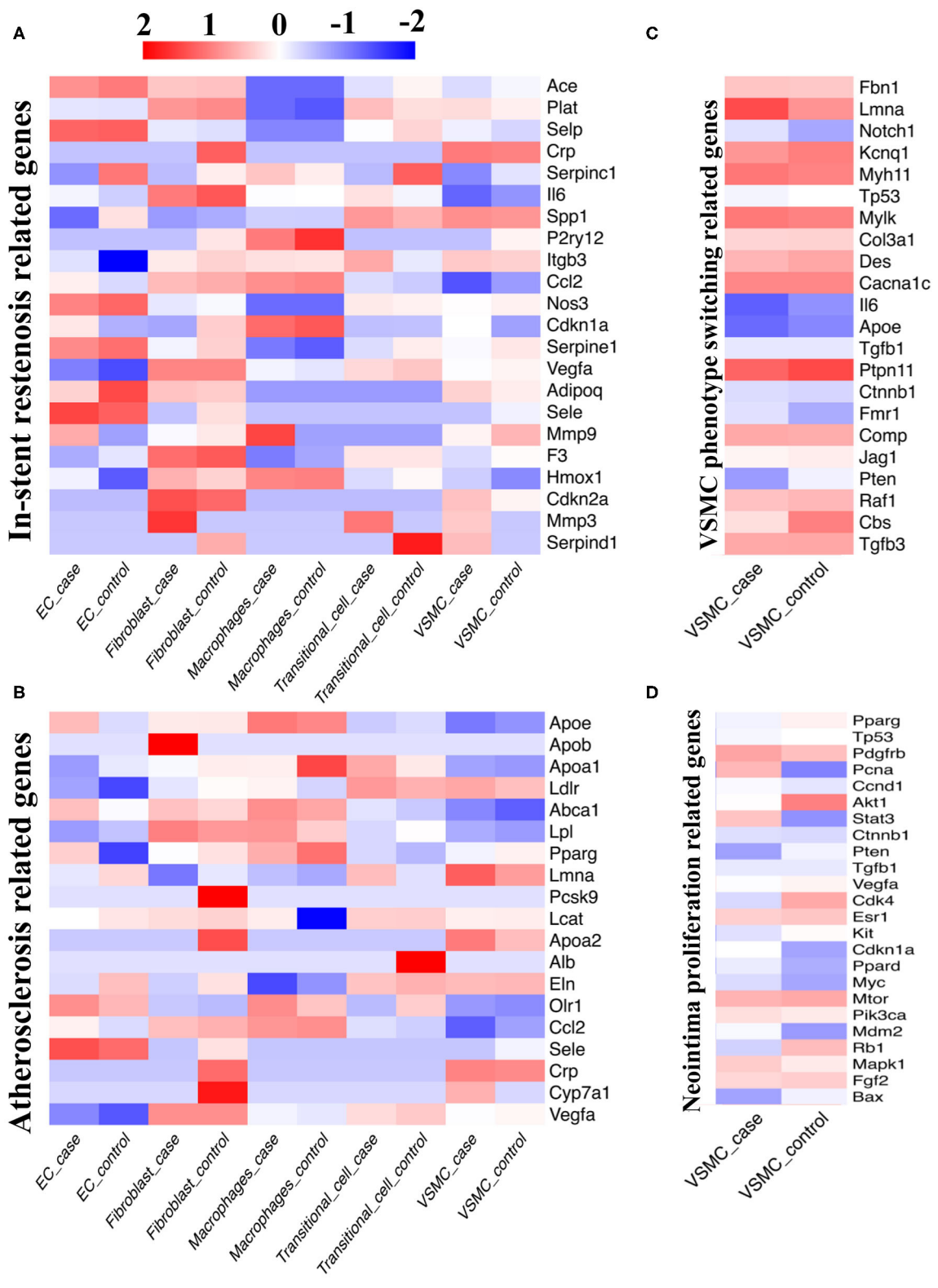

FIGURE 6 | Comparison between single-cell database and disease susceptibility gene databases. **(A)** Our single-cell sequencing compared with database of in-stent restenosis related genes. **(B)** Our single-cell sequencing compared with database of atherosclerosis related genes. **(C)** Our single-cell sequencing compared with database of VSMC phenotype switching related genes. **(D)** Our single-cell sequencing compared with database of neointima proliferation related genes.

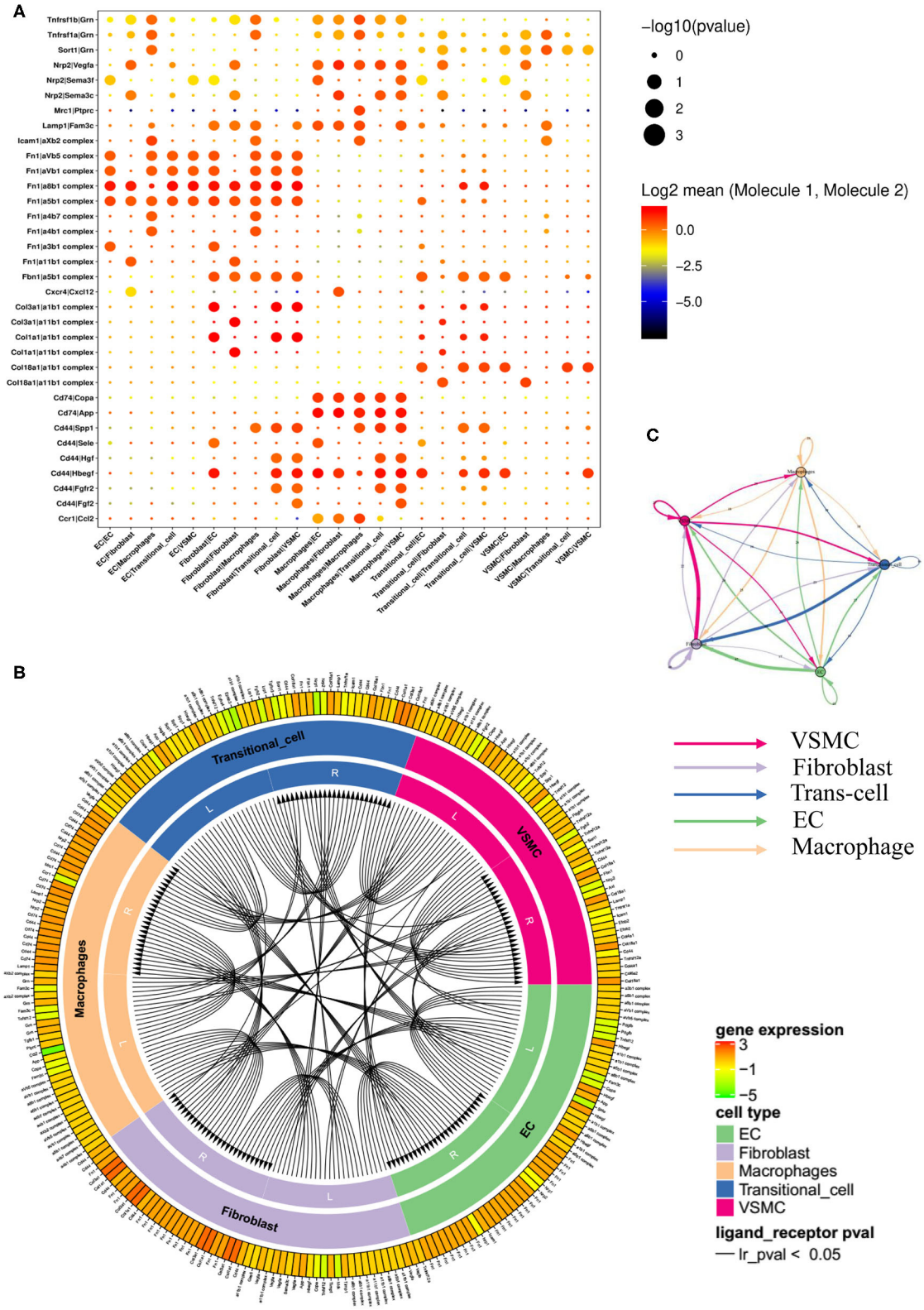

FIGURE 7 | Networks of ligands and receptors in single-cells of case group. **(A)** Dot plot of receptors and ligands analysis. **(B)** Intercellular communication of different cell types. **(C)** Quantitative figure of intercellular communication.

cells between VSMCs and fibroblasts in both normal and stenotic arteries. The specific key genes of these novel cells were also selected by heat map analysis and in a dynamic change trend graph of pseudotime analysis. Second, the phenotype of VSMCs, the major component of blood vessels, switched greatly in the stenotic artery, and we further classified the VSMCs into 6 clusters based on gene enrichment analysis. Finally, disease susceptibility gene analysis confirmed the association of those classical genes and ISR by comparing our data with four previous databases, and we also proposed several novel related target genes, such as Cyp7a1 and Cdk4, which should be validated in future studies.

DES has completely replaced bare-metal stents to be used in ischemic heart disease in daily clinical practice due to the proliferation inhibition effects of coating agents (21), but the relatively high occurrence of restenosis (5–10%) after implantation of DES still cannot be prevented, with a direct financial burden on patients and medical insurance (1). It is warranted to use a novel methodology to investigate the underlying mechanisms of ISR. Single-cell RNA sequencing is a novel bioanalysis technology in recent years that has been extensively used in the field of cancer but less in the cardiovascular field (22). Thus, we conducted the present study and hope to find new clues to explore the mechanisms of ISR in depth.

VSMCs have more plasticity than any other cell type in blood vessels. In atherosclerosis models, VSMC-derived foam cells and macrophage-like VSMCs play major roles within the arterial wall (15). However, our data indicated that specific markers of macrophages showed low expression in VSMCs and ensured the purity of VSMCs. In addition, a previous study revealed that VSMCs could switch into osteoblast-like cells, fibroblast-like cells and senescent VSMCs (23). Wirka et al. reported fibroblast-like cells in atherosclerotic lesions that broke inherent cognition (12). Our data also proved that phenotype switching exists between VSMCs and fibroblasts and found a new cell type: transitional cells. During the transition from VSMCs to fibroblasts, inflammatory factors dropped sharply, and cyclins indicated cell cycle arrest, suggesting that this transition has a protective effect on VSMCs. From another perspective, the transition from fibroblasts to VSMCs means that the elasticity and compliance of hyperplastic tissues are reduced, which may have a certain impact on the long-term prognosis of diseased blood vessels. Therefore, the in-depth investigation of transitional cells is particularly important. By regulating the number and homeostasis of transitional cells, we might seek benefits and avoid disadvantages at the same time.

VSMCs, a major component of blood vessels, were clustered into 6 groups. Obviously, we observed changes in proportions between 6 clusters. We tried to uncover the mechanism of ISR by explaining these changes between 6 clusters during neointima proliferation. In recent years, phenotype switching/modulation of VSMCs has always been a research hotspot and is used to analyze a variety of VSMC-related disease models. Pseudotime analysis helped us distinguish contractile and synthetic VSMCs by the degree of differentiation. Unlike pseudotime analysis of single-cell sequencing, we usually used specific markers to identify different cell types of VSMCs *in vitro*. Nonetheless, classical markers of contractile or synthetic VSMCs are not applicable to all models. For example, secreted phosphoprotein 1 (SPP1)-encoded protein osteopontin (OPN) (24) of synthetic VSMCs, an extracellular matrix-related component that has been frequently reported in VSMC phenotype switching, showed hardly any differences between the case and control groups. Therefore, it is necessary to select several genes suitable for ISR models. Nmt1 might be a new marker in both ISR models *in vivo* and VSMCs *in vitro*. To some extent, Nmt1 is specific not only to the ISR model but also to models related to VSMC phenotype switching, which need more verification.

Moreover, by comparing the database of disease-related susceptibility genes, we revealed target cells of these disease-related susceptibility genes *in vivo.* The expression of disease-related susceptibility genes changed obviously between the case and control groups, which indicated that VSMCs played major roles in neointimal proliferation. Jason LJ et al. reported that Mmp3 mediated the activation of Mmp9, which was required for neointimal proliferation and VSMC migration (25). The serpin gene family, with antithrombin and antiproliferation functions, has been reported to play a protective role in blood vessels (26). As mentioned above, fibronectin1 (Fn1) was found to be a representative ligand and regulate integrins, as suggested by previous studies (27, 28). However, the communication between Fn1 and integrins was enhanced with the progression of ISR and was mainly located in ECs and fibroblasts. In addition, we benefited from the analysis of receptors and ligands. Signals of receptors and ligands aggregated in ECs and macrophages, which was opposite to the results obtained for disease-related susceptibility genes. The results highlighted Fn1/integrins in ECs and fibroblasts and Cd44 in macrophages and showed obvious changes in Fn1/integrins and Cd44 between the case and control groups. However, the number of receptors and ligands of fibroblasts rather than ECs or macrophages was obviously reduced in total.

There are several limitations in our study. First, the rat carotid artery balloon injury model is the most common *in vivo* model widely used to study ISR, but a gap still exists. Second, to obtain live cells for single-cell sequencing, we chose balloon-injured rat carotid arteries instead of frozen human restenotic coronary artery specimens in cold storage. Third, two cases and two controls were selected due to the limited research funding and time, and a relatively small sample size might produce bias. However, the first applied single-cell sequencing in the ISR model could provide novel clues for further study.

In conclusion, maps of heterogeneous cellular landscapes, especially transitional cells, in the carotid artery were defined by single-cell RNA sequencing and revealed several cell types with their internal relations in the ISR model. This study highlights the crucial role of VSMC phenotype switching in the progression of ISR, and we also proposed several novel related target genes, such as Cyp7a1 and Cdk4, providing clues regarding the underlying mechanism of ISR.

DATA AVAILABILITY STATEMENT

The datasets presented in this study can be found in online repositories. The names of the repository/repositories and accession number(s) can be found at: https://www.ncbi.nlm.nih.gov/geo/, GSE174098.

ETHICS STATEMENT

The animal study was reviewed and approved by Experimental Animal Care and Use Committee of Nanjing Medical University.

AUTHOR CONTRIBUTIONS

X-FG and A-QC performed experiments and wrote the manuscript. Z-MW and FW prepared the figures. SL, S-YC, and YG prepared the **Supplementary Materials**. YC and ZG prepared the table. J-JZ and S-LC provided the idea and revised the manuscript. All authors have agreed to the published version of the manuscript.

FUNDING

This study was funded by the National Natural Science Foundation of China (NSFC 81970307 and 81801147), and was jointly supported by Six Talent Peaks Project of Jiangsu Province (2019-WSN-156), Social Development Project of Jiangsu Province (BE2019616), Jiangsu Commission of Health (H2019077), Nanjing Commission of Health (ZKX19027), and Nanjing Health Youth Talent Training project (QRX17017).

ACKNOWLEDGMENTS

We deeply appreciated Xuan Zhou, Xiao-Hua Yao, Yong-Bing Ba, and Jiao-Yang Dong at Shanghai OE Biotech Co. for their support on single-cell RNA sequencing.

SUPPLEMENTARY MATERIAL

The Supplementary Material for this article can be found online at: https://www.frontiersin.org/articles/10.3389/fcvm.2021.751525/full#supplementary-material

REFERENCES

1. Zhang J, Gao X, Kan J, Ge Z, Han L, Lu S, et al. Intravascular ultrasound versus angiography-guided drug-eluting stent implantation: The ULTIMATE trial. *J Am Coll Cardiol.* (2018) 72:3126–37. doi: 10.1016/j.jacc.2018.09.013
2. Gao XF, Ge Z, Kong XQ, Kan J, Han L, Lu S, et al. 3-Year Outcomes of the ULTIMATE Trial comparing intravascular ultrasound versus angiography-guided drug-eluting stent implantation. *JACC Cardiovasc Interven.* (2021) 14:247–57. doi: 10.1016/j.jcin.2020.10.001
3. Zhang JJ, Ye F, Xu K, Kan J, Tao L, Santoso T, et al. Multicentre, randomized comparison of two-stent and provisional stenting techniques in patients with complex coronary bifurcation lesions: the DEFINITION II trial. *Eur Heart J.* (2020) 41:2523–36. doi: 10.1093/eurheartj/ehaa543
4. Shlofmitz E, Iantorno M Waksman R. Restenosis of drug-eluting stents: a new classification system based on disease mechanism to guide treatment and state-of-the-art review. *Circulation Cardiovas Interven.* (2019) 12:e007023. doi: 10.1161/CIRCINTERVENTIONS.118.007023
5. Cochain C, Vafadarnejad E, Arampatzi P, Pelisek J, Winkels H, Ley K, et al. Single-cell RNA-Seq reveals the transcriptional landscape and heterogeneity of aortic macrophages in murine atherosclerosis. *Circulation Res.* (2018) 122:1661–74. doi: 10.1161/CIRCRESAHA.117.312509
6. Dobnikar L, Taylor AL, Chappell J, Oldach P, Harman JL, Oerton E, et al. Disease-relevant transcriptional signatures identified in individual smooth muscle cells from healthy mouse vessels. *Nat Commun.* (2018) 9:4567. doi: 10.1038/s41467-018-06891-x
7. Indolfi C, Mongiardo A, Curcio A Torella D. Molecular mechanisms of in-stent restenosis and approach to therapy with eluting stents. *Trends Cardiovas Med.* (2003) 13:142–8. doi: 10.1016/S1050-1738(03)00038-0
8. Jain M, Dhanesha N, Doddapattar P, Chorawala MR, Nayak MK, Cornelissen A, et al. Smooth muscle cell-specific fibronectin-EDA mediates phenotypic switching and neointimal hyperplasia. *J Clin Investig.* (2020) 130:295–314. doi: 10.1172/JCI124708
9. Gao XF, Wang ZM, Chen AQ, Wang F, Luo S, Gu Y, et al. Plasma small extracellular vesicle-carried miRNA-501-5p promotes vascular smooth muscle cell phenotypic modulation-mediated in-stent restenosis. *Oxidat Med Cell Longevity.* (2021) 2021:6644970. doi: 10.1155/2021/6644970
10. Tulis DA. Rat carotid artery balloon injury model. *Methods Mol Med.* (2007) 139:1–30. doi: 10.1007/978-1-59745-571-8_1
11. Kuro-o M, Nagai R, Nakahara K, Katoh H, Tsai RC, Tsuchimochi H, et al. cDNA cloning of a myosin heavy chain isoform in embryonic smooth muscle and its expression during vascular development and in arteriosclerosis. *J Biol Chem.* (1991) 266:3768–73. doi: 10.1016/S0021-9258(19)67861-0
12. Wirka RC, Wagh D, Paik DT, Pjanic M, Nguyen T, Miller CL, et al. Atheroprotective roles of smooth muscle cell phenotypic modulation and the TCF21 disease gene as revealed by single-cell analysis. *Nat Med.* (2019) 25:1280–9. doi: 10.1038/s41591-019-0512-5
13. Frismantiene A, Philippova M, Erne P Resink TJ. Smooth muscle cell-driven vascular diseases and molecular mechanisms of VSMC plasticity. *Cell Signal.* (2018) 52:48–64. doi: 10.1016/j.cellsig.2018.08.019
14. Allahverdian S, Chaabane C, Boukais K, Francis GA Bochaton-Piallat ML. Smooth muscle cell fate and plasticity in atherosclerosis. *Cardiovasc Res.* (2018) 114:540–50. doi: 10.1093/cvr/cvy022
15. Sorokin V, Vickneson K, Kofidis T, Woo CC, Lin XY, Foo R Shanahan CM. Role of vascular smooth muscle cell plasticity and interactions in vessel wall inflammation. *Front Immunol.* (2020) 11:599415. doi: 10.3389/fimmu.2020.599415
16. Liang J, Xu ZX, Ding Z, Lu Y, Yu Q, Werle KD, et al. Myristoylation confers noncanonical AMPK functions in autophagy selectivity and mitochondrial surveillance. *Nat Commun.* (2015) 6:7926. doi: 10.1038/ncomms8926
17. Owens GK, Kumar MS Wamhoff BR. Molecular regulation of vascular smooth muscle cell differentiation in development and disease. *Physiol Rev.* (2004) 84:767–801. doi: 10.1152/physrev.00041.2003
18. Kageyama R, Ohtsuka T Tomita K. The bHLH gene Hes1 regulates differentiation of multiple cell types. *Mol Cells.* (2000) 10:1–7. doi: 10.1007/s10059-000-0001-0
19. Li Y, Takeshita K, Liu PY, Satoh M, Oyama N, Mukai Y, et al. Smooth muscle Notch1 mediates neointimal formation after vascular injury. *Circulation.* (2009) 119:2686–92. doi: 10.1161/CIRCULATIONAHA.108.790485
20. Arbustini E, Favalli V Narula J. Functionally incomplete re-endothelialization of stents and neoatherosclerosis. *JACC Cardiovas Interven.* (2017) 10:2388–91. doi: 10.1016/j.jcin.2017.08.031
21. Taniwaki M, Stefanini GG, Silber S, Richardt G, Vranckx P, Serruys PW, et al. 4-year clinical outcomes and predictors of repeat revascularization in patients treated with new-generation drug-eluting stents: a report from the RESOLUTE All-Comers trial (A Randomized Comparison of a Zotarolimus-Eluting Stent With an Everolimus-Eluting Stent for Percutaneous Coronary Intervention). *J Am Coll Cardiol.* (2014) 63:1617–25. doi: 10.1016/j.jacc.2013.12.036

22. Yifan C, Fan Y Jun P. Visualization of cardiovascular development, physiology and disease at the single-cell level: Opportunities and future challenges. *J Mol Cell Cardiol.* (2020) 142:80–92. doi: 10.1016/j.yjmcc.2020.03.005
23. Durham AL, Speer MY, Scatena M, Giachelli CM Shanahan CM. Role of smooth muscle cells in vascular calcification: implications in atherosclerosis and arterial stiffness. *Cardiovasc Res.* (2018) 114:590–600. doi: 10.1093/cvr/cvy010
24. Wu M, Rementer C Giachelli CM. Vascular calcification: an update on mechanisms and challenges in treatment. *Calcified Tissue Int.* (2013) 93:365–73. doi: 10.1007/s00223-013-9712-z
25. Johnson JL, Dwivedi A, Somerville M, George SJ Newby AC. Matrix metalloproteinase (MMP)-3 activates MMP-9 mediated vascular smooth muscle cell migration and neointima formation in mice. *Arteriosclerosis Thrombosis Vasc Biol.* (2011) 31:e35–44. doi: 10.1161/ATVBAHA.111.225623
26. Dai E, Guan H, Liu L, Little S, McFadden G, Vaziri S, et al. Serp-1, a viral anti-inflammatory serpin, regulates cellular serine proteinase and serpin responses to vascular injury. *J Biol Chem.* (2003) 278:18563–72. doi: 10.1074/jbc.M209683200
27. Jin L, Lin X, Yang L, Fan X, Wang W, Li S, et al. AK098656, a novel vascular smooth muscle cell-dominant long noncoding RNA, promotes hypertension. *Hypertension.* (2018) 71:262–72. doi: 10.1161/HYPERTENSIONAHA.117.09651
28. Huaman J Ogunwobi OO. Circulating tumor cell migration requires fibronectin acting through integrin B1 or SLUG. *Cells.* (2020) 9:1594. doi: 10.3390/cells9071594

Conflict of Interest: The authors declare that the research was conducted in the absence of any commercial or financial relationships that could be construed as a potential conflict of interest.

Publisher's Note: All claims expressed in this article are solely those of the authors and do not necessarily represent those of their affiliated organizations, or those of the publisher, the editors and the reviewers. Any product that may be evaluated in this article, or claim that may be made by its manufacturer, is not guaranteed or endorsed by the publisher.

frontiers in Cardiovascular Medicine

ORIGINAL RESEARCH
published: 13 December 2021
doi: 10.3389/fcvm.2021.769165

Trends in Bleeding Events Among Patients With Acute Coronary Syndrome in China, 2015 to 2019: Insights From the CCC-ACS Project

Xiao Wang[1†], Guanqi Zhao[1†], Mengge Zhou[2], Changsheng Ma[3], Junbo Ge[4], Yong Huo[5], Sidney C. Smith Jr.[6], Gregg C. Fonarow[7], Yongchen Hao[2], Jun Liu[2], Louise Morgan[8], Wei Gong[1], Yan Yan[1], Jing Liu[2], Dong Zhao[2], Yaling Han[9] and Shaoping Nie[1]* on behalf of the CCC-ACS Investigators*

[1] Center for Coronary Artery Disease, Beijing Anzhen Hospital, Capital Medical University, Beijing, China, [2] Department of Epidemiology, Beijing Anzhen Hospital, Capital Medical University, Beijing Institute of Heart, Lung and Blood Vessel Diseases, Beijing, China, [3] Department of Cardiology, Beijing Anzhen Hospital, Capital Medical University, Beijing, China, [4] Zhongshan Hospital, Fudan University, Shanghai, China, [5] Department of Cardiology, Peking University First Hospital, Beijing, China, [6] Division of Cardiology, University of North Carolina, Chapel Hill, NC, United States, [7] Divisions of Cardiology, University of California, Los Angeles, Los Angeles, CA, United States, [8] International Quality Improvement Department, American Heart Association, New York, NY, United States, [9] Cardiovascular Research Institute and Department of Cardiology, General Hospital of Northern Theater Command, Shenyang, China

Objective: Major bleeding is a common complication following treatment for an acute coronary syndrome (ACS) and is associated with increased mortality. We aimed to explore the temporal trend of bleeding events in relation to changes of therapeutic strategies among patients hospitalized for ACS in China.

Methods: The CCC-ACS project (Improving Care for Cardiovascular Disease in China–Acute Coronary Syndrome) is a collaborative initiative of the American Heart Association and the Chinese Society of Cardiology. We analyzed 113,567 ACS patients from 241 hospitals in China from 2015 to 2019. Major bleeding was defined as intracranial bleeding, retroperitoneal bleeding, a decline in hemoglobin levels ≥3 g/dL, transfusion with overt bleeding, bleeding requiring surgical intervention, and fatal bleeding. Kruskal–Wallis test was used to examine the trend of major bleeding over time.

Results: The rate of in-hospital major bleeding decreased from 6.3% in 2015 to 4.7% in 2019 (unadjusted OR = 0.74, 95% CI: 0.68–0.80, and $P < 0.001$). The relative changes were consistent across almost all subgroups including patients with NSTE-ACS and STEMI, although the trend was more pronounced in NSTE-ACS patients. The decrease in bleeding was accompanied by a decrease in use of GP IIb/IIIa inhibitors and parenteral anticoagulation therapy during hospitalization. The annual reduced risk of bleeding (OR = 0.91, 95% CI: 0.89–0.93) was attenuated after stepwise adjusting for baseline characteristics and antithrombotic treatments (OR = 0.95, 95% CI: 0.93–0.97), but did not change after adjusting for invasive treatment (OR = 0.95, 95% CI: 0.93–0.97).

Conclusions: There was a temporal reduction in in-hospital bleeding among Chinese ACS patients during the last 5 years, which was associated with more evidence-based use of antithrombotic therapies.

OPEN ACCESS

Edited by:
Antonio Greco,
University of Catania, Italy

Reviewed by:
Felice Gragnano,
University of Campania Luigi Vanvitelli, Italy
Marco Di Maio,
University of Salerno, Italy
Claudio Laudani,
University of Catania, Italy
Marco Spagnolo,
Universit'a degli Studi di Catania, Italy

***Correspondence:**
Shaoping Nie
spnie@ccmu.edu.cn
Yaling Han
hanyaling@263.net

[†] These authors have contributed equally to this work

Specialty section:
This article was submitted to Coronary Artery Disease, a section of the journal Frontiers in Cardiovascular Medicine

Received: *01 September 2021*
Accepted: *11 November 2021*
Published: *13 December 2021*

Citation:
Wang X, Zhao G, Zhou M, Ma C, Ge J, Huo Y, Smith SC Jr, Fonarow GC, Hao Y, Liu J, Morgan L, Gong W, Yan Y, Liu J, Zhao D, Han Y and Nie S (2021) Trends in Bleeding Events Among Patients With Acute Coronary Syndrome in China, 2015 to 2019: Insights From the CCC-ACS Project. Front. Cardiovasc. Med. 8:769165. doi: 10.3389/fcvm.2021.769165

Clinical Trial Registration: https://www.clinicaltrials.gov, identifier: NCT02306616.

Keywords: acute coronary syndrome, bleeding, temporal trend, antithrombotic therapy, outcome

INTRODUCTION

The use of intensive antithrombotic therapies coupled with revascularization has been shown to reduce ischemic risk after an acute coronary syndrome (ACS) (1), but such strategies are performed at the expense of an increased risk of bleeding (2). Recent analyses showed that major bleeding events were equivalent or even more prognostic for death than spontaneous myocardial infarction (3, 4).

In particular, East Asian people have different risk profiles for both thrombophilia and bleeding and might be more susceptible to bleeding (5). For potent antithrombotic therapy, various reports have failed to show a net clinical benefit in East Asian patients in contrast to similar studies in Caucasian patients (6). There are several studies describing temporal changes in bleeding rates among Western populations during the past decades (7–9), but no such data are available in East Asian countries. Therefore, we used data from the CCC-ACS project (Improving Care for Cardiovascular Disease in China–Acute Coronary Syndrome) (10) to delineate the temporal trend of in-hospital major bleeding in relation to development of therapeutic strategies and outcomes from 2015 to 2019 among Chinese patients hospitalized for ACS.

METHODS

Study Design and Population

The CCC-ACS project (NCT02306616) is an ongoing nationwide registry and quality improvement project focusing on the quality of care for patients with ACS. The project was launched in November 2014 as a collaborative initiative of the American Heart Association and the Chinese Society of Cardiology. Details of the study design and methodology have been described elsewhere (10). In brief, the study included 159 tertiary hospitals and 82 secondary hospitals in China. In each hospital, the first 20 to 30 ACS patients of each month are consecutively recruited and identified based on principal discharge diagnosis. ACS was defined according to the guidelines published by the Chinese Society of Cardiology for the diagnosis and management of patients with ST-segment-elevation myocardial infarction (STEMI) and non-ST-segment elevation (NSTE)-ACS (11, 12). The Ethics Committee of Beijing Anzhen Hospital, Capital Medical University approved the study with a waiver for informed consent. The research was performed without patient or public involvement.

Overall, 113,650 inpatients with ACS from 241 hospitals were registered between November 2014 and December 2019. Of these, 113,567 patients were included in this study after excluding 83 (0.07%) patients with missing in-hospital outcomes.

Data Collection

A standard web-based data collection platform (Oracle Clinical Remote Data Capture, Oracle) was used. Data elements included patients' characteristics, medical history, clinical presentation, diagnosis and risk evaluation, in-hospital management, discharge medications and in-hospital outcomes. Third-part clinical research associates performed regular quality audits to ensure that cases were reported consecutively rather than selectively.

In-hospital Outcomes

Major bleeding was defined as a composite of intracranial bleeding, retroperitoneal bleeding, a decline in hemoglobin levels $\geq$3 g/dL during hospitalization, transfusion with overt bleeding, or bleeding requiring surgical intervention, and fatal bleeding. Major adverse cardiovascular events (MACE) included cardiac death, reinfarction, stent thrombosis, and ischemic stroke. Cardiac death was defined as death related to proximate cardiac causes, procedure-related complications, or any death unless an unequivocal non-cardiovascular cause could be established. All these outcomes were diagnosed by doctors during patients' hospitalization and recorded in medical records.

Statistical Analysis

Changes in patients' characteristics, in-hospital management and outcomes were evaluated annually (from 2015 to 2019). The number of patients in 2014 was small and thus added to the number of patients in 2015. For in-hospital major bleeding, patients were also stratified by sex, age, type of ACS [STEMI, non ST segment elevation myocardial infarction (NSTEMI), unstable angina pectoris (UAP)], diabetes mellitus, hypertension, eGFR at admission, Killip class, percutaneous coronary intervention (PCI), type of $P2Y_{12}$ inhibitor, parenteral anticoagulation therapy, and GPIIb/IIIa inhibitor use during hospitalization. Continuous variables were shown as mean [standard deviation (SD)] unless otherwise indicated. Categorical variables were presented as the number (percentage). Kruskal–Wallis test was used to examine the trend of major bleeding and ischemic outcomes over time.

To assess the effect of time on major bleeding, assuming a linear association for each 1-year time-block and outcome, a logistic regression model was fitted. These models explored the association for moving forward 1 year, with stepwise adjustments as follows: (1) crude; (2) age and gender; (3) baseline characteristics (diabetes mellitus, hypertension, eGFR$<$ 60 min per 1.73 m^2, STEMI, and Killip class); (4) in-hospital antithrombotic treatments (GPIIb/IIIa inhibitor use, anticoagulant treatment, and ticagrelor use); and (5) invasive treatments [PCI (for STEMI, primary PCI), transradial access]. Standardization of rate of bleeding was performed using logistic regression models to account for the effect of differences in previously described patient characteristics and treatments throughout the observation period.

For variables with a missing rate of $<$15%, we imputed missing values using the sequential regression multiple imputation method implemented by IVEware software version 0.2 (Survey

TABLE 1 | Baseline characteristics.

	2015 (*n* = 29,957)	2016 (*n* = 25,028)	2017 (*n* = 18,979)	2018 (*n* = 19,595)	2019 (*n* = 20,008)	2015–2019 (*n* = 113,567)
Age, y	62.8 ± 12.5	62.9 ± 12.4	63.5 ± 12.4	64.0 ± 12.4	64.4 ± 12.3	63.4 ± 12.4
Female	7,516 (25.1)	6,265 (25.0)	5,117 (27.0)	5,554 (28.3)	6,010 (30.0)	30,462 (27.1)
Hypertension	19,446 (64.9)	16,372 (65.4)	12,637 (66.6)	13,378 (68.3)	13,779 (68.9)	75,612 (67.2)
Diabetes	13,090 (43.7)	11,101 (44.4)	8,829 (46.5)	9,156 (46.7)	9,158 (45.8)	51,334 (45.2)
Hyperlipidemia	25,325 (84.5)	21,015 (84.0)	15,829 (83.4)	16,386 (83.6)	16,396 (82.0)	94,951 (84.4)
Previous MI	2,415 (8.1)	1,826 (7.3)	1,572 (8.3)	1,826 (9.3)	1,885 (8.4)	9,524 (8.4)
Previous PCI	2,267 (7.6)	1,922 (7.7)	1,591 (8.4)	1,762 (9.0)	2,112 (10.6)	9,654 (8.5)
Previous CABG	154 (0.5)	126 (0.5)	104 (0.6)	118 (0.6)	91 (0.5)	593 (0.5)
Previous atrial fibrillation	798 (2.7)	538 (2.2)	424 (2.2)	486 (2.5)	460 (2.3)	2,706 (2.4)
Previous heart failure	730 (2.4)	426 (1.7)	375 (2.0)	570 (2.9)	595 (3.0)	2,696 (2.4)
Previous stroke	3,017 (10.1)	2,314 (9.3)	1,666 (8.8)	1,446 (7.4)	1,570 (7.9)	10,013 (8.9)
Previous peripheral vascular disease	347 (1.2)	217 (0.9)	173 (0.9)	184 (0.9)	229 (1.1)	1,150 (1.0)
Systolic blood pressure, mmHg	129.6 ± 23.5	130.5 ± 23.5	131.1 ± 23.5	132.3 ± 23.5	133.2 ± 24.1	133.2 ± 24.1
Diastolic pressure, mmHg	77.7 ± 14.4	78.2 ± 14.4	78.5 ± 14.2	79.3 ± 14.6	79.9 ± 14.7	79.9 ± 14.7
Heart rate, beats per min	77.2 ± 16.2	77.6 ± 16.3	77.6 ± 16.1	77.9 ± 16.3	78.3 ± 16.7	78.3 ± 16.7
STEMI	19,365 (64.6)	15,429 (61.7)	10,910 (57.5)	10,476 (53.5)	9,390 (46.9)	65,570 (58.3)
Cardiogenic shock	1,257 (6.5)	974 (6.3)	675 (6.2)	599 (5.7)	601 (6.4)	4,106 (6.3)
Cardiac arrest	687 (2.3)	439 (1.8)	195 (1.0)	125 (0.6)	111 (0.6)	1,557 (1.4)
Killip class	20,213 (67.5)	17,096 (68.3)	12,489 (65.8)	12,298 (62.8)	12,637 (63.2)	74,733 (65.8)
Class I						
Class II–III	8,066 (26.9)	6,614 (26.4)	5,484 (28.9)	6,230 (31.8)	6,208 (31.0)	32,602 (28.7)
Class IV	1,678 (5.6)	1,318 (5.3)	1,006 (5.3)	1,067 (5.5)	1,163 (5.8)	6,232 (5.5)
Renal insufficiency (eGFR < 60 min per 1.73 m^2)	5,467 (18.3)	4,362 (17.4)	3,375 (17.8)	3,554 (18.1)	3,580 (17.9)	20,338 (18.1)
Hemoglobin, g/dL	13.6 ± 2.1	13.6 ± 2.0	13.6 ± 2.0	13.7 ± 2.1	13.6 ± 2.1	13.6 ± 2.1

CABG, coronary artery bypass grafting; eGFR, estimated glomerular filtration rate; MI, myocardial infarction; PCI, percutaneous coronary intervention.

Research Center, University of Michigan, Ann Arbor, MI, USA). Missing rates of variables and strategies for the management of missing data are presented in **Supplementary Table 1**. Statistical analyses were performed using SAS 9.4 (SAS Institute, Cary, NC, USA), SPSS 26.0 (IBM SPSS Inc., Armonk, NY) and Stata 14.0 (Stata, College Station, TX, USA). Two-tailed *p*-values of <0.05 were considered statistically significant.

RESULTS

Mean patient age of the whole cohort was 63.4 ± 12.4 years, and 27.1% were female. Most of the patients' characteristics showed only minor changes during the study period. There was a slight increase in the proportion of female patients and the prevalence of hypertension and previous PCI, and a decrease in the prevalence of previous stroke. The proportion of STEMI patients decreased steadily, associated with a temporal decline in patients with cardiac arrest (**Table 1**).

The use of antithrombotic therapies changed over time, with a fall in the use of anticoagulation therapy (77.5–60.6%) during hospitalization among all ACS patients. There was a marked decrease in the use of GP IIb/IIIa inhibitors over time (34.1–19.6%). Use of PCI was high in all ACS patients with extremely high proportion of radial access throughout the whole study period. The proportion of primary PCI in STEMI patients also increased over time (**Table 2**).

In-hospital Bleeding

Overall, the rate of in-hospital major bleeding decreased from 6.3% in 2015 to 4.7% in 2019 (absolute change 1.6%, relative change 25.4%, unadjusted OR = 0.74, 95% CI: 0.68–0.80, and $P < 0.001$; **Tables 3**, **4**; **Figure 1A**). A similar trend was found in patients with overt bleeding and those without overt bleeding but with decline in hemoglobin levels ≥3 g/dL (**Table 4**). The decrease of in-hospital bleeding occurred in parallel to the decreased use of GP IIb/IIIa inhibitors and anticoagulation therapy during hospitalization (**Table 2**; **Figure 1B**). Patients with NSTE-ACS (including NSTEMI and UAP) had a lower rate of bleeding than patients with STEMI, and similar trends were found in patients with NSTEMI and UAP (**Table 4**;

TABLE 2 | In-hospital management*.

	2015 (*n* = 29,957)	2016 (*n* = 25,027)	2017 (*n* = 18,979)	2018 (*n* = 19,595)	2019 (*n* = 20,008)	2015–2019 (*n* = 113,567)
Antiplatelet therapy						
None	828 (2.8)	743 (3.0)	636 (3.4)	813 (4.2)	929 (4.6)	3,949 (3.5)
Aspirin only	499 (1.7)	572 (2.3)	606 (3.2)	984 (5.0)	1,184 (5.9)	3,845 (3.4)
$P2Y_{12}$ receptor inhibitor only	799 (2.7)	592 (2.4)	524 (2.8)	511 (2.6)	546 (2.7)	2,972 (2.6)
DAPT	27,831 (92.9)	23,121 (92.4)	17,213 (90.7)	17,287 (88.2)	17,349 (86.7)	102,801 (91.4)
Ticagrelor	3,863 (13.5)	4,788 (20.2)	4,549 (25.7)	6,408 (36.0)	7,857 (43.9)	27,465 (24.4)
Glycoprotein IIb/IIIa inhibitors†	10,217 (34.1)	7,171 (28.7)	4,520 (23.8)	4,375 (22.3)	3,925 (19.6)	30,208 (26.9)
Anticoagulation therapy‡	23,207 (77.5)	18,205 (72.7)	13,149 (69.3)	12,477 (63.7)	12,130 (60.6)	79,168 (70.4)
UFH‡	1,159 (3.9)	837 (3.3)	657 (3.5)	483 (2.5)	932 (4.7)	4,068 (3.6)
LMWH‡	21,651 (72.3)	16,831 (67.3)	12,109 (63.8)	11,647 (59.4)	11,164 (55.8)	73,402 (65.3)
UFH or LMWH‡	22,449 (74.9)	17,385 (69.5)	12,511 (65.9)	11,935 (60.9)	11,804 (59.0)	76,084 (67.0)
Fondaparinux‡	405 (1.4)	346 (1.4)	270 (1.4)	321 (1.6)	143 (0.7)	1,485 (1.3)
Others‡	438 (1.5)	512 (2.1)	407 (2.1)	253 (1.3)	208 (1.0)	1,818 (1.6)
Warfarin	186 (0.6)	168 (0.7)	142 (0.8)	170 (0.9)	126 (0.6)	792 (0.7)
β-blockers	16,625 (55.5)	13,591 (54.3)	10,822 (57.0)	11,455 (58.5)	10,978 (54.9)	63,471 (55.9)
ACEI or ARB	14,439 (48.2)	11,755 (47.0)	9,178 (48.4)	9,502 (48.5)	8,737 (43.7)	53,611 (47.2)
Statins	28,094 (93.8)	23,349 (93.3)	17,658 (93.0)	18,322 (93.5)	18,665 (93.3)	106,088 (93.4)
Coronary angiography	21,378 (71.4)	18,981 (75.8)	14,893 (78.5)	15,262 (77.9)	14,761 (73.8)	85,275 (75.1)
PCI	19,372 (64.7)	18,142 (72.5)	13,641 (71.9)	13,473 (68.8)	12,917 (64.6)	77,545 (69.0)
DES§	16,556 (85.5)	15,197 (83.8)	11,687 (85.7)	11,934 (88.6)	11,192 (86.7)	66,566 (85.8)
BMS§	126 (0.7)	180 (1.0)	90 (0.7)	39 (0.3)	91 (0.7)	526 (0.7)
PTCA§	2,594 (13.4)	2,575 (14.2)	1,768 (13.0)	1,476 (11.0)	1,570 (12.2)	9,983 (12.9)
Others§	96 (0.5)	190 (1.1)	96 (0.7)	24 (0.2)	64 (0.5)	470 (0.6)
Primary PCI in STEMI patients	10,165 (52.5)	8,537 (55.3)	6,150 (56.4)	6,337 (60.5)	6,048 (64.4)	37,237 (56.8)
Thrombolysis	769 (2.6)	447 (1.8)	607 (3.2)	837 (4.3)	738 (3.7)	3,398 (3.0)
Transradial access	19,792 (92.6)	18,002 (94.8)	14,383 (96.6)	14,668 (96.1)	14,222 (96.3)	81,067 (95.1)

**The medication use is defined as each medication used within 24 h after first medical contact unless otherwise indicated. †Defined as use of glycoprotein IIb/IIIa inhibitors at any time during hospitalization. ‡Defined as use of anticoagulant during hospitalization but not during index procedure. §Denominator is the total number of PCI patients enrolled in each year. ACEI, angiotensin converting enzyme inhibitors; ARB, angiotensin receptor blockers; BMS, bare metal stent; DAPT, dual antiplatelet therapy; DES, drug eluting stent; LMWH, low molecular weight heparin; PCI, percutaneous coronary intervention; PTCA, percutaneous transluminal coronary angioplasty; STEMI, ST-segment elevation myocardial infarction; UFH, unfractionated heparin.*

Figure 1A). The trend of bleeding was consistent across almost all subgroups including age, sex, eGFR, P2Y12 receptor inhibitor, and anticoagulation therapy (**Table 4**).

After adjustment for patient characteristics, medications, and interventions, the downward changes in bleeding were attenuated but remained for all ACS (**Table 5**). To evaluate the impact of changes in baseline characteristics and in-hospital management on outcomes, we did stepwise adjustments and analyzed the association between change in time-period and the risk of major bleeding. Each 1-year advancement was associated with reduced risk of bleeding in the crude analysis (OR = 0.91, 95% CI: 0.89–0.93) and after adjustment for changes in demographics (OR = 0.91, 95% CI: 0.89–0.92). The OR increased to 0.93 (95% CI: 0.91–0.94) after adjusting for baseline characteristics and further increased to 0.95 (95% CI: 0.93–0.97) after adjusting for antithrombotic treatments but did not change after adjusting for invasive treatment (OR = 0.95, 95% CI: 0.93–0.97; **Figure 2**). For patients with NSTE-ACS, only changes in antithrombotic therapy explained the time related reduction in bleeding. However, for patients with STEMI, the association was attenuated after adjusting for changes in antithrombotic therapy and was no longer significant after further adjusting for invasive treatments (mainly primary PCI; **Figure 2).**

Ischemic Outcomes

The annual rate of reinfarction, stent thrombosis, and ischemic stroke remains relatively low and constant. The incidence of MACE decreased steadily with an absolute decrease of 1.5% (from 2.9 to 1.4%), mainly driven by a decrease of cardiac death (from 2.2 to 0.8%; **Table 3**; **Figure 1C**). The rate of all-cause death also decreased over time (from 2.3 to 1.4%; **Table 3**). When combining ischemic and bleeding events together, a significant decrease in total events was also observed (**Figure 1D**).

TABLE 3 | In-hospital outcomes in all ACS patients.

	2015 (*n* = 29,957)	2016 (*n* = 25,027)	2017 (*n* = 18,979)	2018 (*n* = 19,595)	2019 (*n* = 20,008)	*P* for trend
Major bleeding	1,896 (6.3)	1,521 (6.1)	994 (5.2)	865 (4.4)	948 (4.7)	<0.001
MACE	859 (2.9)	528 (2.1)	318 (1.7)	326 (1.7)	288 (1.4)	<0.001
Cardiac death	650 (2.2)	383 (1.5)	212 (1.1)	217 (1.1)	167 (0.8)	<0.001
Reinfarction	124 (0.4)	75 (0.3)	72 (0.4)	86 (0.4)	79 (0.4)	0.14
Stent thrombosis	65 (0.2)	43 (0.2)	15 (0.1)	18 (0.1)	15 (0.1)	<0.0001
Ischemic stroke	87 (0.3)	60 (0.2)	39 (0.2)	32 (0.2)	49 (0.2)	0.06
All-cause death	689 (2.3)	412 (1.7)	249 (1.3)	272 (1.4)	278 (1.4)	<0.001

ACS, acute coronary syndrome; MACE, major adverse cardiovascular events.

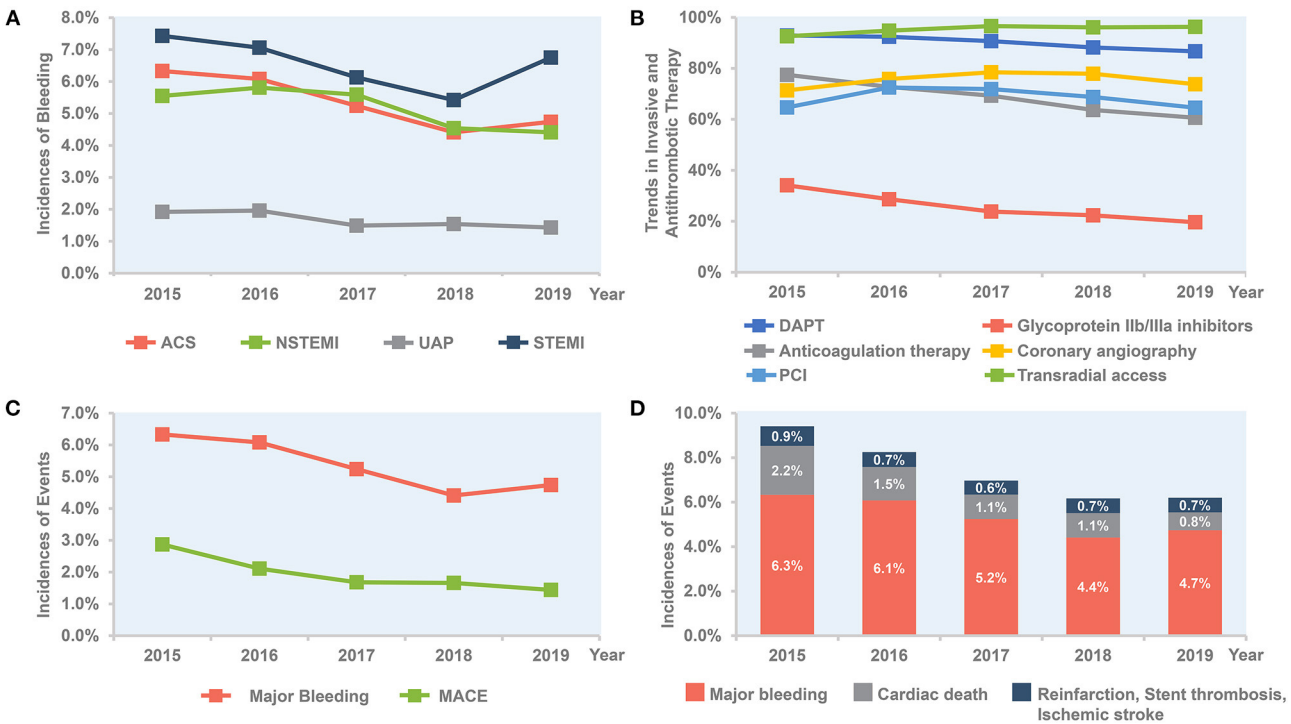

FIGURE 1 | Temporal trend of in-hospital outcomes and treatment, 2015–2019. **(A)** Trends in rate of bleeding for all patients and per subgroup of STEMI, NSTEMI, and UAP. **(B)** Trends in invasive and antithrombotic therapy in all ACS patients. **(C)** Bleeding vs. MACE in all ACS patients. **(D)** Combined bleeding and ischemic outcomes in all ACS patients. ACS, acute coronary syndrome; DAPT, dual antiplatelet therapy; MACE, major adverse cardiovascular events; NSTE-ACS, non-ST-segment elevation acute coronary syndrome; NSTEMI, non-ST-segment elevation myocardial infarction; PCI, percutaneous coronary intervention; STEMI, ST-segment elevation myocardial infarction; UAP, unstable angina pectoris.

DISCUSSION

The present analysis from the large CCC-ACS registry showed an absolute 1.6% decrease in major bleeding in relation to more evidence-based use of antithrombotic therapies in patients hospitalized for ACS in China. Simultaneously, the incidence of ischemic events including cardiac death decreased steadily during the study period. To the best of our knowledge, this is the first report to delineate the temporal changes of bleeding events in East Asian countries with a higher risk profile for bleeding.

The study shows a continuous reduction in bleeding from 2015 to 2019, which is accompanied by a decrease in use of GP IIb/IIIa inhibitors and parenteral anticoagulation therapy during hospitalization. These findings are in line with recent studies from the SWEDEHEART registry (7) and UK database (8) showing a decline in in-hospital bleeding associated with less use of GP IIb/IIIa inhibitors. Specifically, the use of GP IIb/IIIa inhibitors was still as high as 20% in 2019 compared with 4.7% in 2017/2018 in the SWEDEHEART registry (7). Currently, GP IIb/IIIa inhibitors are recommended on a "provisional" basis with decreased TIMI flow or new thrombus. Nevertheless, in

TABLE 4 | Trends in rate of bleeding by patients' characteristics and in-hospital management.

Characteristics	Event rates					%Change from 2015 to 2019		
	2015 (*n* = 29,957)	2016 (*n* = 25,027)	2017 (*n* = 18,979)	2018 (*n* = 19,595)	2019 (*n* = 20,008)	Absolute Change	Relative Change	*P* for trend
Overall major bleeding	1,896 (6.3)	1,521 (6.1)	994 (5.2)	865 (4.4)	948 (4.7)	1.6	25.4	<0.001
Overt bleeding	718 (2.4)	560 (2.2)	310 (1.6)	287 (1.5)	335 (1.7)	0.7	29.2	<0.001
Non-overt bleeding with decline in hemoglobin levels ≥3 g/dL	1,178 (3.9)	961 (3.8)	684 (3.6)	684 (3.0)	613 (3.1)	0.8	20.5	<0.001
Sex								
Male	1,391 (6.2)	1,141 (6.1)	743 (5.4)	642 (4.6)	677 (4.8)	1.4	22.6	<0.001
Female	505 (6.7)	380 (6.1)	251 (4.9)	223 (4.0)	271 (4.5)	2.2	32.8	<0.001
Age								
≥75	458 (7.8)	380 (7.7)	263 (7.0)	222 (5.6)	250 (6.0)	1.8	23.1	<0.001
<75	1,438 (6.0)	1,141 (5.7)	731 (4.8)	643 (4.1)	698 (4.4)	1.6	26.7	<0.001
Type of ACS								
STEMI	1,439 (7.4)	1,089 (7.1)	669 (6.1)	568 (5.4)	634 (6.8)	0.6	8.1	<0.001
NSTE-ACS	457 (4.3)	432 (4.5)	325 (4.0)	297 (3.3)	314 (3.0)	1.3	30.2	<0.001
NSTEMI	388 (5.6)	368 (5.8)	279 (5.6)	237 (4.5)	240 (4.4)	1.1	20.5	<0.001
UAP	69 (1.9)	64 (2.0)	46 (1.5)	60 (1.5)	74 (1.4)	0.5	25.5	0.03
Diabetes mellitus								
Yes	1,001 (7.7)	773 (7.0)	532 (6.0)	443 (4.8)	468 (5.1)	2.6	33.8	<0.001
No	895 (5.3)	748 (5.4)	462 (4.6)	422 (4.0)	480 (4.4)	0.9	11.3	<0.001
Hypertension								
Yes	1,304 (6.7)	1,061 (6.5)	693 (5.5)	619 (4.6)	647 (4.7)	2.0	29.9	<0.001
No	592 (5.6)	460 (5.3)	301 (4.8)	246 (4.0)	301 (4.8)	0.8	14.3	<0.001
eGFR								
<60 mL/min per 1.73 m^2	573 (10.5)	412 (9.5)	279 (8.3)	233 (6.6)	252 (7.0)	3.5	33.3	<0.001
≥60 mL/min per 1.73 m^2	1,323 (5.4)	1,109 (5.4)	715 (4.6)	632 (3.9)	696 (4.2)	1.2	22.2	<0.001
Killip class								
I	1,071 (5.3)	890 (5.2)	574 (4.6)	491 (4.0)	515 (4.1)	1.2	22.6	<0.001
II–III	584 (7.2)	449 (6.8)	306 (5.6)	284 (4.6)	299 (4.8)	2.4	33.3	<0.001
IV	241 (14.4)	182 (13.8)	114 (11.3)	90 (8.4)	134 (11.5)	2.9	20.1	<0.001
PCI								
Yes	1,244 (6.4)	1,096 (6.0)	716 (5.3)	639 (4.7)	709 (5.5)	0.9	14.1	<0.001
No	652 (6.2)	425 (6.2)	278 (5.2)	226 (3.7)	239 (3.4)	2.8	45.2	<0.001
P2Y12 inhibitor								
Ticagrelor	321 (8.3)	345 (7.2)	258 (5.7)	273 (4.3)	392 (5.0)	3.3	39.8	<0.001
Clopidogrel	1,441 (5.8)	1,061 (5.6)	655 (5.0)	516 (4.5)	473 (4.7)	1.1	19.0	<0.001
Anticoagulation therapy								
Yes	1,511 (6.5)	1,167 (6.4)	737 (5.6)	593 (4.8)	613 (5.1)	1.4	21.5	<0.001
No	385 (5.7)	354 (5.2)	257 (4.4)	272 (3.8)	335 (4.3)	1.4	24.6	<0.001
UFH or LMWH								
Yes	1,464 (6.5)	1,121 (6.5)	709 (5.7)	570 (4.8)	602 (5.1)	1.4	21.5	<0.001
No	432 (5.8)	400 (5.2)	285 (4.4)	295 (3.9)	346 (4.2)	1.6	27.6	<0.001
GP IIb/IIIa inhibitor								
Yes	782 (7.7)	574 (8.0)	300 (6.6)	288 (6.6)	302 (7.7)	0.0	0.0	0.096
No	1,114 (5.6)	947 (5.3)	694 (4.8)	577 (3.8)	646 (4.0)	1.6	28.6	<0.001

ACS, acute coronary syndrome; eGFR, estimated glomerular filtration rate; LMWH, low molecular weight heparin; NSTE-ACS, non-ST-segment elevation acute coronary syndrome; NSTEMI, non-ST-segment elevation myocardial infarction; PCI, percutaneous coronary intervention; STEMI, ST-segment elevation myocardial infarction; UAP, unstable angina pectoris; UFH, unfractionated heparin.

many secondary hospitals in China, GP IIb/IIIa inhibitors were almost routinely used during and/or after PCI in STEMI or NSTEMI patients, which actually have no robust evidence but may increase bleeding. Furthermore, anticoagulation therapy (especially the use of LMWH) was regarded as a default therapy following ACS or PCI among many centers in China. However, this strategy was not associated with a lower risk of all-cause death or myocardial infarction but significantly increased risk of major bleeding in the era of PCI and DAPT (13). The decrease from 77.5 to 60.6% in anticoagulation therapy might

TABLE 5 | Standardized rate of bleeding in all ACS patients.

	2015 (*n* = 29,957)	2016 (*n* = 25,027)	2017 (*n* = 18,979)	2018 (*n* = 19,595)	2019 (*n* = 20,008)
Model 1*	6.4 (6.1–6.7)	6.1 (5.8–6.4)	5.2 (4.9–5.6)	4.4 (4.1–4.7)	4.7 (4.4–5.0)
Model 2†	6.1 (5.9–6.4)	6.0 (5.7–6.3)	5.2 (4.9–5.6)	4.5 (4.2–4.8)	5.0 (4.7–5.3)
Model 3‡	5.8 (5.6–6.1)	6.0 (5.7–6.2)	5.4 (5.0–5.7)	4.6 (4.3–4.9)	5.2 (4.9–5.5)

**Adjusted for age and gender.*

†Adjusted for age, gender, and baseline characteristics (diabetes mellitus, hypertension eGFR<60 min per 1.73 m, STEMI, and Killip class).

‡Adjusted for age, gender, baseline characteristics, and in-hospital treatments (GPIIb/IIIa inhibitor use, anticoagulant treatment, ticagrelor use, PCI [for STEMI, primary PCI], and transradial access).

ACS, acute coronary syndrome; eGFR, estimated glomerular filtration rate; PCI, percutaneous coronary intervention; STEMI, ST-segment elevation myocardial infarction.

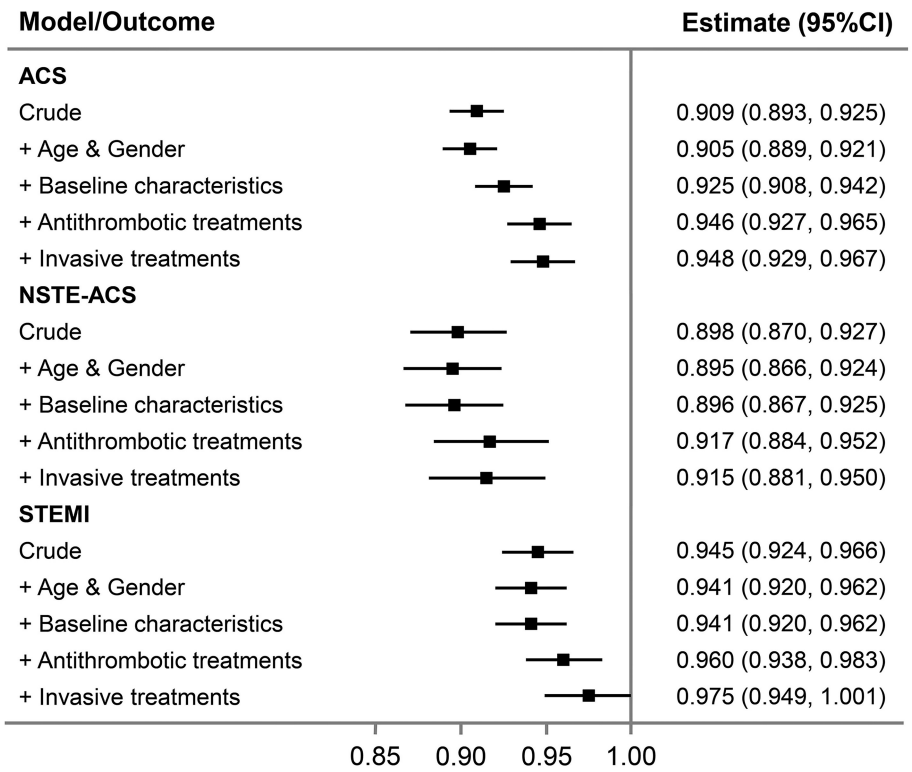

FIGURE 2 | Association between 1 year change in time-period and major bleeding in all ACS patients and per subgroup of NSTE-ACS and STEMI. Stepwise adjustments as follows: (1) crude; (2) age and gender; (3) baseline characteristics (diabetes mellitus, hypertension, eGFR < 60 min per 1.73 m^2, STEMI, and Killip class); (4) in-hospital antithrombotic treatments (GPIIb/IIIa inhibitor use, anticoagulant treatment, and ticagrelor use); and (5) invasive treatments [PCI (for STEMI, primary PCI), transradial access]. ACS, acute coronary syndrome; NSTE-ACS, non-ST-segment elevation acute coronary syndrome; PCI, percutaneous coronary intervention; STEMI, ST-segment elevation myocardial infarction.

also have driven the decline in bleeding events. These findings were supported by stepwise adjustments for antithrombotic therapies, which showed attenuated association of time-period and bleeding trend.

In contrast to prior reports (7, 8, 14), our study was performed on the background of high rates of radial access (95.1% from 2015 to 2019) with no significant change over the past 5 years. This strategy is intuitively a bleeding reduction strategy as recommended by guidelines (15, 16). Recent study of Japanese population also showed low risk of bleeding complications by use of transradial approach or vascular closure device (17). However, data on vascular closure device was not collected in the CCC-ACS registry. Due to high rate of radial access in our study, vascular access strategies were minimally associated with these observed reductions in bleeding rates over time. The use of new-generation DES featuring much lower strut thickness and biodegradable polymers or polymer- free designs allows the shortening of DAPT (18–20). Also, use of intravascular imaging to optimize the PCI procedure and achieve more complete endothelialization is important in patients at high risk of bleeding who might need a short duration of DAPT (21). Additional strategies include the use of proton pump inhibitors to reduce risk of

gastrointestinal bleeding who need antithrombotic medications (22, 23). Although not collected in this project, these factors should be further addressed. Finally, there was a steep rise in the rate of bleeding in STEMI patients from 2018 to 2019. We noted that the proportion of cardiogenic shock in STEMI patients showed a decrease from 2015 to 2018 but a sharp rise from 2018 to 2019, which might at least partially explain this peculiar change. Other potential confounding factors may also take effects and should be further investigated.

In October 2016, the Chinese College of Cardiovascular Physicians Working Group on Thrombosis proposed a multidisciplinary expert consensus on the prevention and management of bleeding in patients with ACS receiving antithrombotic agents (24). The consensus proposed a multidisciplinary bleeding prevention and treatment framework with the cardiologist as the leader and several bleeding avoidance therapies including bleeding risk evaluation, tailored antithrombotic regimen, avoiding unnecessary in-hospital anticoagulation, crossover of anticoagulants, and use of GP IIb/IIIa inhibitors, and early use of PPI, which may partly explain the decline in bleeding rate after 2016.

The higher bleeding rate in our study compared with other reports maybe be partly attributed to higher proportion of STEMI patients and more use of GP IIb/IIIa inhibitors (≈20 vs. <5% in other registries) (7, 8) and anticoagulants. Actually, various studies have reported that East Asian people might be less prone to thrombosis and more prone to bleeding, especially in the context of potent antithrombotic therapy (25). In spite of this, our registry showed a faster and more substantial decrease in bleeding (2015–2019, from 6.3 to 4.7%, absolute change 1.6%) compared with the SWEDEHEART registry (2006/2007 to 2015/2016, from 2.0 to 1.3%, absolute change 0.7%).

On the other hand, the absolute reduction of MACE including cardiac death is also intriguing. In detail, the ischemic events including reinfarction, stent thrombosis, and ischemic stroke did not change a lot across the study. Although precisely causal link should be clearly established, we speculate the reduced rate of cardiac death might be in part owing to the decline of bleeding, as the latter may cause premature discontinuation of antithrombotic medications, reduced myocardial oxygen delivery due to hypotension and anemia, and blood transfusion (26). In the present study, we did not observe plateauing in bleeding rates, indicating that there is room for further lowering of event rates by further expansion of recommended therapies, which have not been fully exploited [e.g., high rate of GP IIb/IIIa inhibitors and anticoagulants use in 2019 compared to other registries (7, 8)].

Limitations

First, bleeding events were self-reported and not adjudicated, possibly leading to underreporting. Second, the standardized bleeding definitions which were usually used in clinical trials were not available in our registry, although the definitions remained unchanged during the study period. However, our bleeding definition is similar to BARC 3 or 5 bleeding. Third, given the observational design of this study, the cause-effect relationship should not be established between change in antithrombotic therapy and temporal reduction in bleeding. Fourth, the information of IABP, which might be associated with bleeding, was only available from 2017 to 2019 and was not presented. Fifth, whether bleeding was access site related or not was not collected in this registry. Sixth, out of hospital events were also not reported. Seventh, data regarding the use of bivalirudin and new oral anticoagulants, which have been related to lower risk of bleeding, were not collected due to their infrequent use. Finally, the effects of timing, dosing, and crossover of anticoagulants and antiplatelets could not be assessed based on this registry.

CONCLUSIONS

The present study shows a temporal reduction in in-hospital bleeding among Chinese ACS patients during the last 5 years. The changes in bleeding are largely associated with the decreased use of GP IIb/IIIa inhibitors and anticoagulation therapy. Given a higher risk profile for bleeding in the Chinese population, a more consistent and systematic application of evidence-based therapies and promotion of new treatment concepts are needed to further reduce bleeding risk and improve overall outcomes.

DATA AVAILABILITY STATEMENT

The datasets analyzed during the current study are not publicly available because of intellectual property rights, but are available from the corresponding author on reasonable request.

ETHICS STATEMENT

The studies involving human participants were reviewed and approved by Ethics Committee of Beijing Anzhen Hospital, Capital Medical University. Written informed consent for participation was not required for this study in accordance with the national legislation and the institutional requirements.

AUTHOR CONTRIBUTIONS

XW, GZ, SN, and YaH: study concept and design. XW, GZ, MZ, YoH, JuL, JiL, DZ, SN, and YaH: acquisition, analysis, or interpretation of data. XW and GZ: drafting of the manuscript. XW, GZ, and SN had full access to all the data in the study and take responsibility for the integrity of the data and the accuracy of the data analysis. All authors critical revision of the manuscript for important intellectual content, read, and approved the final manuscript.

FUNDING

This work was supported by a collaborative program of the American Heart Association (AHA) and the Chinese Society of Cardiology. The AHA was funded by Pfizer for the quality improvement initiative through an independent grant for learning and change.

ACKNOWLEDGMENTS

The authors thank all participating hospitals for their contributions to the CCC-ACS project (Improving Care for Cardiovascular Disease in China-Acute Coronary Syndrome).

SUPPLEMENTARY MATERIAL

The Supplementary Material for this article can be found online at: https://www.frontiersin.org/articles/10.3389/fcvm.2021.769165/full#supplementary-material

REFERENCES

1. Szummer K, Wallentin L, Lindhagen L, Alfredsson J, Erlinge D, Held C, et al. Relations between implementation of new treatments and improved outcomes in patients with non-ST-elevation myocardial infarction during the last 20 years: experiences from SWEDEHEART registry 1995 to 2014. *Eur Heart J.* (2018) 39:3766–76. doi: 10.1093/eurheartj/ehy554
2. Steg PG, Huber K, Andreotti F, Arnesen H, Atar D, Badimon L, et al. Bleeding in acute coronary syndromes and percutaneous coronary interventions: position paper by the Working Group on Thrombosis of the European Society of Cardiology. *Eur Heart J.* (2011) 32:1854–64. doi: 10.1093/eurheartj/ehr204
3. Marquis-Gravel G, Dalgaard F, Jones AD, Lokhnygina Y, James SK, Harrington RA, et al. Post-discharge bleeding and mortality following acute coronary syndromes with or without PCI. *J Am Coll Cardiol.* (2020) 76:162–71. doi: 10.1016/j.jacc.2020.05.031
4. Piccolo R, Oliva A, Avvedimento M, Franzone A, Windecker S, Valgimigli M, et al. Mortality after bleeding versus myocardial infarction in coronary artery disease: a systematic review and meta-analysis. *EuroIntervention.* (2021) 17:550–60. doi: 10.4244/EIJ-D-20-01197
5. Kang J, Park KW, Palmerini T, Stone GW, Lee MS, Colombo A, et al. Racial differences in ischaemia/bleeding risk trade-off during anti-platelet therapy: individual patient level landmark meta-analysis from seven RCTs. *Thromb Haemost.* (2019) 119:149–62. doi: 10.1055/s-0038-1676545
6. Park DW, Kwon O, Jang JS, Yun SC, Park H, Kang DY, et al. Clinically significant bleeding with ticagrelor versus clopidogrel in korean patients with acute coronary syndromes intended for invasive management: a randomized clinical trial. *Circulation.* (2019) 140:1865–77. doi: 10.1161/CIRCULATIONAHA.119.041766
7. Simonsson M, Wallentin L, Alfredsson J, Erlinge D, Hellstrom Angerud K, Hofmann R, et al. Temporal trends in bleeding events in acute myocardial infarction: insights from the SWEDEHEART registry. *Eur Heart J.* (2020) 41:833–43. doi: 10.1093/eurheartj/ehz593
8. Olier I, Carr M, Curzen N, Ludman P, Baumbach A, Kinnaird T, et al. Changes in periprocedural bleeding complications following percutaneous coronary intervention in the United Kingdom between 2006 and 2013 (from the British Cardiovascular Interventional Society). *Am J Cardiol.* (2018) 122:952–60. doi: 10.1016/j.amjcard.2018.06.016
9. Subherwal S, Peterson ED, Dai D, Thomas L, Messenger JC, Xian Y,et al. Temporal trends in and factors associated with bleeding complications among patients undergoing percutaneous coronary intervention: a report from the National Cardiovascular Data CathPCI Registry. *J Am Coll Cardiol.* (2012) 59:1861–9. doi: 10.1016/j.jacc.2011.12.045
10. Hao Y, Liu J, Liu J, Smith SC Jr, Huo Y, Fonarow GC, et al. Rationale and design of the Improving Care for Cardiovascular Disease in China (CCC) project: a national effort to prompt quality enhancement for acute coronary syndrome. *Am Heart J.* (2016) 179:107–15. doi: 10.1016/j.ahj.2016.06.005
11. China Society of Cardiology of Chinese Medical Association. Guideline for diagnosis and treatment of patients with ST-elevation myocardial infarction. *Chin J Cardiol.* (2010) 38:675–90. doi: 10.3760/cma.j.issn.0253-3758.2010.08.002
12. China Society of Cardiology of Chinese Medical Association. Guidelines for the management of acute coronary syndromes in patients presenting without persistent ST-segment elevation 2012. *Chin J Cardiol.* (2012) 40:353–67. doi: 10.3760/cma.j.issn.0253-3758.2012.05.001
13. Chen JY, He PC, Liu YH, Wei XB, Jiang L, Guo W, et al. Association of parenteral anticoagulation therapy with outcomes in Chinese patients undergoing percutaneous coronary intervention for non-ST-segment elevation acute coronary syndrome. *JAMA Intern Med.* (2019) 179:186–94. doi: 10.1001/jamainternmed.2018.5953
14. Elbarouni B, Elmanfud O, Yan RT, Fox KA, Kornder JM, Rose B,et al. Temporal trend of in-hospital major bleeding among patients with non ST-elevation acute coronary syndromes. *Am Heart J.* (2010) 160:420–7. doi: 10.1016/j.ahj.2010.05.036
15. Neumann FJ, Sousa-Uva M, Ahlsson A, Alfonso F, Banning AP, Benedetto U, et al. 2018 ESC/EACTS Guidelines on myocardial revascularization. *EuroIntervention.* (2019) 14:1435–534. doi: 10.4244/EIJY19M01_01
16. Capodanno D, Bhatt DL, Gibson CM, James S, Kimura T, Mehran R, et al. Bleeding avoidance strategies in percutaneous coronary intervention. *Nat Rev Cardiol.* (2021) doi: 10.1038/s41569-021-00598-1. [Epub ahead of print].
17. Sawano M, Spertus JA, Masoudi FA, Rumsfeld JS, Numasawa Y, Inohara T, et al. Bleeding avoidance strategies and percutaneous coronary intervention outcomes: a 10-year observation from a Japanese Multicenter Registry. *Am Heart J.* (2021) 235:113–24. doi: 10.1016/j.ahj.2021.01.010
18. Mehran R, Cao D, Angiolillo DJ, Bangalore S, Bhatt DL, Ge J, et al. 3- or 1-month DAPT in patients at high bleeding risk undergoing everolimus-eluting stent implantation. *JACC Cardiovasc Interv.* (2021) 14:1870–83. doi: 10.1016/j.jcin.2021.07.016
19. Kirtane AJ, Stoler R, Feldman R, Neumann FJ, Boutis L, Tahirkheli N, et al. Primary results of the EVOLVE Short DAPT study: evaluation of 3-month dual antiplatelet therapy in high bleeding risk patients treated with a bioabsorbable polymer-coated Everolimus-eluting stent. *Circ Cardiovasc Interv.* (2021) 14:e010144. doi: 10.1161/CIRCINTERVENTIONS.120.010144
20. Kandzari DE, Kirtane AJ, Windecker S, Latib A, Kedhi E, Mehran R, et al. One-month dual antiplatelet therapy following percutaneous coronary intervention with zotarolimus-eluting stents in high-bleeding-risk patients. *Circ Cardiovasc Interv.* (2020) 13:e009565. doi: 10.1161/CIRCINTERVENTIONS.120.009565
21. Buccheri S, Franchina G, Romano S, Puglisi S, Venuti G, D'Arrigo P, et al. Clinical outcomes following intravascular imaging-guided versus coronary angiography-guided percutaneous coronary intervention with stent implantation: a systematic review and Bayesian network meta-analysis of 31 studies and 17,882 patients. *JACC Cardiovasc Interv.* (2017) 10:2488–98. doi: 10.1016/j.jcin.2017.08.051
22. Capodanno D, Alfonso F, Levine GN, Valgimigli M, Angiolillo DJ. ACC/AHA versus ESC guidelines on dual antiplatelet therapy: JACC guideline comparison. *J Am Coll Cardiol.* (2018) 72:2915–31. doi: 10.1016/j.jacc.2018.09.057
23. Bhatt DL, Cryer BL, Contant CF, Cohen M, Lanas A, Schnitzer TJ, et al. Clopidogrel with or without omeprazole in coronary artery disease. *N Engl J Med.* (2010) 363:1909–17. doi: 10.1056/NEJMoa1007964
24. Chinese College of Cardiovascular P, Chinese College of Cardiovascular Physicians Working Group on T, Chinese Society of Digestive E. Multidisciplinary expert consensus on the prevention and management of bleeding in patients with acute coronary syndrome receiving antithrombotic agents. *Zhonghua Nei Ke Za Zhi.* (2016) 55:813–24. doi: 10.3760/cma.j.issn.0578-1426.2016.10.021
25. Huo Y, Jeong Y-H, Gong Y, Wang D, He B, Chen J, et al. 2018 update of expert consensus statement on antiplatelet therapy in East Asian patients with ACS or undergoing PCI. *Sci Bull.* (2019) 64:166–79. doi: 10.1016/j.scib.2018.12.020
26. Genereux P, Giustino G, Witzenbichler B, Weisz G, Stuckey TD, Rinaldi MJ, et al. Incidence, predictors, and impact of post-discharge bleeding after

percutaneous coronary intervention. *J Am Coll Cardiol.* (2015) 66:1036–45. doi: 10.1016/j.jacc.2015.06.1323

Conflict of Interest: GF consulted for Amgen, AstraZeneca, Bayer, Janssen, and Novartis and served on the AHA's Quality Oversight Committee. CM received honoraria from Bristol-Myers Squibb (BMS), Pfizer, Johnson & Johnson, Boehringer-Ingelheim (BI), Bayer and AstraZeneca for giving lectures. SN received research grants from the institution from Boston Scientific, Abbott, Jiangsu Hengrui Pharmaceuticals, China Resources Sanjiu Medical & Pharmaceuticals, East China Pharmaceuticals.

The remaining authors declare that the research was conducted in the absence of any commercial or financial relationships that could be construed as a potential conflict of interest.

Publisher's Note: All claims expressed in this article are solely those of the authors and do not necessarily represent those of their affiliated organizations, or those of the publisher, the editors and the reviewers. Any product that may be evaluated in this article, or claim that may be made by its manufacturer, is not guaranteed or endorsed by the publisher.

frontiers in Cardiovascular Medicine

ORIGINAL RESEARCH
published: 16 December 2021
doi: 10.3389/fcvm.2021.773200

Nutritional Risk Index Improves the GRACE Score Prediction of Clinical Outcomes in Patients With Acute Coronary Syndrome Undergoing Percutaneous Coronary Intervention

*Xiao-Teng Ma†, Qiao-Yu Shao†, Qiu-Xuan Li, Zhi-Qiang Yang, Kang-Ning Han, Jing Liang, Hua Shen, Xiao-Li Liu, Yu-Jie Zhou and Zhi-Jian Wang**

Department of Cardiology, Beijing Anzhen Hospital, Capital Medical University, Beijing, China

OPEN ACCESS

Edited by:
Tommaso Gori, Johannes Gutenberg University Mainz, Germany

Reviewed by:
Yujing Cheng, Capital Medical University, China
Yasutomi Higashikuni, University of Tokyo, Japan

***Correspondence:**
Zhi-Jian Wang
zjwang1975@hotmail.com

†These authors have contributed equally to this work

Specialty section:
This article was submitted to Coronary Artery Disease, a section of the journal Frontiers in Cardiovascular Medicine

Received: *09 September 2021*
Accepted: *25 November 2021*
Published: *16 December 2021*

Citation:
Ma X-T, Shao Q-Y, Li Q-X, Yang Z-Q, Han K-N, Liang J, Shen H, Liu X-L, Zhou Y-J and Wang Z-J (2021) Nutritional Risk Index Improves the GRACE Score Prediction of Clinical Outcomes in Patients With Acute Coronary Syndrome Undergoing Percutaneous Coronary Intervention. Front. Cardiovasc. Med. 8:773200. doi: 10.3389/fcvm.2021.773200

Background: Malnutrition has been shown to be associated with adverse cardiovascular outcomes in many patient populations.

Aims: To investigate the prognostic significance of malnutrition as defined by nutritional risk index (NRI) in patients with acute coronary syndrome (ACS) undergoing percutaneous coronary intervention (PCI) and whether NRI could improve the GRACE score based prognostic models.

Methods: This study applied NRI among 1,718 patients with ACS undergoing PCI. Patients were divided into three nutritional risk groups according to their baseline NRI: no nutritional risk (NRI $\geq$ 100), mild nutritional risk (97.5 $\leq$ NRI $<$ 100), and moderate-to-severe nutritional risk (NRI $<$ 97.5). The primary endpoint was the composite of major adverse cardiovascular events (MACE), including all-cause death, non-fatal stroke, non-fatal myocardial infarction, or unplanned repeat revascularization.

Results: During a median follow-up of 927 days, 354 patients developed MACE. In the overall population, compared with normal nutritional status, malnutrition was associated with increased risk for MACE [adjusted HR for mild and moderate-to-severe nutritional risk, respectively: 1.368 (95%CI 1.004–1.871) and 1.473 (95%CI 1.064–2.041)], and NRI significantly improved the predictive ability of the GRACE score for MACE (cNRI: 0.070, $P = 0.010$; IDI: 0.005, $P < 0.001$). In the diabetes subgroup, malnutrition was associated with nearly 2-fold high adjusted risk of MACE, and the GRACE score combined with NRI appeared to have better predictive ability than that in the overall population.

Conclusion: Malnutrition as defined by NRI was independently associated with MACE in ACS patients who underwent PCI, especially in individuals with diabetes, and improved the predictive ability of the GRACE score based prognostic models.

Keywords: nutritional risk index (NRI), GRACE score, acute coronary syndrome (ACS), percutaneous coronary intervention, diabetes

INTRODUCTION

Patients with acute coronary syndrome (ACS) are still at an unacceptably high risk of cardiovascular (CV) death and thrombotic events, even after they have undergone percutaneous coronary intervention (PCI). Comprehensive and accurate risk assessment plays an important role in making appropriate treatment decisions for these patients. The GRACE (Global Registry of Acute Coronary Events) score was a strong predictor of 6-month mortality and reinfarction after ACS (1, 2). However, some important predictors associated with poor prognosis are not included in the scoring system. Malnutrition has been proved to be associated with the development of atherosclerosis and a higher rate of CV mortality in elderly patients (3). Alternative nutritional indicators such as body mass index (BMI), serum albumin (ALB), and serum total cholesterol (TC) are predictors of survival in patients with ACS (4–6). Recently, nutritional status has been demonstrated to be a promising prognostic factor (7), and it is considered a modifiable clinical characteristic which physicians may perform interventions on to reduce the risk of adverse CV events.

The nutritional risk index (NRI) was developed as a simplified screening tool to assess nutritional status and predict clinical outcomes based on weight, height, and ALB (8). It has been reported that the malnutrition as defined by NRI was associated with the poor prognosis among patients with advanced age (9, 10), myocardial infarction (MI) (11), heart failure (HF) (12), valvular heart disease (13), atrial fibrillation (14), or chronic kidney disease (CKD) (15). So far, few studies have added nutritional status to the GRACE score for risk stratification assessment, and little is known about whether the predictive value of NRI differs among different subgroups of ACS patients. The present study aimed to evaluate the prognostic significance of nutritional status measured by NRI and the incremental predictive value of adding NRI to the GRACE score in patients with ACS undergoing PCI.

Abbreviations: ACEI, angiotensin converting enzyme inhibitor; ACS, acute coronary syndrome; ALB, serum albumin; ARB, angiotensin II receptor blocker; BMI, body mass index; CAD, coronary artery disease; CADILLAC, Controlled Abciximab and Device Investigation to Lower Late Angioplasty Complications; CI, confidence interval; CKD, chronic kidney disease; cNRI, continuous net reclassification improvement; CONUT, Controlling Nutritional Status; CV, cardiovascular; FPG, fasting plasma glucose, GRACE, Global Registry of Acute Coronary Events; HDL-C, high-density lipoprotein-cholesterol; HF, heart failure; HR, hazard ratio; hs-CRP, high-sensitivity C-reactive protein; IDI, integrated discrimination improvement; IQR, interquartile range; LDL-C, low-density lipoprotein-cholesterol; LVEF, left ventricular ejection fraction; MACE, major adverse cardiovascular events; MI, myocardial infarction; MIA, malnutrition inflammation-atherosclerosis; NRI, nutritional risk index; NSTEMI, non-ST segment elevation myocardial infarction; NSTE-ACS, non-ST segment elevation acute coronary syndrome; PCI, percutaneous coronary intervention; PEM, protein-energy malnutrition; STEMI, ST segment elevation myocardial infarction; SYNTAX, SYNergy between percutaneous coronary intervention with TAXus and cardiac surgery; TC, serum total cholesterol; TG, Triglycerides; TIMI, Thrombolysis in Myocardial Infarction.

MATERIALS AND METHODS

Study Population and Follow-Up Details

The present study is derived from a single-center prospective observational cohort study (ChiCTR1800017417) which was described in detail elsewhere (16). A total of 1770 patients who underwent coronary angiography for ACS and were treated with primary or elective PCI in our CV center were consecutively and prospectively enrolled in the database from June 2016 to November 2017. The exclusion criteria of this study included patients with prior coronary artery bypass graft surgery, cardiogenic shock, left ventricular ejection fraction (LVEF) $< 30\%$, renal failure with creatinine clearance < 15 ml/min, and known cancer history. Four patients were also excluded because of missing follow-up data despite at least four separate attempts to contact them. Ultimately, 1,718 patients were included in the final analysis (**Figure 1**). The study complied with the Declaration of the Helsinki with respect to investigation in humans, was approved by the institutional review committee of Beijing Anzhen Hospital, Capital Medical University, and conducted in accordance with the guidelines of the ethics committee at participating institutions. Written informed consent was obtained from all patients.

All patients were followed up at 1, 6, 12, 18, 24, 30, 36 months after hospital discharge. The information regarding adverse events was collected from the medical records and telephone interviews by three trained personnel blinded to the baseline characteristics. The first participant was recruited in June 2016 and the follow-up ended in December 2019.

Clinical Outcomes

The primary endpoint was the composite of major adverse cardiovascular events (MACE), which included all-cause death, non-fatal stroke, non-fatal MI, or unplanned repeat revascularization. The stroke was defined as ischemic cerebral infarction with evidence of neurological dysfunction requiring hospitalization with clinically documented lesions on brain computed tomography or magnetic resonance imaging. MI was defined as an elevated level of cardiac troponin or creatine kinase greater than the upper limit of the normal range with either ischemic symptoms or electrocardiograph changes implicating ischemia. The presence of new pathological Q waves in ≥ 2 contiguous electrocardiogram leads was also diagnosed as MI. Within 1 week after PCI, only Q-wave MI was defined as MI. Unplanned repeat revascularization referred to any non-staged revascularization after the index PCI. Staged revascularization was defined as scheduled revascularization within 90 days after the index PCI, without a revascularization status of emergency or salvage or without treatment of a coronary artery territory which had been treated. The most severe endpoint event was selected for the primary endpoint analysis if > 1 event occurred during follow-up (death $>$ stroke $>$ MI $>$ revascularization). If more than one stroke or MI or revascularization occurred, the first stroke or MI or revascularization was selected. Meanwhile, the first event was also selected for the primary endpoint analysis.

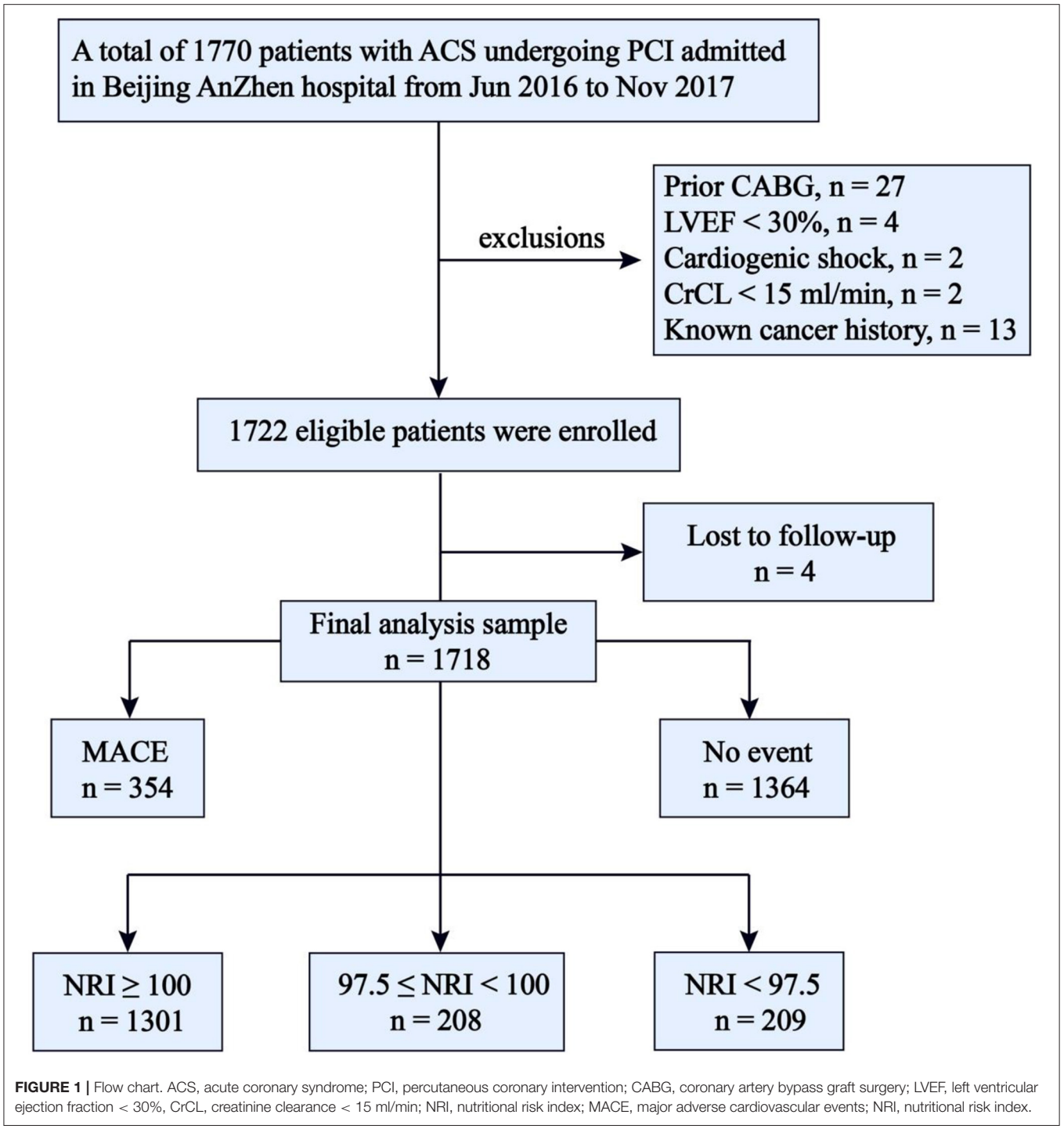

FIGURE 1 | Flow chart. ACS, acute coronary syndrome; PCI, percutaneous coronary intervention; CABG, coronary artery bypass graft surgery; LVEF, left ventricular ejection fraction < 30%, CrCL, creatinine clearance < 15 ml/min; NRI, nutritional risk index; MACE, major adverse cardiovascular events; NRI, nutritional risk index.

Data Collection

Data on demographics, medical history, and medication history were collected using a standard questionnaire. The blood pressure on admission was recorded. The ALB, lipid profiles, fasting plasma glucose (FPG), glycosylated hemoglobin, high-sensitivity C-reactive protein (hs-CRP), and creatinine levels in the first fasting blood samples during the stay in the hospital, which were obtained after 12 h of fasting, were determined at the central laboratory of Beijing Anzhen Hospital. The GRACE score was calculated on admission for predicting 6-month death or MI. The symptoms of diabetes and casual plasma glucose $\geq$ 11.1 mmol/L, FPG $\geq$ 7.0 mmol/L, or 2-h plasma glucose of 75 g oral glucose tolerance test $\geq$ 11.1 mmol/L, and/or antidiabetic drug use were the diagnostic criteria for diabetes. Hypertension

was defined as at least two blood pressure recordings greater than 140/90 mmHg, and/or use of antihypertensive drugs. Fasting TC > 5.17 mmol/L, low-density lipoprotein-cholesterol (LDL-C) > 3.36 mmol/L, triglycerides (TG) > 1.69 mmol/L, high-density lipoprotein-cholesterol (HDL-C) < 1.03 mmol/L, and/or chronic use of lipid-lowering drugs were considered criteria for dyslipidemia.

Calculation of NRI

Baseline NRI was calculated from ALB and BMI obtained on admission as previously described: NRI = 14.89 × ALB (g/dl) + 41.7 × [measured body weight (kg)/ideal body weight (kg)] [8]. The ideal body weight was calculated as follows: body height (cm)−100–{[body height (cm)−150]/4} for males, body height (cm)−100–{[body height (cm)−150]/2.5} for females (17). In accordance with prior studies, we set current body weight/ideal body weight = 1 when current body weight exceeded ideal body weight [7]. In our study, all patients were classified into three nutritional risk groups according to their baseline NRI, as defined in previous studies: normal nutrition (NRI ≥ 100), mild nutritional risk (97.5 ≤ NRI < 100), and moderate-to-severe nutritional risk (NRI < 97.5) (7). Due to the limitation of the sample size in this study, we did not separate a severe group since there was no patient with severe nutritional risk (NRI < 83.5). GRACE score was assessed on admission for predicting 6 months death or MI.

Statistical Analyses

Continuous variables were presented as the mean ± standard deviation or the median and interquartile range (IQR) in the case of normal or non-normal distribution and differences between two groups were examined by independent-sample *t*-test or Manne-Whitney U test correspondingly. Categorical variables were expressed as counts (percentages). The Chi-squared test or Fisher's exact test was used to analyze differences in categorical variables between groups. ANOVA or the Kruskal–Wallis H test was applied to analyze differences in continuous variables between groups. Spearman analysis was used to analyze the correlation between two continuous variables. Kaplan–Meier methods were used to derive the event rates at follow-up and to plot time-to-event curves. The NRI was analyzed in two ways: (1) as a categorical variable; and (2) as a continuous variable. Multivariate Cox proportional hazards analysis was used to estimate the hazard ratio (HR) and 95% confidence interval (CI) of NRI for MACE after adjustment for multiple confounders including other nutrition-related laboratory parameters, clinically relevant risk factors, and variables with statistical significance in the univariate analysis: lymphocyte count, neutrophil count, monocyte count, TC, hs-CRP, GRACE score, sex, BMI, current smoking, family history of CAD, hypertension, dyslipidemia, diabetes, past MI, past PCI, SYNTAX (SYNergy between percutaneous coronary intervention with TAXus and cardiac surgery) score, complete revascularization, discharged with aspirin, angiotensin converting enzyme inhibitor/angiotensin II receptor blockers (ACEI/ARBs), β-blockers, insulins, and oral antidiabetic agents. The interaction effect was tested with a likelihood ratio test, and the proportional hazard assumption was tested by demonstrating no importance of variables multiplied by time as time-dependent variables. The C-statistic, continuous net reclassification improvement (cNRI), and integrated discrimination improvement (IDI) were calculated to assess the discrimination capacity of NRI to predict CV events. All *P*-values were two-sided, and values < 0.05 were considered significant. All statistical analyses were performed using IBM SPSS Statistics version 26.0 (IBM Corporation, Chicago, IL) and R version 4.0.2 software (Vienna, Austria).

RESULTS

The median follow-up duration was 927 days (IQR, 927 to 1,109 days), and during the follow-up period, a total of 354 patients had at least one primary endpoint event, including 239 patients from the normal nutrition group ($n = 1301$), 53 rom the mild nutritional risk group ($n = 208$), and 62 from the moderate-to-severe nutritional risk group ($n = 209$). There were 44 cases of death (37 CV deaths and seven non-CV deaths), 24 cases of non-fatal stroke, 49 cases of non-fatal MI, and 289 cases of unplanned repeat revascularization. Fifty-two patients suffered more than one primary endpoint event. The clinical outcomes according to NRI degree are shown in **Table 1**. The distribution of NRI and incidence rate curve of MACE across continuous NRI are shown in **Figure 2**. The lower the NRI, the significantly higher the incidence of MACE.

At baseline, the majority of patients were male (76.7%), and the mean age was 60 years. The NRI-defined malnutrition rate was 24.3% in the total population, whereas 32.5% in the primary endpoint group, which was significantly higher than that in the event-free population. Patients with a primary endpoint event had higher heart rate, systolic blood pressure, and higher rates of family history of CAD, diabetes, previous MI and prior PCI. In terms of laboratory measurements, patients with a primary endpoint event had higher levels of creatinine, hs-CRP, neutrophil, monocyte, TC, TG, LDL-C, FPG, and glycosylated hemoglobin, but lower levels of ALB and HDL-C. As for the angiographic findings and procedural results, patients with an endpoint event had a higher SYNTAX score, a higher rate of left main or multi-vessel disease, and a lower rate of complete revascularization. Compared with those with normal nutritional status, patients with malnutrition had a higher GRACE score and higher rates of female, non-ST segment elevation MI (NSTEMI), ST segment elevation MI (STEMI), and proximal left anterior descending artery stenosis. Patients with malnutrition had higher levels of hs-CRP, neutrophil, and monocyte, but had a lower rate of complete revascularization. The baseline characteristics of the study population are shown in **Table 2** and **Supplementary Table 1**. One-point decrease of NRI was positively correlated with hs-CRP ($r = 0.231$, $P < 0.001$), neutrophil count ($r = 0.064$, $P = 0.008$), monocyte count ($r = 0.204$, $P < 0.001$), but not significantly correlated with lymphocyte count ($r = -0.024$, $P = 0.325$).

NRI was introduced into multivariate COX regression analysis as a category variable, and after adjustment for

TABLE 1 | Clinical outcomes according to NRI degree during follow-up.

	All subjects (n = 1,718)	NRI ≥ 100 (n = 1,301)	97.5 ≤ NRI < 100 (n = 208)	NRI < 97.5 (n = 209)	*P*-value
MACE-n (%)	354 (20.6)	239 (18.4)	53 (25.5)	62 (29.7)	<0.001
Death-n (%)	44 (2.6)	19 (1.5)	8 (3.8)	17 (8.1)	<0.001
Cardiovascular cause-n (%)	37 (2.2)	16 (1.2)	6 (2.9)	15 (7.2)	<0.001
Non-cardiovascular cause-n (%)	7 (0.4)	3 (0.2)	2 (1.0)	2 (1.0)	0.127
Non-fatal stroke-n (%)	24 (1.4)	12 (0.9)	5 (2.4)	7 (3.3)	0.009
Non-fatal MI-n (%)	49 (2.9)	36 (2.8)	6 (2.9)	7 (3.3)	0.895
Unplanned repeat revascularization -n (%)	289 (16.8)	206 (15.8)	40 (19.2)	43 (20.6)	0.144

Abbreviations as in ***Table 2****.*

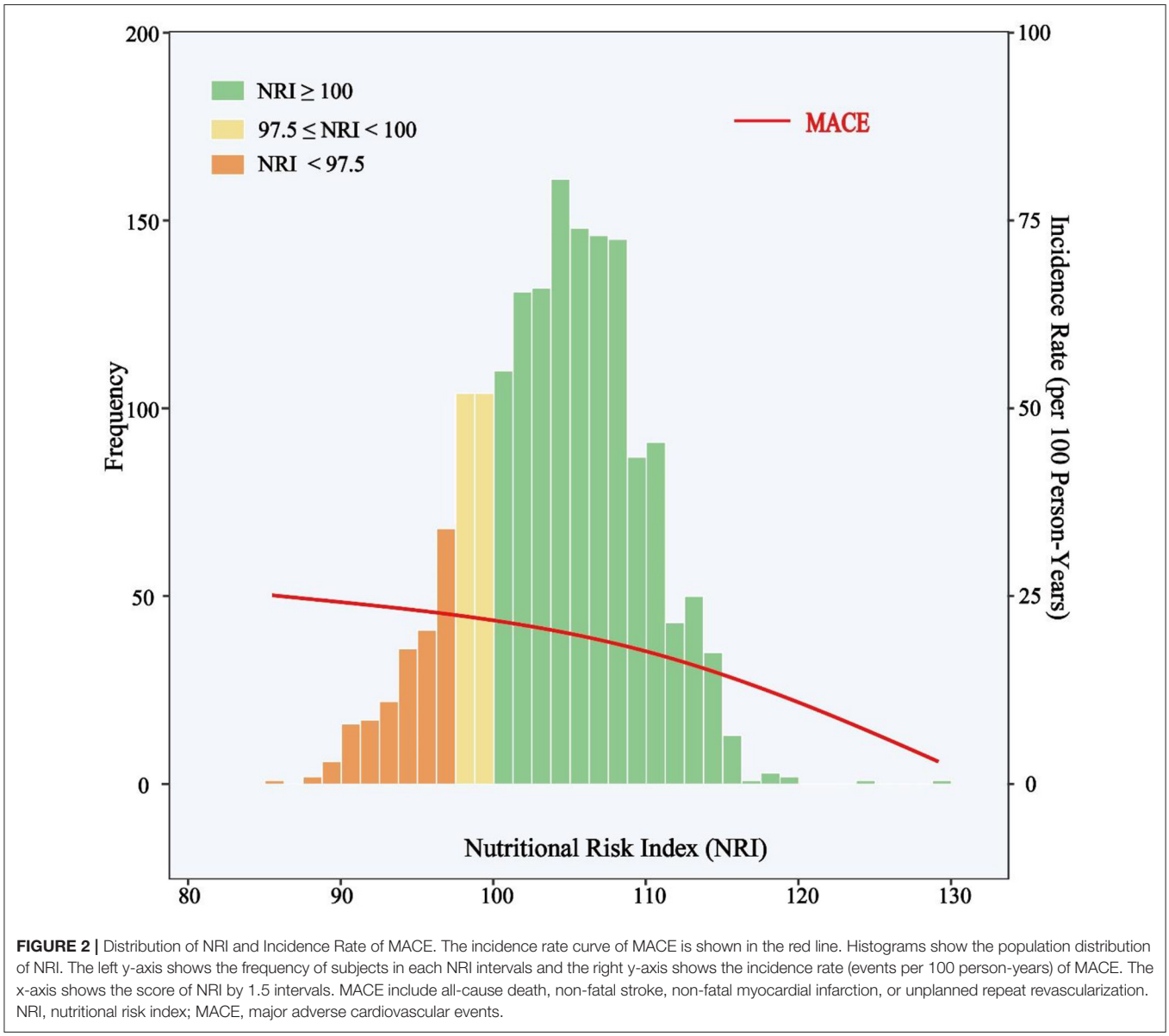

FIGURE 2 | Distribution of NRI and Incidence Rate of MACE. The incidence rate curve of MACE is shown in the red line. Histograms show the population distribution of NRI. The left y-axis shows the frequency of subjects in each NRI intervals and the right y-axis shows the incidence rate (events per 100 person-years) of MACE. The x-axis shows the score of NRI by 1.5 intervals. MACE include all-cause death, non-fatal stroke, non-fatal myocardial infarction, or unplanned repeat revascularization. NRI, nutritional risk index; MACE, major adverse cardiovascular events.

multiple confounding factors, compared with those with normal nutritional status, patients with malnutrition had significantly higher adjusted risk of MACE in both mild and moderate-to-severe group [HR for mild and moderate-to-severe nutritional risk respectively: 1.368 (95%CI 1.004–1.871) and 1.473 (95%CI 1.064–2.041)] (**Table 3**). When NRI

TABLE 2 | Baseline characteristics of study subjects by MACE.

Variable	All subjects (n = 1,718)	MACE (n = 354)	No such event (n = 1,364)	*P*-value
NRI	104.0 ± 5.6	103.0 ± 5.8	104.3 ± 5.5	<0.001
NRI Degree				<0.001
NRI ≥100-n (%)	1,301 (75.7)	239 (67.5)	1,062 (77.9)	
97.5 ≤ NRI < 100-n (%)	208 (12.1)	53 (15.0)	155 (11.4)	
NRI < 97.5-n (%)	209 (12.2)	62 (17.5)	147 (10.8)	
GRACE variables				
Age-years	60 ± 10	60 ± 11	60 ± 10	0.246
HR-bpm	69 ± 9	71 ± 10	68 ± 9	<0.001
SBP-mmHg	130 ± 16	132 ± 17	130 ± 16	0.017
Creatinine-μmol/L	70.3 (62.1–79.7)	72.0 (63.5–83.0)	69.6 (61.6–78.9)	0.003
Heart failure-n (%)	501 (29.2)	118 (33.3)	383 (28.1)	0.061
ST-segment deviation-n (%)	306 (17.8)	74 (20.9)	232 (17.0)	0.103
Elevated cardiac enzymes/markers-n (%)	443 (25.8)	97 (27.4)	346 (25.4)	0.477
Cardiac arrest-n (%)	2 (0.1)	2 (0.6)	0 (0.0)	0.057
GRACE score	104 ± 39	107 ± 41	103 ± 38	0.041
GRACE risk				0.004
Low	1,108 (64.5)	214 (60.5)	894 (65.5)	
Intermediate	287 (16.7)	52 (14.7)	235 (17.2)	
High	323 (18.8)	88 (24.9)	235 (17.2)	
Demographics				
Male-n (%)	1,317 (76.7)	275 (77.7)	1,042 (76.4)	0.659
Height-m	1.68 ± 0.07	1.67 ± 0.07	1.68 ± 0.07	0.322
Weight-kg	73 ± 12	72 ± 11	73 ± 12	0.075
BMI-kg/m^2	25.7 ± 3.1	25.5 ± 3.2	25.8 ± 3.1	0.116
Risk Factors				
Current smokers-n (%)	759 (44.2)	168 (47.5)	591 (43.3)	0.182
Family history of CAD-n (%)	550 (32.0)	131 (37.0)	419 (30.7)	0.028
Hypertension-n (%)	1,094 (63.7)	228 (64.4)	866 (63.5)	0.797
Dyslipidemia-n (%)	1,376 (80.1)	297 (83.9)	1,079 (79.1)	0.053
Diabetes-n (%)	793 (46.2)	195 (55.1)	598 (43.8)	<0.001
Past MI-n (%)	328 (19.1)	92 (26.0)	236 (17.3)	<0.001
Past PCI-n (%)	340 (19.8)	97 (27.4)	243 (17.8)	<0.001
Type of ACS				
UA-n (%)	1,275 (74.2)	257 (72.6)	1,018 (74.6)	0.477
NSTEMI-n (%)	221 (12.9)	51 (14.4)	170 (12.5)	0.377
STEMI-n (%)	222 (12.9)	46 (13.0)	176 (12.9)	1.000
Laboratory Measurements				
ALB (g/L)	42.0 ± 3.7	41.4 ± 3.8	42.2 ± 3.6	<0.001
Lymphocyte count (x10^9/L)	1.83 ± 0.58	1.79 ± 0.60	1.84 ± 0.58	0.130
Neutrophil count (x10^9/L)	4.00 (3.20–4.95)	4.45 (3.56–5.41)	3.90 (3.15–4.76)	<0.001
Monocyte count (x10^9/L)	0.36 (0.29–0.45)	0.40 (0.31–0.49)	0.35 (0.28–0.45)	<0.001
hs-CRP	1.36 (0.65–3.47)	2.22 (0.94–5.32)	1.23 (0.58–3.14)	<0.001
TC (mmol/L)	4.15 ± 0.99	4.28 ± 0.99	4.11 ± 0.99	0.005
LDL-C (mmol/L)	2.44 ± 0.81	2.55 ± 0.78	2.41 ± 0.81	0.006
HDL-C (mmol/L)	1.03 ± 0.23	0.99 ± 0.21	1.05 ± 0.24	<0.001
TG (mmol/L)	1.45 (1.01–2.06)	1.62 (1.11–2.28)	1.41 (0.98–2.01)	<0.001
FPG (mmol/L)	5.79 (5.23–6.94)	6.24 (5.45–8.02)	5.72 (5.21–6.76)	<0.001
Glycosylated hemoglobin (%)	6.1 (5.6–7.1)	6.4 (5.7–7.5)	6.0 (5.5–7.0)	<0.001
LVEF-%	65 (60–68)	62 (58–67)	65 (60–68)	<0.001

(Continued)

TABLE 2 | Continued

Variable	All subjects (n = 1,718)	MACE (n = 354)	No such event (n = 1,364)	P-value
Angiographic Findings				
LM/multi-vessel disease-n (%)	1,458 (84.9)	323 (91.2)	1,135 (83.2)	<0.001
Proximal LAD stenosis-n (%)	862 (50.2)	193 (54.5)	669 (49.0)	0.076
SYNTAX score	21.3 ± 10.9	25.3 ± 11.0	20.2 ± 10.6	<0.001
Procedural Results				
DES-n (%)	1,411 (82.1)	278 (78.5)	1,133 (83.1)	0.057
BRS-n (%)	97 (5.6)	23 (6.5)	74 (5.4)	0.516
DCB-n (%)	111 (27.2)	33 (33.7)	78 (25.2)	0.128
Complete revascularization-n (%)	1,052 (61.2)	151 (42.7)	901 (66.1)	<0.001
Medications				
Aspirin-n (%)	1,702 (99.1)	344 (97.2)	1,358 (99.6)	<0.001
Cilostazol-n (%)	19 (1.1)	10 (2.8)	9 (0.7)	0.001
Clopidogrel-n (%)	1,576 (91.7)	320 (90.4)	1,256 (92.1)	0.358
Ticagrelor-n (%)	142 (8.3)	34 (9.6)	108 (7.9)	0.358
Statins-n (%)	1,718 (100.0)	354 (100.0)	1,364 (100.0)	NA
ACEI/ARBs-n (%)	830 (48.3)	182 (51.4)	648 (47.5)	0.211
β-blockers-n (%)	1,204 (70.1)	231 (65.3)	973 (71.3)	0.031
Any antidiabetic treatment-n (%)	572 (33.3)	158 (44.6)	414 (30.4)	<0.001
Insulin-n (%)	268 (15.6)	80 (22.6)	188 (13.8)	<0.001
Oral antidiabetic agents-n (%)	426 (24.8)	103 (29.1)	323 (23.7)	0.042
Metformin-n (%)	121 (7.0)	32 (9.0)	89 (6.5)	0.126
Alpha-glucosidase inhibitors-n (%)	281 (16.4)	65 (18.4)	281 (16.4)	0.287
Sulfonylurea-n (%)	194 (11.3)	44 (12.4)	150 (11.0)	0.506
DDP-4 inhibitors-n (%)	13 (0.8)	4 (1.1)	9 (0.7)	0.572

MACE indicates major adverse cardiovascular events; NRI, nutritional risk index; GRACE, Global Registry of Acute Coronary Events; HR, heart rate; SBP, systolic blood pressure; BMI, body mass index; CAD, coronary artery disease; MI, myocardial infarction; PCI, percutaneous coronary; ACS, acute coronary syndrome; UA, unstable angina; NSTEMI, non-ST segment elevation myocardial infarction; STEMI, ST segment elevation myocardial infarction; ALB, albumin; hs-CRP, high-sensitivity C-reactive protein; TC, serum total cholesterol; LDL-C, low-density lipoprotein-cholesterol; HDL-C, high-density lipoprotein-cholesterol; TG, triglycerides; FPG, fasting plasma glucose; LVEF, left ventricular ejection fraction; LM, left-main artery; LAD, left anterior descending artery; SYNTAX, SYNergy between percutaneous coronary intervention with TAXus and cardiac surgery; DES, drug eluting stent; BRS, bioresorbable scaffold; DCB, drug coated balloon; ACEI, angiotensin converting enzyme inhibitor; ARB-angiotensin II receptor blocker; DDP-4, dipeptidyl peptidase 4.

was used as a continuous variable in the multivariate Cox regression model, decreased NRI was associated with a higher risk of MACE [HR 1.026, (95%CI 1.004–1.049), $P = 0.022$] (**Supplementary Table 2**). Kaplan–Meier analysis revealed that patients with malnutrition showed higher incidence of the MACE (log-rank $P < 0.001$). This difference was mainly driven by the increase in death (log-rank $P < 0.001$) and stroke (log-rank $P = 0.006$), while the incidence of MI (log-rank $P = 0.870$) and repeat revascularization (log-rank $P = 0.094$) was similar between non-malnourished and malnourished patients during the follow-up. Kaplan–Meier curves of the incidence of the primary endpoint and each component of the primary endpoint for NRI are presented in **Figures 3**, **4**.

Subgroup analyses were also conducted to investigate whether the predictive value of NRI was similar among patients with different demographic characteristics or comorbidities. We found a significant interaction effect between continuous NRI and diabetes subgroup (the predictive value of NRI seemed to be more prominent in patients with diabetes). However, NRI was a significant predictor of MACE regardless of age ≥ or < 60 years, male or female, BMI ≥ or < 25 kg/m^2, current smoking or not, hypertension or not, STEMI or NSTE-ACS (unstable angina + NSTEMI) (all P for interaction > 0.05) (**Figure 5**).

Compared with the baseline GRACE score, the addition of NRI had a significant increase in C-statistic from 0.524 (95%CI 0.493–0.556) to 0.565 (95%CI 0.534–0.596) ($P = 0.006$), and significant improvement in reclassification as assessed by the cNRI (0.070, 95%CI 0.010–0.135, $P = 0.010$) and IDI (0.005, 95% CI 0.001–0.014, $P < 0.001$) (**Table 4**). **Supplementary Table 3** shows the model performance after the addition of NRI to the baseline model in overall population.

We then conducted further analyses to investigate the predictive value of NRI among diabetes subjects. Compared with non-malnourished patients with diabetes, malnourished patients with diabetes had nearly 2-fold high adjusted risk of MACE [HR for mild and moderate-to-severe nutritional risk respectively: 1.601 (95%CI 1.030–2.489) and 1.977 (95%CI 1.283–3.046)] (**Table 5**). Compared with the baseline GRACE score, the addition of NRI had a more significant increase in C-statistic from 0.504 (95%CI 0.461–0.548) to 0.595 (95%CI 0.555–0.636) ($P < 0.001$), and more significant improvement in reclassification as assessed by the cNRI (0.176, 95%CI

TABLE 3 | Relationship between MACE and NRI as a categorical variable in the overall population.

Variables	Univariate analysis		Multivariate analysis	
	HR (95% CI)	*P*-value	HR (95% CI)	*P*-value
NRI				
NRI ≥ 100	ref	ref	ref	ref
97.5 ≤ NRI < 100	1.426 (1.059–1.920)	0.020	1.368 (1.004–1.871)	0.049
NRI < 97.5	1.744 (1.319–2.306)	<0.001	1.473 (1.064–2.041)	0.020
Lymphocyte count	0.879 (0.730–1.059)	0.175	0.834 (0.682–1.020)	0.077
Neutrophil count	1.189 (1.124–1.258)	<0.001	1.117 (1.042–1.198)	0.002
Monocyte count	3.318 (1.952–5.642)	<0.001	1.446 (0.672–3.113)	0.346
TC	1.151 (1.042–1.272)	0.006	1.191 (1.070–1.326)	0.001
hs-CRP	1.032 (1.018–1.046)	<0.001	1.008 (0.988–1.027)	0.442
GRACE score	1.003 (1.000–1.005)	0.036	0.999 (0.996–1.002)	0.355
Sex	1.050 (0.818–1.349)	0.701	0.948 (0.695–1.294)	0.738
BMI	0.974 (0.940–1.008)	0.132	0.974 (0.939–1.011)	0.165
Current smoking	1.168 (0.948–1.438)	0.145	1.354 (1.056–1.736)	0.017
Family history of CAD	1.275 (1.028–1.582)	0.027	1.237 (0.992–1.543)	0.059
Hypertension	1.037 (0.834–1.289)	0.746	1.127 (0.881–1.442)	0.340
Dyslipidemia	1.346 (1.014–1.787)	0.040	1.036 (0.767–1.399)	0.819
Diabetes	1.521 (1.234–1.876)	<0.001	1.323 (0.980–1.785)	0.068
Past MI	1.530 (1.207–1.941)	<0.001	1.101 (0.833–1.457)	0.498
Past PCI	1.582 (1.252–1.998)	<0.001	1.637 (1.239–2.164)	0.001
SYNTAX score	1.036 (1.027–1.045)	<0.001	1.019 (1.009–1.030)	<0.001
Complete revascularization	0.423 (0.342–0.522)	<0.001	0.563 (0.445–0.712)	<0.001
Discharged with Aspirin	0.244 (0.130–0.457)	<0.001	0.428 (0.222–0.823)	0.011
Discharged with ACEI/ARBs	1.147 (0.931–1.412)	0.198	0.990 (0.782–1.255)	0.936
Discharged with β-blockers	0.780 (0.627–0.971)	0.026	0.716 (0.571–0.899)	0.004
Discharged with insulin	1.712 (1.335–2.197)	<0.001	1.359 (1.008–1.831)	0.044
Discharged with oral antidiabetic agents	1.293 (1.028–1.626)	0.028	0.927 (0.690–1.245)	0.615

HR indicates hazard ratio; 95% CI, 95% confidence interval. Other abbreviations as in ***Table 2****.*

0.062-0.278, $P < 0.001$) and IDI (0.022, 95% CI 0.003–0.052, $P < 0.001$) in the diabetes subgroup (**Table 6**). The model performance after the addition of NRI to the baseline model in diabetic population is shown in **Supplementary Table 4**. In addition, **Supplementary Tables 5**, **6** show the relationships between MACE and NRI in the overall population and diabetic population when the first event was selected for the primary endpoint analysis. NRI was an independent predictor of MACE whether the most severe event or the first event was used as the endpoint event.

DISCUSSION

In the present study, we noticed a significant association of NRI with CV outcomes. Compared with those with normal nutritional status, patients with malnutrition as defined by NRI had a higher risk of MACE. Even after adjustment for as many potential confounders as possible, NRI remained an independent predictor of MACE. The addition of NRI significantly improved the ability of the GRACE score to predict MACE. Intriguingly, in the diabetes subgroup, malnutrition was associated with relatively higher adjusted risk of MACE, and the GRACE score combined with NRI seemed to have better predictive ability than that in the overall population. Therefore, the present study supported the utility of NRI in predicting CV outcomes and improving the predictive ability of the model containing the GRACE score among patients with ACS.

Several reliable risk scoring models have been developed to assist clinicians in risk stratification, such as the GRACE (18), TIMI (Thrombolysis in Myocardial Infarction) (19), and CADILLAC (Controlled Abciximab and Device Investigation to Lower Late Angioplasty Complications) scores (20). Of them, the GRACE score is relatively easy to assess, and has been widely accepted as a powerful predictor of adverse CV outcomes after ACS at different time points up to 4 years (2, 18, 21). Malnutrition is common in patients with ACS and is associated with a poor prognosis regardless of GRACE score, BMI, LVEF, coronary revascularization, optimal medical treatment, and other risk factors (7). It is worth noting that variables required for nutritional status calculation are widely available, and malnutrition appears to be a potentially modifiable risk and therapeutic target.

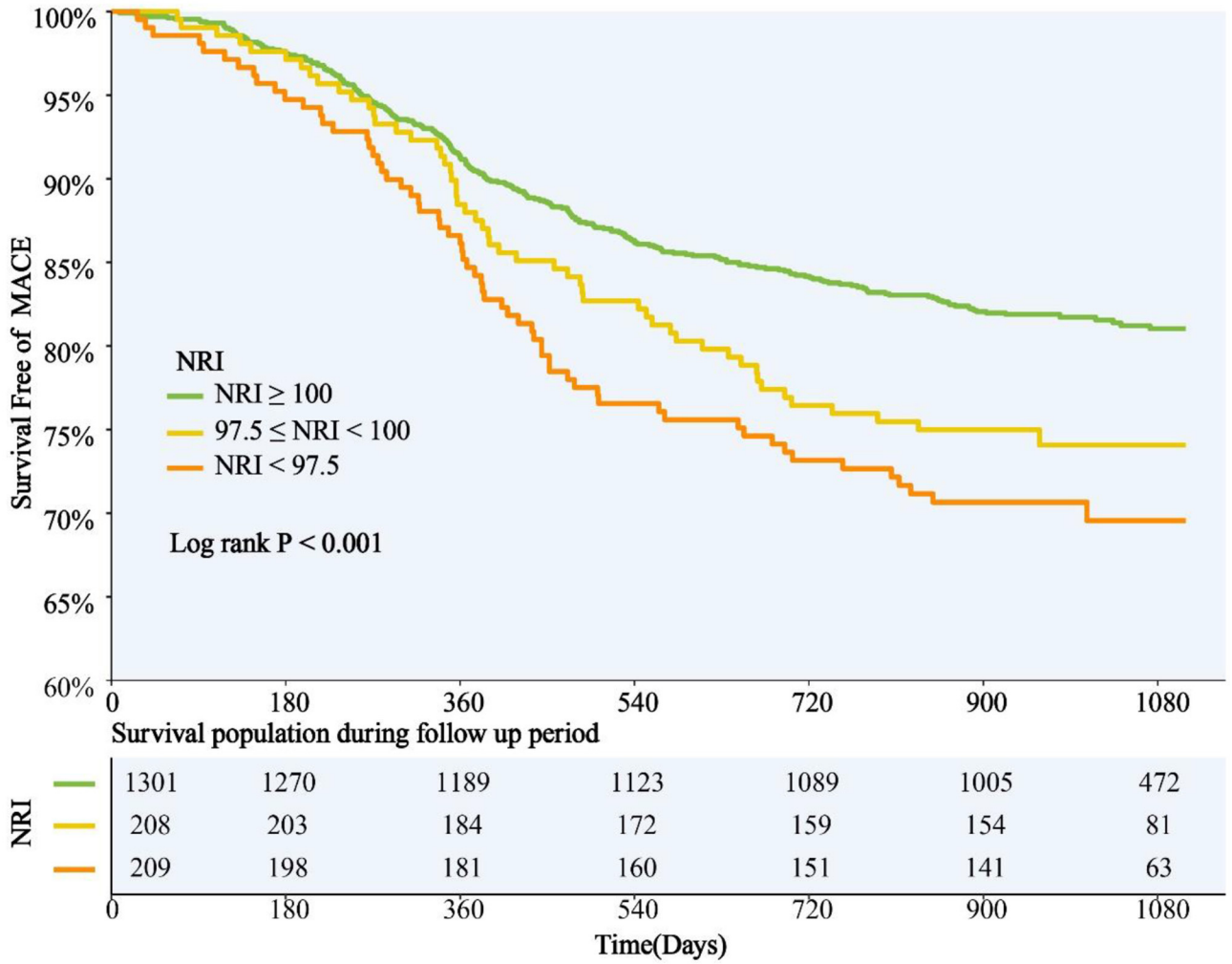

FIGURE 3 | NRI Degree and Risk of MACE. Kaplan-Meier curves for MACE by the NRI degree. NRI, nutritional risk index; MACE, major adverse cardiovascular events.

NRI is a nutritional assessment score that includes ALB as a visceral protein element and actual weight relative to ideal weight as an anthropometric element, both of which are predictors of clinical outcomes in patients with CAD, HF, or diabetes (22, 23). However, albuminemia alone does not appear to be a reliable indicator of nutritional status, as it may be related to inflammation or hydration status rather than malnutrition (24). Hydration status is negatively correlated with ALB concentration, while positively correlated with body weight (8). The combination of both components (i.e., ALB and body weight) in the NRI counteracts the effect of hydration status on nutritional assessment. As to the NRI formula, if the current weight was higher than the ideal weight, we set weight ratio as one, which leads to a higher weighting for albumin than for weight. Otherwise, malnourished patients with overweight would not have been sensitively diagnosed. BMI is often used to define obesity, but it cannot fully reflect the nutritional status. In our study, we found that many obese patients had malnutrition and hypoalbuminemia. The study of Roubín et al. (7) showed that malnutrition was prevalent even in patients with overweight and obesity: a substantial proportion of patients with a BMI of $\geq$ 25 kg/m^2 were malnourished (58% with the NRI). In the study of Sze et al. (25), one-half of heart failure patients with a BMI of $\geq$ 30 kg/m^2 were malnourished as defined by Controlling Nutritional Status (CONUT) scores (another good indicator for nutritional status). These two studies suggest that malnutrition in obese people mainly manifested in low serum albumin levels, which has been shown to reflect active systematic inflammation (26–28). As we known, obesity is associated with active systemic inflammation (29). Of note, inflammation has been shown to reduce serum albumin through several possible mechanisms, including downregulation of synthesis, increased catabolism, and increased vascular permeability (30, 31). These may explain why many obese patients in our study have malnutrition and hypoalbuminemia.

Nutritional status is affected by many factors, and malnourished patients often have complex clinical conditions. In this study, NRI remained strongly associated with MACE after

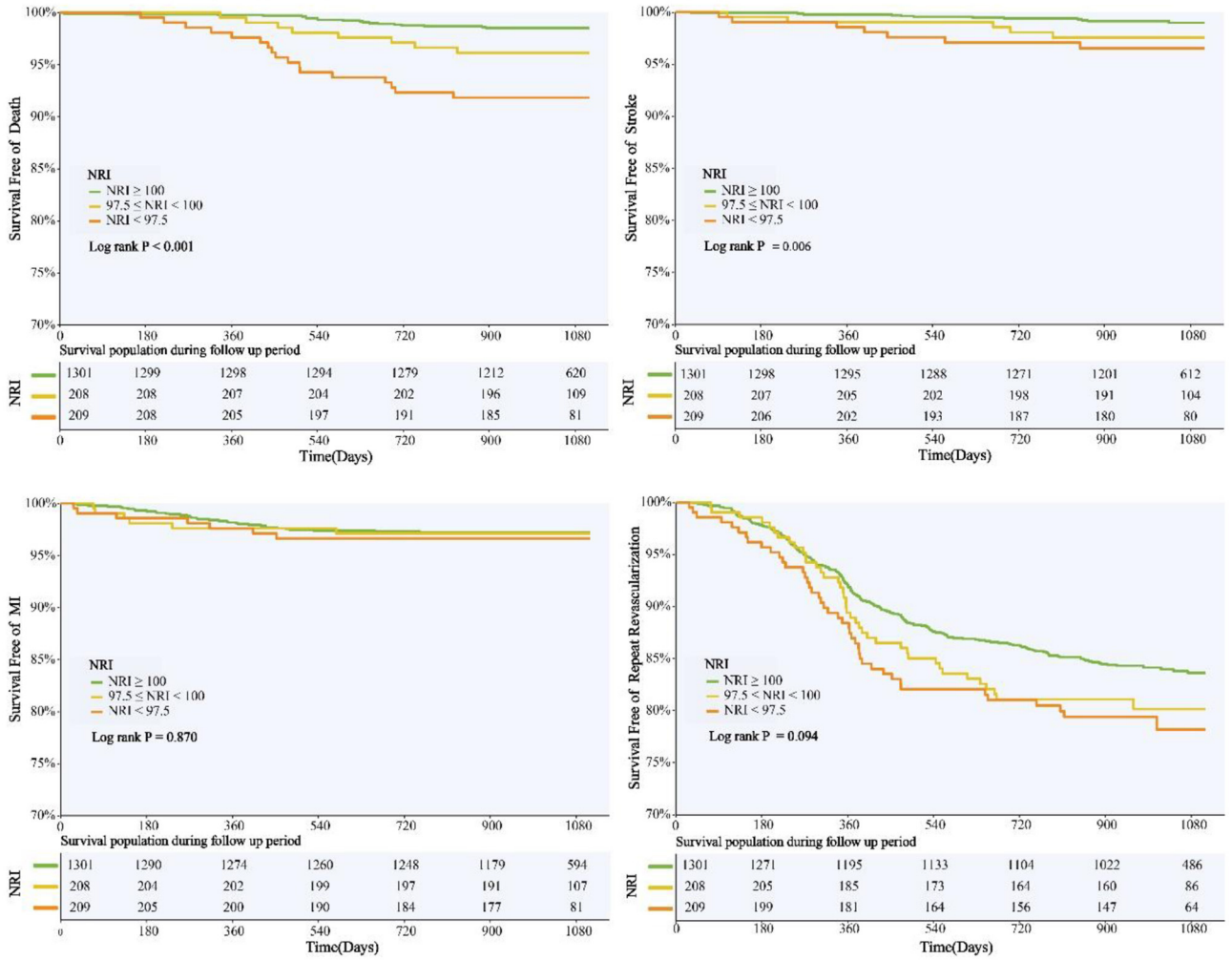

FIGURE 4 | NRI Degree and Risk of Death, Stroke, MI, and Revascularization. Kaplan-Meier curves for all-cause death, non-fatal stroke, non-fatal myocardial infarction, and unplanned repeat revascularization by the NRI degree. NRI, nutritional risk index; MI, myocardial infarction.

adjustment for multiple potential confounders, such as clinical variables, coronary revascularization, and optimal medical treatment. The two components of NRI are widely used and easily collected in the clinical practice. Therefore, NRI could be considered as a feasible and convenient tool to help predict CV outcomes. In fact, NRI was originally used to assess the nutritional status of elderly patients, who are more likely to experience unconscious weight loss (8). Although our study included patients of all ages, we also conducted an age subgroup analysis. We found no difference in the predictive value of NRI for MACE between the younger and older groups, which was consistent with the results of previous studies (15, 32).

Previous studies supported NRI-defined malnutrition as a reliable predictor of adverse CV events in many patient groups, such as patients with acute or chronic HF (12, 33, 34), patients undergoing aortic valve replacement (13, 35), and patients with other systemic diseases (14, 15, 36). Furthermore, several other studies showed that in patients with stable CAD or ACS, lower NRI levels (the lower the NRI levels, the greater the nutritional risk) were associated with in-hospital and long-term adverse CV events after PCI (11, 32, 37–39); however, these studies did not specifically investigate the prognostic value of malnutrition in ACS patients with diabetes. Since a high prevalence of diabetes-related complications and comorbidities may further impair nutritional status (40). Compared with those without diabetes, people with diabetes are more likely to suffer from malnutrition due to the diabetes itself, injuries, medications, and other factors affecting metabolism (41), which suggests that malnutrition may contribute to a higher risk of adverse CV events in ACS patients with diabetes vs. without diabetes.

Malnutrition is a complex pathological condition, and it is difficult to explain how malnutrition affects CV outcomes in patients with ACS from the results of this observational study. We believe that one of the potential mechanisms is malnutrition-inflammation-atherosclerosis (MIA) syndrome (42). ACS is the result of atherosclerotic plaque rupture causing by the chronic

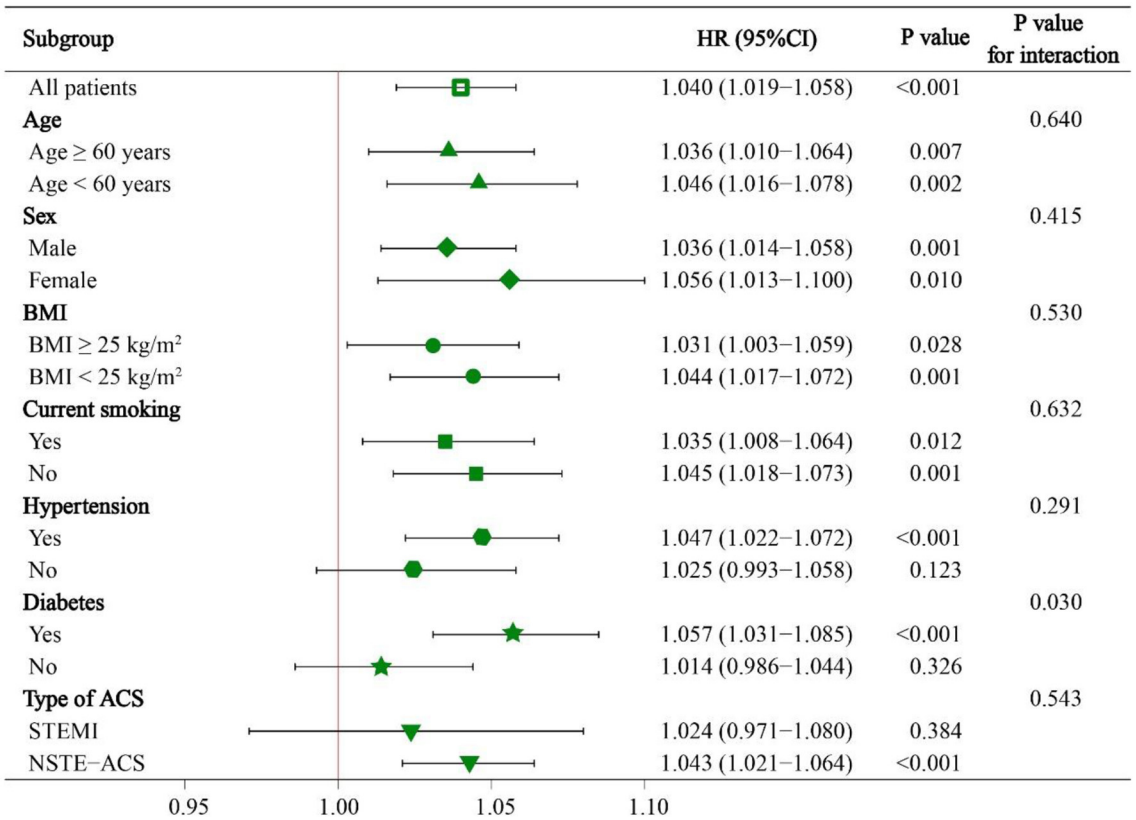

FIGURE 5 | Subgroup analyses of continuous NRI for MACE. HR was evaluated by 1-point decrease of NRI. HR, hazard ratio; CI, confidence interval; BMI, body mass index; STEMI, ST-segment elevation myocardial infarction; NSTE-ACS, non-ST-segment elevation acute coronary syndrome.

TABLE 4 | Model performance after the addition of NRI to the GRACE score in the overall population.

	C-Statistic (95%CI)	*P*-value	cNRI (95%CI)	*P*-value	IDI (95%CI)	*P*-value
MACE						
GRACE	0.524 (0.493–0.556)	ref	ref	ref	ref	ref
GRACE+NRI	0.565 (0.534–0.596)	0.006	0.070 (0.010–0.135)	0.010	0.005 (0.001–0.014)	<0.001
Death						
GRACE	0.671 (0.577–0.764)	ref	ref	ref	ref	ref
GRACE+NRI	0.743 (0.661–0.826)	0.026	0.217 (0.037–0.400)	<0.001	0.018 (0.004–0.051)	<0.001
Death or MI						
GRACE	0.607 (0.540–0.673)	ref	ref	ref	ref	ref
GRACE+NRI	0.625 (0.558–0.693)	0.217	0.063 (−0.057–0.190)	0.179	0.007 (0.001–0.021)	<0.001
Death, stroke, or MI						
GRACE	0.633 (0.578–0.689)	ref	ref	ref	ref	ref
GRACE+NRI	0.650 (0.592–0.709)	0.165	0.088 (−0.012–0.207)	0.090	0.009 (0.002–0.026)	<0.001

cNRI, continuous net-reclassification index; IDI, integrated discrimination improvement. Other abbreviations as in ***Table 2****.*

inflammatory response. Meanwhile, patients with diabetes are more likely to have higher levels of inflammatory markers such as C-reactive protein (43, 44), which may increase the burden of atherosclerosis (45). Thus, when malnutrition is present in patients with ACS and diabetes, hypoalbuminemia may be the result of the combination of malnutrition and inflammation. Malnutrition may be driven by inflammatory cytokines and is characterized by chronic inflammation with an increase in insulin resistance, reduction of appetite, production of catabolic cytokines, and muscle catabolism (46). While increased insulin resistance may in turn inhibit the entry of nutrients into cells and accelerate atherosclerosis (46). Another underlying

TABLE 5 | Relationship between MACE and NRI as a categorical variable in the diabetes subgroup.

Variables	Univariate analysis		Multivariate analysis	
	HR (95% CI)	*P*-value	HR (95% CI)	*P*-value
NRI				
NRI ≥ 100	ref	ref	ref	ref
97.5 ≤ NRI < 100	1.395 (0.925–2.104)	0.112	1.601 (1.030–2.489)	0.037
NRI < 97.5	2.202 (1.564–3.100)	0.000	1.977 (1.283–3.046)	0.002
Lymphocyte count	0.761 (0.590–0.980)	0.035	0.761 (0.571–1.013)	0.061
Neutrophil count	1.184 (1.090–1.287)	<0.001	1.184 (1.059–1.325)	0.003
Monocyte count	2.578 (1.311–5.070)	0.006	1.014 (0.352–2.921)	0.979
TC	1.115 (0.980–1.268)	0.099	1.213 (1.052–1.397)	0.008
hs-CRP	1.035 (1.014–1.055)	0.001	1.001 (0.972–1.031)	0.949
GRACE score	1.002 (0.999–1.005)	0.262	0.997 (0.993–0.001)	0.169
Sex	0.946 (0.691–1.294)	0.727	1.098 (0.732–1.647)	0.650
BMI	0.963 (0.919–1.008)	0.109	0.974 (0.928–0.023)	0.299
Current smoking	1.005 (0.755–1.338)	0.971	1.249 (0.887–1.758)	0.202
Family history of CAD	1.225 (0.911–1.649)	0.179	1.253 (0.916–1.713)	0.158
Hypertension	1.053 (0.777–1.428)	0.737	1.340 (0.949–1.893)	0.096
Dyslipidemia	1.313 (0.869–1.984)	0.197	0.936 (0.604–1.450)	0.766
Past MI	1.516 (1.112–2.068)	0.009	1.090 (0.753–1.579)	0.648
Past PCI	1.751 (1.304–2.351)	<0.001	1.927 (1.339–2.773)	<0.001
SYNTAX score	1.029 (1.016–1.042)	<0.001	1.016 (1.001–1.032)	0.032
Complete revascularization	0.451 (0.339–0.600)	<0.001	0.602 (0.440–0.824)	0.002
Discharged with aspirin	0.109 (0.054–0.222)	<0.001	0.292 (0.128–0.663)	0.003
Discharged with ACEI/ARBs	1.208 (0.912–1.602)	0.188	1.072 (0.778–1.476)	0.673
Discharged with β-blockers	0.776 (0.574–1.049)	0.099	0.690 (0.499–0.953)	0.024
Discharged with insulin	1.411 (1.060–1.878)	0.018	1.429 (1.046–1.951)	0.025
Discharged with oral antidiabetic agents	0.952 (0.719–1.261)	0.732	0.963 (0.710–1.306)	0.808

*Abbreviations as in **Table 2**.*

TABLE 6 | Model performance after the addition of NRI to the GRACE score in the diabetes subgroup.

	C-Statistic (95%CI)	*P*-value	cNRI (95%CI)	*P*-value	IDI (95%CI)	*P*-value
MACE						
GRACE	0.504 (0.461–0.548)	ref	ref	ref	ref	ref
GRACE+NRI	0.595 (0.555–0.636)	<0.001	0.176 (0.062–0.278)	<0.001	0.022 (0.003–0.052)	<0.001
Death						
GRACE	0.735 (0.586–0.884)	ref	ref	ref	ref	ref
GRACE+NRI	0.806 (0.671–0.941)	0.132	0.328 (0.004–0.566)	0.020	0.037 (0.007–0.168)	<0.001
Death or MI						
GRACE	0.656 (0.555–0.757)	ref	ref	ref	ref	ref
GRACE+NRI	0.698 (0.600–0.795)	0.156	0.205 (0.000–0.398)	0.050	0.018 (0.002–0.063)	0.010
Death, stroke, or MI						
GRACE	0.709 (0.637–0.782)	ref	ref	ref	ref	ref
GRACE+NRI	0.738 (0.664–0.812)	0.030	0.191 (0.057–0.331)	0.010	0.023 (0.004–0.062)	<0.001

*Abbreviations as in **Table 2**.*

mechanism of poor prognosis due to malnutrition is protein-energy malnutrition (PEM). PEM refers to a persistent state of inadequate food and nutrient intake, leading to changes in body weight, composition, and functioning (47). The association of PEM with poor prognosis in patients with acute MI, acute ischemic stroke, and HF has been demonstrated (48–50). One study showed that pre-existing PEM impaired the body's healing capability after injury, resulting in devastating clinical outcomes among patients with acute MI (51). We consider that for patients with ACS and diabetes, those who are undernourished

may typically have lower cardiac and systemic muscle and nutrient reserves and may suffer more severe myocardial damage due to weaker baseline cardiac function and limited capacity to repair.

Previous studies have identified several potential risk factors beyond the GRACE score predicting model which enhance the predictive power for CV events after ACS, such as B-type natriuretic peptide (52), neutrophil count (53), and 2-h post-load glucose (54). The combination of NRI and the GRACE score produced a stronger predictive value, which improved the ability of model discrimination and risk reclassification. Our findings suggest that clinicians can apply nutritional status in combination with the GRACE score to identify higher-risk patients with ACS and diabetes and take effective measures to improve their clinical outcomes. In addition, our findings support the necessity and benefits for physicians to integrate the recognition of malnutrition in the clinical practice. Malnutrition screening in patients with ACS and diabetes can identify patients at high residual risk of CV events, who may benefit from optimized secondary prevention therapy and appropriate nutritional supplements. A recent randomized controlled trial which recruited 2,088 medical inpatients at nutritional risk found that the use of individualized nutritional support during the hospital stay improved clinical outcomes, compared with the use of standard hospital food (55). The strong evidence that individualized nutritional support can improve the prognosis of patients with HF is worth learning (56). The benefits of eating plans adjusted by the patient's preference, food fortifications, and oral nutritional supplements have been proved (57, 58). Dietary counseling and educational interventions after discharge should also be provided in the outpatient clinic. Hence, a rehabilitation unit needs physicians to cooperate with dietitians, nurses, care workers, and other professionals involved in the caring process.

This is a single-center observational study with the subsequent limitation to its nature. First, we only assessed the relationship between NRI at admission and CV outcomes and did not focus on changes in nutritional status during the follow-up. Second, the threshold of malnutrition defined by NRI is vague, and different studies set different grading criteria. Hence, there is no authoritative grading reference at present. Third, due to a limited sample size, the range of NRI was relatively small, which may affect the estimation of the relationship between NRI and CV outcomes. Fourth, all patients in this study were Chinese, so these results should be interpreted with caution and generalized to other ethnic groups since dissimilar metabolic levels exist among different races. Fifth, CKD and albuminuria might affect albumin in the blood, and glomerular hyperfiltration is one of important features in diabetic patients. In terms of kidney function, we could only obtain serum creatinine levels from the original cohort. In addition, markers of kidney injury such as albuminuria, abnormal urinary sediment, histological abnormalities, and imaging abnormalities were not routinely detected at our CV center. Therefore, we could not make an accurate diagnosis of CKD and further analyze the effect of CKD on NRI. Albuminuria was only detected qualitatively rather than quantitatively in most patients, so we could not accurately analyze the effect of albuminuria on NRI. Sixth, liver diseases might affect the clinical outcomes, or be associated with hypoalbuminemia; however, it was not taken into account in our study since indicators of liver function and information about liver diseases were not collected in the original cohort. To be clear, deferred PCI for patients with significant liver dysfunction is usually considered at our CV center unless the life-threatening conditions, so few patients with significant liver dysfunction were included in our study. Seventh, malnutrition may influence CV outcomes by promoting inflammation. Therefore, we include hs-CRP, lymphocytes, neutrophils, and monocytes into the analysis. Unfortunately, proinflammatory cytokines were not routinely measured at our CV center, so we could not analyze the correlation between proinflammatory cytokines and malnutrition or prognosis.

CONCLUSION

Malnutrition as defined by NRI was independently and strongly associated with a higher risk of MACE in ACS patients who underwent PCI, especially in individuals with diabetes. NRI also improved the predictive ability of the GRACE score based prognostic models. Clinical trials are needed to determine whether improving nutritional status can improve CV outcomes in these patients.

DATA AVAILABILITY STATEMENT

The original contributions presented in the study are included in the article/**Supplementary Material**, further inquiries can be directed to the corresponding author.

ETHICS STATEMENT

The studies involving human participants were reviewed and approved by the Institutional Review Committee of Beijing Anzhen Hospital, Capital Medical University. The patients/participants provided their written informed consent to participate in this study.

AUTHOR CONTRIBUTIONS

X-TM and Q-YS wrote the first draft of the manuscript. X-TM also made important contributions to the revision of the manuscript. X-TM, Q-YS, Q-XL, Z-QY, K-NH, JL, HS, X-LL, Y-JZ, and Z-JW were involved in the conception and design of the study and the collection, analysis, interpretation of the data, and reviewed the final manuscript. All authors read and approved the final manuscript.

FUNDING

Project funded by National Key Research and Development Program of China (2017YFC0908800, Y-JZ), Beijing

Municipal Administration of Hospitals' Mission plan (SML20180601, Y-JZ), China Postdoctoral Science Foundation (2021M692253, X-TM), Beijing Postdoctoral Research Foundation (2021-ZZ-023, X-TM), Beijing Municipal Health Commission (Jing 19-15, HS).

SUPPLEMENTARY MATERIAL

The Supplementary Material for this article can be found online at: https://www.frontiersin.org/articles/10.3389/fcvm.2021.773200/full#supplementary-material

REFERENCES

1. Fox KAA, Dabbous OH, Goldberg RJ, Pieper KS, Eagle KA, Van de Werf F, et al. Prediction of risk of death and myocardial infarction in the six months after presentation with acute coronary syndrome: prospective multinational observational study (GRACE). *BMJ.* (2006) 333:1091. doi: 10.1136/bmj.38985.646481.55
2. Eagle KA, Lim MJ, Dabbous OH, Pieper KS, Goldberg RJ, Van de Werf F, et al. A validated prediction model for all forms of acute coronary syndrome: estimating the risk of 6-month postdischarge death in an international registry. *JAMA.* (2004) 291:2727–33. doi: 10.1001/jama.291.22.2727
3. Lane JS, Magno CP, Lane KT, Chan T, Hoyt DB, Greenfield S. Nutrition impacts the prevalence of peripheral arterial disease in the United States. *J Vasc Surg.* (2008) 48:897–904. doi: 10.1016/j.jvs.2008.05.014
4. Lee MY, Lin KD, Chang YH, Hsiao PJ, Shin SJ. Albuminuria is the stronger risk factor for peripheral arterial disease than eGFR decline in a type 2 diabetic Taiwanese population. *Kidney Blood Press Res.* (2010) 33:352–9. doi: 10.1159/000317524
5. Kumakura H, Kanai H, Hojo Y, Iwasaki T, Ichikawa S. Long-term survival and fate of the leg in de novo intermittent claudication. *Eur Heart J Qual Care Clin Outcomes.* (2017) 13:208–15. doi: 10.1093/ehjqcco/qcw057
6. Anker SD, Ponikowski P, Varney S, Chua TP, Clark AL, Webb-Peploe KM, et al. Wasting as independent risk factor for mortality in chronic heart failure. *Lancet.* (1997) 349:1050–3. doi: 10.1016/S0140-6736(96)07015-8
7. Raposeiras Roubín S, Abu Assi E, Cespón Fernandez M, Barreiro Pardal C, Lizancos Castro A, Parada JA, et al. Prevalence and prognostic significance of malnutrition in patients with acute coronary syndrome. *J Am Coll Cardiol.* (2020) 76:828–40. doi: 10.1016/j.jacc.2020.06.058
8. Bouillanne O, Morineau G, Dupont C, Coulombel I, Vincent J-P, Nicolis I, et al. Geriatric Nutritional Risk Index: a new index for evaluating at-risk elderly medical patients. *Am J Clin Nutr.* (2005) 82:777–83. doi: 10.1093/ajcn/82.4.777
9. Cereda E, Zagami A, Vanotti A, Piffer S, Pedrolli C. Geriatric nutritional risk index and overall-cause mortality prediction in institutionalised elderly: a 3-year survival analysis. *Clin Nutr.* (2008) 27:717–23. doi: 10.1016/j.clnu.2008.07.005
10. Cereda E, Pusani C, Limonta D, Vanotti A. The ability of the geriatric nutritional risk index to assess the nutritional status and predict the outcome of home-care resident elderly: a comparison with the mini nutritional assessment. *Br J Nutr.* (2009) 102:563–70. doi: 10.1017/S0007114509222677
11. Yoo SH, Kook HY, Hong YJ, Kim JH, Ahn Y, Jeong MH. Influence of undernutrition at admission on clinical outcomes in patients with acute myocardial infarction. *J Cardiol.* (2017) 69:555–60. doi: 10.1016/j.jjcc.2016.05.009
12. Minamisawa M, Seidelmann SB, Claggett B, Hegde SM, Shah AM, Desai AS, et al. Impact of malnutrition using geriatric nutritional risk index in heart failure with preserved ejection fraction. *JACC Heart Fail.* (2019) 7:664–75. doi: 10.1016/j.jchf.2019.04.020
13. Shibata K, Yamamoto M, Kano S, Koyama Y, Shimura T, Kagase A, et al. Importance of geriatric nutritional risk index assessment in patients undergoing transcatheter aortic valve replacement. *Am Heart J.* (2018) 202:68–75. doi: 10.1016/j.ahj.2018.04.021
14. Cheng N, Dang A, Lv N, He Y, Wang X. Malnutrition status in patients of very advanced age with nonvalvular atrial fibrillation and its impact on clinical outcomes. *Nutr Metab Cardiovasc Dis.* (2019) 29:1101–9. doi: 10.1016/j.numecd.2019.06.021
15. Lin T-Y, Hung S-C. Geriatric nutritional risk index is associated with unique health conditions and clinical outcomes in chronic kidney disease patients. *Nutrients.* (2019) 11:2769. doi: 10.3390/nu11112769
16. Ma X, Dong L, Shao Q, Cheng Y, Lv S, Sun Y, et al. Triglyceride glucose index for predicting cardiovascular outcomes after percutaneous coronary intervention in patients with type 2 diabetes mellitus and acute coronary syndrome. *Cardiovasc Diabetol.* (2020) 19:31. doi: 10.1186/s12933-020-01006-7
17. Cereda E, Pedrolli C. The geriatric nutritional risk index. *Curr Opin Clin Nutr Metab Care.* (2009) 12:1–7. doi: 10.1097/MCO.0b013e3283186f59
18. Tang EW, Wong C-K, Herbison P. Global Registry of Acute Coronary Events (GRACE) hospital discharge risk score accurately predicts long-term mortality post acute coronary syndrome. *Am Heart J.* (2007) 153:29–35. doi: 10.1016/j.ahj.2006.10.004
19. Morrow DA, Antman EM, Charlesworth A, Cairns R, Murphy SA, de Lemos JA, et al. TIMI risk score for ST-elevation myocardial infarction: A convenient, bedside, clinical score for risk assessment at presentation: An intravenous nPA for treatment of infarcting myocardium early II trial substudy. *Circulation.* (2000) 102:2031–7. doi: 10.1161/01.CIR.102.17.2031
20. Halkin A, Singh M, Nikolsky E, Grines CL, Tcheng JE, Garcia E, et al. Prediction of mortality after primary percutaneous coronary intervention for acute myocardial infarction: the CADILLAC risk score. *J Am Coll Cardiol.* (2005) 45:1397–405. doi: 10.1016/j.jacc.2005.01.041
21. Bradshaw PJ, Ko DT, Newman AM, Donovan LR, Tu JV. Validity of the GRACE (global registry of acute coronary events). Acute coronary syndrome prediction model for six month post-discharge death in an independent data set. *Heart.* (2006) 92:905–9. doi: 10.1136/hrt.2005.073122
22. Liu M, Chan C-P, Yan BP, Zhang Q, Lam Y-Y, Li R-J, et al. Albumin levels predict survival in patients with heart failure and preserved ejection fraction. *Eur J Heart Fail.* (2012) 14:39–44. doi: 10.1093/eurjhf/hfr154
23. Tobias DK, Pan A, Jackson CL, O'Reilly EJ, Ding EL, Willett WC, et al. Body-mass index and mortality among adults with incident type 2 diabetes. *N Engl J Med.* (2014) 370:233–44. doi: 10.1056/NEJMoa1304501
24. Ballmer PE. Causes and mechanisms of hypoalbuminaemia. *Clin Nutr.* (2001) 20:271–3. doi: 10.1054/clnu.2001.0439
25. Sze S, Pellicori P, Kazmi S, Rigby A, Cleland JGF, Wong K, et al. Prevalence and prognostic significance of malnutrition using 3 scoring systems among outpatients with heart failure: a comparison with body mass index. *JACC Heart Fail.* (2018) 6:476–86. doi: 10.1016/j.jchf.2018.02.018
26. Don BR, Kaysen G. Serum albumin: relationship to inflammation and nutrition. *Semin Dial.* (2004) 17:432–7. doi: 10.1111/j.0894-0959.2004.17603.x
27. Kim S, McClave SA, Martindale RG, Miller KR, Hurt RT. Hypoalbuminemia and clinical outcomes: what is the mechanism behind the relationship? *Am Surg.* (2017) 83:1220–7. doi: 10.1177/000313481708301123
28. Sheinenzon A, Shehadeh M, Michelis R, Shaoul E, Ronen O. Serum albumin levels and inflammation. *Int J Biol Macromol.* (2021) 184:857–62. doi: 10.1016/j.ijbiomac.2021.06.140
29. Monteiro R, Azevedo I. Chronic inflammation in obesity and the metabolic syndrome. *Mediators Inflamm.* (2010) 2010:289645. doi: 10.1155/2010/289645
30. Moshage HJ, Janssen JA, Franssen JH, Hafkenscheid JC, Yap SH. Study of the molecular mechanism of decreased liver synthesis of albumin in inflammation. *J Clin Invest.* (1987) 79:1635–41. doi: 10.1172/JCI113000
31. Fleck A, Raines G, Hawker F, Trotter J, Wallace PI, Ledingham IM, et al. Increased vascular permeability: a major cause of hypoalbuminaemia in disease and injury. *Lancet.* (1985) 1:781–4. doi: 10.1016/S0140-6736(85)91447-3
32. Wada H, Dohi T, Miyauchi K, Doi S, Naito R, Konishi H, et al. Prognostic impact of the geriatric nutritional risk index on long-term outcomes in patients who underwent percutaneous coronary intervention. *Am J Cardiol.* (2017) 119:1740–5. doi: 10.1016/j.amjcard.2017.02.051
33. Honda Y, Nagai T, Iwakami N, Sugano Y, Honda S, Okada A, et al. Usefulness of geriatric nutritional risk index for assessing nutritional status and its

prognostic impact in patients aged ≥65 years with acute heart failure. *Am J Cardiol.* (2016) 118:550–5. doi: 10.1016/j.amjcard.2016.05.045
34. Narumi T, Arimoto T, Funayama A, Kadowaki S, Otaki Y, Nishiyama S, et al. Prognostic importance of objective nutritional indexes in patients with chronic heart failure. *J Cardiol.* (2013) 62:307–13. doi: 10.1016/j.jjcc.2013.05.007
35. Goldfarb M, Lauck S, Webb JG, Asgar AW, Perrault LP, Piazza N, et al. Malnutrition and mortality in frail and non-frail older adults undergoing aortic valve replacement. *Circulation.* (2018) 138:2202–11. doi: 10.1161/CIRCULATIONAHA.118.033887
36. Matsuo Y, Kumakura H, Kanai H, Iwasaki T, Ichikawa S. The geriatric nutritional risk index predicts long-term survival and cardiovascular or limb events in peripheral arterial disease. *J Atheroscler Thromb.* (2020) 27:134–43. doi: 10.5551/jat.49767
37. Katayama T, Hioki H, Kyono H, Watanabe Y, Yamamoto H, Kozuma K. Predictive value of the geriatric nutritional risk index in percutaneous coronary intervention with rotational atherectomy. *Heart Vessels.* (2020) 35:887–93. doi: 10.1007/s00380-020-01558-4
38. Kunimura A, Ishii H, Uetani T, Aoki T, Harada K, Hirayama K, et al. Impact of geriatric nutritional risk index on cardiovascular outcomes in patients with stable coronary artery disease. *J Cardiol.* (2017) 69:383–8. doi: 10.1016/j.jjcc.2016.09.004
39. Cheng L, Rong J, Zhuo X, Gao K, Meng Z, Wen X, et al. Prognostic value of malnutrition using geriatric nutritional risk index in patients with coronary chronic total occlusion after percutaneous coronary intervention. Clin Nutr. (2021) 40:4171–9. doi: 10.1016/j.clnu.2021.01.042
40. Prompers L, Huijberts M, Apelqvist J, Jude E, Piaggesi A, Bakker K, et al. High prevalence of ischaemia, infection and serious comorbidity in patients with diabetic foot disease in Europe. Baseline results from the Eurodiale study. *Diabetologia.* (2007) 50:18–25. doi: 10.1007/s00125-006-0491-1
41. Armstrong DG, Hanft JR, Driver VR, Smith APS, Lazaro-Martinez JL, Reyzelman AM, et al. Effect of oral nutritional supplementation on wound healing in diabetic foot ulcers: a prospective randomized controlled trial. *Diabet Med.* (2014) 31:1069–77. doi: 10.1111/dme.12509
42. Stenvinkel P, Heimbürger O, Lindholm B, Kaysen GA, Bergström J. Are there two types of malnutrition in chronic renal failure? Evidence for relationships between malnutrition, inflammation and atherosclerosis (MIA syndrome). *Nephrol Dial Transplant.* (2000) 15:953–60. doi: 10.1093/ndt/15.7.953
43. Effoe VS, Correa A, Chen H, Lacy ME, Bertoni AG. High-sensitivity C-reactive protein is associated with incident type 2 diabetes among African Americans: the Jackson heart study. *Diabetes Care.* (2015) 38:1694–700. doi: 10.2337/dc15-0221
44. Abe M, Okada K, Maruyama T, Maruyama N, Matsumoto K, Soma M. Relationship between erythropoietin responsiveness, insulin resistance, and malnutrition-inflammation-atherosclerosis (MIA) syndrome in hemodialysis patients with diabetes. *Int J Artif Organs.* (2011) 34:16–25. doi: 10.5301/IJAO.2011.6314
45. Bassuk SS, Rifai N, Ridker PM. High-sensitivity C-reactive protein: clinical importance. *Curr Probl Cardiol.* (2004) 29:439–93. doi: 10.1016/S0146-2806(04)00074-X
46. Merker M, Felder M, Gueissaz L, Bolliger R, Tribolet P, Kägi-Braun N, et al. Association of baseline inflammation with effectiveness of nutritional support among patients with disease-related malnutrition: a secondary analysis of a randomized clinical trial. *JAMA Netw Open.* (2020) 3:e200663. doi: 10.1001/jamanetworkopen.2020.0663
47. Marshall S. Protein-energy malnutrition in the rehabilitation setting: evidence to improve identification. *Maturitas.* (2016) 86:77–85. doi: 10.1016/j.maturitas.2016.01.014
48. Adejumo OL, Koelling TM, Hummel SL. Nutritional Risk Index predicts mortality in hospitalized advanced heart failure patients. *J Heart Lung Transplant.* (2015) 34:1385–9. doi: 10.1016/j.healun.2015.05.027
49. Gariballa SE, Parker SG, Taub N, Castleden CM. Influence of nutritional status on clinical outcome after acute stroke. *Am J Clin Nutr.* (1998) 68:275–81. doi: 10.1093/ajcn/68.2.275
50. Kang MK, Kim TJ, Kim Y, Nam K-W, Jeong H-Y, Kim SK, et al. Geriatric nutritional risk index predicts poor outcomes in patients with acute ischemic stroke - Automated undernutrition screen tool. *PLoS One.* (2020) 15:e0228738. doi: 10.1371/journal.pone.0228738
51. Adejumo AC, Adejumo KL, Adegbala OM, Enwerem N, Ofosu A, Akanbi O, et al. Inferior outcomes of patients with acute myocardial infarction and comorbid protein-energy malnutrition. *JPEN J Parenter Enteral Nutr.* (2020) 44:454–62. doi: 10.1002/jpen.1680
52. Carvalho LSF, Bogniotti LAC, de Almeida OLR, E Silva JCQ, Nadruz W, Coelho OR, et al. Change of BNP between admission and discharge after ST-elevation myocardial infarction (Killip I) improves risk prediction of heart failure, death, and recurrent myocardial infarction compared to single isolated measurement in addition to the GRACE score. *Eur Heart J Acute Cardiovasc Care.* (2019) 8:643–51. doi: 10.1177/2048872617753049
53. Zhang S, Wan Z, Zhang Y, Fan Y, Gu W, Li F, et al. Neutrophil count improves the GRACE risk score prediction of clinical outcomes in patients with ST-elevation myocardial infarction. *Atherosclerosis.* (2015) 241:723–8. doi: 10.1016/j.atherosclerosis.2015.06.035
54. Chattopadhyay S, George A, John J, Sathyapalan T. Adjustment of the GRACE score by 2-hour post-load glucose improves prediction of long-term major adverse cardiac events in acute coronary syndrome in patients without known diabetes. *Eur Heart J.* (2018) 39:2740–5. doi: 10.1093/eurheartj/ehy233
55. Schuetz P, Fehr R, Baechli V, Geiser M, Deiss M, Gomes F, et al. Individualised nutritional support in medical inpatients at nutritional risk: a randomised clinical trial. *Lancet (London, England).* (2019) 393:2312–21. doi: 10.1016/S0140-6736(18)32776-4
56. Hersberger L, Dietz A, Bürgler H, Bargetzi A, Bargetzi L, Kägi-Braun N, et al. Individualized nutritional support for hospitalized patients with chronic heart failure. *J Am Coll Cardiol.* (2021) 77:2307–19. doi: 10.1016/j.jacc.2021.03.232
57. Milne AC, Potter J, Vivanti A, Avenell A. Protein and energy supplementation in elderly people at risk from malnutrition. *Cochrane Database Syst Rev.* 2009:CD003288. doi: 10.1002/14651858.CD003288.pub3
58. Esselstyn CB. A plant-based diet and coronary artery disease: a mandate for effective therapy. *J Geriatr Cardiol.* (2017) 14:317–20. doi: 10.11909/j.issn.1671-5411.2017.05.004

Conflict of Interest: The authors declare that the research was conducted in the absence of any commercial or financial relationships that could be construed as a potential conflict of interest.

The reviewer YC declared a shared affiliation, with the authors X-TM, Q-YS, Q-XL, Z-QY, K-NH, JL, HS, X-LL, Y-JZ, and Z-JW to the handling editor at the time of the review.

frontiers in Cardiovascular Medicine

ORIGINAL RESEARCH
published: 11 January 2022
doi: 10.3389/fcvm.2021.755062

Genetic Variants Associated With Sudden Cardiac Death in Victims With Single Vessel Coronary Artery Disease and Left Ventricular Hypertrophy With or Without Fibrosis

Juha H. Vähätalo[1], Lauri T. A. Holmström[1], Katri Pylkäs[2], Sini Skarp[3], Katja Porvari[4], Lasse Pakanen[4,5], Kari S. Kaikkonen[1], Juha S. Perkiömäki[1], Risto Kerkelä[3], Heikki V. Huikuri[1], Robert J. Myerburg[6] and M. Juhani Junttila[1,7]*

[1] Research Unit of Internal Medicine, Medical Research Center Oulu, Oulu University Hospital, University of Oulu, Oulu, Finland, [2] Laboratory of Cancer Genetics and Tumor Biology, Cancer and Translational Medicine Research Unit, Biocenter Oulu, University of Oulu, Oulu, Finland, [3] Research Unit of Biomedicine and Biocenter Oulu, University of Oulu, Oulu, Finland, [4] Department of Forensic Medicine, Research Unit of Internal Medicine, Medical Research Center Oulu, University of Oulu, Oulu, Finland, [5] Forensic Medicine Unit, Finnish Institute for Health and Welfare, Oulu, Finland, [6] Division of Cardiology, Miller School of Medicine, University of Miami, Miami, FL, United States, [7] Biocenter Oulu, University of Oulu, Oulu, Finland

OPEN ACCESS

Edited by:
Hendrik Tevaearai Stahel,
Bern University Hospital, Switzerland

Reviewed by:
Gaetano Thiene,
University of Padua, Italy
Stefan Michael Sattler,
University of Copenhagen, Denmark

***Correspondence:**
Juha H. Vähätalo
juha.vahatalo@student.oulu.fi

Specialty section:
This article was submitted to Coronary Artery Disease, a section of the journal Frontiers in Cardiovascular Medicine

Received: 07 August 2021
Accepted: 07 December 2021
Published: 11 January 2022

Citation:
Vähätalo JH, Holmström LTA, Pylkäs K, Skarp S, Porvari K, Pakanen L, Kaikkonen KS, Perkiömäki JS, Kerkelä R, Huikuri HV, Myerburg RJ and Junttila MJ (2022) Genetic Variants Associated With Sudden Cardiac Death in Victims With Single Vessel Coronary Artery Disease and Left Ventricular Hypertrophy With or Without Fibrosis. Front. Cardiovasc. Med. 8:755062. doi: 10.3389/fcvm.2021.755062

Objective: Cardiac hypertrophy with varying degrees of myocardial fibrosis is commonly associated with coronary artery disease (CAD) related sudden cardiac death (SCD), especially in young victims among whom patterns of coronary artery lesions do not entirely appear to explain the cause of SCD. Our aim was to study the genetic background of hypertrophy, with or without fibrosis, among ischemic SCD victims with single vessel CAD.

Methods: The study population was derived from the Fingesture study, consisting of all autopsy-verified SCDs in Northern Finland between the years 1998 and 2017 (n = 5,869). We carried out targeted next-generation sequencing using a panel of 174 genes associated with myocardial structure and ion channel function in 95 ischemic-SCD victims (mean age 63.6 ± 10.3 years; 88.4% males) with single-vessel CAD in the absence of previously diagnosed CAD and cardiac hypertrophy with or without myocardial fibrosis at autopsy.

Results: A total of 42 rare variants were detected in 43 subjects (45.3% of the study subjects). Five variants in eight subjects (8.4%) were classified as pathogenic or likely pathogenic. We observed 37 variants of uncertain significance in 39 subjects (40.6%). Variants were detected in myocardial structure protein coding genes, associated with arrhythmogenic right ventricular, dilated, hypertrophic and left ventricular non-compaction cardiomyopathies. Also, variants were detected in ryanodine receptor 2 (*RYR2*), a gene associated with both cardiomyopathies and catecholaminergic polymorphic ventricular tachycardias.

Conclusions: Rare variants associated with cardiomyopathies, in the absence of anatomic evidence of the specific inherited cardiomyopathies, were common findings among CAD-related SCD victims with single vessel disease and myocardial hypertrophy found at autopsies, suggesting that these variants may modulate the risk for fatal arrhythmias and SCD in ischemic disease.

Keywords: sudden cardiac death, left ventricular hypertrophy, coronary artery disease, genetics, medicolegal autopsy

INTRODUCTION

Approximately 80% of sudden cardiac deaths (SCDs) are due to coronary artery disease (CAD) and up to one-half occur in the absence of previously diagnosed cardiac disease (1). Regardless of the cause, cardiac hypertrophy, associated with varying degrees of myocardial fibrosis, is a risk factor for SCD and is associated with increased risk for SCD in patients with or without CAD (2). Left ventricular hypertrophy (LVH) is a common finding in both ischemic and non-ischemic SCD victims at autopsy (3, 4).

Hypertension is the most common cause of LVH in patients with CAD, but LVH is also a common finding in normotensive CAD patients (5). Myocardial weight often increases along with the severity of CAD (4). Three-vessel CAD and cardiac hypertrophy increase the vulnerability to fatal arrhythmias and SCD (4). Nevertheless, some SCDs occur in victims with only single-vessel CAD and cardiac hypertrophy found at autopsy (6).

We hypothesized that a subgroup of SCD victims with less severe CAD and cardiac hypertrophy, with varying degrees of myocardial fibrosis, are associated with rare genetic variants, which could contribute to the development of ischemic heart disease, risk of fatal arrhythmias and SCD. Our aim was to study the association of rare variants in cardiac structure and function encoding genes in SCD victims with single-vessel CAD and myocardial hypertrophy detected at autopsy, in the absence of previously diagnosed CAD.

METHODS

Study Population

The study population was derived from the Fingesture study (The Finnish Genetic Study of Arrhythmic Events; www.clinicaltrials.gov NCT02075866), consisting of 5,869 victims of autopsy-verified SCDs in Northern Finland. Medico-legal autopsies were performed between the years 1998 and 2017 in the Forensic Medicine Unit of the Finnish Institute for Health and Welfare, Oulu, Finland, and at the Department of Forensic Medicine of the University of Oulu, Oulu, Finland by experienced forensic pathologists, using contemporary guidelines for the diagnosis of cause of death. Finnish law requires medico-legal autopsies whenever the death is not caused by a known disease, when the victim was not treated by a physician during his/her last illness, or when the death has been otherwise unexpected (Act on the Inquest into the Cause of Death, 459/1973, 7th paragraph: Finnish Law). As a result of the Finnish legislation, autopsy rates are one of the highest in the Western countries (7). Deaths were defined as sudden if the event was either witnessed within 6 h of the onset of symptoms or an unwitnessed within 24 h when the victim was last seen in a stable state of health. Only sudden deaths considered to be caused by a cardiac disease were included in the Fingesture study. Non-cardiac causes of death such as pulmonary embolism, cerebral hemorrhage as well as intoxications and other non-natural causes were excluded from the SCD cohort.

Autopsy Data

Determination of the cause of death was based on autopsy findings and complementary analyses, available medical records, police reports and specific questionnaires for the relatives of the victim. All postmortem examinations included histological examination from samples taken at autopsy. If autopsy findings were insufficient to define a cause of death, or if a toxic exposure was suspected, toxicologic investigation was conducted. In Finland, meticulous cardiac examinations are performed in all victims during medico-legal autopsies, including macroscopic investigation of myocardium and coronary arteries, heart weight and several histological samples from myocardium. Evidence of an acute coronary event, defined by the presence of an acute intracoronary thrombus, plaque rupture or erosion, intraplaque hemorrhage, critical stenosis (>75%) or complete occlusion of a main coronary artery, was used to classify SCD as ischemic. Possible myocardial scarring was detected macroscopically from cross-sectional samples of the ventricles and microscopically from the myocardial samples. A heart weight > the predicted value based on body surface area (at least 420 g) with hypertrophic myocytes observed at autopsy was identified as cardiac hypertrophy. Methods for the classification of cause of death have been described in our previous studies (3, 8).

Tissue Samples and Gene Sequencing

DNA samples for genetic studies were isolated from formalin-fixed paraffin-embedded myocardial tissue samples taken at autopsy. For library preparation we used The TruSight Cardio gene panel kit, which contains 174 genes associated with hereditary cardiac diseases that are most affected by a genetic predisposition (http://support.illumina.com/downloads/trusight-cardio-product-files.html) (Illumina, San Diego, CA). Genes included in the panel are shown in **Table 1**. Purification of the samples was performed with Agencourt AMPure XP beads (Beckman Coulter Life Sciences, Indianapolis, IN). With quantitative polymerase chain reaction–based formalin-fixed paraffin-embedded quality control kit (Illumina), the

TABLE 1 | Cardiac structure- and function-related genes sequenced in the panel, classified by related diseases.

HCM related	*ACTC1, ACTN2, ANKRD1, CALR3, CAV3, CSRP3, JPH2, MYBPC3, MYH6, MYH7, MYL2, MYL3, MYLK2, MYO6, MYOZ2, MYPN, NEXN, PDLIM3, PLN, PRKAG2, TCAP, TNNC1, TNNI3, TNNT2, TPM1, TRIM63, VCL*
AC related	*DES, DSC2, DSG2, DSP, JUP, LMNA, PKP2, PLN, RYR2, SCN5A, TGFB3, TMEM43*
DCM related	*ABCC9, ACTN2, ACTC1, ANKRD1, BAG3, CRYAB, CSRP3, DES, DMD, DSG2, EYA4, GATAD1, LAMA4, LDB3, LMNA, MYBPC3, MYH6, MYH7, MYPN, NEXN, PLN, RBM20, SCN5A, SGCD, TAZ, TCAP, TMPO, TNNC1, TNNI3, TNNT2, TPM1, TTN, VCL, ZBTB17*
LVNC related	*DTNA, LDB3, LMNA, MIB1, MYBPC3, MYH7, PRDM16, TAZ, TNNT2, TPM1*
Metabolic disorders and syndromes with cardiac diseases and congenital heart defects	*ALMS1, BRAF, CBL, COX15, CRELD1, DNAJC19, DOLK, FXN, GAA, GLA, HFE, HRAS, JAG1, KRAS, LAMP2, MAP2K1, MAP2K2, NKX2-5, NODAL, NOTCH1, NRAS, PTPN11, RAF1, SCO2, SDHA, SHOC2, SMAD4, SOS1, TBX3, TBX20, TBX5, TTR, ZIC3*
Arrhythmic disorders (LQTS, Brugada, familial FA, CPVT etc.)	*AKAP9, ANK2, CACNA1C, CACNA2D1, CACNB2, CALM1, CASQ2, CAV3, DPP6, GJA5, GPD1L, HCN4, KCNA5, KCND3, KCNE1, KCNE2, KCNE3, KCNH2, KCNJ2, KCNJ5, KCNJ8, KCNQ1, NPPA, RANGRF, RYR2, SCN1B, SCN2B, SCN3B, SCN4B, SCN5A, SNTA1, TRDN, TRPM4*
Dyslipidemia	*ABCG5, ABCG8, APOA5, APOB, APOC2, APOE, CETP, GPIHBP1, LDLR, LDLRAP1, LMF1, LPL, PCSK9, SREBF2*
Aortopathies/EDS	*ACTA2, COL3A1, COL5A1, COL5A2, EFEMP2, ELN, FBN1, FBN2, MYH11, MYLK, SLC2A10, SMAD3, TGFB2, TGFB3, TGFBR1, TGFBR2*
Muscular dystrophies/myopathies	*ACTA1, BAG3, EMD, FHL1, FKRP, FKTN, LAMA2, RYR1, SEPN1, SGCB, SGCD, SGCG, SLC25A4, TMEM43*
Other	*APOA4, CBS, CREB3L3, CTF1, FHL2, GCKR, HADHA, HSPB8, ILK, KLF10, LTBP2, MURC, PRKAR1A, SALL4, TXNRD2, ZHX3*

Variants detected in the present study are highlighted (red). AC, Arrhythmogenic right ventricular cardiomyopathy; DCM, Dilated cardiomyopathy; CPVT, Catecholaminergic polymorphic ventricular tachycardia; EDS, Ehlers-Danlos syndrome; FA, Familial arrhythmia; HCM, Hypertrophic cardiomyopathy; LQTS, Long QT syndrome; LVNC, Left ventricular non-compaction cardiomyopathy.

quality of the samples chosen for NGS was verified. The samples that passed quality control (i.e., with a quantitative polymerase chain reaction ΔCq value $\leq$ 2.3) were selected for gene panel sequencing with NextSeq550 platform (Illumina). BWA Enrichment (BWA Genome Aligner Software and the GATK Variant Caller) was used to align sequences and call variants within the BaseSpace Genomics computing environment (Illumina); VariantStudio to annotate, filter, and classify the variants; and Integrative Genomics Viewer visualize the data to exclude falsely annotated variants and sequencing artifacts. Within BaseSpace, the *in silico* prediction tools PolyPhen and SIFT were used to predict the effect of amino acid changes on protein function.

Variant Analysis

We selected all variants with a possible effect on protein for analysis (missense, frameshift, stop gained/lost, initiator codon, in-frame insertion, in-frame deletion, and splice-site alterations). Selected variants were further filtered by excluding variants with minor allele frequency > 0.01 among Finnish subjects from general population in dbSNP or The Genome Aggregation Database (gnomAD) database. Pathogenicity of variants were assessed according to American College of Medical Genetics (ACMG) consensus guidelines (9). Benign variants were excluded from the results. Variants that were not classified as benign were further classified as pathogenic/likely pathogenic or as variants of uncertain significance (VUS), based upon the ACMG guidelines by combining data from previous literature, Human Gene Mutation Database (HGMD), ClinVar database, *in silico* prediction tools (SIFT, PolyPhen) and population frequency databases (gnomAD with > 3,000 Finnish controls), The Sequencing Initiative Suomi (SISu) with >10,000 Finnish controls).

Statistical Analysis

Statistical significance, odds ratios (OR) and 95% confidence intervals (CI) were estimated using $\chi 2$ test with two-sided *p*-value (Fisher's Exact Test if a specific variant was detected in multiple study subjects. The Sequencing Initiative Suomi (SISu) database (10), including data on genetic variants from 10,490 exome sequenced Finnish citizens, was used as a control group. Analyses were performed with the Statistical Package for Social Studies version 24.0 (IBM). *P*-values < 0.05 were considered statistically significant and all *p*-values were two-sided.

RESULTS

Characteristics of the Study Subjects

In the Fingesture study, CAD was determined to be the underlying cause of SCD in 4,392 victims (74.8%), and 3,122 victims (71.1%) had no history of CAD prior to death. Among these victims, single-vessel CAD, determined by evidence of either acute or prior myocardial infarction due to critical stenosis or occlusion of a single epicardial coronary artery, and cardiac hypertrophy were present in 244 individuals. We carried out genetic studies in 95 SCD victims with single-vessel CAD and cardiac hypertrophy in the absence of previously diagnosed CAD, whose DNA passed the quality control for further analysis. No macroscopic or microscopic evidence of cardiomyopathies were

TABLE 2 | Clinical characteristics and autopsy findings of the ischemic-SCD victims with single-vessel CAD and cardiac hypertrophy in the absence of previously diagnosed CAD ($n = 95$).

Characteristic	Value
Age, mean (SD), y	63.6 (10.3)
Male gender, *n* (%)	84 (88.4%)
Hypertension, *n* (%)	25 (26.3%)
Diabetes mellitus, *n* (%)	12 (12.6%)
Dyslipidemia, *n* (%)	8 (8.4%)
Angina, *n* (%)	4 (4.2%)
Dyspnea, *n* (%)	5 (5.3%)
Abundant use of alcohol, *n* (%)	32 (33.7%)
Circumstances at death	
Unwitnessed; dead on initial contact, *n* (%)	89 (93.7%)
During physical activity, *n* (%)	5 (5.3%)
In hospital, health center, or ambulance, *n* (%)	3 (3.2%)
Body mass index, mean (SD), kg/m^2	29.0 (5.3)
Total heart weight, mean (SD), g	514.5 g (87.3), 421-820g range
Occluded coronary artery	
LAD, *n* (%)	80 (84.2%)
CX, *n* (%)	4 (4.2%)
RCA, *n* (%)	11 (11.6%)
Myocardial scar, *n* (%)	22 (23.2%)

CX, Left circumflex coronary artery; LAD, Left anterior descending coronary artery; RCA, Right coronary artery; SD, Standard deviation.

observed among these victims. The mean age of the study subjects was 63.6 ± 10.3 years and the majority were men (88.4%, 84 subjects). The mean heart weight was 514.5 ± 87.3 g (range 421-820 g) and the mean BMI 29.0 ± 5.3 kg/m^2. A healed myocardial infarction scar was detected in 23.2% (22 subjects). 26.3% (25 subjects) had known hypertension, 12.6% (12 subjects) diabetes, 8.4% (8 subjects) dyslipidemia. The most common occluded coronary artery was left anterior descending (84.2% of the subjects; 80 subjects). The characteristics of the study subjects are described in **Table 2**.

Detected Variants

Potentially disease-related variants (pathogenic, likely pathogenic or VUS) were observed in 22 genes among 43 of the study subjects (45.3%), among which pathogenic or likely-pathogenic variants were detected in eight subjects (8.4%). Two or more potentially relevant variants were detected in eight subjects (8.4%).

A summary of the detected pathogenic/likely pathogenic variants is presented in **Table 3**, the VUS's are presented in the **Supplementary Table**. Five variants were classified as pathogenic or likely pathogenic and 37 variants were classified as VUS. All of the potentially disease-related variants were detected in myocardial structure protein coding genes, including those associated with arrhythmogenic cardiomyopathy (AC), hypertrophic cardiomyopathy (HCM), dilated cardiomyopathy (DCM) and left ventricular non-compaction cardiomyopathy (LVNC). *RYR2* has also been associated with catecholaminergic polymorphic ventricular tachycardias (CPVTs). None of SCD subjects with rare variants presented autopsy findings specific for classic expression of HCM, DCM, AC or non-compaction cardiomyopathy. No significant variants in ion channel coding genes were observed in the present study. A healed myocardial scar was detected in 10 subjects (23.4%) with potentially disease relevant variant(s). The DNA sequencing data has been deposited to European Variation Archive.

Pathogenic and Likely-Pathogenic Variants

A novel pathogenic variant was found in the desmosomal gene *DSG2*, of which mutations have been described in patients with AC. This variant (c.523 + 1G > A) was considered as pathogenic because of its effect on splicing site, low population frequency in Finland (<1/10,000) and classification as likely pathogenic by ClinVar database. Additionally, in a previous study (11), similar variant (c.523 + 2T > C) was found in three unrelated patients with AC.

Four likely pathogenic missense variants were identified among the study subjects in *MYBPC3* (two subjects), *MYH7* (three subjects), *DTNA* and *DSG2*. These variants did not quite fulfill the criteria to be considered as pathogenic. However, these variants had low minor population frequency in Finland, are considered as disease causing by ClinVar, and/or are predicted to be damaging by *in silico* tools. The Ala833Thr variant in *MYBPC3* associated with HCM was detected in two unrelated subjects. It was also classified as likely-pathogenic in a previous study (12), and found in familial HCM in a Swedish study (13). Compared to Finnish control population, the difference in the prevalence of affected carriers was statistically significant (2/95 vs. 46/10,480; $p = 0.016$, OR = 4.9, 95% CI 1.2-20.4). The p.Val56Met variant in a conserved region of *DSG2* was previously observed in an AC patient (14), and p.Pro121Leu in *DTNA* has been previously described in family with left ventricular non-compaction (15). We also observed a p.Glu1039Gly variant in a conserved region of *MYH7* in three victims. This variant was previously detected in SCD victims with primary myocardial fibrosis (PMF) (12), and a mutation next to this codon in highly conserved region (p.Leu1038Pro) was previously associated with DCM (16). The difference in the prevalence of affected carriers compared to control population was statistically significant (3/95 vs. 18/10,489; $p = 0.0008$, OR = 19.0, 95% CI 5.5-65.5).

Variants of Uncertain Significance

Variants classified as VUS were observed in 39 study subjects (41.1%). Five of the VUSs were detected in multiple unrelated affected subjects, suggesting possible pathogenicity. These included p.Thr358Ile in *DSC2* ($n = 3$), p.Lys259Glu in *TPM1* ($n = 3$), p.Arg100His in *CSRP3* ($n = 2$), p.Ala936Val in *MYH6* ($n = 2$) and p.Arg634His in *DSC2* ($n = 4$). Previously, p.Arg100His in *CSRP3* has been found in Danish HCM patient (17). p.Ala292Ser in *CASQ2* and p.Arg31Gln in *DTNA* have both been detected in PMF victims (12). p.Ser140Phe in *PKP2* has been described in patients with AC (18, 19), as well as in a previous DCM study (20), which considered this variant as *at least disease modifying if not pathogenic*. p.Thr1373Ala in conserved region of *DSP* was classified earlier as potentially disease causing in a Finnish AC study (21). This study also showed some evidence for a role of

TABLE 3 | Summary of pathogenic and likely pathogenic variants in sudden cardiac death victims with single-vessel coronary artery disease and hypertrophied heart found at medico-legal autopsy.

Mutated gene	Nucleotide change	Effect of protein	Predicted effect	N	NGS coverage	gnomAD > 3,000 Finnish controls MAF	SISu > 10,000 Finnish controls MAF	ACMG score	Clinical features and autopsy findings of the victims
Pathogenic variants									
DSG2	c.523 + 1G > A		Affects canonical splicing	1	75	Not detected	<0.0001	PVS1 + PM2 + PP2 + PP5	Male, in his 70 s, BMI 25, heart weight 446 g, no fibrosis, LAD occluded
Likely pathogenic variants									
MYBPC3	c.2497G > A	p.Ala833Thr	Missense	2	302/363	0.0023	0.0022	PS1 + PP1 + PP2 + PP3	1: Male, in his 50 s, BMI 22, heart weight 450 g, mild fibrosis, LAD occluded 2: Female, in her 70 s, BMI 27, heart weight 598 g, moderate fibrosis, LAD occluded, myocardial scar
MYH7	c.3116A > G	p.Glu1039Gly	Missense	3	146/111/101	0.0011	0.0009	PS4 + PM1 + PP2 + PP3	1: Male, in his 60 s, BMI 31, heart weight 540 g, moderate fibrosis, LAD occluded 2: Male, in his 70 s, BMI 28, heart weight 535 g, substantial fibrosis, LAD occluded 3: Male, in his 60 s, BMI 29, heart weight 575 g, mild fibrosis, CX occluded, myocardial scar
DTNA	c.362C > T	p.Pro121Leu	Missense	1	96	Not detected	<0.0001	PS3 + PM2 + PP1 + PP4 + PP5	Female, in her 40 s, BMI 28, heart weight 430 g, no fibrosis, LAD occluded
DSG2	c.166G > A	p.Val56Met	Missense	1	129	0.0006	0.0004	PM1 + PP2 + PP3 + PP4 + PP5	Male, in his 50 s, BMI 31, heart weight 580 g, moderate fibrosis, LAD occluded, myocardial scar

ACMG criteria:

Very strong evidence of pathogenicity: PVS1, Null variant (nonsense, frameshift, canonical ±1 or 2 splice sites, initiation codon, single or multi-exon deletion) in a gene where loss of function is a known mechanism of disease.

Strong evidence of pathogenicity: PS1, Same amino acid change as a previously established pathogenic variant regardless of nucleotide change; PS2, De novo mutation in a patient with the disease and no family history; PS3, Well-established in vitro or in vivo functional studies supportive of a damaging effect on the gene or gene product; PS4, The prevalence of the variant in affected individuals is significantly increased compared to the prevalence in controls.

Moderate evidence of pathogenicity: PM1, Located in a mutational hot spot and/or critical and well-established.

Functional domain (e.g., active site of an enzyme) without benign variation; PM2, Absent from controls (or at extremely low frequency if recessive).

In exome sequencing project, 1,000 Genomes or gnomAD; PM3, For recessive disorders, detected in trans with a pathogenic variant; PM4, Protein length changes due to in-frame deletions/insertions in a non-repeat region or stop-loss variants; PM5, Novel missense change at an amino acid residue where a different missense change determined to be pathogenic has been seen before; PM6, Assumed de novo, but without confirmation of paternity and maternity.

Supporting evidence of pathogenicity: PP1, Co-segregation with disease in multiple affected family members in a gene definitively known to cause the disease; PP2, Missense variant in a gene that has a low rate of benign missense variation and where missense variants are a common mechanism of disease; PP3, Multiple lines of computational evidence support a deleterious effect on the gene or gene product (conservation, evolutionary, splicing impact, etc.); PP4, Patient's phenotype or family history is highly specific for a disease with a single genetic etiology; PP5, Reputable source recently reports variant as pathogenic but the evidence is not available to the laboratory to perform an independent evaluation.

Rules for combining criteria to classify sequence variants.

Pathogenic:

1. 1 Very Strong (PVS1) AND.
   a. ≥1 Strong (PS1–PS4) OR.
   b. ≥2 Moderate (PM1–PM6) OR.
   c. 1 Moderate (PM1–PM6) and 1 Supporting (PP1–PP5) OR.
   d. ≥2 Supporting (PP1–PP5).
2. ≥2 Strong (PS1–PS4) OR.
3. 1 Strong (PS1–PS4) AND.
   a. ≥3 Moderate (PM1–PM6) OR.
   b. 2 Moderate (PM1–PM6) AND ≥2 Supporting (PP1–PP5) OR.
   c. 1 Moderate (PM1–PM6) AND ≥4 Supporting (PP1–PP5).

Likely pathogenic:

1. 1 Very Strong (PVS1) AND 1 Moderate (PM1–PM6) OR.
2. 1 Strong (PS1–PS4) AND 1–2 Moderate (PM1–PM6) OR.
3. 1 Strong (PS1–PS4) AND ≥ 2 Supporting (PP1–PP5) OR.
4. ≥3 Moderate (PM1–PM6) OR.
5. 2 Moderate (PM1–PM6) AND ≥ 2 Supporting (PP1–PP5) OR.
6. 1 Moderate (PM1–PM6) AND ≥ 4 Supporting (PP1–PP5).

ACMG, American college of molecular genetics; BMI, Body mass index; CX, Left circumflex coronary artery; gnomAD, The Genome Aggregation Database; LAD, Left anterior descending coronary artery; MAF, Minor allele frequency; NGS, Next generation sequencing; SISu, The Sequencing Initiative Suomi.

the variant in risk of tachycardias and association of both PR-interval prolongation and abnormality in the atrioventricular conduction. p.Thr358Ile in *DSC2* was found in three study subjects and earlier in a patient with AC (22). p.Ala2499Thr, p.Arg3597Gly and p.Asp1862Ala in *RYR2* has not been described in previous literature, but p.Arg2518Trp was observed in PMF victim (12). p.Gly154Ser in *CRYAB* was previously classified as likely pathogenic (12), and observed in DCM patients (23). However, the evidence of pathogenicity remains unclear. p.Ala2294Gly in *DSP* has previously been classified as pathogenic (24). The mutation was found in two patients with advanced DCM undergoing cardiac transplantation and the mutation also co-segregated with DCM in the other family. p.Arg1037Gln in *LAMA4* have previously been described in the PMF study (12).

DISCUSSION

In the present study, derived from our large autopsy-based SCD population, we investigated the genetic background for LV hypertrophy, with or without fibrosis, among ischemic SCD victims with single vessel CAD found at autopsy. Our genetic studies demonstrated that many CAD-associated SCD victims with single vessel disease and myocardial hypertrophy carry rare variants in cardiomyopathy-associated genes without anatomical or histopathological findings of the inherited cardiomyopathies. Likely disease-causing gene variants were detected in 8.4% of the subjects and 41.1% carried a variant of uncertain significance. All rare variants were detected predominantly in myocardial structure coding genes associated with DCM, AC, HCM, and LVNC. However, mutations in the *RYR2* gene have been associated with both catecholaminergic polymorphic ventricular tachycardias, in addition to AC (25). No significant variants in ion channel coding genes were detected among our study subjects.

These results raise a question whether, at least in some ischemic SCD victims, variants in myocardial structural genes may possibly contribute to the development of myocardial hypertrophy and/or fibrosis and correlate with the risk for fatal arrhythmias, especially when the severity of CAD does not appear to entirely explain the cause of SCD. However, we cannot exclude the possibility of myocardial hypertrophy with/without fibrosis being only a bystander in specific cases in which an acute coronary event leading to SCD. In addition, about 23% of the study subjects had a myocardial scar detected at autopsy. Healed scar can induce myocardial hypertrophy adjacent to the scar (26), that may associate with risk of arrhythmias, while a genetic predisposition to hypertrophy and fibrosis may associate with these findings in remote, non-infarcted areas, further affecting the vulnerability to arrhythmias. The causes of hypertrophy and fibrosis in the study subjects are likely to be multifactorial, including not only ischemic modulation, but also different levels of treated or untreated hypertension. Nevertheless, it remains interesting that many subjects also have the possibly myocardial disease-causing genetic variants. Perhaps the current approach of labeling each cardiac disease as its own entity is too narrow a view of the actual pathophysiology underlying the risk for sudden death.

Likely disease-causing variants in the present study were detected in genes associated with AC, HCM, DCM, and LVNC. However, none of the subjects in our study presented characteristic autopsy findings related to these specific cardiomyopathies. Rather, all deaths were determined to be caused by CAD in medicolegal investigations, in the presence of LV hypertrophy with varying degrees of fibrosis. As previously observed (12, 27, 28) the phenotypic expression of specific inherited cardiomyopathies may vary significantly. Fibrosis may be the only, or perhaps the earliest, expression of the underlying structural disorder. Inherited structural disorders may have overlapping features (12), which were seen in our results as well. In general, several variants were found in some of the same genes as in PMF victims (12).

Phenotypic expressions and the age at onset of the myocardial disease between gene variants are very heterogenous. For example, variants in *MYBPC3* have been associated with late onset disease and a high rate of incomplete penetrance (29, 30). Even within the same gene, the disease severity and penetrance rate of different gene defects and variants can vary significantly (31). Variable phenotypes can occur also in individuals with the same disease-causing mutation. Although no autopsy findings relating to particular cardiomyopathies were found in any of the study victims, it is reasonable to suggest that the gene defect(s) might have a role in the development of cardiac hypertrophy.

Cardiac hypertrophy is generally known to be associated with increased risk for fatal arrhythmias and SCD (4, 32), and as observed in subjects with CAD (33), it may have an independent mechanistic pathway for ventricular arrhythmias (32). For example, increased left ventricular mass impairs the coronary flow and increases oxygen demand, which can lead to ischemia and arrhythmias, even in the presence of less severe CAD (34). Thus, the risk for SCD was likely higher than with single-vessel disease in the absence of hypertrophy/fibrosis in our study. Almost one-half of the study subjects carried a variant in myocardial structural coding genes, which might have, at least in some cases, explained the cardiac hypertrophy. Even though the panel we used included 174 myocardial genes, we cannot exclude the possibility that some of the study subjects might have had unidentified in other genes.

The number of variants classified as VUS were rather high in the present study. The development of NGS techniques has provided a relatively fast and affordable way for sequencing of large gene panels, which has led to increasing amount of genetic testing and studies. Thus, the number of variants classified as VUS has increased, which is a common challenge in clinical genomics (35). ACMG guidelines are widely used for interpretation and reporting of gene variants. However, since guidelines have not been validated for specific disorders, they may be suboptimal for some genetic diseases like CPVT (36). Even if a genetic variant is not considered pathogenic, it may still be reasonable to consider the possibility of disease-modifying role and contributing effect on the risk of SCD, especially in the presence of CAD.

In cardiomyopathies, the abnormal myocardial structure is considered to act as the substrate for arrhythmias. It has been observed that arrhythmias may occur in the early phase of the disease process or even in the absence of phenotypic features

associated with cardiomyopathies, suggesting that underlying gene defects may have also other arrhythmogenic mechanisms (37). In our CAD-SCD victims, the risk profile for SCD might be a combination of components from both CAD and structural gene defects.

The severity of inherited cardiac diseases has been shown to increase with double or compound mutations (31, 38). Among our study population, 8.4% of the study subjects had at least two potentially relevant variants in structural genes. It is reasonable to consider that individuals with multiple variants might have higher risk for the fatal arrhythmias. Also, it might be possible that even if subject does not have likely disease-causing variant, but multiple VUS variants, the risk for arrhythmias may be higher.

While traditional risk factors for SCD and CAD have been widely studied, the importance and limitations of personalized risk prediction and the role of genetics in the identification of individuals at high risk for SCD has been recognized (39). Evidence for the role of heredity in the risk of SCD have been demonstrated (4), and it is anticipated that genetic profiling will have an increasingly important role in the assessment of the arrhythmogenic risk in the future (37, 39). Based upon the results of this study, we suggest that gene variants in myocardial structure coding genes may associate with the risk of SCD in the presence of single vessel CAD, which would support more intensive CAD treatment strategies for such patients. Additionally, the findings enhance the necessity of primary prevention of CAD (e.g., a healthy lifestyle, cholesterol and blood pressure control), particularly among individuals with variants in myocardial structure coding genes. Therefore, it could be relevant to screen the families of victims with the profiles observed in this report in order to identify those at risk for SCD and to minimize their cardiovascular disease risk burden.

Postmortem genetic analysis improves the accuracy of determining the cause of death, especially when a structurally normal heart is detected at autopsy or when the severity of heart disease does not entirely explain the cause of sudden death (40). Generally, when CAD is detected at autopsy, especially in middle-aged and older populations, postmortem genetic analysis is not considered as necessary to identify the cause of death. These results suggest that rare variants in myocardial structure coding genes might have a contributing role in the development of myocardial disease among patients with less severe coronary artery disease, however, the usefulness in diagnostics, for example, is yet to be solved.

LIMITATIONS

Since our NGS method used is unable of identifying, for example, mutations in intron regions, large deletions or copy number variations, potential variants may go undiscovered. As in most NGS studies, the causal association between detected rare variants and cardiac structural disease remains to be established. Multiple variants with uncertain pathogenicity were observed in the present study, and thus more studies are needed to clarify the specific role of these mutations in the pathophysiology of SCDs. Since none of the subjects in our study had prior knowledge of cardiac disease, it is possible that they had underlying hypertension that could explain the occurrence of LVH. However, this only increases the possibility that, in subjects without prior hypertension, the occurrence and relevance of underlying genetic variants could be even greater. Also, well-recognized limitations are present when extracting DNA from formalin fixed paraffin embedded tissues. However, NGS coverage in all cases were sufficient and Sanger confirmation was not considered necessary.

CONCLUSIONS

Many SCD victims with single vessel CAD and LV hypertrophy observed at autopsy, in the absence of previously diagnosed CAD, had rare variants in myocardial structural coding genes. Variants were detected in disease-associated genes including HCM, DCM, AC, LVNC and CPVT. We identified no variants in genes that are exclusively associated with inherited ion channel defects among the study subjects. The variants identified might contribute to the risk for fatal arrhythmias and sudden death in ischemic heart disease, in SCD victims with less advanced CAD.

DATA AVAILABILITY STATEMENT

The datasets presented in this study can be found in online repositories. The names of the repository/repositories and accession number(s) can be found at: https://www.ebi.ac.uk/eva/; PRJEB47695, ERZ3584884.

ETHICS STATEMENT

This study complies with the Declaration of Helsinki and has been approved by the Ethics Committee of the University of Oulu and Finland's Ministry of Social Affairs and Health. Finnish Institute for Health and Welfare and the Regional State Administrative Agency of Northern Finland approved the review of autopsy data by the investigators. Written informed consent for participation was not required for this study in accordance with the national legislation and the institutional requirements.

AUTHOR CONTRIBUTIONS

JJ, HH, and JP: study design and conception. JV and JJ: drafting of the manuscript and obtained funding. JV and LH: statistical analysis. LH, KPy, SS, KPo, LP, KK, JP, RK, RM, HH, and JJ: critical revision of the manuscript for important intellectual content. JJ and HH: supervision. All authors contributed to the article, acquisition, analysis or interpretation of data, and approved the submitted version.

FUNDING

This work was supported by Aarne Koskelo Foundation, Finnish Foundation for Cardiovascular Research, The

Finnish Medical Foundation, Instrumentarium Science Foundation, The Maud Kuistila Memorial Foundation, Ida Montin Foundation, The University of Oulu Scholarship Foundation, Paavo Nurmi Foundation, and Maire Taponen Foundation.

SUPPLEMENTARY MATERIAL

The Supplementary Material for this article can be found online at: https://www.frontiersin.org/articles/10.3389/fcvm.2021.755062/full#supplementary-material

REFERENCES

1. Myerburg RJ, Junttila MJ. Sudden cardiac death caused by coronary heart disease. *Circulation.* (2012) 125:1043-52. doi: 10.1161/CIRCULATIONAHA.111.023846
2. Marian AJ. Genetic determinants of cardiac hypertrophy. *Curr Opin Cardiol.* (2008) 23:199-205. doi: 10.1097/HCO.0b013e3282fc27d9
3. Hookana E, Junttila MJ, Puurunen VP, Tikkanen JT, Kaikkonen KS, Kortelainen ML, et al. Causes of nonischemic sudden cardiac death in the current era. *Heart Rhythm.* (2011) 8:1570-5. doi: 10.1016/j.hrthm.2011.06.031
4. Kaikkonen KS, Kortelainen ML, Huikuri HV. Comparison of risk profiles between survivors and victims of sudden cardiac death from an acute coronary event. *Ann Med.* (2009) 41:120-7. doi: 10.1080/07853890802213295
5. Ang DS, Pringle SD, Struthers AD. The cardiovascular risk factor, left ventricular hypertrophy, is highly prevalent in stable, treated angina pectoris. *Am J Hypertens.* (2007) 20:1029-35. doi: 10.1016/j.amjhyper.2007.04.021
6. Adabag AS, Peterson G, Apple FS, Titus J, King R, Luepker RV. Etiology of sudden death in the community: results of anatomic, metabolic and genetic evaluation. *Am Heart J.* (2010) 159:33-9. doi: 10.1016/j.ahj.2009.10.019
7. Saukko P. Medicolegal investigative system and sudden death in Scandinavia. *Nihon Hoigaku Zasshi.* (1995) 49:458-65.
8. Vähätalo J, Holmström L, Pakanen L, Kaikkonen K, Perkiömäki J, Huikuri H, et al. Coronary artery disease as the cause of sudden cardiac death among victims < 50 years of age. *Am J Cardiol.* (2021) 147:33-8. doi: 10.1016/j.amjcard.2021.02.012
9. Richards S, Aziz N, Bale S, Bick D, Das S, Gastier-Foster J, et al. Standards and guidelines for the interpretation of sequence variants: a joint consensus recommendation of the American College of Medical Genetics and Genomics and the Association for Molecular Pathology. *Genet Med.* (2015) 17:405-24. doi: 10.1038/gim.2015.30
10. *Sequencing Initiative Suomi Project (SISu).* Helsinki: Institute for Molecular Medicine Finland (FIMM), University of Helsinki. (2021).
11. Fressart V, Duthoit G, Donal E, Probst V, Deharo JC, Chevalier P, et al. Desmosomal gene analysis in arrhythmogenic right ventricular dysplasia/cardiomyopathy: spectrum of mutations and clinical impact in practice. *Europace.* (2010) 12:861-8. doi: 10.1093/europace/euq104
12. Junttila MJ, Holmstrom L, Pylkas K, Mantere T, Kaikkonen K, Porvari K, et al. Primary myocardial fibrosis as an alternative phenotype pathway of inherited cardiac structural disorders. *Circulation.* (2018) 137:2716-26. doi: 10.1161/CIRCULATIONAHA.117.032175
13. Morner S, Richard P, Kazzam E, Hellman U, Hainque B, Schwartz K, et al. Identification of the genotypes causing hypertrophic cardiomyopathy in northern Sweden. *J Mol Cell Cardiol.* (2003) 35:841-9. doi: 10.1016/S0022-2828(03)00146-9
14. Syrris P, Ward D, Asimaki A, Evans A, Sen-Chowdhry S, Hughes SE, et al. Desmoglein-2 mutations in arrhythmogenic right ventricular cardiomyopathy: a genotype-phenotype characterization of familial disease. *Eur Heart J.* (2007) 28:581-8. doi: 10.1093/eurheartj/ehl380
15. Ichida F, Tsubata S, Bowles KR, Haneda N, Uese K, Miyawaki T, et al. Novel gene mutations in patients with left ventricular noncompaction or Barth syndrome. *Circulation.* (2001) 103:1256-63. doi: 10.1161/01.CIR.103.9.1256
16. Moller DV, Andersen PS, Hedley P, Ersboll MK, Bundgaard H, Moolman-Smook J, et al. The role of sarcomere gene mutations in patients with idiopathic dilated cardiomyopathy. *Eur J Hum Genet.* (2009) 17:1241-9. doi: 10.1038/ejhg.2009.34
17. Andersen PS, Havndrup O, Hougs L, Sorensen KM, Jensen M, Larsen LA, et al. Diagnostic yield, interpretation, and clinical utility of mutation screening of sarcomere encoding genes in Danish hypertrophic cardiomyopathy patients and relatives. *Hum Mutat.* (2009) 30:363-70. doi: 10.1002/humu.20862
18. Dalal D, Tandri H, Judge DP, Amat N, Macedo R, Jain R, et al. Morphologic variants of familial arrhythmogenic right ventricular dysplasia/cardiomyopathy a genetics-magnetic resonance imaging correlation study. *J Am Coll Cardiol.* (2009) 53:1289-99. doi: 10.1016/j.jacc.2008.12.045
19. Gerull B, Heuser A, Wichter T, Paul M, Basson CT, McDermott DA, et al. Mutations in the desmosomal protein plakophilin-2 are common in arrhythmogenic right ventricular cardiomyopathy. *Nat Genet.* (2004) 36:1162-4. doi: 10.1038/ng1461
20. Elliott P, O'Mahony C, Syrris P, Evans A, Rivera Sorensen C, Sheppard MN, et al. Prevalence of desmosomal protein gene mutations in patients with dilated cardiomyopathy. *Circ Cardiovasc Genet.* (2010) 3:314-22. doi: 10.1161/CIRCGENETICS.110.937805
21. Lahtinen AM, Lehtonen E, Marjamaa A, Kaartinen M, Helio T, Porthan K, et al. Population-prevalent desmosomal mutations predisposing to arrhythmogenic right ventricular cardiomyopathy. *Heart Rhythm.* (2011) 8:1214-21. doi: 10.1016/j.hrthm.2011.03.015
22. Rasmussen TB, Nissen PH, Palmfeldt J, Gehmlich K, Dalager S, Jensen UB, et al. Truncating plakophilin-2 mutations in arrhythmogenic cardiomyopathy are associated with protein haploinsufficiency in both myocardium and epidermis. *Circ Cardiovasc Genet.* (2014) 7:230-40. doi: 10.1161/CIRCGENETICS.113.000338
23. Pilotto A, Marziliano N, Pasotti M, Grasso M, Costante AM, Arbustini E. alphaB-crystallin mutation in dilated cardiomyopathies: low prevalence in a consecutive series of 200 unrelated probands. *Biochem Biophys Res Commun.* (2006) 346:1115-7. doi: 10.1016/j.bbrc.2006.05.203
24. Garcia-Pavia P, Syrris P, Salas C, Evans A, Mirelis JG, Cobo-Marcos M, et al. Desmosomal protein gene mutations in patients with idiopathic dilated cardiomyopathy undergoing cardiac transplantation: a clinicopathological study. *Heart.* (2011) 97:1744-52. doi: 10.1136/hrt.2011.227967
25. Roux-Buisson N, Gandjbakhch E, Donal E, Probst V, Deharo JC, Chevalier P, et al. Prevalence and significance of rare RYR2 variants in arrhythmogenic right ventricular cardiomyopathy/dysplasia: results of a systematic screening. *Heart Rhythm.* (2014) 11:1999-2009. doi: 10.1016/j.hrthm.2014.07.020
26. Yuan F, Pinto JM, Li Q, Wasserlauf BJ, Yang X, Bassett AL, et al. Characteristics of I(K) and its response to quinidine in experimental healed myocardial infarction. *J Cardiovasc Electrophysiol.* (1999) 10:844-54. doi: 10.1111/j.1540-8167.1999.tb00265.x
27. Caselli S, Pelliccia A. The electrocardiogram and the phenotypic expression of hypertrophic cardiomyopathy. *Eur Heart J.* (2019) 40:982-5. doi: 10.1093/eurheartj/ehy403
28. DeWitt ES, Chandler SF, Hylind RJ, Beausejour Ladouceur V, Blume ED, VanderPluym C, et al. Phenotypic manifestations of arrhythmogenic cardiomyopathy in children and adolescents. *J Am Coll Cardiol.* (2019) 74:346-58. doi: 10.1016/j.jacc.2019.05.022
29. Christiaans I, Birnie E, van Langen IM, van Spaendonck-Zwarts KY, van Tintelen JP, van den Berg MP, et al. The yield of risk stratification for sudden cardiac death in hypertrophic cardiomyopathy myosin-binding protein C gene mutation carriers: focus on predictive screening. *Eur Heart J.* (2010) 31:842-8. doi: 10.1093/eurheartj/ehp539
30. Niimura H, Patton KK, McKenna WJ, Soults J, Maron BJ, Seidman JG, et al. Sarcomere protein gene mutations in hypertrophic cardiomyopathy of the elderly. *Circulation.* (2002) 105:446-51. doi: 10.1161/hc0402.102990
31. Maron BJ, Maron MS, Semsarian C. Double or compound sarcomere mutations in hypertrophic cardiomyopathy: a potential link to sudden death in the absence of conventional risk factors. *Heart Rhythm.* (2012) 9:57-63. doi: 10.1016/j.hrthm.2011.08.009
32. Laukkanen JA, Khan H, Kurl S, Willeit P, Karppi J, Ronkainen K, et al. Left ventricular mass and the risk of sudden cardiac death: a population-based study. *J Am Heart Assoc.* (2014) 3:e001285. doi: 10.1161/JAHA.114.001285

33. Reinier K, Dervan C, Singh T, Uy-Evanado A, Lai S, Gunson K, et al. Increased left ventricular mass and decreased left ventricular systolic function have independent pathways to ventricular arrhythmogenesis in coronary artery disease. *Heart Rhythm.* (2011) 8:1177-82. doi: 10.1016/j.hrthm.2011.02.037
34. Antony I, Nitenberg A, Foult JM, Aptecar E. Coronary vasodilator reserve in untreated and treated hypertensive patients with and without left ventricular hypertrophy. *J Am Coll Cardiol.* (1993) 22:514-20. doi: 10.1016/0735-1097(93)90058-9
35. Bertier G, Hetu M, Joly Y. Unsolved challenges of clinical whole-exome sequencing: a systematic literature review of end-users' views. *BMC Med Genomics.* (2016) 9:52. doi: 10.1186/s12920-016-0213-6
36. Giudicessi JR, Lieve KVV, Rohatgi RK, Koca F, Tester DJ, van der Werf C, et al. Assessment and validation of a phenotype-enhanced variant classification framework to promote or demote RYR2 missense variants of uncertain significance. *Circ Genom Precis Med.* (2019) 12:e002510. doi: 10.1161/CIRCGEN.119.002510
37. Bezzina CR, Lahrouchi N, Priori SG. Genetics of sudden cardiac death. *Circ Res.* (2015) 116:1919-36. doi: 10.1161/CIRCRESAHA.116.304030
38. Van Driest SL, Vasile VC, Ommen SR, Will ML, Tajik AJ, Gersh BJ, et al. Myosin binding protein C mutations and compound heterozygosity in hypertrophic cardiomyopathy. *J Am Coll Cardiol.* (2004) 44:1903-10. doi: 10.1016/j.jacc.2004.07.045
39. Faragli A, Underwood K, Priori SG, Mazzanti A. Is there a role for genetics in the prevention of sudden cardiac death? *J Cardiovasc Electrophysiol.* (2016) 27:1124-32. doi: 10.1111/jce.13028
40. Sanchez O, Campuzano O, Fernandez-Falgueras A, Sarquella-Brugada G, Cesar S, Mademont I, et al. Natural and undetermined sudden death: value of post-mortem genetic investigation. *PLoS ONE.* (2016) 11:e0167358. doi: 10.1371/journal.pone.0167358

Conflict of Interest: The authors declare that the research was conducted in the absence of any commercial or financial relationships that could be construed as a potential conflict of interest.

Publisher's Note: All claims expressed in this article are solely those of the authors and do not necessarily represent those of their affiliated organizations, or those of the publisher, the editors and the reviewers. Any product that may be evaluated in this article, or claim that may be made by its manufacturer, is not guaranteed or endorsed by the publisher.

frontiers in Cardiovascular Medicine

ORIGINAL RESEARCH
published: 13 January 2022
doi: 10.3389/fcvm.2021.756379

A Novel Multiple Risk Score Model for Prediction of Long-Term Ischemic Risk in Patients With Coronary Artery Disease Undergoing Percutaneous Coronary Intervention: Insights From the I-LOVE-IT 2 Trial

*Miaohan Qiu[1,2], Yi Li[2], Kun Na[2,3], Zizhao Qi[2,4], Sicong Ma[2,5], He Zhou[2,6], Xiaoming Xu[2], Jing Li[2,4], Kai Xu[2], Xiaozeng Wang[2] and Yaling Han[2]**

[1] Second Affiliated Hospital of Dalian Medical University, Dalian, China, [2] The Department of Cardiology, General Hospital of Northern Theater Command, Shenyang, China, [3] Postgraduate College, Shenyang Pharmaceutical University, Shenyang, China, [4] Second Affiliated Hospital of Harbin Medical University, Harbin, China, [5] The Second Hospital of Jilin University, Changchun, China, [6] Postgraduate College, Liaoning University of Traditional Chinese Medicine, Shenyang, China

OPEN ACCESS

Edited by:
Masanori Aikawa, Brigham and Women's Hospital and Harvard Medical School, United States

Reviewed by:
Jinwei Tian, The Second Affiliated Hospital of Harbin Medical University, China
Yao-Jun Zhang, Xuzhou Cancer Hospital, China

***Correspondence:**
Yaling Han
hanyaling@163.net

Specialty section:
This article was submitted to Coronary Artery Disease, a section of the journal Frontiers in Cardiovascular Medicine

Received: *10 August 2021*
Accepted: *06 December 2021*
Published: *13 January 2022*

Citation:
Qiu M, Li Y, Na K, Qi Z, Ma S, Zhou H, Xu X, Li J, Xu K, Wang X and Han Y (2022) A Novel Multiple Risk Score Model for Prediction of Long-Term Ischemic Risk in Patients With Coronary Artery Disease Undergoing Percutaneous Coronary Intervention: Insights From the I-LOVE-IT 2 Trial. Front. Cardiovasc. Med. 8:756379. doi: 10.3389/fcvm.2021.756379

Backgrounds: A plug-and-play standardized algorithm to identify the ischemic risk in patients with coronary artery disease (CAD) undergoing percutaneous coronary intervention (PCI) could play a valuable step to help a wide spectrum of clinic workers. This study intended to investigate the ability to use the accumulation of multiple clinical routine risk scores to predict long-term ischemic events in patients with CAD undergoing PCI.

Methods: This was a secondary analysis of the I-LOVE-IT 2 (Evaluate Safety and Effectiveness of the Tivoli drug-eluting stent (DES) and the Firebird DES for Treatment of Coronary Revascularization) trial, which was a prospective, multicenter, and randomized study. The Global Registry for Acute Coronary Events (GRACE), baseline Synergy Between Percutaneous Coronary Intervention with Taxus and Cardiac Surgery (SYNTAX), residual SYNTAX, and age, creatinine, and ejection fraction (ACEF) score were calculated in all patients. Risk stratification was based on the number of these four scores that met the established thresholds for the ischemic risk. The primary end point was ischemic events at 48 months, defined as the composite of cardiac death, nonfatal myocardial infarction, stroke, or definite/probable stent thrombosis (ST).

Results: The 48-month ischemic events had a significant trend for higher event rates (from 6.61 to 16.93%) with an incremental number of risk scores presenting the higher ischemic risk from 0 to ≥3 (p trend < 0.001). In addition, the categories were associated with increased risk for all components of ischemic events, including cardiac death (from 1.36 to 3.15%), myocardial infarction (MI) (from 3.31 to 9.84%), stroke (3.31 to 6.10%), definite/probable ST (from 0.58 to 1.97%), and all-cause mortality (from 2.14 to 6.30%) (all p trend < 0.05). The net reclassification index after combined with four risk scores was 12.5% (5.3–20.0%), 9.4% (2.0–16.8%), 12.1% (4.5–19.7%), and 10.7% (3.3–18.1%),

which offered statistically significant improvement in the performance, compared with SYNTAX, residual SYNTAX, ACEF, and GRACE score, respectively.

Conclusion: The novel multiple risk score model was significantly associated with the risk of long-term ischemic events in these patients with an increment of scores. A meaningful improvement to predict adverse outcomes when multiple risk scores were applied to risk stratification.

Keywords: coronary artery disease, percutaneous coronary intervention, risk score, ischemic events, drug-eluting stent

INTRODUCTION

Personalized medicine is a medical model that separates patients into different groups with tailored medical decisions, practices, and interventions based on their predicted risk of disease. Theoretically, taking a series of risk factors into account to evaluate the individual risk of patients with coronary artery disease (CAD) undergoing percutaneous coronary intervention (PCI) before the decision-making process was superior to "one-size-fits-all" approaches (1–3).

Recently a variety of risk scoring systems, as comprehensive predicted tools for risk assessment, have been developed to support physicians in clinical practice for these patients (4–7). However, to our knowledge, there was not a robust, interoperable, and universal risk score that could be extended to different populations, which is mainly caused by prediction algorithms derived from different cohorts and a complex and time-varying clinical process (8–11). Meanwhile, previous studies demonstrate that an additive value of one risk score combined with a biomarker, angiographic characteristic, and with another risk score to risk predicting (12–14).

Thus, we sought to investigate whether using a strategy assisted by the accumulation of multiple clinical routine risk algorithms could improve the ability of discrimination to predict long-term ischemic events in patients with CAD undergoing PCI.

MATERIALS AND METHODS

Study Design and Patients

This was a secondary analysis of the I-LOVE-IT 2 (Evaluate Safety and Effectiveness of the Tivoli drug-eluting stent (DES) and the Firebird DES for Treatment of Coronary Revascularization; NCT01681381) trial, which was a prospective, multicenter, randomized, assessor-blinded, and non-inferiority study that compared a biodegradable polymer sirolimus-eluting stent (BP-SES, Tivoli, Essen Tech, Beijing, China) with a durable polymer sirolimus-eluting stent (DP-SES, Firebird 2, MicroPort, Shanghai, China). Study details have been previously described (15, 16). In brief, between October 2012 and June 2013, a total of 2,737 patients presenting with stable CAD or acute coronary syndromes (ACS) were randomly assigned to undergo PCI with either BP-SES or DP-SES at a 2:1 ratio at 32 centers in China. Patients who were randomized to the BP-SES group were additionally re-randomized to a 6- or 12-month DAPT group at a 1:1 ratio. All patients were discharged with a prescription for at least 100 mg aspirin indefinitely and 75 mg clopidogrel for 6 or 12 months after stent implantation. Qualitative and quantitative coronary angiography (including Synergy between Percutaneous Coronary Intervention with Taxus and Cardiac Surgery (SYNTAX) score and residual SYNTAX score) were centrally evaluated by a blinded independent core laboratory (CCRF, Beijing, China) using QAngio XA Version 7.3 Analysis Software (Medis Medical Imaging System, Leiden, The Netherlands). The study complies with the provisions of the Declaration of Helsinki, and the study protocol was approved by the institutional review board at each participating site. All patients provided written informed consent.

Risk Assessment

For these analyses, four risk scores, which were supported by an extensive, rigorous external validation process, and/or endorsed by current guidelines, were used to predict the ischemic risk after PCI, as follows. (1) Discharge Global Registry for Acute Coronary Events (GRACE) score (17) was calculated and described based on age, history of congestive heart failure, history of myocardial infarction (MI), resting heart rate, systolic blood pressure, ST-segment depression, initial serum creatinine, elevated cardiac enzymes, and PCI in-hospital. Patients were considered intermediate to high ischemic risk for scores $\geq$88 (18). (2) Baseline SYNTAX score is a comprehensive angiographic scoring system that is derived entirely from the coronary anatomy and lesion characteristics, which was designed to quantify lesion complexity before the procedure (19). The baseline SYNTAX Score may aid in assessing the ischemic events, including cardiac death, MI, and target vessel revascularization (20). The baseline SYNTAX score value of 13 is considered an optimal cutoff point depending on the prognosis of patients (20). (3) Age, creatinine, and ejection fraction (ACEF) score developed by Ranucci et al. (21) was a simple tool for predicting in-hospital mortality in patients undergoing elective cardiac surgery. Meanwhile, a previous study showed that the ACEF score had a good discriminative in patients undergoing PCI (22). The ACEF score $\geq$1.0225 might be useful and applicable for risk stratification in these populations with respect to the long-term clinical prognosis (22). (4) Residual SYNTAX score (rSS) was first proposed by Généreux et al. (23), which was calculated based on the remaining obstructive coronary disease after treatment with PCI. The rSS could be used to quantify the burden and complexity of residual CAD after the procedure. The rSS of $>$0 was associated with long-term ischemic outcomes, including

all-cause mortality and MI (24, 25). Risk score calculations are shown in **Supplementary Appendix S1**.

The method of risk stratification in the current study was calculated using the number of these four scores (called ACE-SYNTAX score) that met the thresholds for the intermediate- or high-risk, ranging from 0 to ≥3, logically a total of four categories, in all patients.

Outcomes

All clinical and laboratory variables included in the present analysis were prospectively collected. The multiple risk score model was developed to predict ischemic events at 48 months, defined as the composite of cardiac death, nonfatal MI, stroke, or definite/probable stent thrombosis (ST). The definitions of those endpoints were described in the previous report (15, 16). All patients were followed-up with by telephone or hospital visits at 1, 6, 9, 12, and 18 months, and annually for up to 5 years. All clinical events were adjudicated by a blinded independent clinical events committee.

Statistical Analysis

Patient characteristics were stratified according to the risk stratification of risk scores. Continuous variables are presented as mean ± SD; categorical variables are displayed as counts and percentages. Comparisons were performed with a chi-square test for categorical variables and one-way ANOVA for continuous variables. Testing for trends in event rates across risk scores was done with the Cochran–Armitage test. Time-to-event data with estimated event rates measured with the Kaplan–Meier method were compared using the log-rank test. An individual risk score was evaluated for the discrimination for 4-year ischemic events. The discrimination of individual risk score was measured by the receiver operator characteristic curve (ROC) with the area under the curve (AUC), which ranges from

TABLE 1 | Baseline demographics and score calculation stratified across cumulative risk-score categories.

	No. of risk scores met the individual thresholds				*P*-value
	0 (*N* = 514)	**1 (*N* = 553)**	**2 (*N* = 632)**	**≥3 (*N* = 508)**	
Age, yrs	53.20 ± 7.89	57.32 ± 8.07	61.80 ± 9.89	68.24 ± 7.34	<0.001
Men, No. (%)	382 (74.32%)	393 (71.07%)	426 (67.41%)	320 (62.99%)	<0.001
Body mass index, mean ± SD	25.67 ± 3.15	25.31 ± 2.87	25.24 ± 3.15	24.77 ± 3.05	<0.001
Diabetes mellitus	108 (21.01%)	115 (20.80%)	145 (22.94%)	136 (26.77%)	0.08
Hypertension	305 (59.34%)	338 (61.12%)	402 (63.61%)	355 (69.88%)	0.003
Hyperlipidemia	140 (27.24%)	151 (27.31%)	143 (22.63%)	117 (23.03%)	0.12
Peripheral arterial disease	3 (0.58%)	6 (1.08%)	6 (0.95%)	9 (1.77%)	0.32
Previous myocardial infarction	55 (10.70%)	82 (14.83%)	118 (18.67%)	112 (22.05%)	<0.001
Previous stroke	30 (5.84%)	62 (11.21%)	75 (11.87%)	57 (11.22%)	0.003
Previous PCI	24 (4.67%)	49 (8.86%)	64 (10.13%)	32 (6.30%)	0.002
Previous CABG	1 (0.19%)	2 (0.36%)	3 (0.47%)	6 (1.18%)	0.15
Smoking history					0.006
Current smoker	223 (43.39%)	222 (40.14%)	228 (36.08%)	283 (55.71%)	
Ex-smoker	55 (10.70%)	64 (11.57%)	73 (11.55%)	159 (31.30%)	
None	236 (45.91%)	267 (48.28%)	331 (52.37%)	66 (12.99%)	
Family history of CAD	41 (7.98%)	44 (7.96%)	35 (5.54%)	23 (4.53%)	
Type of CAD, No. (%)					<0.001
STEMI	47 (9.14%)	62 (11.21%)	89 (14.08%)	78 (15.35%)	
NSTEMI	42 (8.17%)	47 (8.50%)	64 (10.13%)	78 (15.35%)	
Unstable angina	341 (66.34%)	341 (61.66%)	371 (58.70%)	281 (55.31%)	
Others	84 (16.34%)	103 (18.63%)	108 (17.09%)	71 (13.98%)	
Ccr, mean ± SD	110.67 ± 30.00	99.69 ± 32.30	91.36 ± 30.82	72.66 ± 23.67	<0.001
LVEF, %	64.01 ± 5.87	61.54 ± 7.85	60.37 ± 8.38	56.72 ± 8.72	<0.001
Anemia	9 (1.77%)	20 (3.67%)	28 (4.47%)	47 (9.36%)	<0.001
Risk scores					
Baseline SYNTAX score	5.71 ± 3.15	9.50 ± 6.62	13.70 ± 8.25	18.38 ± 8.00	<0.001
Residual SYNTAX score	0.00 ± 0.00	1.65 ± 2.39	4.61 ± 5.65	7.02 ± 6.56	<0.001
ACEF score	0.83 ± 0.12	1.06 ± 0.52	1.31 ± 0.82	1.80 ± 1.09	<0.001
GRACE score	60.31 ± 14.80	68.54 ± 16.33	79.57 ± 20.64	95.41 ± 16.25	<0.001

Values are mean ± SD or No. (%). RS, risk score; BMI, body mass index; PCI, percutaneous coronary intervention; CABG, coronary artery bypass graft; CAD, coronary artery disease; STEMI, ST-segment-elevation myocardial infarction; NSTEMI, non-ST-segment-elevation myocardial infarction; Ccr, creatinine clearance; LVEF, left ventricular ejection fraction; SYNTAX, synergy between PCI with TAXUS and cardiac surgery; ACEF, age, creatinine and ejection fraction; GRACE, global registry for acute coronary events.

0.50 (no discrimination) to 1.0 (perfect discrimination). The net reclassification improvement (NRI) analysis was performed to assess the improved ability of combined risk scores for risk stratification over the single score (26). To deal with the missing components of the risk scores that occurred at random, multiple imputations were performed using chained equations. Missing values were predicted on the basis of all other clinical variables. The Cox regression estimates from each imputed dataset were averaged together to produce an overall hazard ratio (*HR*) computed using the Rubin rule. Unless otherwise specified, a 2-sided *p*-value of < 0.05 was considered to indicate statistical significance. Statistical analysis was performed using SAS software version 9.3 (SAS Institute, Cary, NC, USA).

RESULTS

A total of 2,207 patients with 3,027 lesions were selected and calculated ACE-SYNTAX score and were analyzed in the study. ACEF score was not fully evaluable in 342 patients due to the missing data of ejection fraction (240 cases) or creatinine clearance (102 cases). Meanwhile, the GRACE score could not be calculated in 188 cases with a lack of cardiac enzymes. The outcomes of these 530 patients excluded from the analysis are shown in **Supplementary Table S1**.

The baseline SYNTAX score ranged from 0 to 55, with a mean ± SD of 11.9 ± 8.3, and a median of 10.0 (6.0–16.0). The residual SYNTAX score ranged from 0 to 53, with a mean ± SD of 3.4 ± 5.2, and a median of 0.0 (0.0–5.0). The ACEF score ranged from 0.4 to 7.6, with a mean ± SD of 1.3 ± 0.8, and a median of 1.0 (0.9–1.2). The GRACE score ranged from 16 to 153, with a mean ± SD of 76.0 ± 21.5, and a median of 77.0 (60.0–91.0). By using the previously validated cutoffs described in the methods, 831 patients (37.65%) based on baseline SYNTAX score, 1,053 patients (47.71%) based on residual SYNTAX score, 995 patients (45.08%) based on ACEF score, and 650 patients (29.45%) based on GRACE score met the thresholds for the intermediate or high-risk category. A Venn diagram was shown to demonstrate the coexistence of conditions of these risk scores (**Supplementary Figure S1**).

Among 2,207 patients, the risk score of 514 (23.3%) patients who failed to reach any of the four scores cutoff value was defined as zero. The number of other groups, 1 to ≥3

TABLE 2 | Lesion characteristics and procedural results stratified across cumulative risk-score categories.

	No. of risk scores met the individual thresholds				*P*-value
	0 (514 Patients, 625 Lesions)	**1 (553 Patients, 757 Lesions)**	**2 (632 Patients, 891 Lesions)**	**≥3 (508 Patients, 774 Lesions)**	
Transradial approach	486 (94.55%)	521 (94.21%)	577 (91.30%)	468 (92.13%)	0.09
Target vessel disease extent					<0.001
1-vessel	430 (83.66%)	406 (73.42%)	439 (69.46%)	311 (61.22%)	
2-vessel	63 (12.26%)	123 (22.24%)	162 (25.63%)	149 (29.33%)	
3-vessel	2 (0.39%)	12 (2.17%)	14 (2.22%)	23 (4.53%)	
Left main artery	19 (3.70%)	12 (2.17%)	17 (2.69%)	25 (4.92%)	
Baseline SYNTAX score	5.71 ± 3.15	9.50 ± 6.62	13.70 ± 8.25	18.38 ± 8.00	<0.001
No. of target lesions per patient	1.22 ± 0.43	1.37 ± 0.60	1.41 ± 0.60	1.52 ± 0.68	<0.001
Target vessel location					0.16
Left main artery	19 (3.04%)	12 (1.59%)	17 (1.91%)	26 (3.36%)	
Left anterior descending artery	284 (45.44%)	324 (42.86%)	417 (46.80%)	335 (43.28%)	
Left circumflex artery	142 (22.72%)	183 (24.21%)	183 (20.54%)	173 (22.35%)	
Right coronary artery	180 (28.80%)	237 (31.35%)	274 (30.75%)	240 (31.01%)	
ACC/AHA lesion classification B2+C	501 (80.16%)	635 (83.99%)	757 (84.96%)	685 (88.50%)	<0.001
Bifurcation lesion	181 (28.96%)	235 (31.08%)	280 (31.43%)	317 (40.96%)	<0.001
Total occlusion	42 (6.72%)	75 (9.92%)	127 (14.25%)	116 (14.99%)	<0.001
Severely tortuous or angulated lesion	11 (1.76%)	13 (1.72%)	24 (2.69%)	28 (3.62%)	0.06
Moderate to heavy calcification	13 (2.08%)	15 (1.98%)	27 (3.03%)	41 (5.30%)	<0.001
Pre-procedural QCA					
Reference vessel diameter, mm	2.84 ± 0.49	2.82 ± 0.48	2.76 ± 0.46	2.74 ± 0.43	<0.001
Lesion length, mm	18.62 ± 11.55	19.86 ± 11.16	21.78 ± 12.98	23.66 ± 14.12	<0.001
Procedural results					
Stent per patient	1.51 ± 0.70	1.67 ± 0.83	1.81 ± 0.87	2.02 ± 0.96	<0.001
Total stent length per patient, mm	35.70 ± 20.16	40.42 ± 22.90	44.64 ± 25.20	51.17 ± 27.03	<0.001
Residual SYNTAX score	0.00 ± 0.00	1.65 ± 2.39	4.61 ± 5.65	7.02 ± 6.56	<0.001

Values are mean ± SD or No. (%). ACC/AHA, American College of Cardiology/American Heart Association; QCA, quantitative coronary angiography; Other abbreviations are the same as for ***Table 1****.*

TABLE 3 | Clinical outcomes at 4-year follow-up stratified across cumulative risk-score categories.

	No. of risk scores met the individual thresholds				P for trend*
	0 (*N* = 514)	1 (*N* = 553)	2 (*N* = 632)	≥3 (*N* = 508)	
Ischemic events	34 (6.61%)	51 (9.22%)	83 (13.13%)	86 (16.93%)	<0.001
All-cause mortality	11 (2.14%)	13 (2.35%)	21 (3.32%)	32 (6.30%)	<0.001
Cardiac death	7 (1.36%)	5 (0.90%)	8 (1.27%)	16 (3.15%)	0.025
All MI	17 (3.31%)	26 (4.70%)	41 (6.49%)	50 (9.84%)	<0.001
Target vessel MI	15 (2.92%)	20 (3.62%)	34 (5.38%)	44 (8.66%)	<0.001
Stroke	17 (3.31%)	23 (4.16%)	39 (6.17%)	31 (6.10%)	0.013
Definite/probable ST	3 (0.58%)	4 (0.72%)	5 (0.79%)	10 (1.97%)	0.035

*Values are No. (%). MI, myocardial infarction; ST, stent thrombosis. Ischemic events were defined as a composite of cardiac death, all MI, stroke, and /or definite/probable ST. *Cochran-Armitage trend test.*

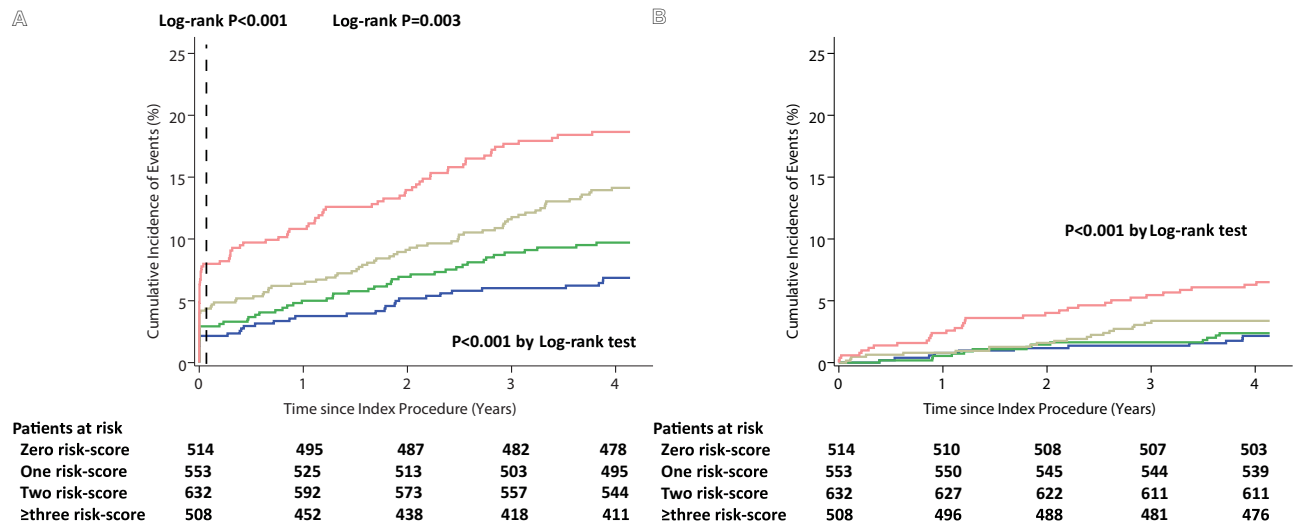

FIGURE 1 | Kaplan–Meier curves during follow-up for 48-month Outcomes among the Cumulative Risk-score Categories. **(A)** Ischemic events (with 30-day landmark analysis). **(B)** All-cause Mortality.

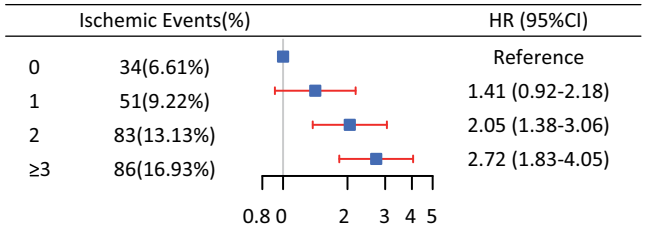

FIGURE 2 | Incidence of ischemic events among cumulative risk-score categories.

risk-score, were 553 (25.1%), 632 (28.6%), and 508(23.0%), respectively. The overall distribution of incremental risk-score categories was displayed in **Supplementary Figure S2**. The baseline demographics and calculation of risk scores are reported in **Table 1**. The antiplatelet therapy during the follow-up period is shown in **Supplementary Table S2**. The lesion characteristics and procedural results are shown in **Table 2** stratified across cumulative risk-score categories.

Stratified Clinical Outcomes

The 48-month ischemic events had a significant trend for higher event rates (from 6.61 to 16.93%) with incremental risk-score categories from 0 to ≥3 ($p_{trend} < 0.001$). The categories were also associated with increased risk for all components of ischemic events, including cardiac death (from 1.36 to 3.15%, $p_{trend} = 0.025$), all MI (from 3.31 to 9.84%, $p_{trend} < 0.001$), stroke (3.31 to 6.10%, $p_{trend} = 0.013$), definite/probable ST (from 0.58 to 1.97%, $p_{trend} = 0.035$), TVMI (from 2.92 to 8.66%, $p_{trend} < 0.001$), and all-cause mortality (from 2.14 to 6.30%, $p_{trend} < 0.001$) at 48 months with a significant trend according to risk-score categories (**Table 3**).

Using the multiple imputations for the missing values (ejection fraction, creatinine clearance, and cardiac enzymes), a

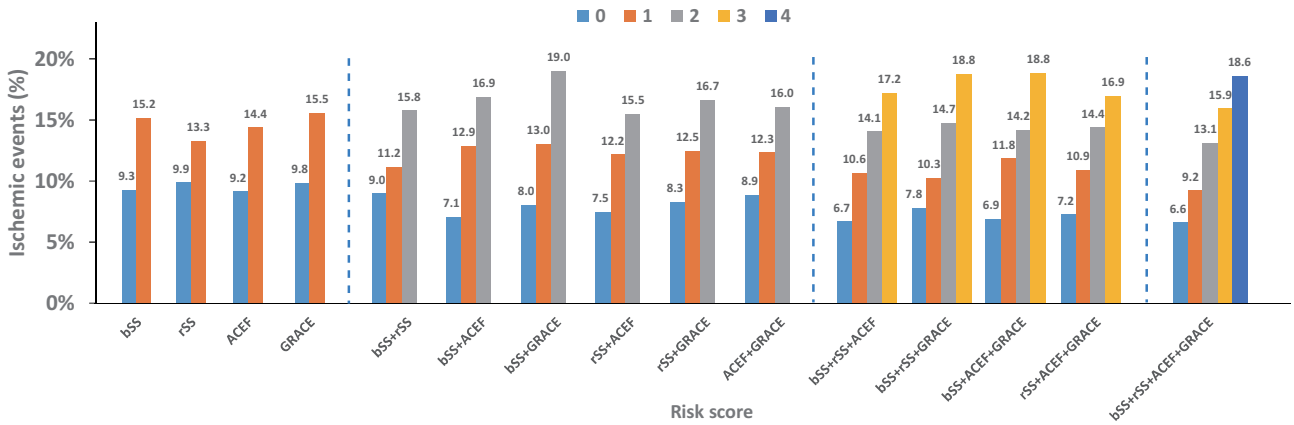

FIGURE 3 | Four-year ischemic events stratified by individual and different combination of risk score (s).

total of 20 imputed datasets were generated. The trend of 48-month ischemic events was robust in each imputed dataset (all $p_{trend} < 0.001$, **Supplementary Table S3**).

There were consistent findings measured with the Kaplan–Meier method. The incidence of ischemic events, all-cause mortality at 4 years experienced a significant increase with the cumulative number of risk scores (both $p < 0.001$ by log-rank test). The landmark analysis showed that the patients with the higher cumulative risk-score were associated with a higher risk of ischemic events in the intervals of 0–30 days as well as 30 days to 4 years (from 2.1 to 7.68%, log-rank $p < 0.001$, and from 4.5 to 9.3%, log-rank $p = 0.003$, respectively) (**Figure 1** and **Supplementary Table S4**). A sensitive analysis was performed and showed that the incidence of 48-month ischemic events had a consistent tendency with incremental risk-score categories with incremental risk-score categories (**Supplementary Table S5**).

It was shown that the 4-year rate of ischemic events was significantly higher in the patients with cumulative risk-score 2 to ≥3, leaving cumulative risk-score 0 as the reference [(*HR*: 2.05, 95% *CI*, 1.38–3.06), and (*HR*: 2.72, 95% CI, 1.83–4.05), respectively], whereas, this did not differ in patients with cumulative risk-scores 0 and 1 (*HR*: 1.41, 95% *CI*, 0.92–2.18) (**Figure 2**).

The ischemic events at 48 months stratified by one and different combinations of risk score (s) are illustrated in **Figure 3** and **Supplementary Figure S3**. Using cumulative risk-score categories could discriminate the risk of ischemia better than any single risk score, especially in patients with lower and higher ischemic risk. The combination with two risk scores of baseline SYNTAX and GRACE score has good discrimination to predict the 48-month ischemic events in all kinds of two risk scores. The combination with three risk scores of baseline SYNTAX, residual SYNTAX, and GRACE score and baseline SYNTAX, ACEF, and GRACE score has a better ability to assess the ischemic risk.

The ROC curves for 48-month ischemic events of the individual and an incremental number of risk scores, as continuous variables, are shown in **Supplementary Figure S4**. The discrimination of individual risk score was moderate, with AUC from 0.55 to 0.58. The AUC of an incremental number of risk scores was 0.61 (0.57–0.64). The best cutoffs of GRACE, baseline SYNTAX, ACEF, and residual SYNTAX score to predict 48-month ischemic events risk were 87, 12.5, 1.11, and 1 point(s), respectively. The optimal threshold of the ACE-SYNTAX model was two points for ischemic events at 48 months. Comparing with the baseline and residual SYNTAX score, the AUC of incremental number of risk scores at 48-month ischemic events had a significant improvement [0.57 (0.53–0.61), $p = 0.038$ and 0.55 (0.51–0.59), $p = 0.001$, respectively]. There was no significant improvement in AUC of ROC when compared ACEF and GRACE score with cumulative risk score [0.58 (0.54–0.62), $p = 0.16$ and 0.57 (0.54–0.61), $p = 0.08$, respectively]. Reclassification of patients into risk categories according to the occurrence of 48-month ischemic events is summarized in **Supplementary Table S6**. The NRI after combined with four risk scores was 12.5% (5.3–20.0%), 9.4% (2.0–16.8%), 12.1% (4.5–19.7%), and 10.7% (3.3–18.1%), which offers statistically significant improvement in the performance, compared with SYNTAX, residual SYNTAX, ACEF, and GRACE score, respectively.

DISCUSSION

The current study, which included data from a prospective, multicenter, and randomized trial, is the first study to investigate the feasibility and effectiveness of the management strategy (ACE-SYNTAX score) that combined with multiple risk scores could modify the discrimination to predict the long-term prognosis of patients with CAD undergoing PCI. The main findings of this analysis were as follows: (1) as the clinical routine risk scores, the baseline SYNTAX, residual SYNTAX, ACEF, and GRACE score demonstrated a certain value with respect to predicted long-term ischemic risk in CAD patients with stents implantation, with moderate discrimination; (2) the

risk of ischemic events, including cardiac death, MI, stroke, definite/probable ST, and all-cause mortality have a significant increasing trend with incremental risk-score categories in these patients; and (3) using combinatory of predicting algorithms properly could play a valuable step to help clinicians identify the risk of these patients with implementation of sufficient treatments both in the post-procedure and long-term period, especially in these with lower or higher risk.

As we all know, the prognosis of patients with CAD is determined by baseline risk factors and the use of guideline-indicated therapies. The appropriately-stratified for these patients after stents implantation, which is a significant management challenge, has the potential to achieve the optimal individualized treatment and improve long-term outcomes (27–29). Thus, it is no doubt that using risk prediction algorithms to stratify the patients according to their estimated risk of future ischemic events could assist clinicians in selecting the optimal intensity and/or duration of secondary prevention therapy in decision-making. However, the gaps between guidelines and clinical practices were that the evidence-recommended tools to predict risk might be not universally applicable and robust. The main reason might be the timeliness of the risk scores, though it might be difficult to solve. The most frequently-used risk scores in our routine clinical practice, such as GRACE and SYNTAX scores, are developed from several years back in time. As the newest risk assessment tools, such as dual antiplatelet therapy (DAPT) and Predicting complications in patients undergoing stent implantation and subsequent Dual antiplatelet therapy (PRECISE-DAPT) scores, the data used to build them from randomized controlled trials or observational studies are still more than 5 years (4, 5). However, clinical practice and technology have advanced at a breathless pace. Over recent decades, medicine has drastically evolved with wider clinical use of more advanced diagnostic and therapeutic techniques, they might misestimate the risk of the disease (30). Meanwhile, the complex interaction between residual risk after PCI and the therapeutic benefit of secondary prevention management increases the complexity of risk stratification in these patients. Although no clinical risk tool is perfect, making use of the scores appropriately could provide convincing evidence in helping clinicians make individualized decisions for their patients. Utility of the accumulation of multiple risk scores could overcome the situation, having a significant improvement to discriminate risk of patients with a better classification.

Of note, evidence from a prior study suggests that medical management based on risk stratification was significantly associated with improved long-term prognosis, nevertheless, the benefits decreased with increasing estimated risk (31). The utilization of risk scores tends to be more successful in improving the reclassification of risk, which may enable monitoring and mobilizing clinical practice managers. Admittedly, there was no significant improvement in AUC of ROC at 48-month ischemic events when compared ACEF and GRACE scores with cumulative risk scores. However, it is intelligible that there is just integrating several validated risk scores without any other factors implantation. Still, the accumulative scores were proved a better net reclassification of risk compared with each single score. As we all know, adjustment of the weight of variables and bringing new factors into the risk score could increase the performance when the algorithm is insufficiently accurate in different races/ethnicity. Both above mentioned methods needed a series of cohorts to re-develop and re-validate the score. Our study demonstrates a plug-and-play strategy to risk assessment, which is especially suitable for these without established tools to carry out.

There is no escaping the fact that physicians routinely overestimated the risk of cardiac events and overvalued the benefits of invasive and secondary prevention management with a strong reliance on their intuition (32–34). Undoubtedly, predicting the adverse risk based on objectively quantified clinical algorithms could provide superior risk discrimination (32, 34). The number of prediction tools, as well as the presence of overlapping risk scores in the same clinical scenarios, is the blowout of a sharp increase, which makes it difficult to select using a universal and interoperable scoring system for the cardiologists. Indeed, in the clinical routine practice, using multiple complex algorithms could be challenging and cumbersome to compute.

However, with the improvement of the digital hospital and laboratory information system and the advent of machine learning based on deep neural networks, an approach may be a viable solution to generate detailed data in high-volume capacity (35, 36). It is convenient to capture all factors relating to the scores in the electronic medical records (EMR), calculate them automatically, and then quickly preset the predicting risk of patients in the system in auto (37, 38). It should be noted that dichotomizing continuous risk scores into a regression model might not be the optimal choice, which could induce a potential risk of inaccuracy. However, predictive accuracy for ischemic events was similar to continuation and dichotomization measurements in our research. Considering the clinical applicability without excessive consumption of accuracy, it might be acceptable to transfer continuous variables into binary variables.

The current study is limited by its *post-hoc* nature. As a retrospective analysis, the results of our study are hypothesis-generating. Thus, it is essential to confirm our findings in several specifically designed trials. Second, even with digital hospital and laboratory information systems, it is still complicated for clinicians to carry out too many risk-assessing tools. Therefore, in order to increase availability, what needs to be done further is investigating the proper combination of risk scores in different races/ethnicity. Third, the patients with missing data of risk scores were excluded in our study, which could have biased the estimates. Nevertheless, multiple imputations were performed to address it. The results were consistent between before and after imputation.

CONCLUSION

The guideline-indicated ischemic risk scores displayed reasonable predictive performance in CAD patients with DES implantation. The novel multiple risk score model was

significantly associated with the risk of long-term ischemic events in these patients with an increment of scores. A meaningful improvement to predict adverse outcomes when multiple risk scores were applied to risk stratification. Further studies are needed to confirm these findings.

DATA AVAILABILITY STATEMENT

The raw data supporting the conclusions of this article will be made available by the authors without undue reservation. Further inquiries can be directed to the corresponding author.

ETHICS STATEMENT

The studies involving human participants were reviewed and approved by Ethics Committee of General Hospital of Northern Theater Command. The patients/participants provided their written informed consent to participate in this study.

AUTHOR CONTRIBUTIONS

MQ designed a statistical plan and verified the underlying data, and was in charge of manuscript writing and statistical analysis. YL designed a statistical plan and verified the underlying data. YL, KN, ZQ, SM, HZ, XX, JL, KX, and XW contributed to recruiting subjects during the whole period of study. YH contributed to the leadership of the whole process of study conduction and acted as the key role of initiating, designing, conducting, and concluding the study. All authors contributed to the article and approved the submitted version.

FUNDING

The I-LOVE-IT 2 trial was sponsored by Essen Technology (Beijing, China), and our study was also supported by the National Key Research and Development Program of China (2016YFC1301300 and 2016YFC1301303).

ACKNOWLEDGMENTS

The authors appreciate the dedicated efforts of clinical research collaborators in the I-LOVE-IT 2 trial organization.

SUPPLEMENTARY MATERIAL

The Supplementary Material for this article can be found online at: https://www.frontiersin.org/articles/10.3389/fcvm.2021.756379/full#supplementary-material

REFERENCES

1. Costa F, Tijssen JG, Ariotti S, Giatti S, Moscarella E, Guastaroba P, et al. Incremental value of the CRUSADE, ACUITY, and HAS-BLED risk scores for the prediction of hemorrhagic events after coronary stent implantation in patients undergoing long or short duration of dual antiplatelet therapy. *J Am Heart Assoc.* (2015) 4. doi: 10.1161/JAHA.115.002524
2. Bueno H, Fernandez-Aviles F. Use of risk scores in acute coronary syndromes. *Heart.* (2012) 98:162–8. doi: 10.1136/heartjnl-2011-300129
3. Tahir UA, Yeh RW. Individualizing dual antiplatelet therapy duration after percutaneous coronary intervention: from randomized control trials to personalized medicine. *Expert Rev Cardiovasc Ther.* (2017) 15:681–93. doi: 10.1080/14779072.2017.1362980
4. Yeh RW, Secemsky EA, Kereiakes DJ, Normand SL, Gershlick AH, Cohen DJ, et al. Development and validation of a prediction rule for benefit and harm of dual antiplatelet therapy beyond 1 year after percutaneous coronary intervention. *JAMA.* (2016) 315:1735–49. doi: 10.1001/jama.2016.3775
5. Costa F, van Klaveren D, James S, Heg D, Räber L, Feres F, et al. Derivation and validation of the predicting bleeding complications in patients undergoing stent implantation and subsequent dual antiplatelet therapy (PRECISE-DAPT) score: a pooled analysis of individual-patient datasets from clinical trials. *Lancet.* (2017) 389:1025–34. doi: 10.1016/S0140-6736(17)30397-5
6. Baber U, Mehran R, Giustino G, Cohen DJ, Henry TD, Sartori S, et al. Coronary thrombosis and major bleeding after PCI with drug-eluting stents: risk scores from PARIS. *J Am Coll Cardiol.* (2016) 67:2224–34. doi: 10.1016/j.jacc.2016.02.064
7. Eagle KA, Lim MJ, Dabbous OH, Pieper KS, Goldberg RJ, Van de Werf F, et al. A validated prediction model for all forms of acute coronary syndrome: estimating the risk of 6-month postdischarge death in an international registry. *JAMA.* (2004) 291:2727–33. doi: 10.1001/jama.291.22.2727
8. Harada Y, Michel J, Lohaus R, Mayer K, Emmer R, Lahmann AL, et al. Validation of the DAPT score in patients randomized to 6 or 12 months clopidogrel after predominantly second-generation drug-eluting stents. *Thromb Haemost.* (2017) 117:1989–99. doi: 10.1160/TH17-02-0101
9. Song L, Guan C, Yan H, Qiao S, Wu Y, Yuan J, et al. Validation of contemporary risk scores in predicting coronary thrombotic events and major bleeding in patients with acute coronary syndrome after drug-eluting stent implantations. *Catheter Cardiovasc Interv.* (2018) 91:573–81. doi: 10.1002/ccd.27468
10. Ueda P, Jernberg T, James S, Alfredsson J, Erlinge D, Omerovic E, et al. External validation of the DAPT Score in a nationwide population. *J Am Coll Cardiol.* (2018) 72:1069–78. doi: 10.1016/j.jacc.2018.06.023
11. Zhao XY, Li JX, Tang XF, Xu JJ, Song Y, Jiang L, et al. Validation of predictive value of patterns of nonadherence to antiplatelet regimen in stented patients thrombotic risk score in chinese population undergoing percutaneous coronary intervention: a prospective observational study. *Chin Med J.* (2018) 131:2699–704. doi: 10.4103/0366-6999.245263
12. Zhao X, Jiang L, Xu L, Tian J, Xu Y, Zhao Y, et al. Predictive value of in-hospital white blood cell count in Chinese patients with triple-vessel coronary disease. *Eur J Prev Cardiol.* (2019) 26:872–82. doi: 10.1177/2047487319826398
13. Reindl M, Reinstadler SJ, Tiller C, Kofler M, Theurl M, Klier N, et al. ACEF score adapted to ST-elevation myocardial infarction patients: the ACEF-STEMI score. *Int J Cardiol.* (2018) 264:18–24. doi: 10.1016/j.ijcard.2018.04.017
14. Morici N, Tavecchia GA, Antolini L, Caporale MR, Cantoni S, Bertuccio P, et al. Use of PRECISE-DAPT score and admission platelet count to predict mortality risk in patients with acute coronary syndrome. *Angiology.* (2019) 70:867–77. doi: 10.1177/0003319719848547
15. Han Y, Xu B, Jing Q, Lu S, Yang L, Xu K, et al. A randomized comparison of novel biodegradable polymer- and durable polymer–coated cobalt-chromium sirolimus-eluting stents. *JACC Cardiovasc Interv.* (2014) 7:1352–60. doi: 10.1016/j.jcin.2014.09.001
16. Han Y, Xu B, Xu K, Guan C, Jing Q, Zheng Q, et al. Six versus 12 months of dual antiplatelet therapy after implantation of biodegradable polymer sirolimus-eluting stent: randomized substudy of the I-LOVE-IT 2 trial. *Circ Cardiovasc Interv.* (2016) 9:e003145. doi: 10.1161/CIRCINTERVENTIONS.115.003145

17. Fox KA, Dabbous OH, Goldberg RJ, Pieper KS, Eagle KA, Van de Werf F, et al. Prediction of risk of death and myocardial infarction in the six months after presentation with acute coronary syndrome: prospective multinational observational study (GRACE). *BMJ.* (2006) 333:1091. doi: 10.1136/bmj.38985.646481.55
18. Hamm CW, Bassand JP, Agewall S, Bax J, Boersma E, Bueno H, et al. ESC Guidelines for the management of acute coronary syndromes in patients presenting without persistent ST-segment elevation: the task force for the management of acute coronary syndromes (ACS) in patients presenting without persistent ST-segment elevation of the European Society of Cardiology (ESC). *Eur Heart J.* (2011) 32:2999–3054. doi: 10.1093/eurheartj/ehr236
19. Sianos G, Morel MA, Kappetein AP, Morice MC, Colombo A, Dawkins K, et al. The SYNTAX Score: an angiographic tool grading the complexity of coronary artery disease. *EuroIntervention.* (2005) 1:219–27. Available online at: https://eurointervention.pcronline.com/article/the-syntax-score-an-angiographic-tool-grading-the-complexity-of-coronary-artery-disease
20. Palmerini T, Genereux P, Caixeta A, Cristea E, Lansky A, Mehran R, et al. Prognostic value of the SYNTAX score in patients with acute coronary syndromes undergoing percutaneous coronary intervention: analysis from the ACUITY (Acute Catheterization and Urgent Intervention Triage StrategY) trial. *J Am Coll Cardiol.* (2011) 57:2389–97. doi: 10.1016/j.jacc.2011.02.032
21. Ranucci M, Castelvecchio S, Menicanti L, Frigiola A, Pelissero G. Risk of assessing mortality risk in elective cardiac operations: age, creatinine, ejection fraction, and the law of parsimony. *Circulation.* (2009) 119:3053–61. doi: 10.1161/CIRCULATIONAHA.108.842393
22. Wykrzykowska JJ, Garg S, Onuma Y, de Vries T, Goedhart D, Morel MA, et al. Value of age, creatinine, and ejection fraction (ACEF score) in assessing risk in patients undergoing percutaneous coronary interventions in the "All-Comers" LEADERS trial. *Circ Cardiovasc Interv.* (2011) 4:47–56. doi: 10.1161/CIRCINTERVENTIONS.110.958389
23. Genereux P, Palmerini T, Caixeta A, Rosner G, Green P, Dressler O, et al. Quantification and impact of untreated coronary artery disease after percutaneous coronary intervention: the residual SYNTAX (Synergy Between PCI with Taxus and Cardiac Surgery) score. *J Am Coll Cardiol.* (2012) 59:2165–74. doi: 10.1016/j.jacc.2012.03.010
24. Qiu M, Li Y, Li J, Xu K, Jing Q, Dong S, et al. Impact of six versus 12 months of dual antiplatelet therapy in patients with drug-eluting stent implantation after risk stratification with the residual SYNTAX score: Results from a secondary analysis of the I-LOVE-IT 2 trial. *Catheter Cardiovasc Interv.* (2017) 89:565–73. doi: 10.1002/ccd.26948
25. Farooq V, Serruys PW, Bourantas CV, Zhang Y, Muramatsu T, Feldman T, et al. Quantification of incomplete revascularization and its association with five-year mortality in the synergy between percutaneous coronary intervention with taxus and cardiac surgery (SYNTAX) trial validation of the residual SYNTAX score. *Circulation.* (2013) 128:141–51. doi: 10.1161/CIRCULATIONAHA.113.001803
26. Pencina MJ, D'Agostino RB, Sr., D'Agostino RB, Jr., Vasan RS. Evaluating the added predictive ability of a new marker: from area under the ROC curve to reclassification and beyond. *Stat Med.* (2008) 27:157–72. doi: 10.1002/sim.2929
27. Valgimigli M, Bueno H, Byrne RA, Collet JP, Costa F, Jeppsson A, et al. 2017 ESC focused update on dual antiplatelet therapy in coronary artery disease developed in collaboration with EACTS: the task force for dual antiplatelet therapy in coronary artery disease of the European Society of Cardiology (ESC) and of the European Association for Cardio-Thoracic Surgery (EACTS). *Eur Heart J.* (2018) 39:213–60. doi: 10.1093/eurheartj/ehx419
28. Ibanez B, James S, Agewall S, Antunes MJ, Bucciarelli-Ducci C, Bueno H, et al. 2017 ESC Guidelines for the management of acute myocardial infarction in patients presenting with ST-segment elevation: the task force for the management of acute myocardial infarction in patients presenting with ST-segment elevation of the European Society of Cardiology (ESC). *Eur Heart J.* (2018) 39:119–77. doi: 10.1093/eurheartj/ehx393
29. Levine GN, Bates ER, Bittl JA, Brindis RG, Fihn SD, Fleisher LA, et al. 2016 ACC/AHA guideline focused update on duration of dual antiplatelet therapy in patients with coronary artery disease: a report of the American College of Cardiology/American Heart Association Task Force on clinical practice guidelines. *J Am Coll Cardiol.* (2016) 68:1082–115. doi: 10.1016/j.jacc.2016.03.513
30. Bawamia B, Mehran R, Qiu W, Kunadian V. Risk scores in acute coronary syndrome and percutaneous coronary intervention: a review. *Am Heart J.* (2013) 165:441–50. doi: 10.1016/j.ahj.2012.12.020
31. Hall M, Bebb OJ, Dondo TB, Yan AT, Goodman SG, Bueno H, et al. Guideline-indicated treatments and diagnostics, GRACE risk score, and survival for non-ST elevation myocardial infarction. *Eur Heart J.* (2018) 39:3798–806. doi: 10.1093/eurheartj/ehy517
32. Chew DP, Junbo G, Parsonage W, Kerkar P, Sulimov VA, Horsfall M, et al. Perceived risk of ischemic and bleeding events in acute coronary syndromes. *Circ Cardiovasc Qual Outcomes.* (2013) 6:299–308. doi: 10.1161/CIRCOUTCOMES.111.000072
33. Yan AT, Yan RT, Tan M, Fung A, Cohen EA, Fitchett DH, et al. Management patterns in relation to risk stratification among patients with non-ST elevation acute coronary syndromes. *Arch Intern Med.* (2007) 167:1009–16. doi: 10.1001/archinte.167.10.1009
34. Bing R, Goodman SG, Yan AT, Fox K, Gale CP, Hyun K, et al. Use of clinical risk stratification in non-ST elevation acute coronary syndromes: an analysis from the CONCORDANCE registry. *Eur Heart J Qual Care Clin Outcomes.* (2018) 4:309–17. doi: 10.1093/ehjqcco/qcy002
35. Liang H, Tsui BY Ni H, Valentim CCS, Baxter SL, Liu G, et al. Evaluation and accurate diagnoses of pediatric diseases using artificial intelligence. *Nat Med.* (2019) 25:433–8. doi: 10.1038/s41591-018-0335-9
36. Leyh-Bannurah S-R, Tian Z, Karakiewicz PI, Wolffgang U, Sauter G, Fisch M, et al. Deep learning for natural language processing in urology: state-of-the-art automated extraction of detailed pathologic prostate cancer data from narratively written electronic health records. *JCO Clin Cancer Inform.* (2018) (2):1–9. doi: 10.1200/CCI.18.00080
37. Ness SL, Manyakov NV, Bangerter A, Lewin D, Jagannatha S, Boice M, et al. JAKE(R) multimodal data capture system: insights from an observational study of autism spectrum disorder. *Front Neurosci.* (2017) 11:517. doi: 10.3389/fnins.2017.00517
38. Malke JC, Jin S, Camp SP, Lari B, Kell T, Simon JM, et al. Enhancing case capture, quality, and completeness of primary melanoma pathology records *via* natural language processing. *JCO Clin Cancer Inform.* (2019) 3:1–11. doi: 10.1200/CCI.19.00006

Conflict of Interest: The authors declare that the research was conducted in the absence of any commercial or financial relationships that could be construed as a potential conflict of interest.

The reviewer JT declared a shared affiliation, with two of the authors ZQ and JL to the handling editor at the time of the review.

frontiers in Cardiovascular Medicine

ORIGINAL RESEARCH
published: 31 January 2022
doi: 10.3389/fcvm.2021.780198

Prognostic Implications of a Second Peak of High-Sensitivity Troponin T After Myocardial Infarction

Tau S. Hartikainen[1], Alina Goßling[1], Nils A. Sörensen[1,2], Jonas Lehmacher[1], Johannes T. Neumann[1,2,3], Stefan Blankenberg[1,2] and Dirk Westermann[1,2]*

[1] Department of Cardiology, University Heart and Vascular Center Hamburg, Hamburg, Germany, [2] German Center for Cardiovascular Research (DZHK), Partner Site Hamburg/Kiel/Lübeck, Hamburg, Germany, [3] Department of Epidemiology and Preventive Medicine, School of Public Health and Preventive Medicine, Monash University, Melbourne, VIC, Australia

Background: After an acute myocardial infarction (MI), repeated measurement of cardiac biomarkers is commonly performed, although not recommended in current guidelines. There is only limited data on the kinetics of troponin in this phase. For high-sensitivity cardiac troponin T (hs-cTnT), but not high-sensitivity cardiac troponin I (hs-cTnI), late increases in terms of a second peak have been described. Their impact on the prognosis of patients with MI remains unclear.

Methods: We included 2,305 patients presenting to the emergency department with symptoms suggestive of MI. Five hundred and seven were diagnosed with MI. Hs-cTnT, creatine kinase (CK) and the MB fraction of CK (CK-MB) were measured at admission, after 1 and 3 h and thereafter as indicated by the treating physician. A mixed-model approach was applied for modeling the biomarker kinetics. All patients were followed up to assess a composite endpoint of mortality, recurrent MI, revascularization and rehospitalization and to investigate the effect of a second hs-cTnT peak on prognosis.

Results: Out of 507 patients with MI, 192 had a sufficient amount of hs-cTnT measurements after the index MI. In 111 (57.8%) patients a second hs-cTnT peak was found after 4.48 days. For CK and CK-MB a second peak could not be identified. Regarding the composite endpoint there was no significant difference between patients with and without a second hs-cTnT peak.

Conclusion: In our analyses, a second peak of hs-cTnT after an acute MI was common, but not associated with poorer outcome. Thus, the clinical value of hs-cTnT for monitoring myocardial ischemia might be limited in this phase and other biomarkers might be more suitable.

Trial Registration: www.ClinicalTrials.gov, identifier: NCT02355457, Date of registration: February 4, 2015.

Keywords: myocardial infarction, biomarker, acute coronary syndrome, troponin, kinetics, second peak

OPEN ACCESS

Edited by:
Karin Wildi, Critical Care Research Group (CCRG), Australia

Reviewed by:
Alma Mingels, Maastricht University Medical Centre, Netherlands
Marco Zimarino, Asl Lanciano Vasto Chieti, Italy

****Correspondence:***
Tau S. Hartikainen
t.hartikainen@uke.de

Specialty section:
This article was submitted to Coronary Artery Disease, a section of the journal Frontiers in Cardiovascular Medicine

Received: *20 September 2021*
Accepted: *27 January 2022*
Published: *31 January 2022*

Citation:
Hartikainen TS, Goßling A, Sörensen NA, Lehmacher J, Neumann JT, Blankenberg S and Westermann D (2022) Prognostic Implications of a Second Peak of High-Sensitivity Troponin T After Myocardial Infarction. Front. Cardiovasc. Med. 8:780198. doi: 10.3389/fcvm.2021.780198

INTRODUCTION

High sensitivity cardiac troponin (hs-cTn) has evolved as being the gold-standard biomarker for diagnosing myocardial injury and infarction (MI) (1, 2). Even though not recommended in current guidelines, repeated measurement of hs-cTn is commonly performed in clinical practice in the first days after MI. However, there is only limited data on the kinetics of hs-cTn after an acute MI and

their consecutive clinical and prognostic implications. For hs-cTnT, but hs-cTnI, late increases in terms of a second peak several days after the index event have been observed (3). We aimed to investigate the prognostic value of late hs-cTnT increases after an acute MI in a large, contemporary cohort study.

MATERIALS AND METHODS

For this analysis we used data from the Biomarkers in Acute Cardiac Care study population (4). Briefly, we prospectively recruited patients presenting to the emergency department with symptoms suggestive of MI. Hs-cTnT (Elecsys; Roche Diagnostics), creatine kinase (CK) and the MB fraction of CK (CK-MB) were measured at admission, after 1 and 3 h and thereafter as indicated by the treating physician. Measurements until the 10th day after admission were included. A second peak of hs-cTnT was defined as an increase of at least 15% after the concentrations had already decreased after the first maximum troponin value. Patients without a second peak and <3 measurements between day 1 and 5 were excluded due to possible missing of an existing second peak. The final diagnosis was adjudicated by two physicians separately in a blinded fashion based on all available clinical findings and according to the Third Universal Definition of MI (5). A follow-up was performed up to 4 years. Cox regression analyses were conducted for a composite endpoint of all-cause mortality, recurrent MI, revascularization and rehospitalization. Event rates were calculated using the Kaplan-Meier estimator. For modeling the hs-cTnT kinetics a mixed-model approach was used.

RESULTS

Among 2,305 patients presenting with suspected MI, 507 (22.0%) were diagnosed as having MI. Out of these, 365 (72%) were patients with type 1 MI, 140 (27.6%) patients with type 2 MI and 2 (0.4%) patients with type 4 MI. Three hundred and eleven of all patients with MI were excluded from the analyses due to an insufficient number of available biomarker results after MI. Out of 192 remaining patients, 111 (57.8%) patients presented a second hs-cTnT peak, mostly between day 2 and 5 after the index event (**Figure 1**). The median troponin concentration at the first peak was 1,213 ng/L (interquartile range (IQR) 1,107–1,319 ng/L) and at the second peak 866 ng/L (IQR 727–1,005 ng/L), thus the second peak was 28.6% (IQR 23.8-34.3%) lower as compared to the first peak. In 81 patients (42.2%) a second peak could not be identified. There were no significant differences in the baseline characteristics between patients with and without a second hs-cTnT peak (**Table 1**). Angiography for the index event was performed in 97.5% in patients without and 92.8% with a second hs-cTnT peak. Angiography was followed by a percutaneous coronary intervention significantly more often in patients without a second peak (85.2% of patients without and 72.1% patients with a second peak, $p = 0.048$).

Regarding the composite endpoint there was no significant difference between patients with and without a second hs-cTnT peak for both unadjusted analyses [hazard ratio (HR) 0.93, 95% confidence interval (CI) 0.58–1.48, $p = 0.75$] and after adjustment for sex, age and cardiovascular risk factors (HR 0.78, CI 0.48–1.28, $p = 0.33$) (**Figure 1**). In comparison to hs-cTnT, CK and CK-MB showed an almost linear decrease after the index-event.

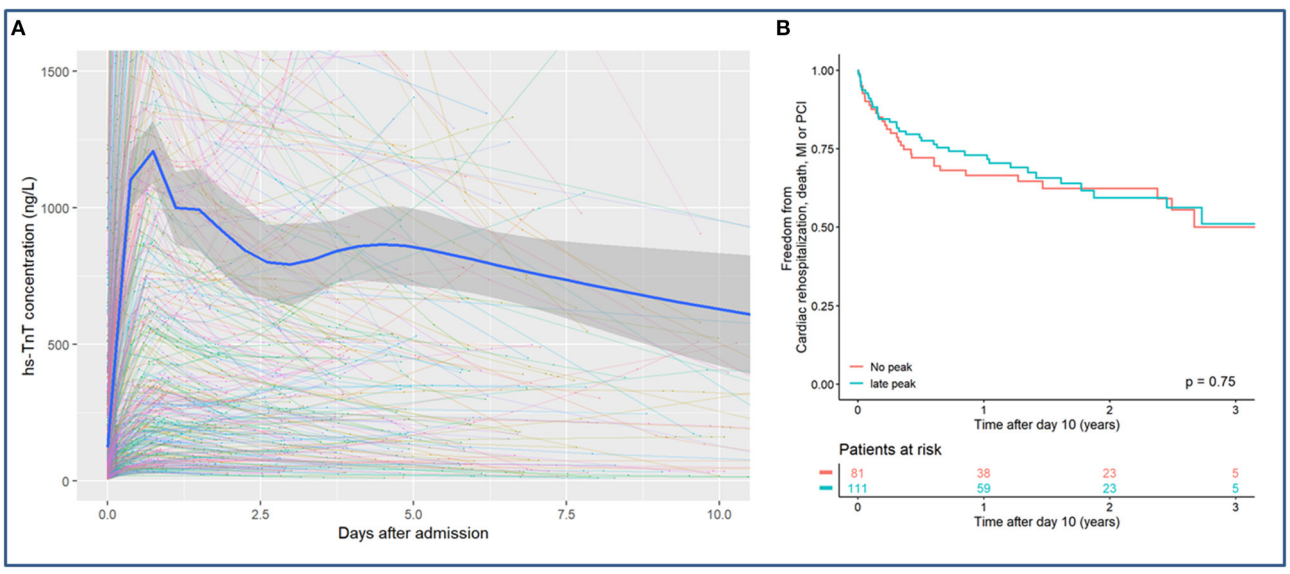

FIGURE 1 | (A) Kinetics of hs-cTnT during the first 10 days after myocardial infarction presented using mixed-model statistics. A second hs-cTnT peak can be detected after 4.48 days after the index event. **(B)** Kaplan-Meier curve for the combined endpoint of all-cause mortality, rehospitalization, MI or PCI for patients with and without a second hs-cTnT peak.

TABLE 1 | Baseline characteristics of patients with and without a second hs-cTnT peak.

	All ($N = 192$)	No 2nd peak ($N = 81$)	2nd peak ($N = 111$)	*p*-value
Age (years)	68.0 (56.0, 76.0)	67.0 (50.0, 75.0)	69.0 (60.0, 77.8)	0.11
Male No. (%)	147 (76.6)	64 (79.0)	83 (74.8)	0.61
BMI (kg/m²)	27.0 (24.1, 30.2)	27.0 (24.3, 30.9)	27.2 (23.9, 29.7)	0.77
Hypertension No. (%)	151 (78.6)	62 (76.5)	89 (80.2)	0.67
Hyperlipoproteinemia No. (%)	85 (44.3)	31 (38.3)	54 (48.6)	0.20
Diabetes No. (%)	36 (18.8)	11 (13.6)	25 (22.7)	0.16
Current smoker No. (%)	57 (29.8)	18 (22.5)	39 (35.1)	0.085
History of CAD No. (%)	80 (41.7)	29 (35.8)	51 (45.9)	0.21
Angiography No. (%)	182 (94.8)	79 (97.5)	103 (92.8)	0.26
PCI No. (%)	149 (77.6)	69 (85.2)	80 (72.1)	0.048

For continuous variables median and interquartile ranges are given. For binary variables absolute and relative frequencies are shown.
No., Number; BMI, body mass index; CAD, coronary artery disease; PCI, percutaneous coronary intervention.

DISCUSSION

Our findings indicate that a second peak of hs-cTnT after MI is very common but not associated with impaired outcome compared to patients without a second peak. Our results regarding the timepoint and the height of the second peak in relation to the first peak are in line with earlier findings (3). Most of the previously published studies investigating the second hs-cTnT peak included only patients with ST-segment elevation MI (STEMI). However, we were able to confirm that a second peak was also detectable in other MI patients. Since hs-cTnT is a widely used biomarker, these novel findings are highly relevant for clinical practice. A second increase of hs-cTnT after MI can be misinterpreted as ongoing or recurrent ischemia and might lead to unnecessary coronary re-catheterization. In previous studies, a second peak after MI has only been found for hs-cTnT but not for cTnI, hs-cTnI, CK or CK-MB—irrespective of the manufacturer, the sensitivity of the assay or renal function of the patient (3). Therefore the latter might be more suitable for post-MI monitoring since a second peak of these biomarkers might indicate ischemia more accurately. Importantly, Schaaf et al. were able to find a high correlation between the second hs-cTnT peak and infarct size measured in cardiac magnetic resonance, which would somewhat disagree with our findings, since the prognosis after MI is related to the extent of the infarction (6). These investigations emphasize the need for further studies regarding the cause and impact of the second hs-cTnT peak. Several different mechanisms for the genesis of the second peak of hs-cTnT have been suggested, however, the etiology still remains unclear (3, 7). Since a second peak has only been detected for hs-cTnT but not hs-cTnI, the cause might be associated with different clearance pathways, the different molecular weight or variable fragments of the two troponins.

Our analyses and the consecutive conclusions are limited by the relatively small number of patients. Larger studies are necessary to validate the findings of this study. Also, there might be a selection bias since troponin was not measured systematically in all included patients but as indicated by the treating physician. Therefore, a second hs-cTnT peak might have been missed in some patients. The cut-off of 15%, which was required for an increase of troponin to be defined as a second peak in this study, was chosen to exclude a random variability of two consecutive hs-cTnT measurements. However, this cut-off value should be validated in a larger study. Lastly, due to the limited number of patients in this study, we cannot make conclusions on whether the second peak has other characteristics or a different clinical value in certain types of MI.

In summary, the clinical value of hs-cTnT measurements after MI might be limited due a frequently occurring second peak, which was not associated with impaired outcome in our analyses. Prospective studies are needed to further evaluate the role of hs-cTnT after MI.

DATA AVAILABILITY STATEMENT

The raw data supporting the conclusions of this article will be made available by the authors, without undue reservation.

ETHICS STATEMENT

The studies involving human participants were reviewed and approved by the local ethics committee. The patients/participants provided their written informed consent to participate in this study.

AUTHOR CONTRIBUTIONS

TH, JN, and DW made significant contributions to the conception and design of the study. AG contributed to the analysis of the data. TH and JN drafted the manuscript. All authors critically revised the manuscript for intellectual content, approved it for submission, and were involved in the acquisition and interpretation of the data.

FUNDING

This work was supported by the German Center of Cardiovascular Research (DZHK) and with an unrestricted grant by Abbott Diagnostics. JN was recipient of a research fellowship by the Deutsche Forschungsgemeinschaft (DFG).

REFERENCES

1. Thygesen K, Alpert JS, Jaffe AS, Chaitman BR, Bax JJ, Morrow DA, et al. Fourth universal definition of myocardial infarction 2018. *Eur Heart J*. (2019) 40:237–69. doi: 10.1093/eurheartj/ehy856
2. Neumann JT, Twerenbold R, Ojeda F, Sorensen NA, Chapman AR, Shah ASV, et al. Application of high-sensitivity troponin in suspected myocardial infarction. *N Engl J Med*. (2019) 380:2529–40. doi: 10.1056/NEJMoa1803377
3. Laugaudin G, Kuster N, Petiton A, Leclercq F, Gervasoni R, Macia JC, et al. Kinetics of high-sensitivity cardiac troponin T and I differ in patients with ST-segment elevation myocardial infarction treated by primary coronary intervention. *Eur Heart J Acute Cardiovasc Care*. (2016) 5:354–63. doi: 10.1177/2048872615585518
4. Hartikainen TS, Sorensen NA, Haller PM, Gossling A, Lehmacher J, Zeller T, et al. Clinical application of the 4th Universal Definition of Myocardial Infarction. *Eur Heart J*. (2020) 41:2209–16. doi: 10.1093/eurheartj/ehaa035
5. Thygesen K, Alpert JS, Jaffe AS, Simoons ML, Chaitman BR, White HD, et al. Third universal definition of myocardial infarction. *Eur Heart J*. (2012) 33:2551–67. doi: 10.1016/j.gheart.2012.08.001
6. Schaaf M, Huet F, Akodad M, Gorce-Dupuy AM, Adda J, Macia JC, et al. Which high-sensitivity troponin variable best characterizes infarct size and microvascular obstruction? *Arch Cardiovasc Dis*. (2019) 112:334–42. doi: 10.1016/j.acvd.2018.12.001
7. Michielsen EC, Diris JH, Kleijnen VW, Wodzig WK, Van Dieijen-Visser MP. Investigation of release and degradation of cardiac troponin T in patients with acute myocardial infarction. *Clin Biochem*. (2007) 40:851–5. doi: 10.1016/j.clinbiochem.2007.04.004

Conflict of Interest: SB has received honoraria from Abbott Diagnostics, Siemens, Thermo Fisher, and Roche Diagnostics and is a consultant for Thermo Fisher; DW reports personal fees from Bayer, Boehringer-Ingelheim, Berlin Chemie, Astra Zeneca, Biotronik and Novartis.

The remaining authors declare that the research was conducted in the absence of any commercial or financial relationships that could be construed as a potential conflict of interest.

Publisher's Note: All claims expressed in this article are solely those of the authors and do not necessarily represent those of their affiliated organizations, or those of the publisher, the editors and the reviewers. Any product that may be evaluated in this article, or claim that may be made by its manufacturer, is not guaranteed or endorsed by the publisher.

frontiers in Cardiovascular Medicine

ORIGINAL RESEARCH
published: 04 February 2022
doi: 10.3389/fcvm.2021.760178

GSVMA: A Genetic Support Vector Machine ANOVA Method for CAD Diagnosis

Javad Hassannataj Joloudari[1], Faezeh Azizi[1], Mohammad Ali Nematollahi[2], Roohallah Alizadehsani[3], Edris Hassannatajjeloudari[4], Issa Nodehi[5] and Amir Mosavi[6,7,8,9,10]**

[1] Department of Computer Engineering, Faculty of Engineering, University of Birjand, Birjand, Iran, [2] Department of Computer Sciences, Fasa University, Fasa, Iran, [3] Institute for Intelligent Systems Research and Innovation, Deakin University, Geelong, VIC, Australia, [4] Department of Nursing, School of Nursing and Allied Medical Sciences, Maragheh Faculty of Medical Sciences, Maragheh, Iran, [5] Department of Computer Engineering, University of Qom, Qom, Iran, [6] Faculty of Informatics, Technische Universität Dresden, Dresden, Germany, [7] Faculty of Civil Engineering, TU-Dresden, Dresden, Germany, [8] John von Neumann Faculty of Informatics, Óbuda University, Budapest, Hungary, [9] Institute of Information Society, University of Public Service, Budapest, Hungary, [10] Institute of Information Engineering, Automation and Mathematics, Slovak University of Technology in Bratislava, Bratislava, Slovakia

Background: Coronary artery disease (CAD) is one of the crucial reasons for cardiovascular mortality in middle-aged people worldwide. The most typical tool is angiography for diagnosing CAD. The challenges of CAD diagnosis using angiography are costly and have side effects. One of the alternative solutions is the use of machine learning-based patterns for CAD diagnosis.

Methods: Hence, this paper provides a new hybrid machine learning model called genetic support vector machine and analysis of variance (GSVMA). The analysis of variance (ANOVA) is known as the kernel function for the SVM algorithm. The proposed model is performed based on the Z-Alizadeh Sani dataset so that a genetic optimization algorithm is used to select crucial features. In addition, SVM with ANOVA, linear SVM (LSVM), and library for support vector machine (LIBSVM) with radial basis function (RBF) methods were applied to classify the dataset.

Results: As a result, the GSVMA hybrid method performs better than other methods. This proposed method has the highest accuracy of 89.45% through a 10-fold crossvalidation technique with 31 selected features on the Z-Alizadeh Sani dataset.

Conclusion: We demonstrated that SVM combined with genetic optimization algorithm could be lead to more accuracy. Therefore, our study confirms that the GSVMA method outperforms other methods so that it can facilitate CAD diagnosis.

Keywords: coronary artery disease, genetic algorithm, support vector machine, machine learning, diagnosis

OPEN ACCESS

Edited by:
Stéphane Cook,
Université de Fribourg, Switzerland

Reviewed by:
Rajiv Rampat,
William Harvey Hospital,
United Kingdom
Dominique Monlezun,
University of Texas MD Anderson Cancer Center, United States

****Correspondence:***
Javad Hassannataj Joloudari
javad.hassannataj@birjand.ac.ir
Amir Mosavi
amir.mosavi@mailbox.tu-dresden.de

Specialty section:
This article was submitted to Coronary Artery Disease, a section of the journal Frontiers in Cardiovascular Medicine

Received: *17 August 2021*
Accepted: *22 December 2021*
Published: *04 February 2022*

Citation:
Hassannataj Joloudari J, Azizi F, Nematollahi MA, Alizadehsani R, Hassannatajjeloudari E, Nodehi I and Mosavi A (2022) GSVMA: A Genetic Support Vector Machine ANOVA Method for CAD Diagnosis. Front. Cardiovasc. Med. 8:760178. doi: 10.3389/fcvm.2021.760178

INTRODUCTION

Cardiovascular disease (CVD) is one of the most prevalent diseases which cause a lot of deaths worldwide (1). As crucial evidence for this fact, one can refer to the CVD fact sheet published by the World Health Organization (WHO), which estimated 17.9 million deaths from CVDs in 2019, representing 32% of all global deaths. Of these deaths, 85% were due to heart attack and stroke (2). An essential type of CVDs is coronary artery disease (CAD) (3). One of the reasons that made CAD such a necessary and stressful disease is the fact that nearly 25% of people who have been diagnosed with CAD died unexpectedly without any prior symptoms (4).

Nowadays, electrocardiogram, cardiac stress test, coronary computed tomographic angiography, and coronary angiogram are some of the prevalent techniques used as diagnostic methods for CAD. The downside facts about all these methods are having side effects and imposing high costs on patients and health systems. Hence, today, applying machine learning methods for diagnosing CAD has become a general tendency. These techniques are important for modeling and knowledge extraction from row dataset (5).

To evaluate the performance of these new techniques, various CAD datasets have been prepared. Among these datasets, the Z-Alizadeh Sani dataset, Cleveland, and Hungarian are public.

In recent years, studies have been presented using machine learning methods for CAD diagnosis on different datasets. The well-known dataset, namely the Z-Alizadeh Sani dataset in the field of heart disease, is utilized. It is worth noting that until now, dozens of studies on the Z-Alizadeh Sani dataset have been published (5–25). The main goal of recent studies is to utilize feature selection methods to improve the accuracy of CAD diagnosis. In (10), a classification accuracy of 87.85 was obtained for CAD diagnosis by ANN classifier, so that 25 features were identified. In (14), a hybrid model titled nested ensemble nu-support vector classification method was presented to predict CAD. An accuracy of 94.66% was obtained using the hybrid method on the Z-Alizadeh Sani dataset so that 16 features were selected.

In a recent study (25), the CAD diagnosis was conducted using the weighted-average voting ensemble method. An accuracy of 98.97% was achieved using the ensemble method on five features.

We obtained the highest area under the curve (AUC) and accuracy with more valuable and important features.

The previous studies demonstrate that Support Vector Machine (SVM) performs better for binary classification and dimension reduction on a small dataset (16, 26).

Hence, we utilized the SVM method with kernel types such as analysis of variance (ANOVA), linear SVM (LSVM), and library for support vector machine (LIBSVM) with radial basis function (RBF) on the Z-Alizadeh Sani dataset. Also, a genetic algorithm as an optimizer is used to select important features in the SVM modeling process. Ultimately, among the proposed methods used in this paper, the genetic optimizer method combined with SVM and ANOVA kernel has the most accuracy of 89.45% on 31 features.

In summary, the main contributions of our paper are as follows:

1) Performing data preprocessing (transforming nominal data to numerical data and normalization)
2) Using genetic algorithm as a feature selection method for selecting important features
3) Specifying ANOVA kernel as the best kernel compared to the other kernels
4) Generating the hybrid model consist of genetic training for feature selection, SVM for classification, and a 10-fold crossvalidation technique
5) Obtaining a maximum AUC of 100% on the Z-Alizadeh Sani dataset

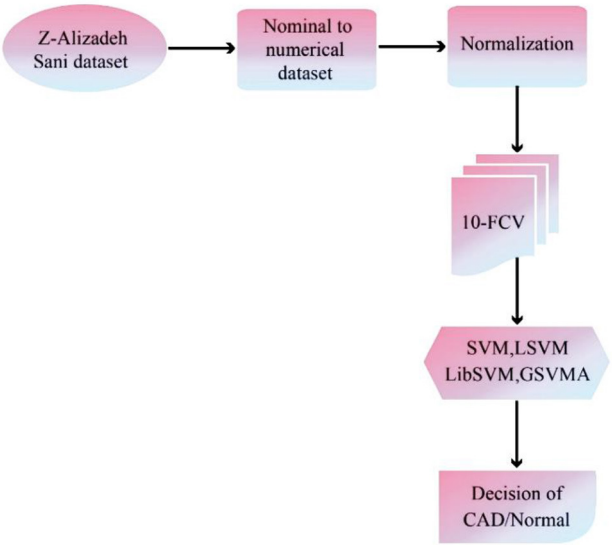

FIGURE 1 | The proposed methodology framework.

MATERIALS AND METHODS

The proposed methodology has been performed in three subsections. Section Z-Alizadeh Sani Dataset describes the Z-Alizadeh Sani dataset. Also, in section Data Preprocessing, data preprocessing will be done. In addition, data classification using SVM with ANOVA, LSVM, and LIBSVM with RBF and GSVMA methods is described in section Used Classification Methods. The proposed methodology framework is shown in **Figure 1**.

Z-Alizadeh Sani Dataset

The Z-Alizadeh Sani dataset is one of the most common datasets used in machine learning for automatic CAD detection. This dataset is constructed from 303 patients referred to Shaheed Rajaie Cardiovascular, Medical, and Research Center[1] A patient is categorized as a patient with CAD if one or more of his/her coronary arteries are stenosis. A coronary artery is categorized as stenosis if its diameter narrowing is $\geq$50% (27). Accordingly, 216 patients had CAD, and the dataset contains 88 patients with the normal situation on the Z-Alizadeh Sani. Each record in this dataset has 55 features that can be used as indicators of CAD for a patient. These features are grouped into four categories include demographic, symptom and examination, laboratory and echo, and ECG features as explained in **Table 1**.

Data Preprocessing

In the data analysis process, preprocessing is required after data gathering. The Z-Alizade Sani dataset was numerical and string. First, the values of features are transformed from nominal data to numerical data. The features such as sex, chronic renal failure, cerebrovascular accident, airway disease, thyroid disease, congestive heart failure, dyslipidemia, etc., are

[1]https://archive.ics.uci.edu/ml/datasets/Z-Alizadeh+Sani

TABLE 1 | Description of the Z-Alizadeh-Sani dataset (5).

Feature type	Feature name	Range	Std. error of mean
Demographic	Age	(30–80)	0.6
Demographic	Weight	(48–120)	0.69
Demographic	Length	(140–188)	0.54
Demographic	Sex	Male, Female	—
Demographic	Body mass index (BMI) (Kb/m^2)	(18-41)	0.24
Demographic	Diabetes mellitus (DM)	(0, 1)	0.03
Demographic	Hypertension (HTN)	(0, 1)	0.03
Demographic	Current smoker	(0, 1)	0.02
Demographic	Ex-smoker	(0, 1)	0.01
Demographic	Family history (FH)	(0, 1)	0.02
Demographic	Obesity	Yes if MBI $>$ 25, No otherwise	—
Demographic	Chronic renal failure (CRF)	Yes, No	—
Demographic	Cerebrovascular accident (CVA)	Yes, No	—
Demographic	Airway disease	Yes, No	—
Demographic	Thyroid disease	Yes, No	—
Demographic	Congestive heart failure (CHF)	Yes, No	—
Demographic	Dyslipidemia (DLP)	Yes, No	—
Symptom and examination	Blood pressure (BP) (mmHg)	(90–190)	1.09
Symptom and examination	Pulse rate (PR) (ppm)	(50–110)	0.51
Symptom and examination	Edema	(0, 1)	0.01
Symptom and examination	Weak peripheral pulse	Yes, No	—
Symptom and examination	Lung rales	Yes, No	—
Symptom and examination	Systolic murmur	Yes, No	—
Symptom and examination	Diastolic murmur	Yes, No	—
Symptom and examination	Typical chest pain	(0, 1)	0.03
Symptom and examination	Dyspnea	Yes, No	—
Symptom and examination	Function class	1, 2, 3, 4	0.06
Symptom and examination	Atypical	Yes, No	—
Symptom and examination	Nonanginal chest pain	Yes, No	—
Symptom and examination	Exertional chest pain	Yes, No	—
Symptom and examination	Low TH Ang (low-threshold angina)	Yes, No	—
ECG	Rhythm	Sin, AF	—
ECG	Q wave	(0, 1)	0.01
ECG	ST elevation	(0, 1)	0.01
ECG	ST depression	(0, 1)	0.02
ECG	T inversion	(0, 1)	0.03
ECG	LVH (left ventricular hypertrophy)	Yes, No	—
ECG	Poor R-wave progression	Yes, No	—
Laboratory and echo	FBS (fasting blood sugar mg/dl)	(62–400)	2.99
Laboratory and echo	Cr (creatine mg/dl)	(0.5–2.2)	0.02
Laboratory and echo	TG (triglyceride mg/dl)	(37–1050)	5.63
Laboratory and echo	LDL (low-density lipoprotein mg/dl)	(18–232)	2.03
Laboratory and echo	HDL (high-density lipoprotein mg/dl)	(15–111)	0.61
Laboratory and echo	BUN (blood urea nitrogen mg/dl)	(6–52)	0.4
Laboratory and echo	ESR (erythrocyte sedimentation rate mm/h)	(1–90)	0.92
Laboratory and echo	HB (hemoglobin g/dl)	(8.9–17.6)	0.09
Laboratory and echo	K (potassium mEq/lit)	(3.0–6.6)	0.03
Laboratory and echo	Na (sodium mEq/lit)	(128–156)	0.22
Laboratory and echo	WBC (white blood cell cells/ml)	(3,700–18.000)	138.67
Laboratory and echo	Lymph (lymphocyte %)	(7–60)	0.57
Laboratory and echo	Neut (neutrophil %)	(32–89)	0.59
Laboratory and echo	PLT (platelet 1,000/ml)	(25–742)	3.49
Laboratory and echo	EF (ejection fraction %)	(15–60)	0.51
Laboratory and echo	Region with RWMA	(0–4)	0.07
Laboratory and echo	VHD (valvular heart disease)	Normal, Mild, Moderate, Severe	—
Categorical	Target classes	CAD, Normal	—

Std: Standard.

transformed. Then, the data normalization is performed. The range transformation technique is a common technique for normalizing data related to features between 0 and 1 (5). In other words, changing the range of data to zero and one means changing the mean and variance to mean zero and variance 1. Normalizing the data helps all features have an equal effect and role in diagnosing the input class so that normalizing efforts to allow all features an equal weight.

The values of features such as diabetes mellitus (DM), hypertension (HTN), current smoker, ex-smoker, etc., are transformed between zero and one. In general, normalization leads to an increase in the accuracy of the classification methods. Furthermore, a 10-fold crossvalidation (10-FCV) technique (28, 29) for partitioning the dataset was utilized so that the dataset was divided into training (90%) and test (10%) subsets. The 10-FCV process was run 10 times in which the results of the methods were obtained by averaging every 10 times.

Used Classification Methods

SVM

For the first time, the SVM algorithm has been developed for data classification in (30–32), which is an optimal selection when robust predictive power is required. The SVM is a supervised machine learning algorithm that transforms data to a high dimensional space, that is, Hilbert space. Then kernel-based methods due to the visions presented by the generalization theory are exploited, and the optimization theory is performed (33). Indeed, SVM is an area parting model in which the data allocated into the support vectors are based on machine learning and model construction (34, 35).

In general, the SVM aims to find the best separator line (optimal hyperplane) between the data of the two classes so that it has the most significant possible distance from all the support vectors of the two classes. These classes are partitioned as linear and nonlinear statuses (34, 36). In these statuses, the SVM is considered that there is a set of training data x_1,$x2$,...,$x3 \in R^n$ with class $y_1 \in\{1,-1\}$ that are binary (x_i, y_i), $(i=1, 2,...n)$, and n represents the number of training data points.

In this paper, we used methods such as LSVM, library SVM with RBF, SVM with ANOVA, and genetic support vector machine with ANOVA (GSVMA). RapidMiner software version 9.9 has been used to implement the methods. We described these methods in the following.

Linear SVM

The linear kernel is the most common kernel function for LSVM (37). The LSVM model generates an optimized hyperplane that discrete the data points of the two classes.

For an LSVM, a decision function or separator function is defined as follows:

$$f(x_i) = sign(< w, x_i > + b) \tag{1}$$

$$= \begin{cases} 1 \text{ if } y_i = 1 \\ -1 \text{ if } y_i = -1 \end{cases}$$

In equation (1), the w parameter represents the weight of inertia, b is the width of the origin point, in which $w \in Z$ and $b \in R$. Based on the LSVM model, an optimized hyperplane is shown in **Figure 2** (34).

In **Figure 2**, x_i is the data points of the two classes labeled $y_i = \{1,-1\}$ such that $<w,x> + b=0$ represents the optimal hyperplane assigned in the average of the other two lines, that is, $\{x|<w,x> + b = +1\}$ and $\{x|<w,x> + b = -1\}$. Also, w denotes a normal vector for the optimal hyperplane, and b is the offset between the hyperplane and the origin plane. Moreover, the margin $M=w/2$ of the separator is the distance among support vectors. Therefore, the maximum margin can be obtained in the form of the following constraint optimization equation (2):

$$Minimize: \frac{1}{2}|w|^2 subjectto: yi(w.x + b) - 1 \geq 0 \ \forall i \tag{2}$$

Based on the objective function (2), the most common approach for solving an optimization problem is to transform it into a dual problem. First, to get the dual form of the problem, the positive Lagrangian coefficients are multiplied by $\alpha_i \geq 0$ and deducted from the objective function, causing in the following equation named a primal problem (Lagrange's initial equation, L_p):

$$\mathrm{L_p} = \frac{1}{2}|w|^2 - \sum_i \alpha_i(\mathrm{y_i}\left(\mathrm{w.x} + \mathrm{b}\right)) - 1 \tag{3}$$

To solve equation (3), we are employed the Karush–Kuhn–Tucker (KKT) conditions, which perform an essential role in constraint optimization problems. These conditions state the necessary and adequate needs for the optimal solution to constraint formulas and must be a derivative of the function regarding the variables equal to zero. Exploiting KKT conditions into L_p has been derived from the $L_p$relation to w and b, and it sets to zero. So, the equations (4–7) are obtained as follows:

$$\frac{\partial}{\partial w_v} L_p = w_v - \sum_i \alpha_i y_i x_{iv} = 0 v = 1, ..., d \tag{4}$$

$$\frac{\partial}{\partial b} L_p = -\sum_i \alpha_i y_i = 0 \tag{5}$$

$$\alpha_i(y_i(w.x + b)) - 1 \geq 0 i = 1, ..., l \alpha_i \geq 0 \forall_i \tag{6}$$

$$\alpha_i(y_i(w.x + b)) - 1 \geq 0 \forall_i \tag{7}$$

Consequently, with the assignment of the above formulas into equation (3), equation (8) is gained.

$$Maximize: L_D = \sum_i \alpha_i - \frac{1}{2} \sum_i \sum_j \alpha_i \alpha_j y_i y_j (x_i . x_j) \tag{8}$$

Equation (8) is named the dual problem. Hence, L_p and L_D are both obtained from the same condition. So, the optimal problem can be solved by achieving the minimum L_p or the maximum L_p, the L_p double with the condition $\alpha_i \geq 0$.

The parameters setting of the used LSVM method is given in **Table 2**.

The pseudocode of the LSVM is presented below.

Algorithm 1: The used LSVM method for CAD diagnosis.

Input: Extract the Z-Alizadeh Sani dataset include 303 records and 55 features.

Output: The diagnosed (CAD/normal) class of each test record by the generated LSVM model and determined the evaluation criteria such as accuracy, positive predictive value (PPV), F-measure, sensitivity, specificity, negative predictive value, and AUC

Begin
    Data preprocessing: Transforming nominal records to numerical records and normalizing between zero and one
    Divide the data using a 10-fold crossvalidation technique
    Choose the value of the parameters setting based on **Table 2**
    While (terminating condition is not happened by 10-fold crossvalidation) do
        Employ LSVM train for each record
        Generate LSVM model
        Employ LSVM classify for testing records
    End while
    Return obtaining the evaluation criteria
End

Library SVM With RBF

The SVM is a binary classifier that it can only classify two classes. LIBSVM (38, 39) also supports the multiclass state. The difference between the two-class and multiclass problems regarding training and testing the data is that larger sets or multiclass conditions may be time-consuming. Indeed, the LIBSVM supports four different kernels by default: linear, polynomial, RBF, and sigmoid kernels, so that the RBF is the essential tool for SVM and regression classifications developed by Chavhan et al. (36). The RBF kernel is applied in the training phase (37). The advantage of using the RBF kernel is that it handles the training data to assign specified boundaries. Moreover, the RBF kernel nonlinearly maps samples into a higher-dimensional space. It can handle the training data when the relation between class labels and features is nonlinear. The RBF kernel has fewer numerical difficulties than the polynomial kernel, linear, and sigmoid.

The SVM types are selected through LIBSVM, such as the C-SVC and nu-SVC for classification tasks. Also, the epsilon-SVR and nu-SVR are used for regression tasks, and the one-class SVM is performed for distribution estimation. In this paper, the RBF kernel is selected for SVM as formulated in (9).

The most common kernel type is the RBF for SVM.

$$K(x_i, x_j) = \exp\left(-\frac{\left\|x_i - x_j\right\|^2}{2\sigma^2}\right) = \exp\left(-\gamma \left\|x_i - x_j\right\|^2\right) \quad (9)$$

According to (9), σ is the radial of the kernel function. Also, $\gamma =$ represents the kernel parameter. The value of the kernel parameter affects the training rate and the test rate. It should be noted that the efficiency of SVM regarding the accuracy of diagnosis and generalization power is related to the situation of the penalty factor "c" and the kernel parameter "γ" (34).

TABLE 2 | The parameters setting of the LSVM method.

Parameters	Setting
Kernel cache	200
C	0.1
Convergence epsilon	0.001
Max iterations	100,000
L pos	1.0
L neg	1.0
Balance cost	✓

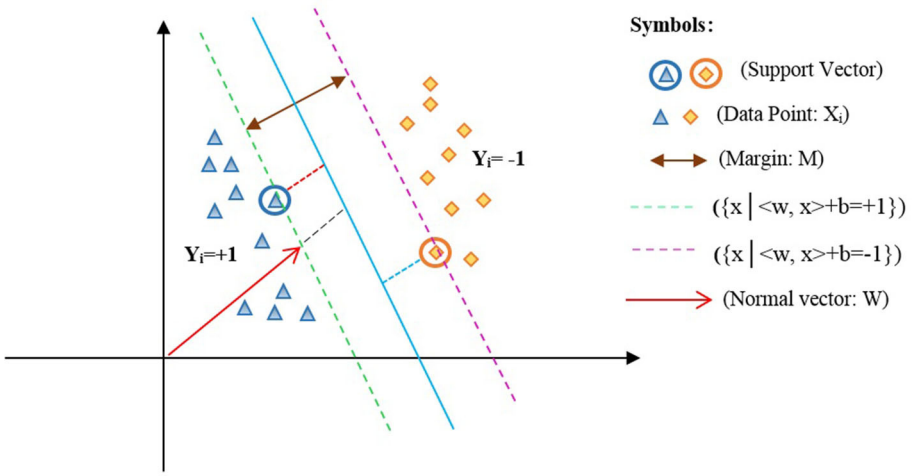

FIGURE 2 | Optimized hyperplane for two-dimensional space.

Moreover, the C-SVC is used to classify data.

The parameters setting of the used LIBSVM with RBF method is described in **Table 3**.

The pseudocode of the LIBSVM is given below.

Algorithm 2: The used LIBSVM method for CAD diagnosis.

Input: Extract the Z-Alizadeh Sani dataset include 303 records and 55 features.

Output: The diagnosed (CAD/normal) class of each test record and determined the evaluation criteria

Begin
    Data preprocessing: Transforming nominal records to numerical records and normalizing between zero and one
    Divide the data using a 10-fold crossvalidation technique
    Choose the value of the parameters setting based on **Table 3**
    While (terminating condition is not happened by 10-fold crossvalidation) do
    Employ LIBSVM train for each record
    Generate LIBSVM model
    Employ LIBSVM classify for testing records
    End while
    Return obtaining the evaluation criteria
End

SVM With Analysis of Variance

In general, kernel types are supported by the SVM such as dot, radial, polynomial, neural, ANOVA, Epachnenikov, Gaussian combination, and multiquadric. The ANOVA kernel is defined by raised to the power "d" of summation of $exp(-\gamma\ (x-y))$ where "γ" is gamma, and "d" is degree. The "γ" and "d" are regulated by the kernel gamma and kernel degree parameters, respectively. Indeed, the ANOVA kernel is also a RBF kernel. It is said to perform well in multidimensional regression and classification problems (40). The ANOVA kernel is formulated as follows:

$$k(x, y) = \sum_{k=1}^{n} \exp(-\sigma(\overset{k}{x} - \overset{k}{y})^2)^d \tag{10}$$

TABLE 3 | The parameters setting of the LIBSVM method.

Parameters	Setting
SVM type	C-SVC
Kernel type	RBF
Gamma	1.0
C	0.1
Cache size	80
Epsilon	0.001
Shrinking	✓

The parameters setting of the used SVM with the ANOVA method is given in **Table 4**.

The pseudocode of the SVM with the ANOVA method is presented below.

Algorithm 3 : The used SVM with ANOVA method for CAD diagnosis.

Input: Extract the Z-Alizadeh Sani dataset include 303 records and 55 features.

Output: The diagnosed (CAD/normal) class of each test record and determined the evaluation criteria

Begin
    Data preprocessing: Transforming nominal records to numerical records and normalizing between zero and one
    Divide the data using a 10-fold cross-validation technique
    Choose the value of the parameters setting based on **Table 4**
    While (terminating condition is not happened by 10-fold crossvalidation) do
    Employ SVM with ANOVA train for each record
    Generate SVM with ANOVA model
    Employ SVM with ANOVA classify for testing records
    End while
    Return obtaining the evaluation criteria
End

Genetic Support Vector Machine Along With ANOVA

A genetic algorithm is a search heuristic method for solving optimization problems. This optimization algorithm uses heuristic biology techniques such as inheritance and mutation. In a genetic algorithm, to obtain the optimal response, the appropriate generation solutions are combined based on the principle of survival of the most desirable living organisms. In fact, in this algorithm, the solutions to a problem are defined in a chromosome form, consisting of a set of parameters called a gene. So, chromosomes are the proposed solutions to the problem of the genetic algorithm.

TABLE 4 | The parameters setting of the SVM with the ANOVA method.

Parameters	Setting
Kernel type	ANOVA
Kernel gamma	1.0
Kernel degree	2.0
Kernel cache	200
C	0.1
Convergence epsilon	0.001
Max iterations	100,000
L pos	1.0
L neg	1.0
Balance cost	✓

The most important application of the genetic algorithm is feature selection. Feature selection can be defined as the process of identifying related features and removing unrelated and duplicate features. The feature selection by the genetic algorithm is caused to the better efficiency of the classification methods. Hence, in this paper, we used a genetic algorithm for subset feature selection.

The stages of the genetic algorithm are as follows:

1) Initial population

The parameter of the initial population specifies the population size, that is, the number of members per generation. The genetic algorithm starts with a set of chromosomes so that several solutions with different combinations of features are randomly generated. Indeed, the chromosomes of the initial population, which are the initial solutions, comprise different combinations of the features. These combinations were randomly incorporated for each chromosome and formed the initial solutions to the problem. Hence, in this paper, using this algorithm, the best subset of the features is selected from the Z-Alizadeh Sani dataset (5). These essential features are fed to the SVM classification algorithm to classify the input dataset. In the genetic algorithm process, we set the population size to 50 and set the maximum number of generations to ten. Therefore, the size of each chromosome is related to the number of features, including 55 genes for all features.

2) Determining the fitness function

The value of each chromosome is determined by the fitness function. This function is used to examine the solutions generated in the initial population. In this paper, the fitness function is equal to accuracy, F-measure, sensitivity, specificity, PPV, and negative predictive value (NPV) (28) as determined in equations (11-16):

$$Specificity = TN/TN + FP \tag{11}$$

$$Accuracy = TP + TN/TP + TN + FP + FN \tag{12}$$

$$\text{Positive Predictive Value} = TP/TP + FP \tag{13}$$

$$Sensitivity = TP/TP + FN \tag{14}$$

$$F - measure = 2 * \frac{precision * Sensitivity}{precision + Sensitivity} \tag{15}$$

$$\text{Negative Predictive Value} = TN/TN + FN \tag{16}$$

Based on the equations (11-16), the elements of the false positive (FP), false negative (FN), true positive (TP), and true negative (TN) are described as follows:

- FP: The number of samples predicted to be positive is negative.
- FN: The number of samples predicted to be negative is positive.
- TP: The number of samples predicted to be positive is positive.
- TN: The number of samples predicted to be negative is negative.

The performance of the GSVMA method is evaluated using the mentioned fitness functions. Therefore, we tested the generated GSVMA model based on the fitness functions.

3) Selection scheme

In this stage, based on the fitness criterion, a member of a generation is selected so that members with more compatibility have more probability of making the next generation. The selection schemes such as uniform, roulette wheel (RW), stochastic universal sampling, Boltzmann, rank, tournament, and nondominated sorting exist in the genetic algorithm (6). In this paper, the RW is applied as a select scheme. Based on the scheme, the member with a higher fitness value has more probability of being selected. This scheme is one of the weighted random selection schemes. The probability of choosing each member is obtained according to the equation (17).

$$P_i = \frac{f_i}{\sum_{k=1}^{N} f_k} \tag{17}$$

In (17), P_i indicates the probability of choosing the member, "i" f_i indicates member fitness, "i" and N, the number of members in the initial population. In this paper, the initial $P = 0.5$. The higher value of P_i represents that the probability of choosing the chromosome is high. In other words, this chromosome has a better chance to produce the next generation.

4) The operation of crossover

After the parent chromosomes are selected by the RW, they must be merged to generate two new children for both parents by the crossover operator. In general, there are three crossover types such as one-point, uniform, and shuffle (6, 41). Using the one-point crossover, a point on two-parent chromosomes is selected and divided into two parts so that one part of the first parent is replaced by one part of the second parent. The other type of crossover is a shuffle that two points on two-parent chromosomes are randomly selected and divided into three parts. Then, one part of the first parent is replaced by one part of the second parent, and the children in three parts are a combination of two parents. The third type of crossover is uniform. Using the uniform crossover, all the chromosome points are selected as the merge points. First, a random number between zero and one for each part of the chromosome is generated. If the generated value is less than a constant value, the genes are moved. In this paper, the shuffle has been selected as the crossover type. Also, crossover "p" is given 0.75.

5) Mutation action

After crossover, the mutation action is one of the essential actions to create a new generation. The mutation action is used to modify a member of the current generation to produce a new member. Due to the mutation action by random, the possibility of reaching a better member and

escaping the local optimization can be efficient. In this paper, the probability value of 1.0 has been considered. This value demonstrates that mutation action is performed to create a new generation.

When the mutation action is performed, the cycle of the genetic algorithm is terminated due to convergence conditions. The convergence condition is determined based on the number of generations (number of generations = 10). Again, construction action of the new generation should be repeated (6, 41).

The parameters setting of the used genetic optimization method is given in **Table 5**.

The pseudocode of the GSVMA method is presented below.

Algorithm 4: The used GSVMA method for CAD diagnosis.

Input: Extract the Z-Alizadeh Sani dataset include 303 records and 55 features.

Output: The diagnosed (CAD/normal) class of each test record and determined the 31 features as the most important features

1: **Begin**
2: Data preprocessing: Transforming nominal records to numerical records and normalizing between zero and one
3: Divide the data using a 10-fold crossvalidation technique
4: Generating a new population of members randomly (the population size= 50 and the maximum number of generations=10) based on **Table 5**
5: **For** i=1 to 55(chromosome size)
6: set a random of (0,1) value to gene(i) of the chromosome
7: **End For**
8: Determining the fitness function based on evaluation criteria
9: select a member of a generation (the selection scheme: uniform, roulette wheel) based on formula (16)
10: Performing crossover (crossover type: shuffle)
11: Performing mutation action (Probability of mutation=1.0)
12: **While** (terminating condition is not happened by 10-fold crossvalidation or number of generations) do
13: Execute the most important features using Genetic optimization algorithm
14: Feeding feathers SVM with ANOVA model based on algorithm 3
15: Employ SVMA classify for testing records
16: **End while**
17: **Return** obtaining the evaluation criteria and selecting the best model with 31 features
18: **End**

Based on algorithm 4, the genetic optimization method has been applied for feature selection, and the SVM with the ANOVA model has been used for classifying the dataset.

TABLE 5 | The parameters setting of the genetic optimization algorithm.

Parameters	Setting
Population size	50
Maximum number of generations	10
Normalize weights	✓
Plot generations	10
Draw dominated points	✓
Initial probability	0.5
Size of each chromosome = total of features	55
Probability of mutation	1.0
Crossover probability	0.75
Crossover type	Shuffle
Maximum fitness	Infinity
Fitness function	Accuracy, PPV, F-measure, sensitivity, specificity, and NPV

TABLE 6 | Confusion matrix for diagnosis of CAD.

The predicted class	The actual class	
	CAD	Normal
Positive	True positive	False positive
Negative	False negative	True negative

RESULTS

In this section, the evaluation results for the classification methods are obtained. These methods are the SVM with ANOVA, LSVM, LIBSVM with RBF, and GSVMA. Based on **Table 6**, accuracy (ACC), PPV, F-measure, sensitivity, specificity, NPV, and AUC had been achieved by the confusion matrix. In this paper, we have used RapidMiner Studio version 9.9 to implement the methods in the CAD diagnosis and classification process.

The evaluation criteria of the methods were obtained based on equations (11-16) (28).

By comparing the performance of the methods, the ACC rates of the SVM with ANOVA, LSVM, and LIBSVM with RBF were achieved 85.13, 86.11, and 84.78%, respectively, whereas the ACC rate of the GSVMA method is 89.45% based on the 10-FCV technique. According to the other criteria, the GSVMA method had the highest PPV, F-measure, sensitivity, and specificity. Moreover, another crucial criterion used to determine the classification methods is the AUC criterion. The AUC indicates the measure of the area under the Receiver Operating Characteristic (ROC). In other words, the AUC transforms the ROC curve into a numeric demonstration of performance for classification models. The AUC of the GSVMA method is obtained 100%. The results of the evaluation criteria for methods through the 10-FCV are indicated in **Table 7**. Also, the ROC curve was illustrated for the GSVMA method in **Figure 3**.

Based on **Figure 3**, the ROC diagram for the GSVMA method demonstrates that the AUC value = 100%.

TABLE 7 | The comparison of the methods based on the Z-Alizadeh Sani dataset in this study.

Methods	ACC(%)	PPV(%)	F-measure (%)	Sensitivity (%)	Specificity(%)	NPV(%)	AUC(%)
SVM with ANOVA	85.13	80.24	72.01	69.19	91.62	68.97	89
Linear SVM	86.11	77.21	75.55	74.75	90.71	74.71	92.4
LIBSVM with RBF	84.78	76.24	72.38	70.03	90.74	70.11	82.1
GSVMA	**89.45**	**100**	**80.49**	**81.22**	**100**	**92.9**	**100**

Bold the best values of the proposed method (GSVMA) to show our method is the best.

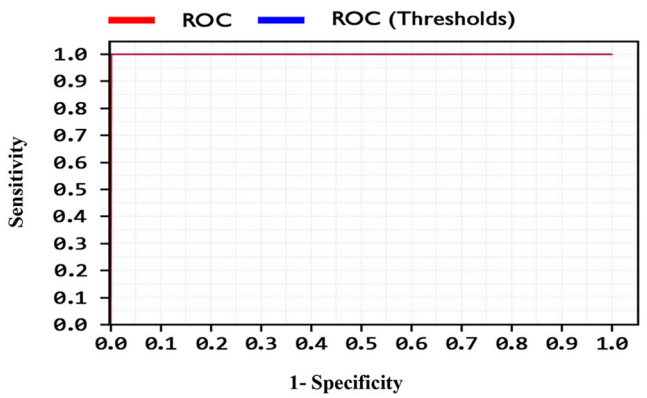

FIGURE 3 | ROC curve for GSVMA method.

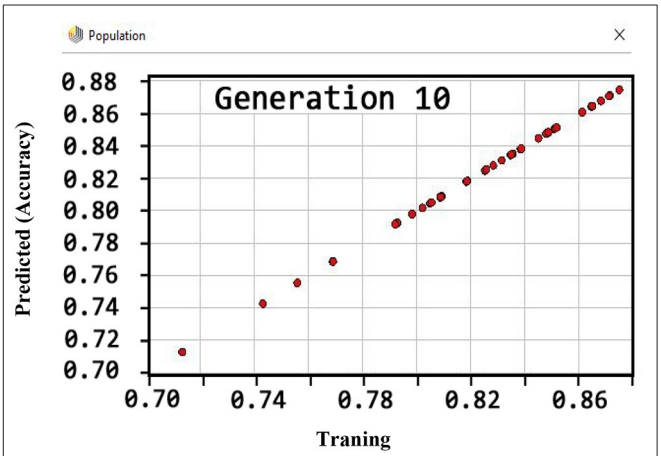

FIGURE 4 | ACC diagram for GSVMA method for generation 10.

Also, the criteria of the ACC, F-measure, PPV, sensitivity, specificity, and NPV are illustrated in **Figures 4–9**, respectively. Moreover, in the 10-FCV technique, the GSVMA method was trained for 10 generations on the Z-Alizadeh Sani dataset. To find the optimal response of the evaluation criteria (fitness function = criteria), a set of initial responses are generated in each generation so that the set of responses converges toward the optimal response. In this study, convergence is related to the tenth generation. Therefore, the mentioned criteria were obtained based on the best generation (generation 10).

According to **Figure 4**, the ACC rate has obtained more than 88% (89.45%) through the GSVMA method for generation 10.

Based on **Figure 5**, the performance of the GSVMA method achieved F-measure of 80.49% for generation 10.

Figure 6 shows that the PPV has reached a maximum of 100% for the tenth generation.

By observing **Figure 7**, it can be inferred that the sensitivity has been more than 80% (81.22) using the GSVMA method for the tenth generation.

Regarding the specificity criterion, **Figure 8** shows the maximum value of 100% using the GSVMA method for the tenth generation.

Another crucial evaluation criterion is the NPV in clinical practice. The NPV is the probability that subjects with a negative test rightly have healthy. The NPV was obtained on average 92.9% as shown in **Figure 9**. Similarly, three methods such as LIBSVM with RBF, LSVM, and SVM with ANOVA have been applied to the Z-Alizadeh Sani dataset. We presented the results

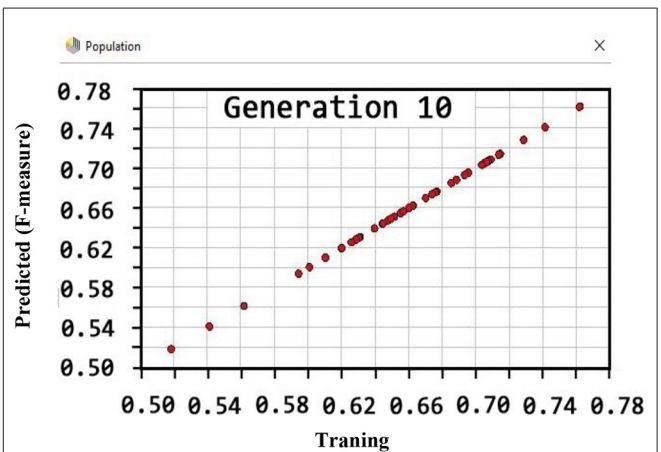

FIGURE 5 | F-measure diagram for GSVMA method for generation 10.

of these methods in **Table 7**. Based on **Table 7**, the accuracy of the LSVM, SVM with ANOVA, and LIBSVM with RBF is 86.11, 85.13, and 84.78%, respectively. The PPV for the SVM with ANOVA, LSVM, and LIBSVM with RBF models is obtained as 80.24, 77.21, and 76.24, respectively. In terms of the F-measure, sensitivity, specificity, and NPV criteria, the LSVM method has a better performance compared to the other two methods.

In addition, one of the important criteria of the evaluation of methods is the AUC criterion. The AUC of methods was

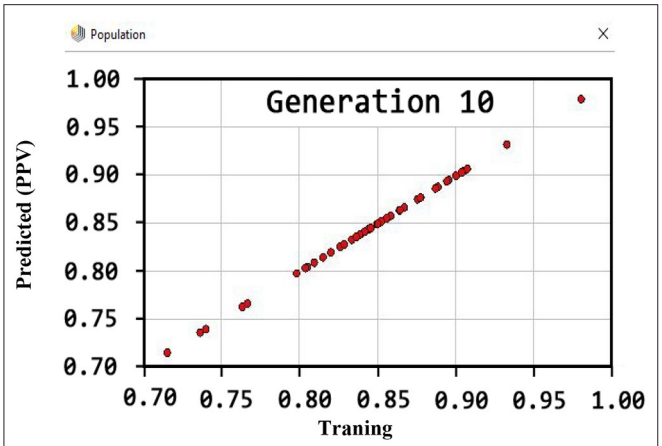

FIGURE 6 | PPV diagram for GSVNA method for generation 10.

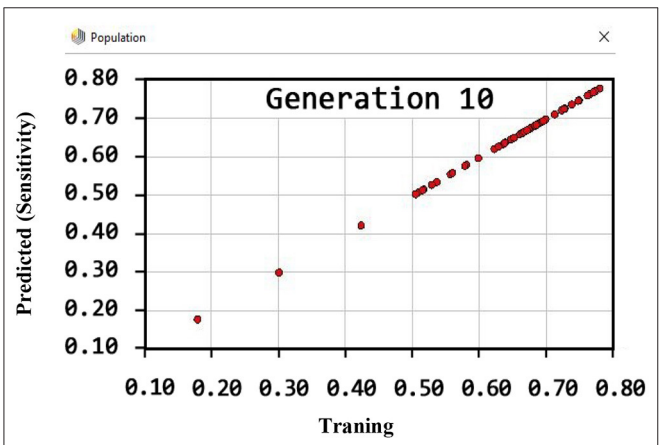

FIGURE 7 | Sensitivity diagram for GSVMA method for generation 10.

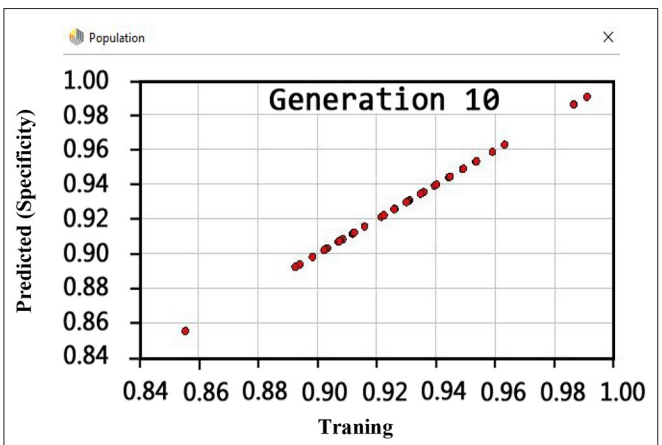

FIGURE 8 | Specificity diagram for GSVNA method for generation 10.

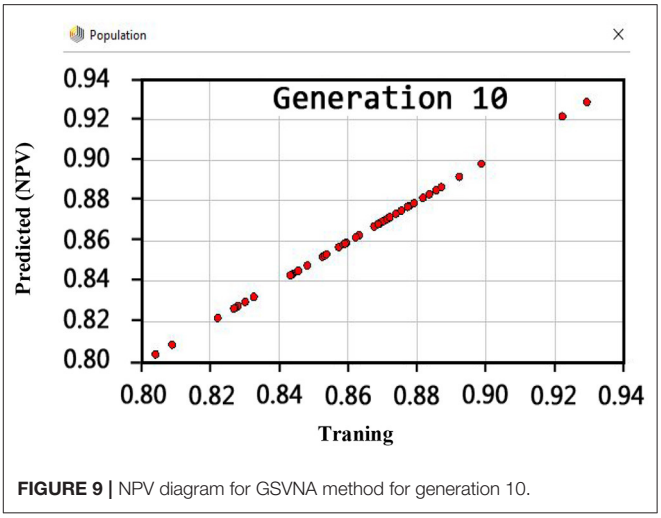

FIGURE 9 | NPV diagram for GSVNA method for generation 10.

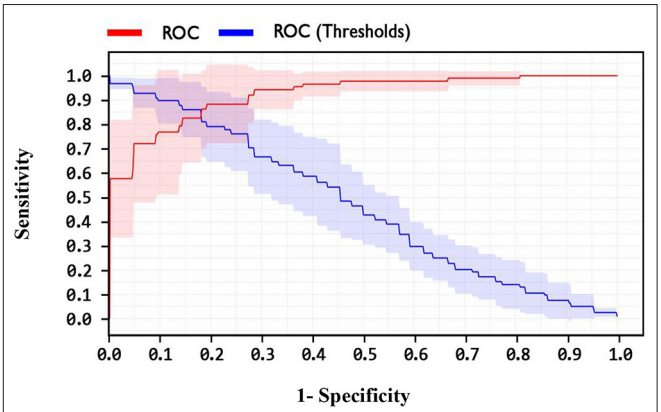

FIGURE 10 | ROC curve for LSVM method.

achieved as 92.4, 89, and 82.1% for LSVM, SVM with ANOVA, and LIBSVM with RBF methods, respectively. The ROC curve for the LSVM, SVM with ANOVA, and LIBSVM with RBF methods is shown in **Figures 10–12**, respectively.

By observing the **Figures 10–12**, it can be concluded that the LSVM method has better performance with an AUC of 92.4% than SVM with ANOVA and LIBSVM with RBF methods.

Overall, the proposed GSVMA method has the best performance compared to the other methods in terms of accuracy, F-measure, PPV, NPV, sensitivity, specificity, and AUC. **Figure 13** shows the comparison between the methods based on the seven criteria.

Moreover, according to the proposed method, out of 35 features, 31 features were selected using the genetic optimization algorithm. The crucial features include sex, CRF, CVA, airway disease, thyroid disease, CHF, systolic murmur, diastolic murmur, low TH ang, LVH, poor R progression, VHD, age, HTN, ex-smoker, FH, PR, typical chest pain, function class, Q wave, St elevation, T inversion, FBS, TG, LDL, ESR, lymph, Neut, PLT, EF-TTE, and region RWMA.

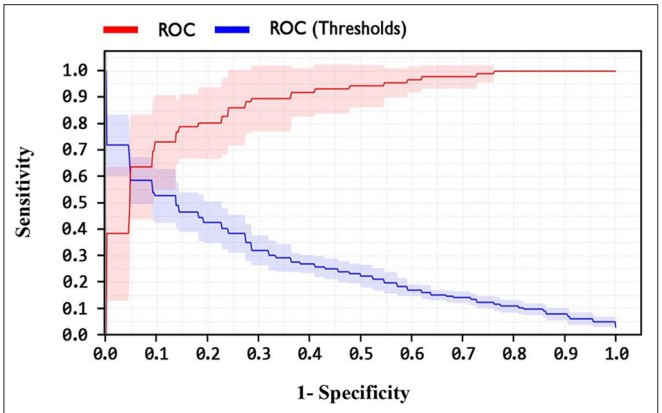

FIGURE 11 | ROC curve for SVM with ANOVA method.

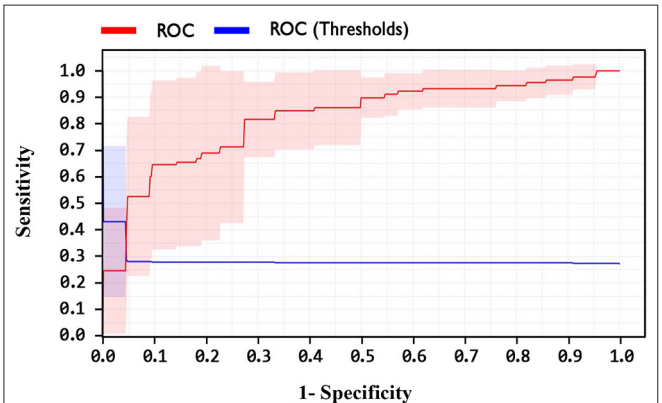

FIGURE 12 | ROC curve for LIBSVM with RBF method.

DISCUSSION

In this paper, we demonstrate the accuracy of 89.45% using the proposed GSVMA method for CAD diagnosis on the Z-Alizadeh Sani dataset by identifying 31 features. Finally, we compared our proposed method with the work of other researchers based on the Z-Alizadeh Sani dataset, as demonstrated in **Table 8**.

Based on **Table 8**, in the Qin et al. study (8), several feature selection methods had been implemented on the Z-Alizadeh Sani CHD dataset. The various assessment criteria to evaluate features coupled with a heuristic search strategy and seven classification methods are utilized. They further proposed an ensemble algorithm based on multiple feature selection (EA-MFS). The proposed EA-MFS method had better results with a reported accuracy of 93.70 and 95.53% F1-measure. In Cüvitoglu and Işik's study (10), an ensemble learner based on the combination of naïve Bayes, random forest, SVM, artificial neural networks (ANNs), and k-nearest neighbor algorithm is developed to diagnose CAD. Also, each of these methods is applied to the dataset separately. The authors performed a *t*-test for feature selection and reduced the feature space from 54 to 25. Moreover, they implemented PCA to reduce dimensionality further. Between the six methods, the best performance of the ANN achieved an AUC of 93%. Kiliç and Keleş (12) attempted to select the most convenient features to achieve better performance. They have used the artificial bee colony method on the Z-Alizadeh Sani dataset. The results showed that 16 of 56 features are more meaningful to predict CAD. They reported that a higher accuracy was achieved employing the selected features. Abdar et al. (14) proposed a model combining several traditional ML methods using ensemble learning techniques titled nested ensemble nu-support vector classification (NE-nu-SVC) to predict CAD. Also, they employed a feature selection routine based on a genetic algorithm and a filtering method to adjust data. The reported that accuracy of the NE-nu-SVC method is 94.66% for Z-Alizadeh Sani and 98.60% for Cleveland CAD datasets. In (16), Abdar et al. introduced the N2Genetic optimizer, which is a genetic-based algorithm and particle swarm optimization. Using the N2Genetic-nuSVM proposed, they achieved an accuracy of 93.08% and F1-score of 91.51% in the Z-Alizadeh Sani dataset for predicting CAD. In another study, Kolukisa et al. (17) examined two feature selection approaches to extract the most convenient set of features for the Z-Alizadeh Sani dataset. First, the features were selected based on medical doctor recommendations. According to clinically significant findings and Framingham heart study risk factors labeled features. The second method of feature selection was reported to improve the performance of ML algorithms. A combination of three ensemble learners, random forest, gradient boosting machine, and extreme gradient boosting, form a classifier to predict coronary heart disease in the work of Tama et al. (19). Moreover, a particle swarm optimization-based feature selection model takes the most valuable data features to feed the classifier efficiently. The functionality of the proposed system is verified by having Z-Alizadeh Sani, Statlog, Cleveland, and Hungarian datasets as the input data. The authors claim that the performance of their proposed model outperforms the present methods established on traditional classifier ensembles. They report a 98.13% accuracy, 96.60% F1-score, and 0.98 AUC to classify the Z-Alizadeh Sani dataset. The effectiveness of ANN and adaptive boosting algorithms to predict CAD was tested in the work of Terrada et al. (20). Data for this study were collected from Z-Alizadeh Sani, Hungarian, UCI repository, and Cleveland datasets, and 17 features were manually selected based on the atherosclerosis risk factors. The results indicated that ANNs show more promising performance over the adaptive boosting method. In (22), a hybrid algorithm based on emotional neural networks (EmNNs) and particle swarm optimization (PSO) is proposed by Shahid and Singh for CAD diagnosis. In addition, they implemented four unique feature selection techniques on the Z-Alizadeh Sani dataset to boost the functionality of the proposed model. Generally, their method has a better performance than the PSO-ANFIS model. The F1-score, accuracy, sensitivity, specificity, and PPV of the model are 92.12, 88.34, 91.85, 78.98, and 92.37%, respectively. According to Ghiasi et al. (23), only 40 independent parameters of the Z-Alizadeh Sani dataset affect the diagnosis of CAD. The authors apply the classification and regression tree (CART) method for this purpose. They further developed three additional CARD models utilizing 5,

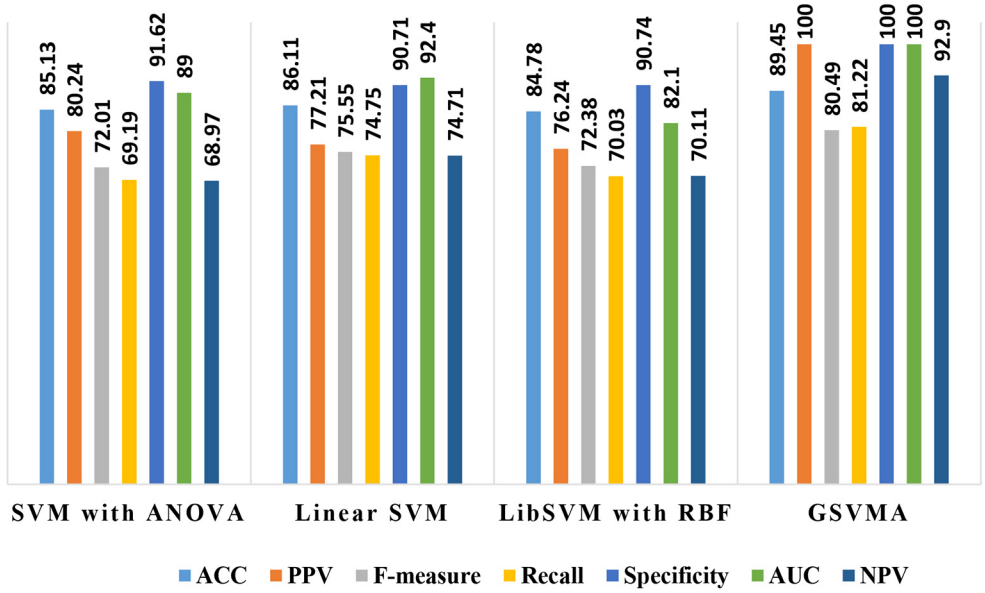

FIGURE 13 | A comparison between the performance of methods based on the seven criteria.

TABLE 8 | Comparison between the proposed GSVMA method and the work of other researchers based on the original Z-Alizadeh Sani dataset.

References	Techniques	No. of crossvalidation	No. of features	ACC (%)	AUC (%)
Qin et al. (8)	Ensemble algorithm-multiple feature selection, (EA-MFS)	10-FCV	34	93.70 + −0.48%	NC
Cüvitoglu et al. (10)	Artificial neural network	10-FCV	25	87.85	93
Kiliç et al. (12)	Artificial Bee colony	-	16	89.4	NC
Abdar et al. (14)	NE-nu-SVC	10-FCV	16	94.66	NC
Abdar et al. (16)	N2Genetic-nuSVM	10-FCV	29	93.08	NC
Kolukisa et al. (17)	Ensemble classifier with Fisher linear discriminant analysis	5, 10, 20-FCV	55	92.07	95.3
Tama et al. (19)	Two-tier ensemble particle swarm optimization(PSO)-based feature selection	10-FCV	27	98.13	98.7
Terrada et al. (20)	(ANN)	-	17	94	94
Shahid et al. (22)	Hybrid PSO-EmNN	10-FCV	22	88.34	NC
Ghiasi et al. (23)	CART	10-FCV	5	92.41	NC
Dahal et al. (24)	SVM	10-FCV	15	89.47	88.68
Velusamy et al. (25)	Weighted-average Voting ensemble (WAVEn)	10-FCV	5	98.97	NC
Hassannataj et al. (5)	Random trees	10-FCV	40	91.47	96.7
The Proposed Method	GSVMA	10-FCV	31	89.45	100

NC, Not considered.

10, and 18 selected features. For the developed model with five features, the reported accuracy is 92.41%. Also, a 77.01% true negative rate and 98.61% true positive value are reported for the model.

Dahal et al. (24) performed logistic regression, random forest, SVM, and K-nearest neighbors algorithms for CAD detection on the Z-Alizadeh Sani dataset to determine the most efficient technique. The results indicate that SVM has a better performance over other tested methods with 89.47% of accuracy. In (25), a study of CAD diagnosis was conducted using the weighted-average voting ensemble (WAVEn) method. Using this method, an accuracy of 98.97% was obtained on five features.

Hassannataj et al. (5) used the random trees (RTs) on the 303 samples with 55 features. They have compared the RTs model with SVM, the C5.0 decision tree, and the CHAID decision tree. As a result, using the RTs model, 40 features were ranked with an accuracy of 91.47%, which RTs model has the best performance compared to the other models.

The results demonstrate the robustness of our proposed method in the diagnosis and prediction of CAD. Applying the GSVMA method, an accuracy of 89.45% was obtained by identifying 31 features. To the best of our knowledge, using this method, the AUC was achieved 100% on the original Z-Alizadeh Sani for the first time. Also, no previous works in the literature have investigated the NPV in CAD diagnosis, so that this criterion is essential in clinical practice. Despite these advances in the diagnosis of heart disease, there are limitations to the diagnosis process that we list below.

- Need a larger dataset to apply to the proposed GSVMA method.
- Lack of access to the real laboratory environment to record people's data in electronic profiles.
- Requiring the interaction of physicians and researchers to evaluate the results obtained properly.

CONCLUSIONS

In this study, a hybrid method, namely GSVMA, is proposed to help the effective diagnosis and prediction of CAD by selecting essential features. This method was evaluated on the Z-Alizadeh Sani dataset. The GSVMA method consists of two main blocks. The first is the genetic optimization algorithm, in which essential features are selected by this algorithm. The second is the SVM algorithm with ANOVA kernel, which is used for classifying the input dataset. We carried out data preprocessing by converting nominal data to numerical data and performing a range transformation technique. Also, the 10-fold crossvalidation technique is used to split the dataset into two groups: 90% for training and 10% for testing. Moreover, other methods such as SVM with ANOVA, LSVM, and LIBSVM with RBF have been utilized to diagnose CAD. The proposed GSVMA method had the best performance compared to the mentioned methods regarding the accuracy of 89.45%, a PPV of 100%, a F-measure of 80.49%, a specificity of 100%, a sensitivity of 81.22%, a NPV of 92.9%, and an AUC of 100%, on 31 features among 55 features. By comparing the proposed method with related works, we found that the GSVMA method has good accuracy and AUC rates with the essential features. Besides, no previous works have studied the NPV in CAD diagnosis. In future work, if a larger dataset is available, the GSVMA method could be utilized. In addition, metaheuristic methods that include tabu search, iterated local search, simulated annealing, and variable neighborhood search can be used for feature selection. Then, each of these methods can be combined with machine learning methods.

DATA AVAILABILITY STATEMENT

The datasets presented in this study can be found in online repositories. The names of the repository/repositories and accession number(s) can be found at: https://archive.ics.uci.edu/ml/datasets/Z-Alizadeh+Sani, 20403598.

AUTHOR CONTRIBUTIONS

JH, FA, and RA designed the study. JH, FA, MN, and RA wrote the paper. JH, FA, MN, RA, and AM edited the paper. JH carried out the software on the Z-Alizadeh Sani dataset. JH, FA, RA, and IN generated all figures and tables. All authors have read and approved the final version of the paper.

FUNDING

This work was supported by Alexander von Humboldt Foundation under project AvH0019272.

REFERENCES

1. Martin-Isla C, Campello VM, Izquierdo C, Raisi-Estabragh Z, Baeßler B, Petersen SE, et al. Image-based cardiac diagnosis with machine learning: a review. *Front Cardiovasc Med.* (2020) 7:1. doi: 10.3389/fcvm.2020.00001
2. Bagula AB, Djenouri D, Karbab E. On the relevance of using interference and service differentiation routing in the internet-of-things. In: *Internet of Things, Smart Spaces, and Next Generation Networking.* Berlin; Heidelberg: Springer (2013). p. 25–35. doi: 10.1007/978-3-642-40316-3_3
3. Hampe N, Wolterink JM, Van Velzen SG, Leiner T, Išgum I. Machine learning for assessment of coronary artery disease in cardiac CT: a survey. *Front Cardiovasc Med.* (2019) 6:172. doi: 10.3389/fcvm.2019.00172
4. Lilly LS, Braunwald E. *Braunwald's Heart Disease: A Textbook of Cardiovascular Medicine.* Philadelphia, PA: Elsevier Health Sciences (2012).
5. Joloudari JH, Hassannataj Joloudari E, Saadatfar H, Ghasemigol M, Razavi SM, Mosavi A, et al. Coronary artery disease diagnosis; ranking the significant features using a random trees model. *Int J Environ Res Public Health.* (2020)731:17. doi: 10.3390/ijerph17030731
6. Arabasadi Z, Alizadehsani R, Roshanzamir M, Moosaei H, Yarifard AA. Computer aided decision making for heart disease detection using hybrid neural network-Genetic algorithm. *Comput Methods Prog Biomed.* (2017) 141:19-26.. doi: 10.1016/j.cmpb.2017.01.004
7. Alizadehsani R, Habibi J, Hosseini MJ, Mashayekhi H, Boghrati R, Ghandeharioun A, et al. A data mining approach for diagnosis of coronary artery disease. *Comput Methods Prog Biomed.* (2013) 111:52-61. doi: 10.1016/j.cmpb.2013.03.004
8. Qin C-J, Guan Q, Wang X-P. Application of ensemble algorithm integrating multiple criteria feature selection in coronary heart disease detection. *Biomed Eng Appl Basis Commun.* (2017) 29:1750043. doi: 10.4015/S1016237217500430
9. Alizadehsani R, Zangooei MH, Hosseini MJ, Habibi J, Khosravi A, Roshanzamir M, et al. Coronary artery disease detection using computational intelligence methods. *Knowled Based Syst.* (2016) 109:187-97. doi: 10.1016/j.knosys.2016.07.004
10. Cüvitoglu A, I sik Z. Classification of CAD dataset by using principal component analysis and machine learning approaches. In: *2018 5th International Conference on Electrical and Electronic Engineering (ICEEE).* Istanbul: IEEE (2018). p. 340–3. doi: 10.1109/ICEEE2.2018.8391358
11. Alizadehsani R, Hosseini MJ, Sani ZA, Ghandeharioun A, Boghrati R. Diagnosis of coronary artery disease using cost-sensitive algorithms. In: *2012*

IEEE 12th International Conference on Data Mining Workshops. Brussels: IEEE (2012). p. 9–16. doi: 10.1109/ICDMW.2012.29
12. Kiliç Ü, Keleş MK. Feature selection with artificial bee colony algorithm on Z-Alizadeh Sani dataset. In: *2018 Innovations in Intelligent Systems and Applications Conference (ASYU)*. Adana: IEEE (2018). p. 1–3. doi: 10.1109/ASYU.2018.8554004
13. Alizadehsani R, Hosseini MJ, Khosravi A, Khozeimeh F, Roshanzamir M, Sarrafzadegan N, et al. Non-invasive detection of coronary artery disease in high-risk patients based on the stenosis prediction of separate coronary arteries. *Comput Methods Prog Biomed.* (2018) 162:119-27. doi: 10.1016/j.cmpb.2018.05.009
14. Abdar M, Acharya UR, Sarrafzadegan N, Makarenkov V. NE-nu-SVC: a new nested ensemble clinical decision support system for effective diagnosis of coronary artery disease. *IEEE Access.* (2019) 7:167605-20. doi: 10.1109/ACCESS.2019.2953920
15. Alizadehsani R, Habibi J, Sani ZA, Mashayekhi H, Boghrati R, Ghandeharioun A, et al. Diagnosing coronary artery disease via data mining algorithms by considering laboratory and echocardiography features. *Res Cardiovasc Med.* (2013) 2:133. doi: 10.5812/cardiovascmed.10888
16. Abdar M, Ksiazek W, Acharya UR, Tan R-S, Makarenkov V, Pławiak P. A new machine learning technique for an accurate diagnosis of coronary artery disease. *Comput Methods Prog Biomed.* (2019) 179:104992. doi: 10.1016/j.cmpb.2019.104992
17. Kolukisa B, Hacilar H, Kuş M, Bakir-Güngör B, Aral A, Güngör VÇ. Diagnosis of coronary heart disease via classification algorithms and a new feature selection methodology. *Int J Data Mining Sci.* (2019) 1:8-15.
18. Nasarian E, Abdar M, Fahami MA, Alizadehsani R, Hussain S, Basiri ME, et al. Association between work-related features and coronary artery disease: A heterogeneous hybrid feature selection integrated with balancing approach. *Pattern Recogn Lett.* (2020) 133:33-40. doi: 10.1016/j.patrec.2020.02.010
19. Tama BA, Im S, Lee S. Improving an intelligent detection system for coronary heart disease using a two-tier classifier ensemble. *BioMed Research International.* (2020) 2020:9816142. doi: 10.1155/2020/9816142
20. Terrada O, Cherradi B, Hamida S, Raihani A, Moujahid H, Bouattane O. Prediction of patients with heart disease using artificial neural network and adaptive boosting techniques. In: *2020 3rd International Conference on Advanced Communication Technologies and Networking (CommNet)*. Marrakech: IEEE (2020). p. 1–6. doi: 10.1109/CommNet49926.2020.9199620
21. Shahid AH, Singh MP, Roy B, Aadarsh A. Coronary artery disease diagnosis using feature selection based hybrid extreme learning machine. In: *2020 3rd International Conference on Information and Computer Technologies (ICICT)*. San Jose, CA: IEEE (2020). p. 341–6. doi: 10.1109/ICICT50521.2020.00060
22. Shahid AH, Singh MP. A novel approach for coronary artery disease diagnosis using hybrid particle swarm optimization based emotional neural network. *Biocybernet Biomed Eng.* (2020) 40:1568-85. doi: 10.1016/j.bbe.2020.09.005
23. Ghiasi MM, Zendehboudi S, Mohsenipour AA. Decision tree-based diagnosis of coronary artery disease: CART model. *Comput Methods Prog Biomed.* (2020) 192:105400. doi: 10.1016/j.cmpb.2020.105400
24. Dahal KR, Gautam Y. Argumentative comparative analysis of machine learning on coronary artery disease. *Open J Stat.* (2020) 10:694-705. doi: 10.4236/ojs.2020.104043
25. Velusamy D, Ramasamy K. Ensemble of heterogeneous classifiers for diagnosis and prediction of coronary artery disease with reduced feature subset. *Comput Methods Prog Biomed.* (2021) 198:105770. doi: 10.1016/j.cmpb.2020.105770
26. Pławiak P. Novel genetic ensembles of classifiers applied to myocardium dysfunction recognition based on ECG signals. *Swarm Evolution Comput.* (2018) 39:192-208. doi: 10.1016/j.swevo.2017.10.002
27. Alizadehsani R, Roshanzamir M, Abdar M, Beykikhoshk A, Khosravi A, Panahiazar M, et al. A database for using machine learning and data mining techniques for coronary artery disease diagnosis. *Sci Data.* (2019) 6:227. doi: 10.1038/s41597-019-0206-3
28. Joloudari JH, Saadatfar H, Dehzangi A, Shamshirband S. Computer-aided decision-making for predicting liver disease using PSO-based optimized SVM with feature selection. *Informat Med Unlocked.* (2019) 17:100255. doi: 10.1016/j.imu.2019.100255
29. Joloudari JH, Haderbadi M, Mashmool A, GhasemiGol M, Band SS, Mosavi A. Early detection of the advanced persistent threat attack using performance analysis of deep learning. *IEEE Access.* (2020) 8:186125-37. doi: 10.1109/ACCESS.2020.3029202
30. Boser BE, Guyon IM, Vapnik VN, editors. A training algorithm for optimal margin classifiers. In: *Proceedings of the Fifth Annual Workshop on Computational Learning Theory*. Pittsburgh Pennsylvania. ACM (1992). p. 144–52. doi: 10.1145/130385.130401
31. Cortes C, Vapnik V. Support-vector networks. *Machine Learn.* (1995) 20:273-97. doi: 10.1007/BF00994018
32. Cristianini N, Shawe-Taylor J. *An Introduction to Support Vector Machines and Other Kernel-Based Learning Methods.* Cambridge University Press (2000).
33. Chang Y-W, Hsieh C-J, Chang K-W, Ringgaard M, Lin C-J. Training and testing low-degree polynomial data mappings via linear SVM. *J Machine Learn Res.* (2010) 11:1471–90. doi: 10.5555/1756006.1859899
34. Shamshirband S, Joloudari JH, GhasemiGol M, Saadatfar H, Mosavi A, Nabipour N. FCS-MBFLEACH: designing an energy-aware fault detection system for mobile wireless sensor networks. *Mathematics.* (2020) 8:28. doi: 10.3390/math8010028
35. Sharifrazi D, Alizadehsani R, Roshanzamir M, Joloudari JH, Shoeibi A, Jafari M, et al. Fusion of convolution neural network, support vector machine and Sobel filter for accurate detection of COVID-19 patients using X-ray images. *Biomed Signal Process Control.* (2021) 68:102622. doi: 10.1016/j.bspc.2021.102622
36. Chavhan YD, Yelure BS, Tayade KN. Speech emotion recognition using RBF kernel of LIBSVM. In: *2015 2nd International Conference on Electronics and Communication Systems (ICECS)*. Coimbatore: IEEE (2015). p. 1132–35. doi: 10.1109/ECS.2015.7124760
37. Souza CR. Kernel functions for machine learning applications. *Creative Commons Attribut Noncommercial Share Alike.* (2010) 3:29.
38. Wankhade SB, Tijare P, Chavhan Y. Speech emotion recognition system using SVM AND LIBSVM. *Int J Comput Sci Applications.* (2011) 4.
39. Chang C-C, Lin C-J. LIBSVM: a library for support vector machines. *ACM Transac Intel Syst Technol.* (2011) 2:1-27. doi: 10.1145/1961189.1961199
40. Hofmann T, Schölkopf B, Smola AJ. Kernel methods in machine learning. *Ann Stat.* (2008) 36:1171-220. doi: 10.1214/009053607000000677
41. Kaya Y, Uyar M. A novel crossover operator for genetic algorithms: ring crossover. *arXiv [Preprint].* (2011). arXiv: 11050355. Available online at: https://arxiv.org/abs/1105.0355 (accessed January 11, 2021).

Conflict of Interest: The authors declare that the research was conducted in the absence of any commercial or financial relationships that could be construed as a potential conflict of interest.

frontiers in Cardiovascular Medicine

ORIGINAL RESEARCH
published: 17 February 2022
doi: 10.3389/fcvm.2022.752964

Association of Residential Proximity to the Coast With Incident Myocardial Infarction: A Prospective Cohort Study

Zhuang Xiao-dong[1,2†], *Zhang Shao-zhao*[1,2†], *Hu Xun*[1,2†], *Liao Xin-xue*[1,2*] and *Liao Li-zhen*[3,4*]

[1] Department of Cardiology, The First Affiliated Hospital of Sun Yat-sen University, Guangzhou, China, [2] NHC Key Laboratory of Assisted Circulation, Sun Yat-sen University, Guangzhou, China, [3] Health Department, Guangdong Provincial Key Laboratory of Pharmaceutical Bioactive Substances, Guangzhou Higher Education Mega Center, Guangdong Pharmaceutical University, Guangzhou, China, [4] Guangdong Engineering Research Center for Light and Health, Guangzhou Higher Education Mega Center, Guangzhou, China

OPEN ACCESS

Edited by:
Stéphane Cook,
Université de Fribourg, Switzerland

Reviewed by:
Xin Li,
Third Affiliated Hospital of Sun Yat-sen University, China
Jiezhen Qi,
Dongguan University of Technology, China

***Correspondence:**
Liao Xin-xue
liaoxinx@mail.sysu.edu.cn
Liao Li-zhen
liaolizhen2013gy@163.com

[†]These authors have contributed equally to this work

Specialty section:
This article was submitted to Coronary Artery Disease, a section of the journal Frontiers in Cardiovascular Medicine

Received: 04 August 2021
Accepted: 10 January 2022
Published: 17 February 2022

Citation:
Xiao-dong Z, Shao-zhao Z, Xun H, Xin-xue L and Li-zhen L (2022) Association of Residential Proximity to the Coast With Incident Myocardial Infarction: A Prospective Cohort Study. Front. Cardiovasc. Med. 9:752964. doi: 10.3389/fcvm.2022.752964

Background: Little is known about how the residential distance to the coast is associated with incident myocardial infarction (MI) and which mechanisms may explain the association. We aim to explore this association using data from a prospective, population-based cohort with unprecedented sample size, and broad geographical coverage.

Methods: In this study, 377,340 participants from the UK Biobank were included.

Results: It was shown that 4,059 MI occurred during a median 8.0 years follow-up. Using group (<1 km) as reference, group (20–50 km) was associated with a lower risk of MI (hazard ratio, *HR* 0.79, 95% *CI* 0.64–0.98) and a *U*-shaped relation between distance to the coast and MI was shown with the low-risk interval between 32 and 64 km ($p_{non-linear} = 0.0012$). Using participants of the intermediate region (32–64 km) as a reference, participants of the offshore region (<32 km) and inland region (>64 km) were both associated with a higher risk of incident MI (*HR* 1.12, 95% *CI* 1.04–1.21 and *HR* 1.09, 95% *CI* 1.01–1.18, respectively). *HR* for offshore region (<32 km) was larger in subgroup with low total physical activity (<24 h/week) (*HR* 1.24, 95% *CI* 1.09–1.42, $p_{interaction} = 0.043$). *HR* for inland region (>64 km) was larger in subgroup in urban area (*HR* 1.12, 95% *CI* 1.03–1.22, $p_{interaction} = 0.065$) and in subgroup of high nitrogen dioxide (NO_2) air pollution (*HR* 1.29, 95% *CI* 1.11–1.50, $p_{interaction} = 0.021$).

Conclusion: We found a *U*-shaped association between residential distance to the coast and incident MI, and the association was modified by physical activity, population density, and air pollution.

Keywords: myocardial infarction, distance to coast, cohort, UK Biobank, association

KEYPOINTS

Question

- Proximity to the coast, an essential natural outdoor environment attribute, is positively related to self-reported general and mental health.

Findings

- We found a *U*-shaped association between residential distance to the coast and incident myocardial infarction (MI). The association of offshore region with incident MI was modified by total physical activity. The association of inland region with incident MI was modified by urban/rural area or nitrogen dioxide (NO_2) air pollution.

Meaning

- The harmful effect of residential distance to coast on incident MI may vary with the distance of coastline and is regulated by various factors. Therefore, when possible, advice on the living environment and health should be personalized.

BACKGROUND

Natural outdoor environment attributes, such as green spaces (i.e., forests or parks), blue spaces (i.e., visible bodies of water), and coastal proximity, have long-term effects on behavior and health (1–3). Researchers have provided preliminary evidence that proximity to the coast, an essential natural outdoor environment attribute, is positively related to both self-reported general and mental health, and the beneficial effect of coastal proximity was mainly mediated by improving behavioral pathways (such as physical activity, sleep, and diet), alleviating stress, and avoiding environmental pollution (4–6). However, most of these studies are limited by a small sample size, weak geographical representation, insufficient adjustment for confounders, and unclear definition of exposure. Besides, most of the outcomes of previous reports were self-reported and not relating to specific diseases. Hence, little is known about how the residential distance to the coast is associated with the incidence of myocardial infarction (MI) and which mechanisms may explain the association.

To deal with these limitations, we explored the association between distance to the coast and incident MI using data from UK Biobank, a prospective, population-based cohort study with unprecedented sample size and broad geographical coverage.

METHODS

Study Population

UK Biobank is a large prospective cohort of middle-aged adults designed to support biomedical analysis focused on improving the prevention, diagnosis, and treatment of chronic disease, the methods and aim of which have been reported elsewhere (7). In brief, between April 2007 and December 2010, UK Biobank recruited 502,628 participants (5.5% response rate, most of whom were age 40–70 years) from the general population (8). Participants attended 1 of 22 assessment centers across England, Wales, and Scotland and completed a touch screen questionnaire, had physical measurements taken, and provided biological samples. All participants provided written informed consent, and the study was approved by the NHS National Research Ethics Service. This research has been conducted using the UK Biobank Resource under Application Number 56,925.

In the present study, we included participants with data of distance from participant's residence location to the coast ($n = 440{,}874$), excluded participants with previous cardiovascular diseases (CVDs) (coronary heart disease and stroke, $n = 28{,}980$) or cancer ($n = 34{,}544$) at baseline, leaving 377,340 participants remained for analysis (**Supplementary Figure S1**).

Ascertainment of Outcome

In UK Biobank, hospital admissions were identified *via* record linkage to Health Episode Statistics records for England and Wales and the Scottish Mortality Records for Scotland (8). Detailed information about recorded linkage procedures is available online. Incident MI, comprising fatal and non-fatal ST-segment elevation and non-ST-segment elevation MI, was defined as ICD 10 (international classification of diseases, 10th revision) code of I21, I21.4, and I21.9 recorded on hospital admission. At the time of analysis, the last recorded MI was on March 31, 2017, which was used as the censoring date for other participants if no outcome had been recorded, whichever occurred first.

Ascertainment of Exposures

Environmental indicators attributed to participants were based on home location grid references. Data on the natural environment were linked using CEH 2007 Land Cover Map data. Measures of residential greenspace were estimated for England residents using the 2005 Generalized Land Use Database for England. It provides data on land use distribution for 2001 Census Output Areas in England and is consistent with the previous related research (9, 10). Residential distance to the coast was defined as the participant's residence location to the coast according to the participant's address, measured in Kilometers (km). The Euclidean distance raster from the coastline was calculated for a small grid cell size, then values from the grid allocated to UKB point locations. Based on existing literature, distances to the coast were collapsed into five categories: 0–1 km, 1–5 km, 5–20 km, 20–50 km, and over 50 km (11). To obtain approximately equal sample sizes per category, we divided the data into five quintiles for the current analyzes.

Data on Potential Confounders and Effect Modifiers

Sociodemographic factors (age, gender, ethnicity, Townsend deprivation index, professional qualifications, income, employment, and month of recruitment), health-related variables (overall health rating, mental health, handgrip strength, family history of heart diseases, medication for aspirin, cholesterol, and blood pressure, prevalent diabetes, and hypertension at baseline), lifestyle factors (smoking status, drinking status, body mass index, total physical activity, sedentary lifestyle, sleep duration, and dietary intake), residential air and noise pollution (nitrogen oxides, nitrogen dioxide [NO_2], particulate matter [PM], traffic intensity, average daytime/night sound level of noise pollution),

Abbreviations: MI, myocardial infarction; NO_2, nitrogen dioxide; PM, particulate matter; HR, hazard ratios; Q1, first quintile; CVDs, cardiovascular diseases.

home area population density classified as urban or rural, and greenspace (domestic garden percentage, greenspace percentage, natural environment percentage, and water percentage) were treated as potential confounders.

Age was calculated from dates of birth and baseline assessment. Qualification, average total household income, current employment status, overall health rating, mental health status, family history of heart diseases, the medication used, and sleep pattern were recorded using an electronic questionnaire completed by participants. Smoking status and drinking status were categorized into never, former and current smoker or drinker. Area-based socioeconomic status was derived from the postal code of residence by using the Townsend deprivation score (12). Dietary information was collected *via* the Oxford WebQ; a web-based 24 recall questionnaire developed specifically for large population studies (13). Physical activity was based on self-report by using the International Physical Activity Questionnaire short form, and total physical activity was calculated as the sum of walking, moderate, and vigorous exercise measured as metabolic equivalents (MET-h/week) (14). Grip strength was accessed through the use of a hydraulic hand dynamometer while sitting (14, 15). Total time spent in sedentary behaviors was derived from the sum of self-reported time spent driving, using a computer, and watching television. Land use regression (LUR)-based estimates of NO_2, PM10, and PM2.5 for 2010 were generated as part of the European Study of Cohorts for Air Pollution Effects (ESCAPE) and link to geocoded residential addresses of UK Biobank participants (16). Noise estimates were derived from a simplified version of the Common Noise Assessment Methods in the European Union (CNOSSOS-EU) framework (17). Home area population density classified as urban or rural was derived by combining each participant's home postcode with data generated from the 2001 census from the Office of National Statistics, using the Geoconvert tool from Census Dissemination Unit. More details for each variable are available on the UK Biobank website http://www.ukbiobank.ac.uk/.

Statistical Analysis

Baseline characteristics of 377,340 participants were described as means or percentages and were compared between groups using the one-way ANOVA test, the $\chi 2$ test, and the Kruskal–Wallis test, as appropriate. We coded missing data as a missing indicator category for categorical variables, such as smoking status, and mean values for continuous variables.

The association between residential distance to coast and MI was explored using Cox proportional hazard models. The proportional hazard assumption was checked by tests based on Schoenfeld residuals. The results were reported as hazard ratios (*HRs*) together with 95% *CIs*. First, distance to the coast was treated as continuous variables, and *HRs* were calculated per 1 SD (26.7 km) difference in distance to the coast. Then we categorized the distance to coast into <1 km, 1–5 km, 5–20 km, 20–50 km, and ≥50 km groups and calculated the *HRs* for the other four groups taking the first group (<1 km) as reference. We also categorized distance to coast into quintiles (Q1–Q5) base on the sample distribution and calculated the HRs for the last four groups taking the first quintile (Q1) as reference. Models were arranged a priori to investigate the impact of incremental adjustment. Model 1 adjusted for age, gender, ethnicity, social deprivation, income, employment status, total physical activity, overall health rating, smoking, drinking status, BMI, and handgrip strength. Model 2 additionally adjusted for family history of heart diseases, medication for aspirin, cholesterol, and blood pressure, prevalent diabetes, and hypertension. Model 3 further adjusted for air pollution, noise pollution, sleep duration, dietary intake, and home area population density.

To examine the overall statistical significance and the non-linearity of the exposure, we used likelihood ratio tests. A multivariable restricted cubic spline with 3 knots was used to express the dose-response relationship. We calculated *HRs* for living in the offshore region (<32 km) and inland region (>64 km) using Cox-proportional hazard models with incremental adjustment separately, taking participants in the intermediate area (32–64 km) within the lowest risk interval as a reference, according to the result of the restricted cubic spline. We conducted subgroup analyses to assess potential modification effects by the following factors: sex, age, BMI, sedentary behavior, sleep duration, total physical activity, smoking status, drinking status, income, area-based socioeconomic status, mental health status, urban area, air pollution, noise pollution, and hypertension. A sensitivity analysis was also conducted to investigate the effect of removing MI occurring within the first 24 months of follow-up to reduce the possible impact of reverse causation. Effect modifiers were investigated by adding to the fully adjusted model an interaction term between exposure and each of these variables.

All analyses were performed with SPSS V26 (IBM) and Stata V15 (Stata Corporation, College Station, TX, USA). A two-sided value of $p < 0.05$ was considered statistically significant.

RESULTS

The baseline characteristics of the participants are summarized in **Table 1**. The mean value of residential distance to the coast for 377,340 participants was 45.7 ± 26.7 km. Briefly, participants who lived proximal to the coast (<1 km) were more likely to be white, retired, less social deprivation, less diabetes, more physically active, and exposed to less NO_2 air pollution and traffic intensity. **Supplementary Table S1** shows the characteristics of participants by quintiles (Q1–Q5) of residential distance to the coast.

During a median of 8.0 years (3.0 million person-years) of follow-up, 4,059 cases of MI occurred. **Table 2** shows the association between residential distance to the coast and incident MI. After adjusting potential confounders, no significant association with MI was observed for distance to coast as continuing variable (*HR* 0.98 per SD increase, 95% *CI* 0.95–1.02, $p = 0.321$). Using group (<1 km) as reference, group (20–50 km) was associated with a statistically significant lower risk of MI (*HR* 0.79, 95% *CI* 0.64–0.98, $p = 0.033$). When using the lowest quintile Q1 (<14.1 km) as reference, Q2 (14.1–40.2 km), and Q3 (40.2–56.4 km) were both associated with a statistically

TABLE 1 | The baseline characteristics of the participants by residential distance to the coast.

Characteristic	Total (n = 377,340)	Distance to coast, km					*P*-value
		≤1 km (n = 6,893)	1–5 km (n = 19,402)	5–20 km (n = 68,104)	20–50 km (n = 96,586)	>50 km (n = 186,355)	
Distance to coast, km	45.7 ± 26.7	0.6 ± 0.3	2.6 ± 1.1	11.6 ± 3.8	37.5 ± 8.0	68.6 ± 12.2	<0.001
Male	169,741 (45.0%)	3,072 (44.6%)	8,558 (44.1%)	30,205 (44.4%)	43,112 (44.6%)	84,794 (45.5%)	<0.001
Age, years	55.9 ± 8.1	56.7 ± 7.9	56.4 ± 8.1	55.6 ± 8.2	56.0 ± 8.1	55.9 ± 8.1	<0.001
White	352,453 (93.4%)	6,793 (98.5%)	19,083 (98.4%)	66,106 (97.1%)	87,157 (90.2%)	173,314 (93.0%)	<0.001
Education							<0.001
College or University degree	122,650 (32.5%)	2,110 (30.6%)	4,628 (23.9%)	19,548 (28.7%)	37,293 (38.6%)	59,071 (31.7%)	
A levels/AS levels	42,306 (11.2%)	799 (11.6%)	2,236 (11.5%)	7,382 (10.8%)	11,294 (11.7%)	20,595 (11.1%)	
O levels/GCSEs	80,726 (21.4%)	1,608 (23.3%)	4,834 (24.9%)	15,765 (23.1%)	18,775 (19.4%)	39,744 (21.3%)	
CSEs or other	65,306 (17.3%)	1,323 (19.2%)	4,041 (20.8%)	13,158 (19.3%)	14,943 (15.5%)	31,841 (17.1%)	
None	66,352 (17.6%)	1,053 (15.3%)	3,663 (18.9%)	12,251 (18.0%)	14,281 (14.8%)	35,104 (18.8%)	
Income, £							<0.001
< 18,000	125,367 (33.2%)	2,152 (31.2%)	7,013 (36.1%)	22,610 (33.2%)	29,810 (30.9%)	63,782 (34.2%)	
18,000–30,999	80,207 (21.3%)	1,573 (22.8%)	4,553 (23.5%)	15,351 (22.5%)	19,149 (19.8%)	39,581 (21.2%)	
31,000–51,999	85,267 (22.6%)	1,620 (23.5%)	4,549 (23.4%)	15,929 (23.4%)	21,515 (22.3%)	41,654 (22.4%)	
52,000–100,000	68,140 (18.1%)	1,305 (18.9%)	2,857 (14.7%)	11,880 (17.4%)	18,996 (19.7%)	33,102 (17.8%)	
>100,000	18,359 (4.9%)	243 (3.5%)	430 (2.2%)	2,334 (3.4%)	7,116 (7.4%)	8,236 (4.4%)	
Current employment status							<0.001
In paid employment	227,225 (60.2%)	3880 (56.3%)	11,012 (56.8%)	411.83 (60.5%)	58,411 (60.5%)	112,739 (60.5%)	
Retired	115,064 (30.5%)	2,457 (35.6%)	6,594 (34.0%)	20,703 (30.4%)	28,380 (29.4%)	56,930 (30.5%)	
Looking after home	11,055 (2.9%)	195 (2.8%)	549 (2.8%)	1,995 (2.9%)	3,053 (3.2%)	5,263 (2.8%)	
Others	23,996 (6.4%)	361 (5.2%)	1,247 (6.4%)	4,223 (6.2%)	6,742 (7.0%)	11,423 (6.1%)	
Drinking status							<0.001
Never	17,831 (4.7%)	228 (3.3%)	694 (3.6%)	2,587 (3.8%)	4,814 (5.0%)	9,508 (5.1%)	
Previous	12,506 (3.3%)	220 (3.2%)	646 (3.3%)	2,269 (3.3%)	3,311 (3.4%)	6,060 (3.3%)	
Current	347,003 (92.0%)	6,445 (93.5%)	18,062 (93.1%)	63,248 (92.9%)	88,461 (91.6%)	170,787 (91.6%)	
Smoking status							<0.001
Never	212,622 (56.3%)	3,910 (56.7%)	10,999 (56.7%)	38,124 (56.0%)	53,350 (55.2%)	106,239 (57.0%)	
Previous	125,960 (33.4%)	2,367 (34.3%)	6,456 (33.3%)	22,972 (33.7%)	32.860 (34.0%)	61,305 (32.9%)	
Current	38,758 (10.3%)	616 (8.9%)	1,947 (10.0%)	7,008 (10.3%)	10,376 (10.7%)	18,811 (10.1%)	
BMI, kg/m^2	27.3 ± 4.7	27.4 ± 4.7	27.6 ± 4.7	27.4 ± 4.8	27.1 ± 4.7	27.3 ± 4.7	<0.001
Waist-hip ratio	0.87 ± 0.09	0.87 ± 0.09	0.87 ± 0.09	0.87 ± 0.09	0.87 ± 0.09	0.87 ± 0.09	<0.001
Total physical activity, hours/week	44.6 ± 40.7	45.6 ± 40.9	47.1 ± 43.1	45.4 ± 41.8	43.5 ± 40.7	44.5 ± 40.7	<0.001
Sedentary behavior, hours/day	4.5 ± 2.6	4.6 ± 2.5	4.8 ± 2.5	4.6 ± 2.6	4.5 ± 2.6	4.5 ± 2.5	<0.001
Home area							<0.001
Urban	323,552 (85.7%)	6,122 (88.8%)	17,039 (87.8%)	58,997 (86.6%)	84,105 (87.1%)	157,289 (84.4%)	
Rural	53,788 (14.3%)	771 (11.2%)	2,363 (12.2%)	9,107 (13.4%)	12,481 (12.9%)	29,066 (15.6%)	
Handgrip strength, Kg	29.6 ± 11.3	29.1 ± 11.1	29.1 ± 11.3	29.3 ± 11.3	29.7 ± 11.1	29.8 ± 11.3	<0.001
Townsend deprivation index	−1.3 ± 3.0	−1.7 ± 2.6	−1.5 ± 2.9	−1.5 ± 3.0	−0.6 ± 3.4	−1.6 ± 2.8	<0.001
Mental health	124,765 (33.1%)	2,372 (34.4%)	6,526 (33.6%)	23,130 (34.0%)	31,085 (32.2%)	61,652 (33.1%)	<0.001
Overall health rating							<0.001
Excellent	67,413 (17.9%)	1,210 (17.6%)	3,251 (16.8%)	12,011 (17.6%)	17,716 (18.3%)	33,225 (17.8%)	
Good	224,017 (59.4%)	4,210 (61.1%)	11,448 (59.0%)	40,310 (59.0%)	57,145 (59.2%)	110,904 (59.5%)	
Fair	73,088 (19.4%)	1,273 (18.5%)	3,967 (20.4%)	13,485 (19.8%)	18,462 (19.1%)	35,901 (19.3%)	
Poor	12,822 (3.4%)	200 (2.9%)	736 (3.8%)	2,298 (3.4%)	3,263 (3.4%)	6,325 (3.4%)	
Family history of heart diseases	144,592 (38.3%)	2,775 (40.3%)	7,698 (39.7%)	26,665 (39.2%)	36,132 (37.4%)	71,322 (38.3%)	<0.001
Hypertension	89,704 (23.8%)	1,614 (23.4%)	4,861 (25.1%)	16,121 (23.7%)	22,747 (23.6%)	44,361 (23.8%)	<0.001
Diabetes	13.626 (3.6%)	217 (3.1%)	632 (3.3%)	2,079 (3.1%)	3,674 (3.8%)	7,024 (3.8%)	<0.001

(Continued)

TABLE 1 | Continued

Characteristic	Total (n = 377,340)	Distance to coast, km					*P*-value
		≤1 km (n = 6,893)	1–5 km (n = 19,402)	5–20 km (n = 68,104)	20–50 km (n = 96,586)	>50 km (n = 186,355)	
Aspirin	36,598 (9.7%)	692 (10.0%)	1,908 (9.8%)	6,431 (9.4%)	9,426 (9.8%)	18,141 (9.7%)	0.132
Anti-hypertension medicine	20,667 (5.5%)	385 (5.6%)	1,236 (6,4%)	3,743 (5.5%)	5,225 (5.4%)	10,078 (5.4%)	<0.001
Lipid-lowering medicine	21,138 (5.6%)	386 (5.6%)	1,224 (6.3%)	3.662 (5.4%)	5,850 (6.1%)	10,016 (5.4%)	<0.001
Nitrogen dioxide air pollution, microg/m^3	26.7 ± 7.6	24.4 ± 6.0	26.0 ± 7.0	27.4 ± 7.3	28.7 ± 8.9	25.6 ± 6.8	<0.001
Nitrogen oxides, air pollution, micro/m^3	44.0 ± 15.5	43.6 ± 13.8	44.7 ± 15.5	45.5 ± 14.8	47.3 ± 18.2	41.7 ± 13.8	<0.001
PM10, microg/m^3	16.2 ± 1.9	15.9 ± 1.9	16.1 ± 1.7	16.3 ± 1.8	16.5 ± 2.0	16.1 ± 1.8	<0.001
PM2.5, microg/m^3	10.0 ± 1.0	10.2 ± 1.1	10.3 ± 1.2	10.2 ± 1.1	10.2 ± 1.1	9.8 ± 0.9	<0.001
Traffic intensity on the nearest road, vehicles/day	1513.1 ± 4933.5	934.8 ± 2339.8	1228.2 ± 3815.1	1271.9 ± 4277.8	1764.7 ± 5606.4	1521.8 ± 4950.9	<0.001
Inverse distance to the nearest road, 1/meters	0.05 ± 0.07	0.05 ± 0.07	0.05 ± 0.07	0.05 ± 0.07	0.05 ± 0.07	0.05 ± 0.08	<0.001
Average daytime sound level of noise pollution, dB	55.4 ± 4.3	55.3 ± 3.7	55.3 ± 4.0	55.2 ± 4.0	55.9 ± 4.6	55.2 ± 4.2	<0.001
Average evening sound level of noise pollution, dB	51.7 ± 4.3	51.6 ± 3.7	51.5 ± 4.0	51.5 ± 4.0	52.1 ± 4.6	51.5 ± 4.2	<0.001
Average night-time sound level of noise pollution, dB	46.6 ± 4.3	46.5 ± 3.7	46.5 ± 4.0	46.4 ± 4.0	47.1 ± 4.6	46.4 ± 4.2	<0.001
Food weight, g	3263.1 ± 374.0	3268.4 ± 388.7	3258.9 ± 419.2	3264.1 ± 311.6	3262.8 ± 444.9	3263.1 ± 348.3	<0.001
Energy, KJ	8826.7 ± 1284.0	8836.9 ± 1277.4	8834.5 ± 1498.0	8835.6 ± 1065.4	8823.8 ± 1531.1	8823.8 ± 1189.4	<0.001
Protein, g	81.8 ± 12.4	81.9 ± 12.7	81.8 ± 13.9	81.9 ± 10.2	81.8 ± 14.9	81.8 ± 11.6	<0.001
Fat, g	76.8 ± 14.5	77.0 ± 15.2	76.9 ± 16.5	76.8 ± 12.1	76.8 ± 17.4	76.7 ± 13.4	<0.001
Carbohydrate, g	258.1 ± 43.1	258.1 ± 42.0	258.8 ± 50.0	258.4 ± 35.9	257.6 ± 51.4	258.3 ± 39.9	<0.001
Englyst dietary fiber, g	16.6 ± 3.1	16.7 ± 3.4	16.7 ± 3.5	16.7 ± 2.6	16.6 ± 3.7	16.6 ± 2.9	<0.001
Sleep duration, hours/day	7.14 ± 1.1	7.19 ± 1.1	7.15 ± 1.1	7.15 ± 1.1	7.13 ± 1.1	7.15 ± 1.1	<0.001

TABLE 2 | Association between distance to the coast and incident myocardial infarction (MI).

Subgroup	Events rate	Model 1		Model 2		Model 3		
		HR (95% CI)	*P*-value	HR (95% CI)	*P*-value	HR (95% CI)	*P*-value	*P* for trend
Per SD (26.7 km)	4,059/377,340	0.97 (0.94, 1.00)	0.085	0.97 (0.94, 1.00)	0.092	0.98 (0.95, 1.02)	0.321	
<1 km	94/6,893	Reference	-	Reference	-	Reference	-	
1–5 km	245/19,402	0.90 (0.71, 1.14)	0.372	0.89 (0.71, 1.13)	0.355	0.93 (0.73, 1.18)	0.564	
5–20 km	765/68,104	0.82 (0.66, 1.01)	0.067	0.82 (0.66, 1.01)	0.066	0.89 (0.71, 1.10)	0.280	
20–50 km	906/96,586	0.72 (0.58, 0.89)	0.002	0.72 (0.58, 0.89)	0.002	0.79 (0.64, 0.98)	0.033	
>50 km	2,049/186,355	0.77 (0.63, 0.95)	0.015	0.77 (0.63, 0.95)	0.015	0.84 (0.68, 1.04)	0.109	
Q1 (<14.1 km)	901/75,663	Reference	-	Reference	-	Reference	-	0.586
Q2 (14.1–40.2 km)	717/75,249	0.84 (0.76, 0.93)	0.001	0.84 (0.76, 0.93)	0.001	0.86 (0.78, 0.95)	0.003	
Q3 (40.2–56.4 km)	768/75,723	0.82 (0.75, 0.91)	<0.001	0.82 (0.75, 0.91)	<0.001	0.85 (0.77, 0.94)	0.001	
Q4 (56.4–70.2 km)	841/75,426	0.90 (0.82, 0.99)	0.033	0.90 (0.82, 0.99)	0.035	0.91 (0.83, 1.00)	0.058	
Q5 (≥70.2 km)	832/75,279	0.92 (0.84, 1.01)	0.079	0.92 (0.84, 1.01)	0.086	0.95 (0.86, 1.04)	0.265	

Model 1: adjusted for age, gender, race, qualification, income, employ status, physical activity, sedentary behavior, mental health status, overall health rating, smoking status, drinking status, body mass index, waist to hip ratio, grip strength, and area-based socioeconomic status; Model 2: further adjusted for family history of heart diseases, the medication used of aspirin, antihypertension medicine and lip-lowing medicine, previous of hypertension and diabetes; Model 3: further adjusted for air pollution, noise pollution, dietary, sleep pattern, and home area population density.

HR, hazard ratio; CI, confident interval; SD, standard difference; Km, kilometer.

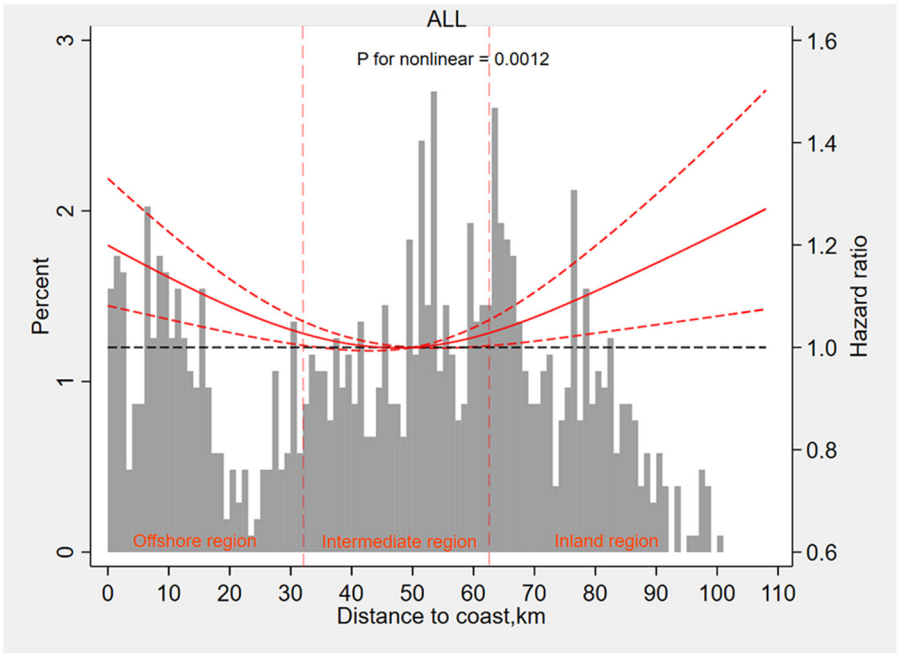

FIGURE 1 | The restricted cubic spline curve to explore potential non-linear patterns between distance to the coast and myocardial infarction. Km, kilometers.

TABLE 3 | Hazard ratio for participants of offshore region and inland region with MI.

Space	Events rate	Model 1		Model 2		Model 3	
		HR (95% CI)	*P*-value	HR (95% CI)	*P*-value	HR (95% CI)	*P*-value
Offshore (<32 km)	2,866/268,449	1.16 (1.08, 1.25)	<0.001	1.16 (1.08, 1.25)	<0.001	1.12 (1.04, 1.21)	0.004
Inland (>64 km)	2,685/257,210	1.10 (1.02, 1.19)	0.014	1.10 (1.02, 1.19)	0.013	1.09 (1.01, 1.18)	0.027

Model 1: adjusted for age, gender, race, qualification, income, employ status, physical activity, sedentary behavior, mental health status, overall health rating, smoking status, drinking status, BMI, waist to hip ratio, grip strength, and area-based socioeconomic status; Model 2: further adjusted for family history of heart diseases, the medication used of aspirin, antihypertension medicine and lip-lowing medicine, previous of hypertension and diabetes; Model 3: further adjusted for air pollution, noise pollution, dietary, sleep pattern, and home area population density.
HR, hazard ratio; CI, confident interval; Km, kilometer.

significant lower risk of MI (*HR* 0.86, 95% *CI* 0.78–0.95, $p = 0.003$; and *HR* 0.85, 95% *CI* 0.77–0.94, $p = 0.001$, respectively; p for trend = 0.586, **Table 2**).

We then applied the restricted cubic spline curve to explore potential non-linear patterns. **Figure 1** shows a *U*-shaped relation between distance to coast and MI with a relatively lower risk interval between 32 and 64 km (p for non-linear = 0.0012). According to the curve, we divided the population into three categories: offshore region (<32 km), inland region (>64 km), and intermediate area (32–64 km). Using participants of the intermediate region (32–64 km) as a reference, participants of the offshore region (<32 km), and inland region (>64 km) were both associated with a higher risk of incident MI and *HRs* were 1.12 (95% CI 1.04–1.21, $p = 0.004$) and 1.09 (95% *CI* 1.01–1.18, $p = 0.027$) after adjusting for all confounders, respectively (**Table 3**).

Figure 2 shows the associations between participants living in the offshore region (<32 km) and incident MI in subgroups analyses. *HR* for the offshore area (<32 km) was higher in the subgroup with low total physical activity (<24 h/week) (*HR* 1.24, 95% *CI* 1.09–1.42, $p = 0.001$), compared with subgroups with moderate and high total physical activity (p for interaction = 0.043). **Figure 3** shows the associations between participants living in the inland region (>64 km) and incident MI in subgroups stratified by potential effect modifiers. *HR* for the inland region (>64 km) was significantly larger in the subgroup of the urban area (*HR* 1.12, 95% *CI* 1.03–1.22, $p = 0.007$), compared with the subgroup of the rural area (p for interaction 0.065). Also, *HR* for the inland region (>64 km) was significantly larger in the subgroup of high NO_2 air pollution exposure (*HR* 1.29, 95% *CI* 1.11–1.50, $p = 0.001$), compared with middle and low NO_2 air pollution (p for interaction = 0.021).

DISCUSSION

The main finding of the current study was that residential distance to coast had a *U*-shaped relation with incident MI in

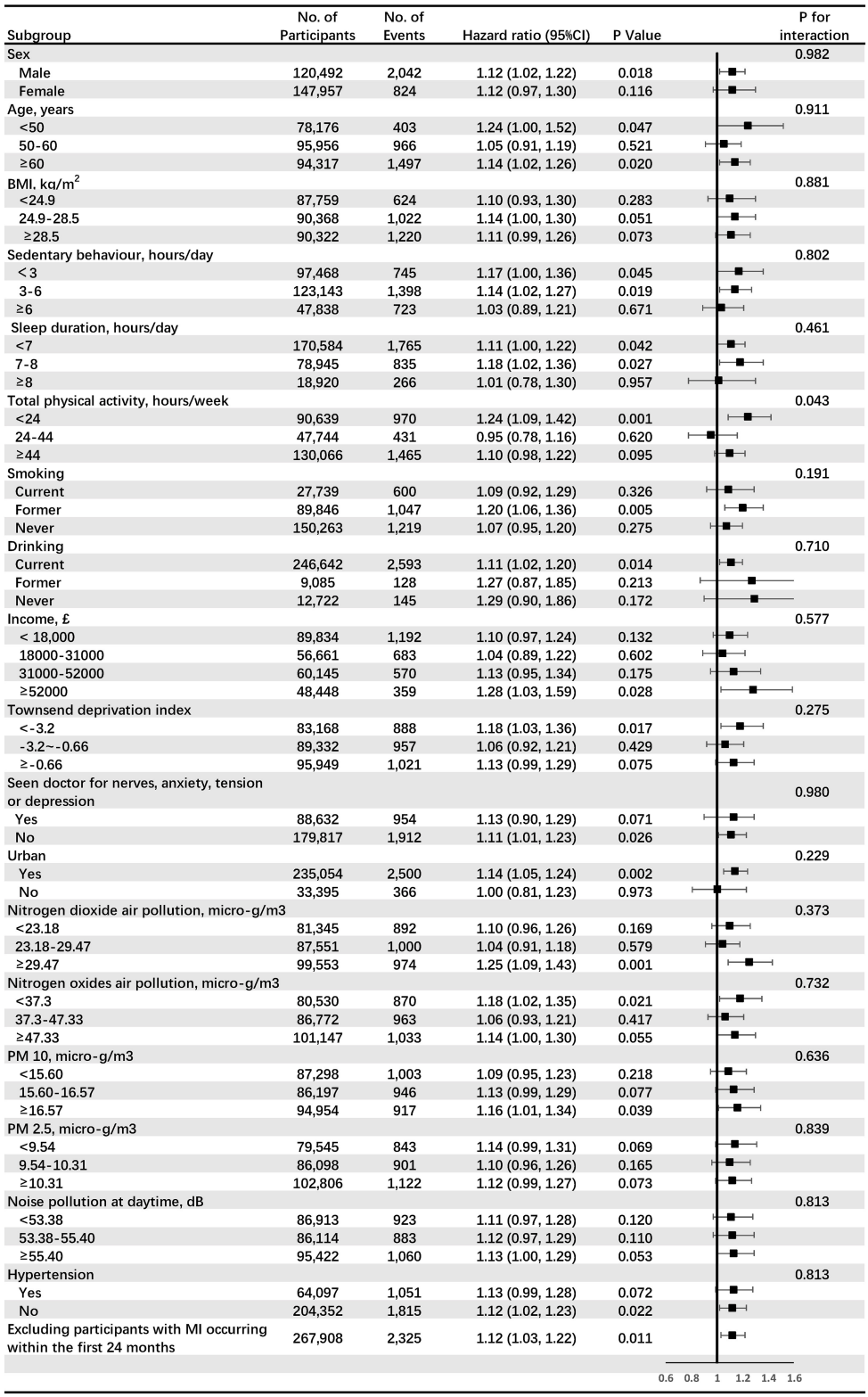

FIGURE 2 | The associations between participants living in the offshore region (<32 km) and incident myocardial infarction (MI) in subgroups analyses. BMI, body mass index; PM, particulate matter.

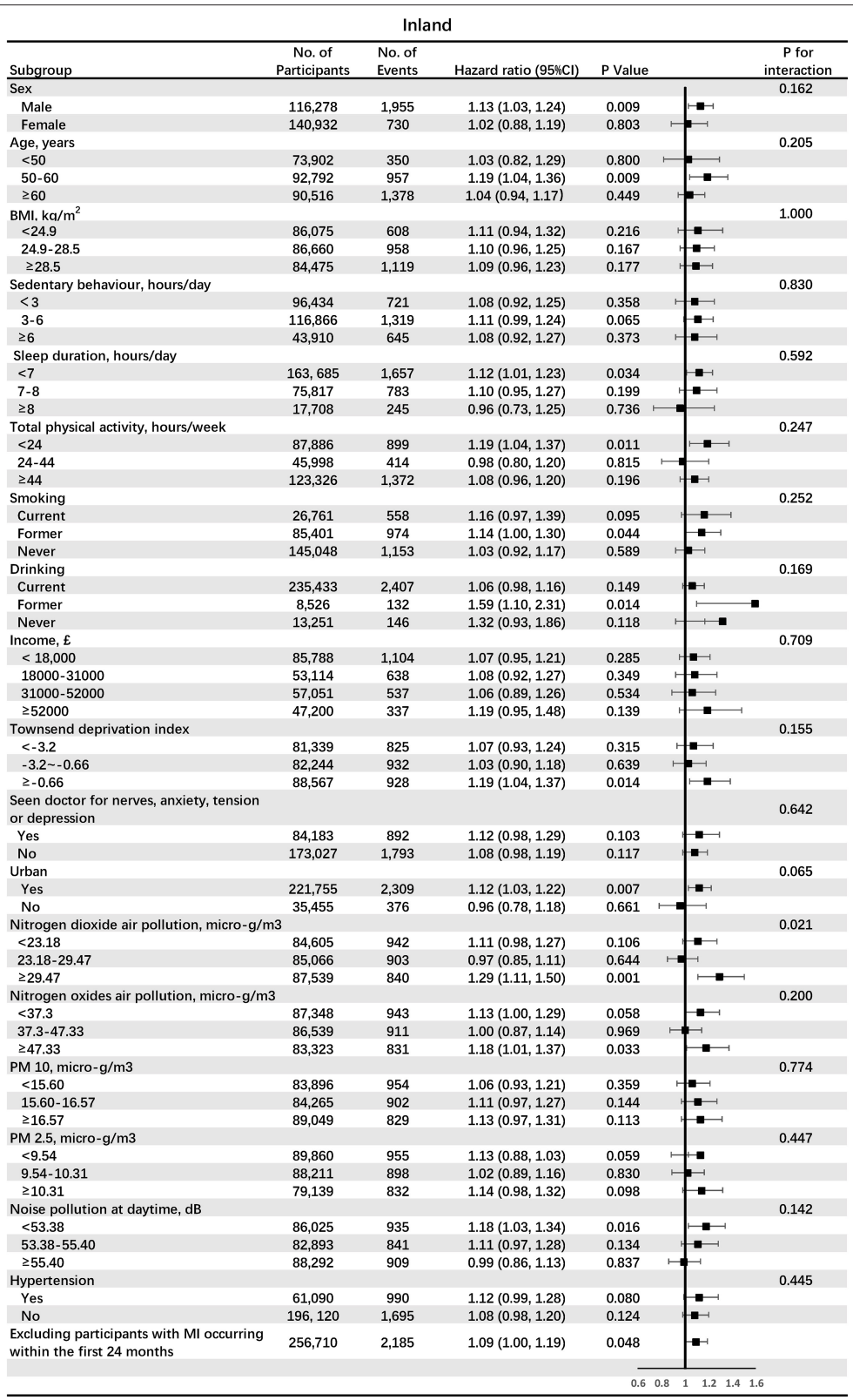

FIGURE 3 | The associations between participants living in the inland region (>64 km) and incident MI in subgroups analyses. BMI, body mass index; PM, particulate matter.

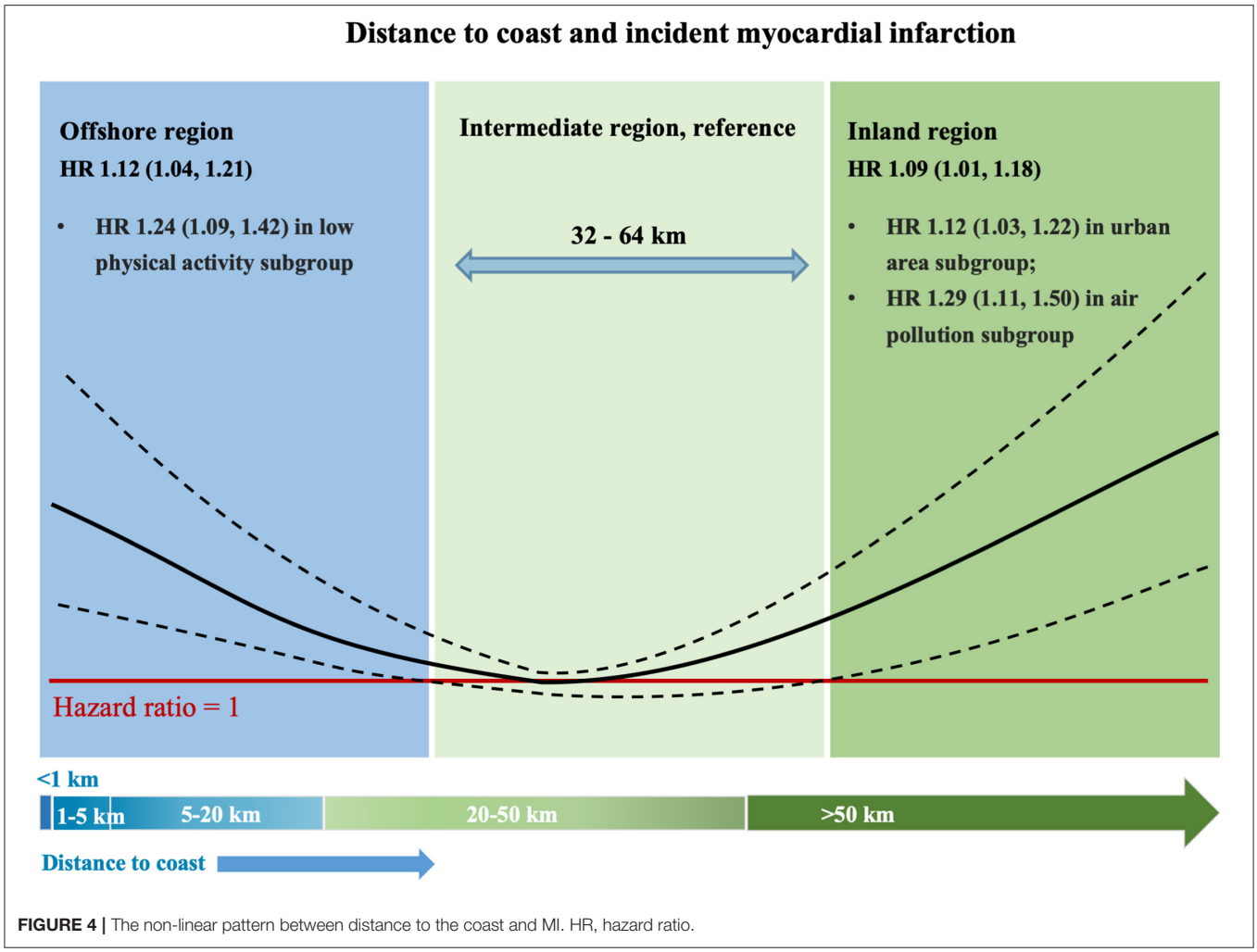

FIGURE 4 | The non-linear pattern between distance to the coast and MI. HR, hazard ratio.

over 370,000 individuals followed for over 3.0 million person-years and that both residents of the offshore region (<32 km) and that of the inland region (>64 km) had around 10% increase risk of MI compared with residents of the intermediate region (32–64 km) (**Figure 4**). Moreover, the associations of offshore region and inland region with incident MI were modified by various factors. Participants of offshore regions with low total physical activity had a higher risk of MI (increased by 24%), suggesting that this subgroup may benefit from increased physical activity. Meanwhile, participants of inland regions living in the urban area or exposed to high NO_2 air pollution had a higher risk of MI (increased by 12 and 29%, respectively), suggesting that urban environment improvement and air pollution control played a crucial role in these population. The results were mostly consistent in a series of sensitivity and subgroup analyses.

Unlike previous research that commonly reported linear associations, we investigated the non-linear association of coastal proximity with disease outcome. Our findings highlight the complex and diverse associations between residential distance to the coast and incident MI. Although modifying the residential environment tends to be problematic in the short term, our findings suggest that targeting based on coastal proximity and various effect modifiers (physical activity, population density, and air pollution) could help identify high-risk individuals and provide personalized interventions for diverse populations. However, the classification of the offshore, inland, and intermediate regions was constructed for illustrative purposes; hence the cut-off values of distance to coast identified in this study cannot be simply generalized. This classification is more about raising public awareness of the residential location than about being implemented as a real-world tool. The harmful effect of residential distance to coast on incident MI may vary with the coastline's distance and is regulated by various factors. Therefore, when possible, advice on the living environment and health should be personalized.

Scientific and public interest in the role of the natural outdoor environment in preventing CVDs is growing. A tremendous body of studies has provided evidence on the associations between various outdoor environment attributes, behavioral pathways, CV risk factors, and mortality (18–21). A meta-analysis of longitudinal studies found inverse relationships between neighborhood walkability and risk factors, such as

obesity, hypertension, and type 2 diabetes mellitus (20). Similarly, another meta-analysis found that more residential greenspace was associated with reduced CVD mortality (22). The links between air and noise pollution, stress, and CVDs have also been recognized (23). The previous research suggested that living near and regularly visiting the coast or other large waterbodies was associated with better general and mental health. However, most of the outcomes used were self-reported and not disease-specific (24–26). However, the association of residential distance to the coast with CVD incidence is relatively less well studied, and high-quality epidemiological evidence was too scant to draw a conclusion. To investigate this issue at a broad level of disease specificity, we set out to address the question: does the incidence of MI increase or decrease with proximity to the coast?

The results of the study were somewhat unexpected, particularly the finding that MI risk increased in coastal areas, which contradicts most of the previous studies that have shown the benefits of living near the sea. However, our study was based on sufficient confounding adjustment and subgroup analyses, and the results were reliable and consistent. One possible explanation is that the same environment attribute might have diverse effects on cardiometabolic risk factors and different population subgroups. For example, whereas high population density might help improve the weight status through better availability of physical activity destinations and healthy food options, high population density might also have adverse effects on airway and CVD through more exposure to air pollution. Similarly, a previous study showed that individuals living in the <1 km coastal category had an average a 4 nmol/l higher vitamin D status compared to those living inland through increased solar irradiance, which can provide benefits in terms of vitamin D status but may also pose a risk due to higher skin cancer rates (27). Examining single environmental attributes with multiple behaviors and risk factors in single studies can provide insights into the differential effects of the natural environment on CVD. Further interdisciplinary research initiatives involving cardiology and urban design researchers must disentangle the complex relationships between the residential coastal distance and CVD.

Strengths of this study include its prospective design, a large sample size with harmonized exposure, health, and covariate data. We could adjust for a wide range of health, demographic, behavioral, and environmental confounders. The possibility of confounding was dealt with through statistical adjustment for a wide range of covariates, such as health, demographic, behavioral, and ecological confounders, and a series of sensitivity analyses. This study has several limitations. First, we were not able to consider the impact on the exposure of residential changes during follow-up, which will contribute to misclassification of long-term exposure relevant to the development of MI. These misclassifications are believed to be non-differential for cases, and non-cases likely bias the risk estimates toward the null. Second, as is the case for any observational study, residual confounding is always possible, and associations may not imply causation. We cannot rule out the possibility of residual confounding by other unaccounted factors, such as coastal climate, humidity, and sun exposure. Third, the UK Biobank represents the general population for age, sex, ethnicity, and deprivation within the age range recruited but is not representative in other regards, which may indicate a healthy volunteer selection bias. While this limits the ability to generalize prevalence rates, it should be possible to generalize the estimates of the associations' magnitude. Forth, the offshore, inland, and intermediate regions were constructed for illustrative purposes rather than as a tool ready for implementation. The cut-off values of distance to coast (32 km, 64 km) have not been validated.

CONCLUSIONS

The study found a *U*-shaped association between residential distance to the coast and incident MI. Moreover, the association of offshore region with incident MI was modified by total physical activity. The association of inland region with incident MI was limited by urban/rural area or NO_2 air pollution. Our findings highlight the complex and diverse associations between residential distance to the coast and incident MI, and residential advice should be personalized.

DATA AVAILABILITY STATEMENT

The datasets presented in this study can be found in online repositories. The names of the repository/repositories and accession number(s) can be found in the article/**Supplementary Material**.

AUTHOR CONTRIBUTIONS

ZX-d performed statistical analysis. LL-z handled funding and supervision. LX-x acquired the data. ZS-z conceived and designed the research. HX drafted the manuscript and made critical revision of the manuscript for critical intellectual content. All authors contributed to the article and approved the submitted version.

FUNDING

The UK Biobank was supported by the Welcome Trust, Medical Research Council, Department of Health, Scottish Government, and the Northwest Regional Development Agency. It has also had funding from the Welsh Assembly Government and the British Heart Foundation. The research was designed, conducted, analyzed, and interpreted by the authors entirely independently of the funding sources.

SUPPLEMENTARY MATERIAL

The Supplementary Material for this article can be found online at: https://www.frontiersin.org/articles/10.3389/fcvm.2022.752964/full#supplementary-material

REFERENCES

1. Koohsari MJ, McCormack GR, Nakaya T, Oka K. Neighbourhood built environment and cardiovascular disease: knowledge and future directions. *Nat Rev Cardiol.* (2020) 17:261–3. doi: 10.1038/s41569-020-0343-6
2. Gascon M, Sánchez-Benavides G, Dadvand P, Martínez D, Gramunt N, Gotsens X, et al. Long-term exposure to residential green and blue spaces and anxiety and depression in adults: a cross-sectional study. *Environ Res.* (2018) 162:231–9. doi: 10.1016/j.envres.2018.01.012
3. Huang B, Liu Y, Feng Z, Pearce JR, Wang R, Zhang Y, et al. Residential exposure to natural outdoor environments and general health among older adults in Shanghai, China. *Int J Equity Health.* (2019) 18:178. doi: 10.1186/s12939-019-1081-4
4. Pasanen TP, White MP, Wheeler BW, Garrett JK, Elliott LR. Neighbourhood blue space, health and wellbeing: the mediating role of different types of physical activity. *Environ Int.* (2019) 131:105016. doi: 10.1016/j.envint.2019.105016
5. Wood SL, Demougin PR, Higgins S, Husk K, Wheeler BW, White M. Exploring the relationship between childhood obesity and proximity to the coast: a rural/urban perspective. *Health Place.* (2016) 40:129–36. doi: 10.1016/j.healthplace.2016.05.010
6. Garrett JK, Clitherow TJ, White MP, Wheeler BW, Fleming LE. Coastal proximity and mental health among urban adults in England: The moderating effect of household income. *Health Place.* (2019) 59:102200. doi: 10.1016/j.healthplace.2019.102200
7. Collins R. What makes UK Biobank special? *Lancet. Mar.* (2012) 379:1173–4. doi: 10.1016/S0140-6736(12)60404-8
8. Sudlow C, Gallacher J, Allen N, Beral V, Burton P, Danesh J, et al. UK biobank: an open access resource for identifying the causes of a wide range of complex diseases of middle and old age. *PLoS Med.* (2015) 12:e1001779. doi: 10.1371/journal.pmed.1001779
9. Alcock I, White MP, Wheeler BW, Fleming LE, Depledge MH. Longitudinal effects on mental health of moving to greener and less green urban areas. *Environ Sci Technol.* (2014) 48:1247–55. doi: 10.1021/es403688w
10. White P, Ruble CL, Lane ME. The effect of changes in land use on nitrate concentration in water supply wells in southern Chester County, Pennsylvania. *Environ Monit Assess.* (2013) 185:643–51. doi: 10.1007/s10661-012-2581-5
11. Wheeler BW, White M, Stahl-Timmins W, Depledge MH. Does living by the coast improve health and wellbeing? *Health Place.* (2012) 18:1198–201. doi: 10.1016/j.healthplace.2012.06.015
12. Aveyard P, Manaseki S, Chambers J. The relationship between mean birth weight and poverty using the townsend deprivation score and the super profile classification system. *Public Health.* (2002) 116:308–14. doi: 10.1016/S0033-3506(02)00554-1
13. Liu B, Young H, Crowe FL, Benson VS, Spencer EA, Key TJ, et al. Development and evaluation of the Oxford WebQ, a low-cost, web-based method for assessment of previous 24 h dietary intakes in large-scale prospective studies. *Public Health Nutr.* (2011) 14:1998–2005. doi: 10.1017/S1368980011000942
14. Guo W, Bradbury KE, Reeves GK, Key TJ. Physical activity in relation to body size and composition in women in UK Biobank. *Ann Epidemiol.* (2015) 25:406–13.e6. doi: 10.1016/j.annepidem.2015.01.015
15. Celis-Morales CA, Petermann F, Hui L, Lyall DM, Iliodromiti S, McLaren J, et al. Associations between diabetes and both cardiovascular disease and all-cause mortality are modified by grip strength: evidence from UK Biobank, a prospective population-based cohort study. *Diabetes Care.* (2017) 40:1710–8. doi: 10.2337/dc17-0921
16. Doiron D, de Hoogh K, Probst-Hensch N, Fortier I, Cai Y, De Matteis S, et al. Air pollution, lung function and COPD: results from the population-based UK Biobank study. *Eur Respir J.* (2019). 54:1802140. doi: 10.1183/13993003.02140-2018
17. Kephalopoulos S, Paviotti M, Anfosso-Lédée F, Van Maercke D, Shilton S, Jones N. Advances in the development of common noise assessment methods in Europe: the CNOSSOS-EU framework for strategic environmental noise mapping. *Sci Total Environ.* (2014) 482–3:400–10. doi: 10.1016/j.scitotenv.2014.02.031
18. Nieuwenhuijsen MJ. Influence of urban and transport planning and the city environment on cardiovascular disease. *Nat Rev Cardiol.* (2018) 15:432–8. doi: 10.1038/s41569-018-0003-2
19. Stevenson M, Thompson J, de Sá TH, Ewing R, Mohan D, McClure R, et al. Land use, transport, and population health: estimating the health benefits of compact cities. *Lancet.* (2016) 388:2925–35. doi: 10.1016/S0140-6736(16)30067-8
20. Chandrabose M, Rachele JN, Gunn L, Kavanagh A, Owen N, Turrell G, et al. Built environment and cardio-metabolic health: systematic review and meta-analysis of longitudinal studies. *Obes Rev.* (2019) 20:41–54. doi: 10.1111/obr.12759
21. Garg PK, Jorgensen N, Moore K, Soliman EZ, Heckbert SR. Neighborhood environments and risk of incident atrial fibrillation: the multi-ethnic study of atherosclerosis. *Eur J Prev Cardiol.* (2020) 27:1440–1. doi: 10.1177/2047487319885196
22. Gascon M, Triguero-Mas M, Martínez D, Dadvand P, Rojas-Rueda D, Plasència A, et al. Residential green spaces and mortality: a systematic review. *Environ Int.* (2016) 86:60–7. doi: 10.1016/j.envint.2015.10.013
23. Al-Kindi SG, Brook RD, Biswal S, Rajagopalan S. Environmental determinants of cardiovascular disease: lessons learned from air pollution. *Nat Rev Cardiol.* (2020) 17:656–72. doi: 10.1038/s41569-020-0371-2
24. Garrett JK, White MP, Huang J, Ng S, Hui Z, Leung C, et al. Urban blue space and health and wellbeing in Hong Kong: results from a survey of older adults. *Health Place.* (2019) 55:100–10. doi: 10.1016/j.healthplace.2018.11.003
25. Dempsey S, Devine MT, Gillespie T, Lyons S, Nolan A. Coastal blue space and depression in older adults. *Health Place.* (2018) 54:110–7. doi: 10.1016/j.healthplace.2018.09.002
26. Dzhambov AM, Markevych I, Hartig T, Tilov B, Arabadzhiev Z, Stoyanov D, et al. Multiple pathways link urban green- and bluespace to mental health in young adults. *Environ Res.* (2018) 166:223–3. doi: 10.1016/j.envres.2018.06.004
27. Cherrie MP, Wheeler BW, White MP, Sarran CE, Osborne NJ. The coastal climate is associated with elevated solar irradiance and higher 25(OH)D level. *Environ Int.* (2015) 77:76–84. doi: 10.1016/j.envint.2015.01.005

Conflict of Interest: The authors declare that the research was conducted in the absence of any commercial or financial relationships that could be construed as a potential conflict of interest.

frontiers in Cardiovascular Medicine

ORIGINAL RESEARCH
published: 22 February 2022
doi: 10.3389/fcvm.2022.764622

The Early Predictive Value of Circulating Monocytes and Eosinophils in Coronary DES Restenosis

Shumei Li[1*†], *Hong Qiu*[2†], *Zhaorong Lin*[1], *Lin Fan*[1], *Yongzhe Guo*[1], *Yujie Zhang*[1] and *Lianglong Chen*[1]

[1] Department of Cardiology, Fujian Institute of Coronary Heart Disease, Fujian Medical University Union Hospital, Fuzhou, China, [2] JC School of Public Health and Primary Care, The Chinese University of Hong Kong, Shatin, Hong Kong SAR, China

Background: Monocytes and eosinophils are involved in intracoronary inflammatory responses, aggravating coronary artery plaque instability and in-stent restenosis (ISR).

Aims: To investigate an early prediction of ISR in patients undergoing stenting by circulating monocytes and eosinophils.

Methods: The single-center data of patients undergoing successful drug-eluting stents (DES) implantation from January 1, 2017 to April 30, 2020 were retrospectively analyzed. Of the 4,392 patients assessed, 140 patients with restenosis and 141 patients without restenosis were enrolled. A scheduled postoperative follow-up was proceeded in four sessions: 0–3 months, 3–6 months, 6–12 months, and >12 months. The hematological and biochemical measurement was collected. The angiographic review was completed within two postoperative years.

Results: Significant associations of monocyte count and percentage with ISR were evident [odds ratio (OR): 1.44, 95% CI: 1.23–1.68, $P < 0.001$; OR: 1.47, 95%CI: 1.24–1.74, $P < 0.001$, respectively], which began at 3 months postoperatively and persisted throughout the follow-up period. Eosinophil count and percentage were associated with ISR (OR: 1.22, 95%CI: 1.09–1.36, $P = 0.001$; OR: 1.23, 95%CI: 1.07–1.40, $P = 0.003$, respectively), with ISR most significantly associated with the baseline eosinophils. The receiver operating characteristic (ROC) curve analysis showed that the cutoff points of monocyte count and percentage in the ISR prediction were 0.46×10^9/L and 7.4%, respectively, and those of eosinophil count and percentage were 0.20×10^9/L and 2.5%, respectively.

Conclusion: This study, with a long-term follow-up, first provides evidence that the elevated monocytes at three postoperative months and baseline eosinophils may be strong early predictors of ISR after drug-eluting stent implantation. Persistent elevation of monocytes may also be a signal of ISR after percutaneous coronary intervention (PCI).

Keywords: monocyte, eosinophil, in-stent restenosis, drug-eluting stent, coronary heart disease

OPEN ACCESS

Edited by:
Stéphane Cook,
Université de Fribourg, Switzerland

Reviewed by:
Rocco Antonio Montone,
Agostino Gemelli University Polyclinic (IRCCS), Italy
Yujie Zhou,
Capital Medical University, China

****Correspondence:***
Shumei Li
lsmzssdoctor@126.com

†These authors share first authorship

Specialty section:
This article was submitted to Coronary Artery Disease, a section of the journal Frontiers in Cardiovascular Medicine

Received: *25 August 2021*
Accepted: *03 January 2022*
Published: *22 February 2022*

Citation:
Li S, Qiu H, Lin Z, Fan L, Guo Y, Zhang Y and Chen L (2022) The Early Predictive Value of Circulating Monocytes and Eosinophils in Coronary DES Restenosis. Front. Cardiovasc. Med. 9:764622. doi: 10.3389/fcvm.2022.764622

INTRODUCTION

Although percutaneous coronary intervention (PCI), a widely-prescribed treatment for symptomatic coronary disease, has proven effective, in-stent restenosis (ISR) remains a clinical challenge. It may result in repeated revascularization and poor long-term prognosis for afflicted patients, despite the reduced neointimal hyperplasia and incidence rate of <10% due to the emergence of drug-eluting stents (DES) (1, 2).

As a key feature of atherosclerosis, inflammation represents a well-known pathogenic mechanism underlying both coronary plaque progression and instability and adverse events following stent implantation. Available evidence suggests that effector cells of allergic inflammation such as eosinophils, as well as classic inflammatory cells, including monocytes, macrophages, lymphocytes, and neutrophils, play an important role in ISR (3–5).

Several studies have investigated whether laboratory parameters of complete blood count or biochemical analysis could predict ISR, but yielded inconsistent results (6–12). Moreover, previous studies only employed bare-metal stent (BMS) and blood samples from the peri-interventional period and did not supplement with a dynamic follow-up. In the current study, we monitored the serial changes of monocytes and eosinophils by a simple blood draw after stent implantation, attempting to investigate whether circulating monocytes and eosinophils can identify the ISR in those patients undergoing stenting at an early phase.

METHODS

Study Population

Patients, who had been diagnosed with stable angina pectoris or acute coronary syndrome and underwent successful DES implantation during January 1, 2017 and April 30, 2020, were enrolled at the Affiliated Union Hospital of Fujian Medical University. The excluding criteria were as follows: no follow-up coronary angiography (CAG) within 2 years after PCI, requiring PCI for other vessels at the follow-up visit, severe hepatic and renal diseases, thyroid disease, malignancy, allergic diseases, hematological disorders, immunological disorder, and active infection. ISR referred to the plaque within 5 mm of the edge of the stent after PCI and had stenosis >50% (13). Of the 4,392 patients who underwent PCI during this study period, 140 patients with restenosis met the inclusion criteria, and 141 patients without restenosis in the same period were selected randomly as controls. Patients were advised to return for scheduled postoperative follow-up analysis during 4 periods: 0–3 months, 3–6 months, 6–12 months, and >12 months.

The study protocol observed the recommendations of the Declaration of Helsinki on Biomedical Research involving human subjects and was approved by the institutional ethics committee of Fujian medical university Union Hospital (Ethics approval number: 2021KY080). The written informed consent was obtained from all study participants.

Measurements of Blood Parameters

Blood samples were collected during the clinical visit. Specimens were used for hematological and biochemical measurement. Total white blood cells and each fraction were measured with an automated hematology analyzer (Sysmex XN2000, Japan). Plasma total cholesterol, low-density lipoprotein cholesterol, high-density lipoprotein cholesterol, triglyceride, apolipoprotein A, apolipoprotein B, creatinine, and uric acid were analyzed in fasting blood samples with an automatic biochemical detector (Cobas 8000, Roche, Germany). High-sensitivity C-reactive protein was determined by immune turbidimetry with an analyzer (Beckman immage800, USA). HbA1c, as a marker of glycemic control level, was detected on a glycosylated hemoglobin analyzer (Sysmex G7, Japan). Serum homocysteine (HCY) was quantified by the chemiluminescent method with Architect i2000sr (Abbott, USA).

In-stent Restenosis Assessment

For all patients, the PCI procedure and the implantation of DES were performed according to the PCI guideline. For patients without clinical contraindications, coronary angiography was routinely performed within the 2-year follow-up. Angiograms were analyzed with a validated quantitative coronary angiography system (Philips UNIQ FD20, Holland). Angiographic restenosis was defined as percent diameter stenosis >50% during the follow-up and the patients were accordingly divided into the ISR and non-ISR groups.

Statistical Analyses

The essential characteristics and the hematological and biochemical indices were compared between postoperative in-stent restenosis (ISR) and non-ISR group. The continuous variables with approximately normal distribution were presented as mean and SD, and compared by independent samples *t*-test; continuous variables with skewed distribution were described as median (25th, 75th percentiles) and compared by Mann-Whitney *U*-Test; categorical variables were described as the frequency with percentage and compared by the Chi-square test.

As it is a case-control study design with longitudinal repeated measurements of hematological and biochemical indices, we applied mixed-effect logistic regression in the generalized linear mixed model family to examine the associations of each hematological and biochemical parameter with the risk of ISR. The follow-up month (times of repeated measurements) was included as a random intercept in the model to account for the within-subject correlation, and individual essential characteristics at baseline (age, sex, BMI, smoking status, chronic diseases of hypertension, or diabetes mellitus) as fixed effects to adjust the between-subject confounders (14, 15).

In order to evaluate whether the main hematological indices (monocyte and eosinophil count/percentage) have an early prediction of ISR or not, we conducted a follow-up period-specific analysis. The logistic regression in the generalized linear model family was applied to examine the risk of ISR associated with each of the main hematological indices during each follow-up period, with the individual essential characteristics adjusted.

The optimal cutoff points for monocyte and eosinophil count/percentage in the prediction of ISR were identified according to the receiver operating characteristic (ROC) curve analysis (16). The optimal cutoff points were then used to categorize monocyte and eosinophil count/percentage into low and high levels, respectively, and examine their joint effect and potential biological interaction (17). The predictive values of monocyte and eosinophil count/percentage were also evaluated by the area under the ROC curve (AUC) (18).

All analyses were conducted within the R statistical environment version 3.5.3 using the "lme4" package for generalized mixed effect model, and "cutpointr" and "ModelGood" packages to identify the optimal cutoff point and to obtain ROC curves based on the logistic regression (19).

RESULTS

The comparison of clinical characteristics between the ISR and non-ISR groups was summarized in **Table 1**.

The effect estimates were presented as the odds ratio (OR) of ISR with the 95% CI associated with an interquartile range (IQR) increment of each hematological and biochemical index. We observed the statistically significant associations of ISR with monocyte and eosinophil count and percentage, respectively (**Table 2**). The OR of ISR was 1.44 (95%CI: 1.23–1.68, $P < 0.001$) per IQR increase of monocyte count (0.21×10^9/L) and 1.47 (95%CI: 1.24–1.74, $P < 0.001$) per IQR increase of monocyte percentage (2.42%). The follow-up period-specific analysis (**Table 3**) showed that significant associations began at 3 months after the operative intervention and persisted throughout the following observation period, which suggests an early prediction of ISR by monocytes. Meanwhile, the OR of ISR was 1.22 (95%CI: 1.09–1.36, $P = 0.001$) per IQR increase of eosinophil count (0.13×10^9/L) and 1.23 (95%CI: 1.07–1.40, $P = 0.003$) per IQR increase of eosinophil percentage (2.00%). The most significant association between ISR and eosinophils occurred at baseline and lasted for about 1 year, supporting the early prediction of ISR by eosinophils. The mean levels of monocytes and eosinophil percentage and count at each follow-up period between ISR and non-ISR groups supported the above-mentioned observations (**Figure 1**). Besides, lower high-density lipoprotein cholesterol (OR = 0.8, 95%CI.67–0.95, $P = 0.012$) and higher HbA1c (OR = 1.28, 95%CI 1.03–1.60, $P= 0.025$) raised the ISR risk. Other parameters did not show a significant correlation with ISR (**Table 2**).

The ROC and AUC were employed to explore the diagnostic value of monocyte and eosinophil count and percentage in ISR prediction. On ROC analysis, the optimal cutoff points were identified as 0.46×10^9/L and 7.4% for monocyte count and percentage, respectively (AUC: 74%, 95% CI: 71.1–77%, $P < 0.001$; AUC: 73.7%, 95% CI: 70.7–76.6%, $P < 0.001$). The optimal cutoff points were identified as 0.20×10^9/L and 2.5% for eosinophil count and percentage, respectively (AUC: 73.5%, 95% CI: 70.5–76.5%, $P < 0.001$; AUC: 73.4%, 95% CI: 70.4–76.3%, $P < 0.001$) (**Figure 2**).

TABLE 1 | Data description of basic characteristics and main hematological and biochemical indices between postoperative in-stent restenosis (ISR) and non-ISR group*.

	ISR group	Non-ISR group	*P*-value
Basic characteristics	***N* = 140**	***N* = 141**	
Age	65.1 ± 10.1	61.8 ± 9.9	<0.001
Sex, men	115 (82.1%)	106 (75.2)	0.201
BMI	23.9 ± 3.0□	24.4 ± 2.9	<0.001
Smoking			0.857
Never-smoker	73 (52.1%)	71 (50.4%)	
Ever-smoker	67 (47.9%)	70 (49.6%)	
Hypertension	97 (69.3%)	86 (61.0%)	0.182
Diabetes Mellitus	70 (50.0%)	41 (29.1%)	<0.001
Hematological and biochemical indices with repeated measurements	*n* = 507	n = 594	
White blood cell count ($\times 10^9$/L)	7.054 ± 2.066	6.942 ± 1.903	0.348
Neutrophil count ($\times 10^9$/L)	4.452 ± 1.713	4.486 ± 2.932	0.818
Lymphocyte count ($\times 10^9$/L)	1.859 ± 0.654	1.893 ± 0.661	0.386
Monocyte count ($\times 10^9$/L)	0.525 ± 0.202	0.469 ± 0.181	<0.001
Eosinophil count ($\times 10^9$/L)	0.189 ± 0.182	0.151 ± 0.140	<0.001
Neutrophil percentage (%)	63.41 ± 30.88	61.95 ± 8.69	0.303
Lymphocyte percentage (%)	26.99 ± 7.80	28.31 ± 8.46	0.007
Monocyte percentage (%)	7.53 ± 2.07	6.83 ± 1.87	<0.001
Eosinophil percentage (%)	2.70 ± 2.25	2.24 ± 1.74	<0.001
Total cholesterol (mmol/L)	3.732 ± 1.022	3.913 ± 1.097	0.005
Low-density lipoprotein cholesterol (mmol/L)	2.216 ± 0.882	2.374 ± 0.970	0.005
High-density lipoprotein cholesterol (mmol/L)	1.024 ± 0.264	1.082 ± 0.297	<0.001
Triglyceride (mmol/L)	1.791 ± 1.380	1.734 ± 1.030	0.450
Apolipoprotein A (g/L)	1.202 ± 0.268	1.235 ± 0.241	0.030
Apolipoprotein B (g/L)	0.816 ± 0.258	0.841 ± 0.268	0.122
Serum creatinine (μmol/L)	83.38 ± 21.09	81.94 ± 21.21	0.268
Estimated glomerular filtration rate (mL/min/1.73m^2)	71.46 ± 26.16	79.54 ± 21.60	< 0.001
Serum uric acid (μmol/L)	384.75 ± 101.18	375.97 ± 111.27	0.177
High-sensitivity C-reactive protein (mg/L)#	1.71 (0.51, 5.90)	1.55 (0.45, 5.35)	0.441
HBA1c (%)	7.22 ± 1.75	6.63 ± 1.33	<0.001
Homocysteine (umol/L)	10.51 ± 4.61	10.05 ± 5.50	0.320

**Continuous variables with approximately normal distribution are described as Mean±SD, and compared with independent samples t-test; Categorical variables were described as N (%) and compared with Chi-square test.*

#Continuous variables with skewed distribution were described as median (25th, 75th percentiles), and compared with Mann-Whitney U-Test.

Furthermore, we observed the joint effect of monocyte and eosinophil count and percentage on the risk of postoperative ISR. The value beyond the cutoff points was defined as high levels. When both monocyte and eosinophil count and percentage were high (OR of ISR: 3.04, 95%CI: 2.06–4.49, $P < 0.001$ for the joint count; OR of ISR: 3.06, 95%CI: 2.08–4.51, $P < 0.001$ for joint percentage), the risk of ISR was higher than that of a single index (**Table 4**).

TABLE 2 | OR (95%CI) of ISR associated with per interquartile range (IQR) increment of each hematological and biochemical index*.

Hematological and biochemical indices	IQR	OR (95% CI)	*P*-value
White blood cell count ($\times 10^9$/L)	2.52	1.18 (1.00, 1.40)	0.052
Neutrophil count ($\times 10^9$/L)	1.91	1.01 (0.91, 1.11)	0.916
Lymphocyte count ($\times 10^9$/L)	0.77	1.15 (0.99, 1.35)	0.074
Monocyte count ($\times 10^9$/L)	0.21	**1.44 (1.23, 1.68)**	<0.001
Eosinophil count ($\times 10^9$/L)	0.13	**1.22 (1.09, 1.36)**	0.001
Neutrophil percentage (%)	11.49	1.04 (0.98, 1.12)	0.209
Lymphocyte percentage (%)	10.96	0.94 (0.79, 1.13)	0.525
Monocyte percentage (%)	2.42	**1.47 (1.24, 1.74)**	<0.001
Eosinophil percentage (%)	2.00	**1.23 (1.07, 1.40)**	0.003
Total cholesterol (mmol/L)	1.34	0.89 (0.75, 1.05)	0.169
Low-density lipoprotein cholesterol (mmol/L)	1.19	0.90 (0.76, 1.06)	0.211
High-density lipoprotein cholesterol (mmol/L)	0.34	**0.80 (0.67, 0.95)**	0.012
Triglyceride (mmol/L)	0.92	1.04 (0.94, 1.16)	0.417
Apolipoprotein A (g/L)	0.31	0.88 (0.75, 1.04)	0.137
Apolipoprotein B (g/L)	0.32	1.02 (0.87, 1.19)	0.832
Serum creatinine (μmol/L)	23.00	0.94 (0.80, 1.09)	0.408
Estimated glomerular filtration rate (mL/min/1.73 m^2)	31.42	0.89 (0.71, 1.11)	0.309
Serum uric acid (μmol/L)	126.00	1.12 (0.96, 1.32)	0.142
High-sensitivity C-reactive protein (mg/L)	5.12	0.97 (0.91, 1.03)	0.260
HBA1c (%)	1.60	**1.28 (1.03, 1.60)**	0.025
Homocysteine (umol/L)	3.59	1.07 (0.93, 1.23)	0.344

**Generalized linear mixed models (mixed-effects logistic regression) were used to examine the odds ratio (ORs) of ISR with the hematological and biochemical indices, adjusting for follow-up time as a random effect and individual basic characteristics (age, sex, BMI, smoking status, chronic diseases of hypertension or diabetes mellitus) as fixed effects. Each of the blood biochemical indices was included into the model one at a time. Statistically significant effect estimates are in bold.*

TABLE 3 | OR (95%CI) of ISR associated with per interquartile range (IQR) increment of each hematological index during the follow-up period*.

	ISR	Non-ISR	OR (95% CI)	*P*-value
Monocyte count (10^9/L)#	507	594	**1.44 (1.23, 1.68)**	<0.001
Baseline	140	141	1.13 (0.89, 1.42)	0.313
>0 & <3 M	87	107	1.22 (0.87, 1.70)	0.244
≥3 & <6 M	69	72	**2.35 (1.25, 4.42)**	0.008
≥6 & <12 M	99	141	**2.25 (1.38, 3.68)**	0.001
≥12 M	112	133	**2.26 (1.44, 3.56)**	<0.001
Monocyte percentage (%)#	507	594	**1.47 (1.24, 1.74)**	<0.001
Baseline	140	141	1.16 (0.87, 1.55)	0.317
>0 & <3 M	87	107	1.25 (0.86, 1.81)	0.242
≥3 & <6 M	69	72	**1.82 (1.04, 3.17)**	0.034
≥6 & <12 M	99	141	**2.03 (1.23, 3.33)**	0.005
≥12 M	112	133	**2.02 (1.33, 3.08)**	0.001
Eosinophil count (10^9/L)#	507	594	**1.22 (1.09, 1.36)**	0.001
Baseline	140	141	**1.30 (1.00, 1.70)**	0.050
>0 & <3 M	87	107	1.31 (0.99, 1.73)	0.057
≥3 & <6 M	69	72	1.30 (0.94, 1.81)	0.109
≥6 & <12 M	99	141	1.18 (0.92, 1.51)	0.185
≥12 M	112	133	1.14 (0.88, 1.47)	0.334
Eosinophil percentage (%)#	507	594	**1.23 (1.07, 1.40)**	0.003
Baseline	140	141	**1.49 (1.06, 2.10)**	0.021
>0 & <3 M	87	107	1.25 (0.92, 1.70)	0.155
≥3 & <6 M	69	72	1.24 (0.86, 1.78)	0.251
≥6 & <12 M	99	141	1.25 (0.92, 1.70)	0.159
≥12 M	112	133	1.11 (0.83, 1.49)	0.465

**Generalized linear models (logistic regression) were used to examine the odds ratio (ORs) of ISR with an IQR increment of the hematological indices during each follow-up period, adjusting for individual basic characteristics including age, sex, BMI, smoking status, chronic diseases of hypertension and diabetes mellitus. The IQR for monocyte and eosinophil count was 0.21×10^9/L and 0.13×10^9/L, respectively; and the IQR for monocyte and eosinophil percentage was 2.42% and 2.00%, respectively.*

*#ORs were estimated from the generalized linear mixed models, as those in **Table 2**. Each of the blood biochemical indices was included into the model one at a time. Statistically significant effect estimates are in bold.*

DISCUSSION

Inflammation is an important player both for the initiation and progression of coronary artery disease and for coronary plaque instability. Moreover, experimental studies have demonstrated that local and systemic inflammation may promote neointimal proliferation, which serves as the leading mechanism involved in the pathogenesis of ISR.

Classic inflammatory cells such as monocytes have been demonstrated to infiltrate into and accumulate to the stenting site, secreting numerous growth factors, cytokines and promoting the migration and proliferation of vascular smooth muscle cells (SMCs) to the subendothelial space. Some studies believe that the activated monocytes may differentiate into the neointimal SMCs, becoming a component of the neointima (6, 20). Hong YJ and Fukuda D et al. reported that circulating pre-interventional monocyte count may be related to in-stent neointimal volume (6, 7). But no serial blood parameters have been monitored in these studies. Intimal hyperplasia after BMS usually peaks between 6 months−1 year, after which a quiescent period resumes (21, 22); however, this typically occurs earlier within 6 months of stenting in DES (23, 24). Different from previous studies, our results indicate that monocyte count and percentage within 3 months after stent implantation had no predictive value for restenosis. The increase of monocytes in both groups may be related to plaque rupture, inflammation activation, and endothelial repair after stenting. Significant associations of ISR with monocyte percentage and count began at 3 months and lasted for more than 1 year, which suggests the strong early prediction of ISR by monocytes. The optimal cutoff points of monocyte count and percentage were 0.46 (10^9/L) and 7.4%, respectively.

Besides classic inflammation, mounting evidence derived from both experimental and clinical studies suggests an important, yet under-recognized, role for effector cells of allergic inflammation in both the pathogenesis of coronary artery disease and adverse events following stent implantation. Eosinophils may promote thrombus formation, endothelial damaging and coronary plaque instability (5). The metal stent struts and the

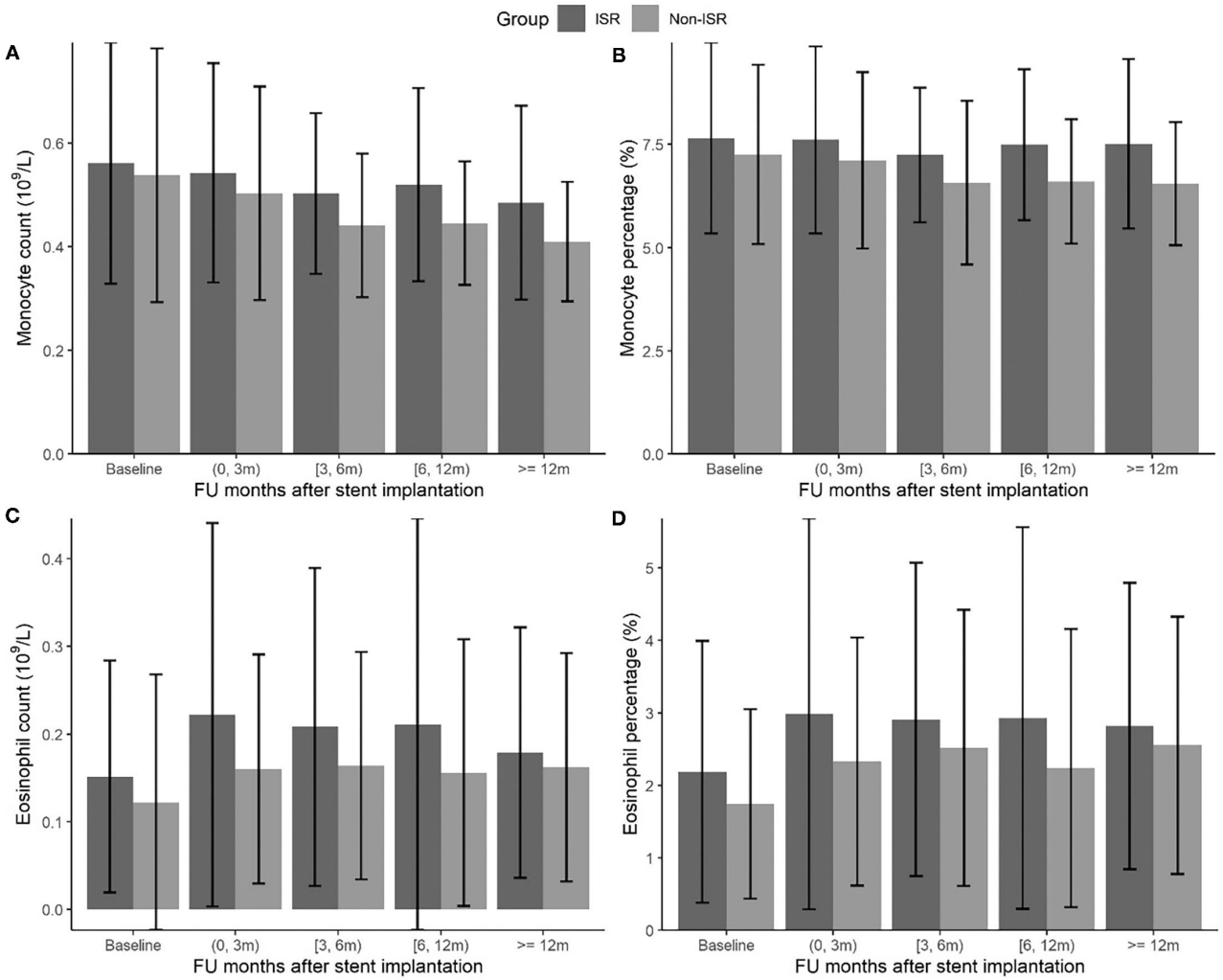

FIGURE 1 | The changes of monocyte and eosinophil count (10^9/L) **(A,C)** and percentage (%) **(B,D)** during the follow-up months between ISR and non-ISR groups.

polymer may trigger local recruitment and activation of allergic inflammation. Histopathologic studies showed that eosinophils were observed to infiltrate into DES at a higher concentration when compared with BMS (25, 26). These findings suggest that allergy-mediated inflammation plays a greater role in DES-related ISR.

Eosinophil count, in epidemiological studies, has been associated with future ischemic heart disease (IHD) (27). Eotaxin, a potent eosinophil chemokine, has been involved in an increased coronary atherosclerotic burden (28) and the baseline serum levels of ECP, a sensitive marker of eosinophil activation can predict the clinical outcome after the implantation of first-generation DES (29). Inconsistencies still arise with regards to the association between eosinophil count and ISR. Hajizadeh R et al. reported that blood eosinophil count measured 6 weeks after PCI has a significant association with the development of ISR within 6-month after DES implantation (30). However, Verdoia M et al. argued that eosinophils levels are not independently associated with the prevalence and extent of coronary artery disease (31).

Different from the above findings, we demonstrated a higher prevalence of ISR in patients with a blood eosinophil count >0.20 (10^9/L) and a percentage $>2.5\%$ ($P = 0.001$, $P = 0.003$ respectively) at baseline. In the supplementary materials, we furthermore analyzed the changes of eosinophils in two groups before and after operation separately. The levels of postinterventional eosinophils in ISR and non-ISR groups were both higher than those at baseline, with the increase in the ISR group significantly greater than that in the non-ISR group (**Supplementary Figure 1**). This result supports the induction of allergic inflammation after stenting. For the insignificant association between ISR and postinterventional eosinophil count and percentage, a possible explanation may lie in the relatively small sample size. Accordingly, our results show that enhanced eosinophilic activation at baseline or post-intervention may possess an early predictive value for ISR.

We also confirmed that low HDL cholesterol increased ISR rates, which is consistent with the finding that HDL cholesterol enhances stent biocompatibility (32). Similar results have also

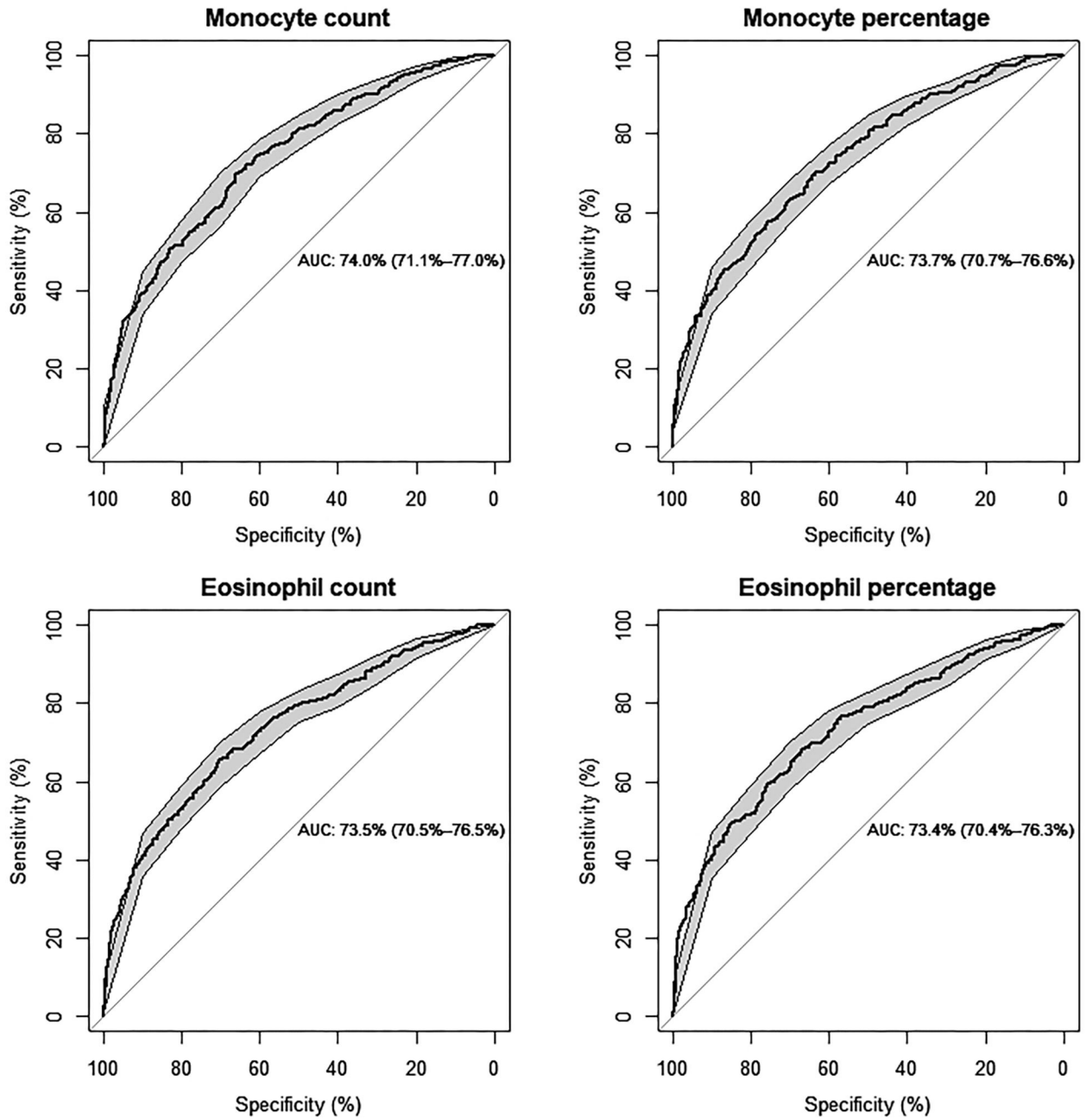

FIGURE 2 | Predictive values of monocyte and eosinophil count (10^9/L) and percentage (%) for the risk of ISR, respectively, by ROC curve analysis (Models are adjusted for individual basic characteristics, including age, sex, BMI, smoking status, chronic diseases of hypertension and diabetes mellitus, and follow-up time. AUC: area under the curve with 95% confidence interval).

been reported in patients with diabetes with coronary heart disease and carotid artery stents implantation (33, 34).

Diabetes mellitus (DM) has been consistently found to be an independent risk factor for poor outcomes following PCI in several previous studies (35). Although the introduction of DES reduces the restenosis rates, diabetic patients as a group continue to experience poor outcomes (36). Although with currently available therapies, some believe that DM is not a risk factor for poor outcomes following DES (37, 38), in our study, HbA1c is still an independent risk factor for ISR, which is in agreement with most previous studies.

In conclusion, our study demonstrates that circulating monocytes at 3 months after DES implantation and baseline eosinophils can strongly predict the risk of ISR. Persistent elevation of monocytes also may be a signal of ISR after PCI. Lower high-density lipoprotein cholesterol and increased HbA1c are significantly associated with ISR. Persistent elevation of monocytes also may be a signal of ISR after PCI.

TABLE 4 | The joint effect of monocyte and eosinophil Count or percentage on the risk of postoperative in-stent restenosis (ISR).

Joint effect	ISR ($n = 507$)	Non-ISR ($n = 594$)	OR (95% CI)*	*P*-value
Monocyte and eosinophil Count[a]				
Both monocyte and eosinophil count are low	153 (30.2)	292 (49.3)	1.00	-
Only monocyte count is high	180 (35.5)	167 (28.2)	2.21 (1.61, 3.04)	< 0.001
Only eosinophil cunt is high	49 (9.7)	57 (9.6)	1.82 (1.14, 2.91)	0.012
Both monocyte and eosinophil count are high	125 (24.7)	76 (12.8)	3.04 (2.06, 4.49)	< 0.001
Monocyte and eosinophil Percentage[b]				
Both monocyte% and eosinophil% are low	149 (29.4)	273 (46.1)	1.00	-
Only monocyte% is high	135 (26.6)	125 (21.1)	1.85 (1.30, 2.62)	< 0.001
Only eosinophil% is high	95 (18.7)	125 (21.1)	1.32 (0.92, 1.91)	0.135
Both monocyte% and eosinophil% are high	128 (25.2)	69 (11.7)	3.06 (2.08, 4.51)	< 0.001

**Generalized linear mixed models (mixed-effects logistic regression) were used to examine the odds ratio (ORs) of ISR.*

[a]The optimal cutoff points were identified as 0.46×10^9/L and 0.20×10^9/L for monocyte and eosinophil count, respectively, to categorize them into low and high levels.

[b]The optimal cutoff points were identified as 7.4% and 2.5% for monocyte and eosinophil percentage, respectively, to categorize them into low and high levels.

DATA AVAILABILITY STATEMENT

The data analyzed in this study is subject to the following licenses/restrictions: We have a series of relevant studies in progress and need to wait until all the results are published. Requests to access these datasets should be directed to Shumei Li, lsmzssdoctor@126.com.

ETHICS STATEMENT

The studies involving human participants were reviewed and approved by Institutional Ethics Committee of Fujian Medical University Union Hospital (Ethics approval number: 2021KY080). The patients/participants provided their written informed consent to participate in this study. Written informed consent was obtained from the individual(s) for the publication of any potentially identifiable images or data included in this article.

AUTHOR CONTRIBUTIONS

SL responsible for the design, manuscript drafting and overall research management. HQ statistical analysis and interpretation. ZL data collection and manuscript drafting. LF and LC guidance and content revision. YG and YZ data collection and implementation of data. LC guidance and supportive contributions. All authors contributed to the article and approved the submitted version.

FUNDING

This project is supported by the funds for the National Natural Science Foundation of China (grant No 8217033).

ACKNOWLEDGMENTS

The authors are grateful to the following colleagues (Hong Zheng, Qiong Jang et al.) for the data collection. We also thank our co-workers (Chaogui Lin, Yafei Peng, Xingchun Zheng, Yukun Luo, Dan Ke, Enhui Yao, Ziwen Zhao, Wei Cai) for their technical support and the volunteers for their cooperation in this study.

SUPPLEMENTARY MATERIAL

The Supplementary Material for this article can be found online at: https://www.frontiersin.org/articles/10.3389/fcvm.2022.764622/full#supplementary-material

Supplementary Figure 1 | The basic and postoperative dynamic changes of monocytes count (10^9/L) **(A)** and percentage (%) **(B)** in ISR and non-ISR groups were observed. All values are presented as mean ± SD. Comparisons were conducted using the one-way ANOVA. A P value of <0.05 was considered to be statistically significant. #P<0.05, ##<0.01 vs ISR; *P<0.05, **P<0.01 vs non-ISR.

REFERENCES

1. Moses JW, Leon MB, Popma JJ, Fitzgerald PJ, Holmes DR, O'Shaughnessy C, et al. Sirolimus-eluting stents versus standard stents in patients with stenosis in a native coronary artery. *N Engl J Med.* (2003) 349:1315–23. doi: 10.1056/NEJMoa035071
2. Ertaş G, Van Beusekom H. Drug eluting stents: current status and new developments. *Anadolu Kardiyol Derg.* (2012) 12:676–83. doi: 10.5152/akd.2012.220
3. Hansson GK. Inflammation, atherosclerosis, and coronary artery disease. *N Engl J Med.* (2005) 352:1685–95. doi: 10.1056/NEJMra043430
4. Dennis W, Klaus L. Immunity and inflammation in atherosclerosis. *Circ Res.* (2019) 124:315–27. doi: 10.1161/CIRCRESAHA.118.313591
5. Niccoli G, Montone RA, Sabato V, Crea F. Role of allergic inflammatory cells in coronary artery disease. *Circulation.* (2018) 38:1736–48. doi: 10.1161/CIRCULATIONAHA.118.035400
6. Hong YJ, Jeong MH, Lim SY, Lee SR, Kim KH, Sohn IS, et al. Preinterventional peak monocyte count and in-stent intimal hyperplasia after coronary stent implantation in human coronary arteries. *Clin Cardiol.* (2005) 28: 512–8. doi: 10.1002/clc.4960281105
7. Fukuda D, Shimada K, Tanaka A, Takahiko K. Circulating monocytes and in-stent neointima after coronary stent implantation. *J Am Coll Cardiol.* (2004) 43:18–23. doi: 10.1016/j.jacc.2003.08.026

8. Murat SN, Yarlioglues M, Celik IE, Kurtul A, Duran M. The relationship between lymphocyte-to-monocyte ratio and bare-metal stent in-stent restenosis in patients with stable coronary artery disease. *Clin Appl Thromb Hemost*. (2017) 23:235–40. doi: 10.1177/1076029615627340
9. Agarwal R, Aurora RG, Siswanto BB, Muliawan HS. The prognostic value of neutrophil-to-lymphocyte ratio across all stages of coronary artery disease. *Coron Artery Dis*. (2021) 33:137–43. doi: 10.1097/MCA.0000000000001040
10. Ösken A, Akdeniz E, Keskin M, Ipek G, Zehir R, Barutça H, et al. Glomerular filtration rate as a predictor of restenosis after carotid stenting using first-generation stents. *Angiology*. (2021) 72:762–9. doi: 10.1177/00033197211014684
11. Cui S, Li K, Ang L, Liu J, Cui L, Song X, et al. Plasma phospholipids and sphingolipids identify stent restenosis after percutaneous coronary intervention. *JACC Cardiovasc Interv*. (2017) 10:1307–16. doi: 10.1016/j.jcin.2017.04.007
12. Zurakowski A, Wojakowski W, Dzielski T, Milewski K, Gościńska-Bis K, endera M, et al. Plasma levels of C-reactive protein and interleukin-10 predict late coronary in-stent restenosis 6 months after elective stenting. *Kardiol Pol*. (2009) 67:623–30.
13. Alfonso F, Cequier A, Angel J, Martí V, Zueco J, Bethencourt A, et al. Value of the American College of Cardiology/American Heart Association angiographic classification of coronary lesion morphology in patients with in-stent restenosis. Insights from the Restenosis Intra-stent Balloon angioplasty versus elective Stenting (RIBS) randomized trial. *Am Heart J*. (2006) 151:e681–689. doi: 10.1016/j.ahj.2005.10.014
14. Bashir SA, Duffy SW, Qizilbash N. Repeat measurement of case-control data: Corrections for measurement error in a study of ischaemic stroke and haemostatic factors. *Int J Epidemiol*. (1997) 26:64–70. doi: 10.1093/ije/26.1.64
15. Schildcrout JS, Schisterman EF, Mercaldo ND, Rathouz PJ, Heagerty PJ. Extending the case-control design to longitudinal data: stratified sampling based on repeated binary outcomes. *Epidemiology*. (2018) 29:67–75. doi: 10.1097/EDE.0000000000000764
16. Ucar FM. A potential marker of bare metal stent restenosis: monocyte count - to- HDL cholesterol ratio. *BMC Cardiovasc Disord*. (2016) 16:1–7. doi: 10.1186/s12872-016-0367-3
17. Källberg H, Ahlbom A, Alfredsson L. Calculating measures of biological interaction using R. *Eur J Epidemiol*. (2006) 21:571–3. doi: 10.1007/s10654-006-9037-6
18. Zhao J, Wang X. Wang H, Zhao Y, Fu X. Occurrence and predictive factors of restenosis in coronary heart disease patients underwent sirolimus-eluting stent implantation. *Ir J Med Sci*. (2020) 189:907–15. doi: 10.1007/s11845-020-02176-9
19. *R Core Team. R: A language and environment for statistical computing R Foundation for Statistical Computing, Vienna, Austria* (2019). Available online at: https://www.r-project.org/ (accessed June 19, 2021).
20. Buja LM. Vascular responses to percutaneous coronary intervention with bare-metal stents and drug-eluting stents: a perspective based on insights from pathological and clinical studies. *J Am Coll Cardiol*. (2011) 57:1323–6. doi: 10.1016/j.jacc.2010.11.033
21. Libby P. Inflammation in atherosclerosis. *Arterioscler Thromb Vasc Biol*. (2012) 32:2045–51. doi: 10.1161/ATVBAHA.108.179705
22. Komatsu R, Ueda M, Naruko T. Kojima A, Becker AE. Neointimal tissue response at sites of coronary stenting in humans: macroscopic, histological, and immunohistochemical analyses. *Circulation*. (1998) 98:224–33. doi: 10.1161/01.CIR.98.3.224
23. Crea F, Libby P. Acute coronary syndromes: the way forward from mechanisms to precision treatment. *Circulation*. (2017) 136:1155–66. doi: 10.1161/CIRCULATIONAHA.117.029870
24. Park SJ, Kang SJ, Virmani R, Nakano M, Ueda Y. In-stent neoatherosclerosis: a final common pathway of late stent failure. *J Am Coll Cardiol*. (2012) 59:2051–7. doi: 10.1016/j.jacc.2011.10.909
25. Rittersma SZ, Meuwissen M, van der Loos CM. Koch KT, de Winter RJ, Piek JJ, et al. Eosinophilic infiltration in restenotic tissue following coronary stent implantation. *Atherosclerosis*. (2006) 184:157–62. doi: 10.1016/j.atherosclerosis.2005.03.049
26. Niccoli G, Montone RA. Ferrante G, Crea F. The evolving role of inflammatory biomarkers in risk assessment after stent implantation. *J Am Coll Cardiol*. (2010) 56:1783–93. doi: 10.1016/j.jacc.2010.06.045
27. Sweetnam PM, Thomas HF, Yarnell JW. Baker IA, Elwood PC. Total and differential leukocyte counts as predictors of ischemic heart disease: the Caerphilly and Speedwell studies. *Am J Epidemiol*. (1997) 145:416–21. doi: 10.1093/oxfordjournals.aje.a009123
28. Emanuele E, Falcone C, D'Angelo A, Minoretti P, Buzzi MP, Bertona M, et al. Association of plasma eotaxin levels with the presence and extent of angiographic coronary artery disease. *Atherosclerosis*. (2006) 186:140–5. doi: 10.1016/j.atherosclerosis.2005.07.002
29. Niccoli G, Schiavino D, Belloni F, Ferrante G, La Torre G, Conte M, et al. Pre-intervention eosinophil cationic protein serum levels predict clinical outcomes following implantation of drug-eluting stents. *Eur Heart*. (2009) 30:1340–7. doi: 10.1093/eurheartj/ehp120
30. Hajizadeh R, Ghaffari S, Separham A, Shokouhi B, Kavandi H, Pourafkari L, et al. The value of peripheral blood eosinophil count in predicting in-stent restenosis in patients with stable angina pectoris undergoing drug eluting stenting. *Rom J Intern Med*. (2017) 55:1–18 doi: 10.1515/rjim-2017-0024
31. Verdoia M, Schaffer A, Cassetti E, Di Giovine G, Marino P, Suryapranata H, et al. Absolute eosinophils count and the extent of coronary artery disease: a single centre cohort study. *J Thromb Thrombolysis*. (2015) 39:459–66. doi: 10.1007/s11239-014-1120-3
32. Vanags LZ, Wong NKP, Nicholls SJ, Bursill CA. High-density lipoproteins and apolipoprotein A-I improve stent biocompatibility. *Arterioscler Thromb Vasc Biol*. (2018) 38:1691–701. doi: 10.1161/ATVBAHA.118.310788
33. Topakian R, Sonnberger M, Nussbaumer K, Haring HP, Trenkler J, Aichner FT. Postprocedural high-density lipoprotein cholesterol predicts carotid stent patency at 1 year. *Eur J Neurol*. (2008) 15:179–84. doi: 10.1111/j.1468-1331.2007.02026.x
34. Sukhija R, Aronow WS, Sureddi R, Aleti S, Molavi B, Sachdeva R, et al. Predictors of in-stent restenosis and patient outcome after percutaneous coronary intervention in patients with diabetes mellitus. *Am J Cardiol*. (2007) 100:777–80. doi: 10.1016/j.amjcard.2007.03.097
35. Stettler C, Allemann S, Wandel S, Kastrati A, Morice MC,Schömig A, et al. Drug eluting and bare metal stents in people with and without diabetes: collaborative network meta-analysis. *BMJ*. (2008) 337:a1331. doi: 10.1136/bmj.a1331
36. Kedhi E, Généreux P, Palmerini T, McAndrew TC, Parise H, Mehran R, et al. Impact of coronary lesion complexity on drug-eluting stent outcomes in patients with and without diabetes mellitus: analysis from 18 pooled randomized trials. *J Am Coll Cardiol*. (2014) 63:2111–8. doi: 10.1016/j.jacc.2014.01.064
37. Paramasivam G, Devasia T, Jayaram A, UK AR, Rao MS, Vijayvergiya R, et al. In-stent restenosis of drug-eluting stents in patients with diabetes mellitus: Clinical presentation, angiographic features, and outcomes. *Anatol J Cardiol*. (2020) 23:28–34. doi: 10.14744/AnatolJCardiol.2019.72916
38. Zhao L, Zhu W, Zhang X, He D, Guo C. Effect of diabetes mellitus on long-term outcomes after repeat drug-eluting stent implantation for in-stent restenosis. *BMC Cardiovasc Disord*. (2017) 17:1–7. doi: 10.1186/s12872-016-0445-6

Conflict of Interest: The authors declare that the research was conducted in the absence of any commercial or financial relationships that could be construed as a potential conflict of interest.

frontiers in Cardiovascular Medicine

ORIGINAL RESEARCH
published: 28 February 2022
doi: 10.3389/fcvm.2022.762351

A Novel Classification for Predicting Chronic Total Occlusion Percutaneous Coronary Intervention

Dongfeng Zhang[1], Haoran Xing[1], Rui Wang[2], Jinfan Tian[1], Zhiguo Ju[3], Lijun Zhang[4], Hui Chen[5], Yi He[2†] and Xiantao Song[1*†]*

[1] Department of Cardiology, Beijing Anzhen Hospital, Capital Medical University, Beijing, China, [2] Department of Radiology, Beijing Friendship Hospital, Capital Medical University, Beijing, China, [3] College of Medical Imaging, Shanghai University of Medicine & Health Science, Shanghai, China, [4] Department of Radiology, Beijing Anzhen Hospital, Capital Medical University, Beijing, China, [5] Department of Cardiology, Beijing Friendship Hospital, Capital Medical University, Beijing, China

Aims: Chronic total occlusion (CTO) percutaneous coronary intervention (PCI) is characterized by a low success rate and an increase in complications. This study aimed to explore a new and simple classification method based on plaque composition to predict guidewire (GW) crossing within 30 min of CTO lesions.

Methods: This study consecutively enrolled individuals undergoing attempted PCI of CTO who underwent coronary computed tomographic angiography (CCTA) within 2 months. Lesions were divided into soft and hard CTO groups according to the necrotic core proportion.

Results: In this study, 207 lesions were divided into soft (20.3%) and hard CTO (79.7%) groups according to a necrotic core percentage cutoff value of 72.7%. The rate of successful GW crossing within 30 min (57.6 vs. 85.7%, $p = 0.004$) and final success (73.3 vs. 95.2%, $p = 0.001$) were much lower in the hard CTO group. For patients with hard CTO, previous failed attempt, proximal side branch, bending $>$ 45 degrees calcium $\geq$ 50% cross-sectional area (CSA), and distal reference diameter $\leq$ 2.5 mm were demonstrated to be associated with GW failure within 30 min. For patients with soft CTO, only blunt entry was proved to be an independent predictive factor of GW failure within 30 min.

Conclusions: Grouping CTO lesions according to the proportion of necrotic core is reasonable and necessary in predicting GW crossing within 30 min. A soft CTO with a necrotic core is more likely to be recanalized compared with a hard CTO with fibrous and/or dense calcium. Different plaque types have variable predictive factors.

Keywords: chronic total occlusion, percutaneous coronary intervention, computed tomographic angiography, plaque composition, coronary artery disease

OPEN ACCESS

Edited by:
Marouane Boukhris, Tunis El Manar University, Tunisia

Reviewed by:
Takahide Kodama, Toranomon Hospital, Japan
Robert Jeenchen Chen, Stanford University, United States

***Correspondence:**
Xiantao Song
songxiantao0929@qq.com
Yi He
heyi139@sina.com

† These authors have contributed equally to this work

Specialty section:
This article was submitted to Coronary Artery Disease, a section of the journal Frontiers in Cardiovascular Medicine

Received: *21 August 2021*
Accepted: *10 January 2022*
Published: *28 February 2022*

Citation:
Zhang D, Xing H, Wang R, Tian J, Ju Z, Zhang L, Chen H, He Y and Song X (2022) A Novel Classification for Predicting Chronic Total Occlusion Percutaneous Coronary Intervention. Front. Cardiovasc. Med. 9:762351. doi: 10.3389/fcvm.2022.762351

INTRODUCTION

A coronary chronic total occlusion (CTO) is generally accepted as 100% occlusion of a coronary artery for a duration $\geq$ 3 months. Approximately, one-third of coronary artery disease (CAD) is partly due to CTO lesions that are identified by coronary angiography (1). CTO was once treated as the last frontier of interventional cardiology because of its lower success rate and higher risk of

complications. Nevertheless, continuous efforts have been made to increase the success rate of CTO percutaneous coronary intervention (PCI) in view of numerous clinical benefits, including reduced angina pectoris, increased ventricular function, and improved quality of life (2, 3).

In the past few decades, the rate of successful CTO PCI has steadily increased due to the development of equipment, progression of technology, and accumulation of operation experience. Meanwhile, several systems were developed to determine the grade of difficulty likely to be encountered in CTO PCI (4–9), using scoring systems helped in selecting the appropriate candidates and optimizing treatment strategies. However, subsequent validation trials have revealed that the predictive values of existing models are unsatisfactory (10). Patients with low scores indicating low difficulty always experience failed procedures and vice versa. We thus assume that some potential factors significantly influence CTO PCI outcomes.

Plaque compositions vary with CAD type and are significantly associated with prognosis (11). CTO pathophysiology revealed that plaque composition with the gradual replacement of cholesterol and foam cells with fibrous and calcification may be an important factor associated with the feasibility of passaging the occlusion with a wire (12). However, previous scoring systems only considered the impact of calcification and disregarded other components. Coronary computed tomographic angiography (CCTA) is a useful diagnostic tool for the analysis of coronary plaques (13). Therefore, this study aimed to explore a new classification method based on CCTA derived plaque composition to predict the guidewire (GW) crossing within 30 min of CTO lesions.

MATERIALS AND METHODS

Study Design and Population

We retrospectively enrolled consecutive patients undergoing attempted PCI of invasive coronary angiography (ICA) confirmed CTO with a CCTA performed within 2 months before ICA in the time period between September 2015 and September 2019 from two high volume centers (Beijing Anzhen Hospital and Beijing Friendship Hospital, Beijing, China). CTO was defined as Thrombolysis in Myocardial Infarction (TIMI) flow grade 0 in a native vessel and estimated to have lasted for at least 3 months according to the first onset of angina pectoris, previous history of myocardial infarction, or comparison with a prior angiogram. All enrolled candidates had either typical angina symptoms or functional tests that demonstrated myocardial ischemia.

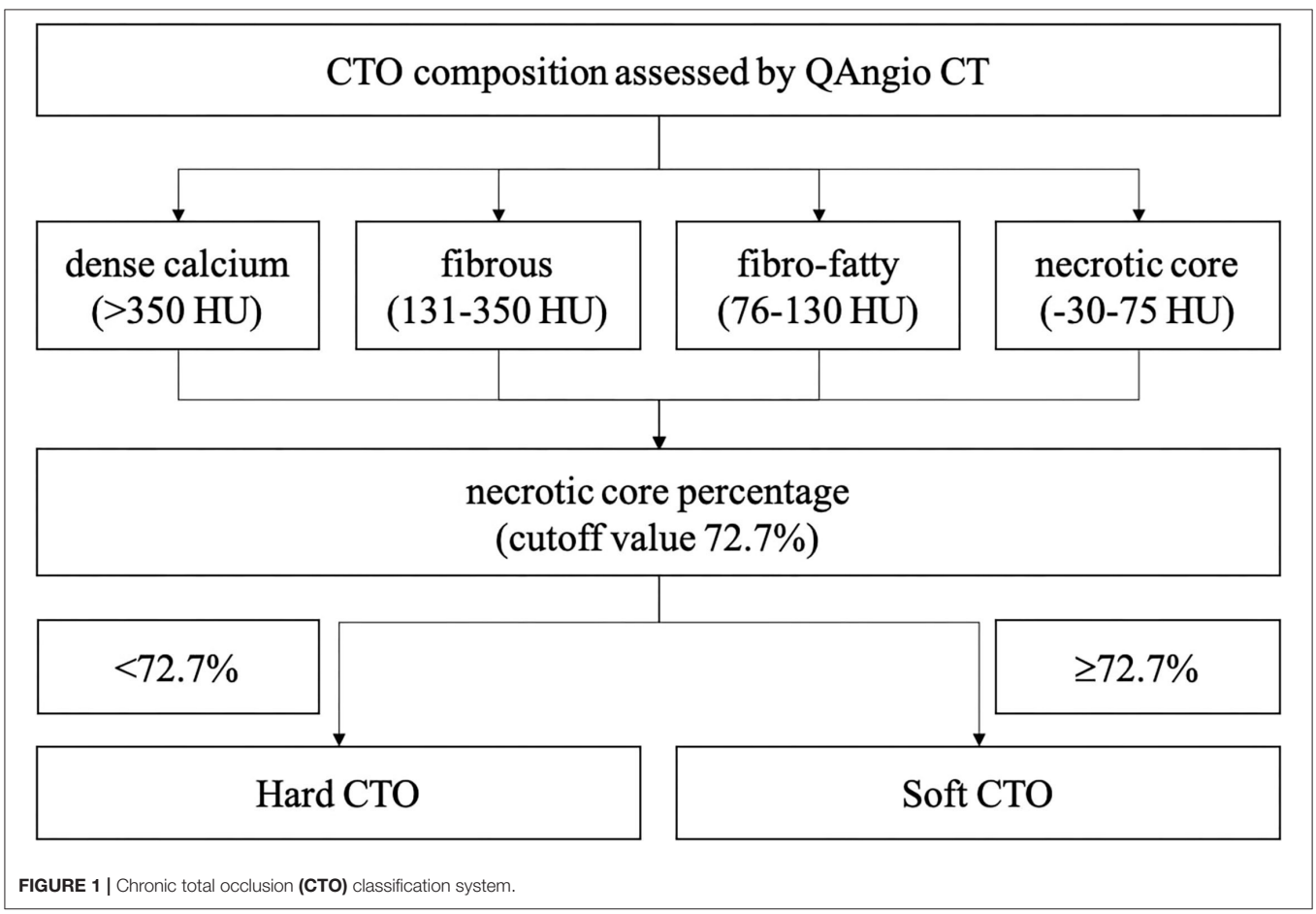

FIGURE 1 | Chronic total occlusion **(CTO)** classification system.

TABLE 1 | Baseline clinical characteristics.

	Overall ($n = 207$)	Soft CTO ($n = 42$)	Hard CTO ($n = 165$)	*p*-Value
Age, years	58.7 ± 10.7	57.5 ± 12.1	59.0 ± 10.3	0.295
Male, *n* (%)	176 (85.0)	39 (92.9)	137 (83.0)	0.111
BMI, kg/m^2	26.3 ± 3.3	26.5 ± 3.5	26.3 ± 3.3	0.759
Smoking history, *n* (%)	112 (54.1)	24 (57.1)	88 (53.3)	0.658
Hypertension, *n* (%)	131 (63.3)	24 (57.1)	107 (64.8)	0.355
Diabetes, *n* (%)	62 (30.0)	13 (31.0)	49 (29.7)	0.874
Hyperlipidemia, *n* (%)	82 (39.6)	14 (33.3)	68 (41.2)	0.351
Previous MI, *n* (%)	53 (25.6)	12 (28.6)	41 (24.8)	0.622
Previous PCI, *n* (%)	39 (18.8)	6 (14.3)	33 (20.0)	0.398
Previous CABG, *n* (%)	2 (1.0)	0 (0)	2 (1.2)	1.000
Prior stroke, *n* (%)	19 (9.2)	5 (11.9)	14 (8.5)	0.699
Renal disease, *n* (%)	13 (6.3)	2 (4.8)	11 (6.7)	0.922
PVD, *n* (%)	10 (4.8)	2 (4.8)	8 (4.8)	1.000
LVEF (%)	61.7 ± 8.3	61.0 ± 5.8	61.8 ± 8.8	0.113
eGFR, mL/min/1.73 m^2	94.1 ± 16.1	92.8 ± 19.6	94.4 ± 15.2	0.987
TG, mmol/L	1.8 ± 1.0	1.7 ± 0.9	1.8 ± 1.0	0.692
TC, mmol/L	3.9 ± 1.0	3.7 ± 1.0	3.9 ± 0.9	0.205
LDL, mmol/L	2.3 ± 0.8	2.1 ± 0.8	2.3 ± 0.8	0.312
HDL, mmol/L	1.0 ± 0.2	1.0 ± 0.2	1.0 ± 0.2	0.126
FBG, mmol/L	6.6 ± 2.3	6.5 ± 2.3	6.6 ± 2.3	0.393
HbA1c (%)	6.4 ± 1.1	6.4 ± 1.1	6.4 ± 1.1	0.487
Occlusion time ≥ 12 months or unknown, *n* (%)	137 (66.2)	31 (73.8)	106 (64.2)	0.242
Reattempt of failed CTO PCI, *n* (%)	28 (13.5)	4 (9.5)	24 (14.5)	0.396

CTO, chronic total occlusion; BMI, body mass index; MI, myocardial infarction; PCI, percutaneous coronary intervention; CABG, coronary artery bypass grafting; PVD, peripheral vascular disease; LVEF, left ventricular ejection fraction; eGFR, estimated glomerular filtration rate; TG, triglyceride; TC, total cholesterol; LDL, low-density lipoprotein; HDL, high-density lipoprotein; FBG, fasting blood glucose.

The percutaneous coronary intervention was performed by experienced interventional cardiologists with a minimum of 50 CTO cases per year. The interventional strategies, including GW selection and crossing approach, were left to the discretion of the operator. Except for CTO vessels that were supplied only by ipsilateral collaterals, the use of bilateral injection was essential. Crossing wires were selected in a step-up approach beginning with soft polymeric wires and then stiff flat or tapered wires. Antegrade approaches including the manipulation of stiff wires and parallel wire technique as well as retrograde approach were used.

The primary endpoint was a successful GW crossing through the CTO lesion within 30 min as described in the J-CTO trial (4). Furthermore, GW crossing at any time was set as a secondary outcome. The study protocol was approved by the Institutional Review Boards of Beijing Anzhen Hospital (2020070X) and Beijing Friendship Hospital (2020-P2-228-01) and was conducted according to the principles of the Declaration of Helsinki.

CCTA Protocol

Coronary computed tomographic angiography was performed within 2 months (median interval of 6 days) before ICA using a dual-source CT scanner (Somatom Definition FLASH, Siemens Healthcare, Germany) or a 256-slice CT scanner (Revolution CT, General Electric, MA, USA). For the prospectively ECG-triggered CCTA, the patients with body mass index (BMI) < 24 kg/m^2 were scanned at 100 kV, and those with BMIs of ≥ 24 kg/m^2 were scanned at 120 kV. The tube current was regulated by automatic exposure control. The acquisition window was performed within the 70% R-R interval for heart rates (HR) of < 60 bpm, 40–70% R-R interval for HRs of 60–80 bpm, and 30–40% R-R interval for HRs of > 80 bpm. Bolus-tracking was conducted by placing the region of interest in the root of the aorta, and images were automatically acquired 6 s after a predefined threshold of 100 Hounsfield units (HU) was reached. The scanning range was set from the tracheal bifurcation to 1 cm below the diaphragm. The contrast agent was injected with a dual-head power injector (Stellant D, Medrad, PA, USA) through an 18–20-gauge intravenous needle placed in the right antecubital vein. Then, 50–70 ml of contrast agent (Ultravist, 370 mg iodine/ml, Bayer, Germany) were injected, followed by 30 ml of saline as a bolus chaser with an injection rate of 4.5–5 ml/s for all phases.

CCTA Analysis

Image quality was assessed by the two experienced radiologists based on trans-axial images following the Society of CCT guidelines.

A separate commercial software with a semi-automated 3-dimensional contour detection algorithm (QAngio CT Research

TABLE 2 | Angiographic and procedural characteristics.

	Overall (*n* = 207)	Soft CTO (*n* = 42)	Hard CTO (*n* = 165)	*p*-Value
Angiographic characteristics				
Target vessel				0.177
LM, *n* (%)	2 (1.0)	0 (0)	2 (1.2)	
LAD, *n* (%)	85 (41.1)	12 (28.6)	73 (44.2)	
LCX, *n* (%)	22 (10.6)	7 (16.7)	15 (9.1)	
RCA, *n* (%)	98 (47.3)	23 (54.8)	75 (45.5)	
Multiple occlusion, *n* (%)	9 (4.3)	2 (4.8)	7 (4.2)	1.000
Ostial location, *n* (%)	10 (4.8)	1 (2.4)	9 (5.5)	0.670
Blunt stump at entry, *n* (%)	76 (36.7)	12 (28.6)	64 (38.8)	0.220
Side branch at entry, *n* (%)	90 (43.5)	14 (33.3)	76 (46.1)	0.137
Bending > 45°, n (%)	48 (23.2)	11 (26.2)	37 (22.4)	0.606
Calcium, any, *n* (%)	45 (21.7)	2 (4.8)	43 (26.1)	0.003
Heavy calcium, *n* (%)	20 (9.7)	0 (0)	20 (12.1)	0.037
Occlusion length ≥ 20 mm, *n* (%)	85 (41.1)	16 (38.1)	69 (41.8)	0.661
Bridging collaterals, *n* (%)	21 (10.1)	5 (11.9)	16 (9.7)	0.891
Retrograde collaterals grade ≥ 2, *n* (%)	195 (94.2)	37 (88.1)	158 (95.8)	0.127
Severe proximal vessel disease, *n* (%)	68 (32.9)	16 (38.1)	52 (31.5)	0.418
Severe distal vessel disease, *n* (%)	86 (41.5)	16 (38.1)	70 (42.4)	0.611
Procedural characteristics				
Radial access, *n* (%)	85 (41.3)	17 (40.5)	68 (41.5)	0.908
Guiding catheter				0.609
6-F, *n* (%)	136 (65.7)	29 (69.0)	107 (64.8)	
7-F, *n* (%)	71 (34.3)	13 (31.0)	58 (35.2)	
Retrograde injection, *n* (%)	97 (46.9)	18 (42.9)	79 (47.9)	0.560
Retrograde wiring approach, *n* (%)	19 (9.2)	0 (0)	19 (11.5)	0.045
Over-the-wire balloon support, *n* (%)	10 (4.8)	0 (0)	10 (6.1)	0.218
Simultaneous PCI for non-CTO lesion, *n* (%)	73 (35.3)	17 (40.5)	56 (33.9)	0.429
Mean number of wires, *n* (%)	3.6 ± 1.8	3.0 ± 1.2	3.8 ± 2.0	0.016
Successful GW crossing within 30, *n* (%)	131 (63.3)	36 (85.7)	95 (57.6)	0.001
Final successful GW crossing, *n* (%)	161 (77.8)	40 (95.2)	121 (73.3)	0.002
Successful implantation of stent, *n* (%)	152 (73.4)	36 (85.7)	116 (70.3)	0.044
Dissection or perforation, *n* (%)	9 (4.2)	2 (4.8)	7 (4.2)	1.000

CTO, chronic total occlusion; LM, left main; LAD, left anterior descending; LCX, left circumflex; RCA, right coronary artery; PCI, percutaneous coronary intervention; GW, guidewire.

Edition version 3.1.4, MEDIS Medical Imaging Systems, Leiden, the Netherlands) was used to quantify CTO lesion metrics. Predefined fixed intensity cutoff values on the HU were selected to assess the plaque constitution. Currently, different cut-off values are available in the literature, which is obtained by comparing CTA with intravascular ultrasound virtual histology (IVUS VH) or histological examination. For the current analysis, the fixed HU cut-off values used for classifying were: dense calcium (>350 HU), fibrous (131–350 HU), fibro-fatty (76–130 HU), and necrotic core (−30 to 75 HU). These values were initially based on the paper by Brodoefel et al. (14) and empirically optimized using three representative training sets. The volume and proportion of each component were calculated.

Coronary tree lumen and wall were automatically extracted and manually corrected when necessary. All CTO characteristics were retrieved. Multiple occlusion was defined as at least two completely interrupted contrast media opacities with an interval of at least 5 mm. Stump morphology was categorized as tapered or blunt. Proximal side branch was defined as any side branch within 3 mm near the entrance. Bending was recognized as the presence of at least one bend of >45 degrees throughout the occlusion route. Severe calcium was defined as the presence of high-density plaque involving ≥50% of the vessel cross-sectional area (CSA). Additionally, occlusion length and proximal and distal vessel diameters were analyzed quantitatively. Occlusion length was then categorized as either <20 or ≥20 mm. CT-RECTOR, KCCT,

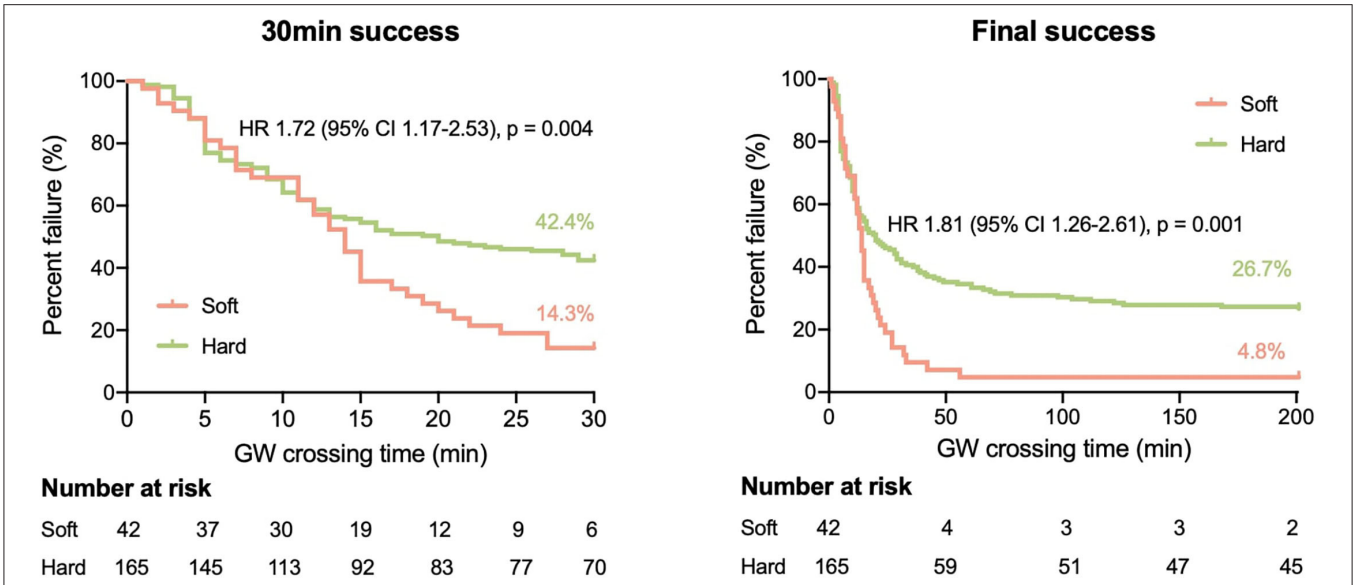

FIGURE 2 | Kaplan–Meier curves of successful 30 min (left) and final (right) guidewire (GW) crossing in patients with soft and hard CTO.

and CTA J-CTO scores for each individual CTO were then calculated.

Coronary Angiography and PCI Procedure Analysis

Coronary angiographic analyses were conducted by the two experienced cardiologists blinded to the results from clinical characteristics and CCTA. Angiographic variables, including target vessel, multiple occlusions, ostial CTO, blunt entry site, side branch, bending, calcification, occlusion length, bridging collaterals, the degree of retrograde collaterals according to the Rentrop classification, and severe proximal and distal vessel diseases, were determined as previously described. Procedural indexes were retrieved, including access site, guiding catheter size, retrograde approach, over-the-wire balloon support, GW numbers, and procedure outcomes. J-CTO and PROGRESS-CTO scores were then calculated according to previous studies.

Statistical Analysis

Continuous variables were described as the mean and SD or median with interquartile range (IQR). The Student's *t*-test or the Mann–Whitney *U*-test was used to assess differences in continuous variables among groups. Categorical variables were expressed as absolute numbers and frequencies (%) and were compared with Pearson's chi-squared test or Fisher's exact test. As calcium and fibrous were both considered to be hard compositions, the receiver operating characteristic (ROC) curve of necrotic core percentage was generated, and the cutoff value was used to divide the patients into soft or hard CTO groups. Kaplan–Meier analysis was performed to compare outcomes between groups. A Log-rank test was adopted to compare rates of endpoints. To explore the risk factors associated with successful GW crossing of the CTO within 30 min, we performed multivariate regression using the overall, soft, and hard cohorts. Independent variables were selected to develop a prediction model for hard CTOs. The difficulty score for each hard CTO lesion was calculated by assigning points for each factor and then summing all points. The performance of the prediction model was assessed by the ROC curve. All analyses were performed using SPSS 21.0 (IBM Corp., Armonk, NY, USA). Differences obtained using a two-tailed test and $p < 0.05$ were deemed statistically significant.

RESULTS

Clinical Characteristics

A total of 201 patients (207 lesions) were enrolled. A ROC curve of necrotic core percentage was generated, and the cutoff value of 72.7% was used to divide the patients into soft or hard CTO groups. Lesions with the necrotic core proportion of ≥72.7% of the entire CTO plaque were defined as soft CTO ($n = 42$), whereas those with < 72.7% were defined as hard CTO ($n = 165$). **Figure 1** shows how the CTO classification system works. No differences in baseline clinical characteristics, including age, sex, smoking history, and medical histories, were observed (**Table 1**). Most of the patients were attempted for the first time PCI (86.5%).

Coronary Angiographic Characteristics

The most common target vessel for both groups was the right coronary artery (RCA) (**Table 2**). No obvious difference in plaque characteristics was detected except for calcium (4.8 vs. 26.1%, $p = 0.003$). Only two (4.8%) soft CTOs had calcium. Patients with hard CTO underwent the retrograde wiring approach more frequently (11.5 vs. 0%, $p = 0.045$) and consumed more guiding wires (3.8 ± 2.0 vs. 3.0 ± 1.2, $p = 0.016$). However, the rate of successful GW crossing within 30 min (57.6 vs. 85.7%, $p = 0.004$)

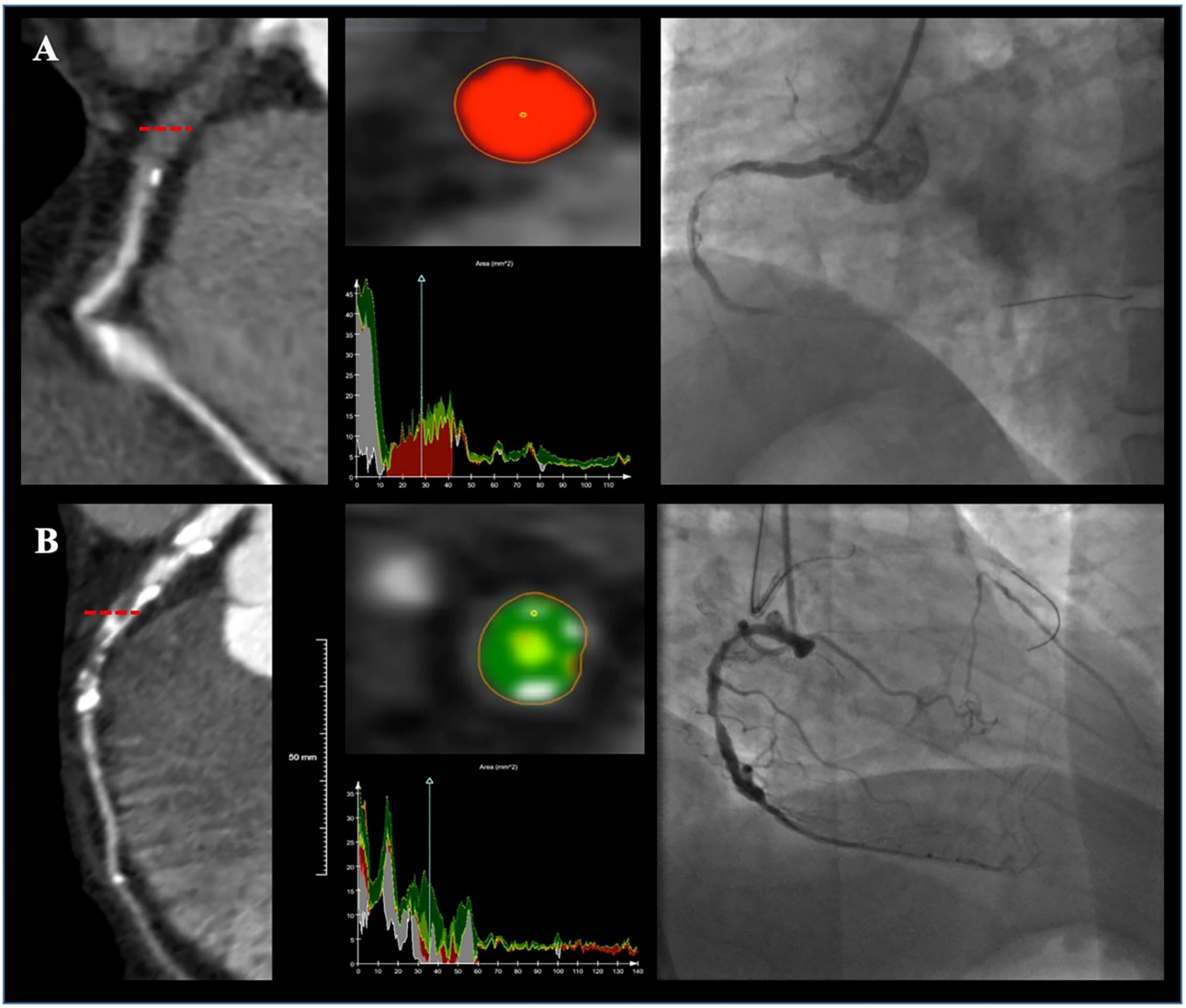

FIGURE 3 | Two representative cases showing plaque compositions and guidewire (GW) crossing outcomes. Lesion **(A)** was a right coronary artery (RCA) lesion with soft CTO (80.7% necrotic core, 17.4% fibrous fatty, 1.6% fibrous, and 0% dense calcium) and the GW was successfully passed at 20 min. Lesion **(B)** was a left anterior descending artery (LAD) lesion with hard CTO (46.4% fibrous, 21.9% dense calcium, 17.8% fibrous fatty, and 13.5% necrotic core) and the GW was failed to be advanced cross the CTO.

and final success (73.3 vs. 95.2%, $p = 0.001$) was much lower in the hard CTO group. The difference was observed beginning at about 13 min (**Figure 2**). Eventually, stents were implanted in 36 (85.7%) lesions of the soft CTO group and 116 (70.3%) of the hard CTO group. **Figure 3** shows representative cases of plaque compositions and GW crossing outcomes.

CCTA Characteristics

In terms of characteristics detected by CCTA, the proximal reference vessel diameter in lesions with hard CTO was much larger (3.0 ± 0.7 vs. 2.8 ± 0.7, $p = 0.013$) (**Table 3**). Hard CTO was more likely to characterized by blunt stump at the entry (39.4 vs. 21.4%, $p = 0.030$), proximal side branch (35.8 vs. 14.3%, $p = 0.007$), and calcification ($p < 0.001$).

Risk Scoring Systems

We compared the current predictive scores between the soft CTO and hard CTO groups (**Table 4**). The J-CTO, KCCT, and PROGRESS-CTO scores were similar between the two groups. CT-RECTOR (1.8 ± 1.2 vs. 1.2 ± 0.9, $p = 0.002$) and CTA-J CTO (1.6 ± 1.3 vs. 0.8 ± 0.9, $p < 0.001$) were much higher in the hard CTO group. The predictive values of each scoring system, as evaluated by ROC curves, are shown in **Figure 4**.

Independent Predictive Factors

To investigate the independent predictors of successful 30 min GW crossing, we performed the multivariate analysis that included clinical and CCTA variables, such as age, sex, BMI,

TABLE 3 | Computed tomographic characteristics.

	Overall ($n = 207$)	Soft CTO ($n = 42$)	Hard CTO ($n = 165$)	*p*-Value
Occlusion length, mm	20.3 ± 15.8	16.3 ± 10.4	21.3 ± 16.8	0.066
Occlusion length ≥ 15 mm, *n* (%)	107 (51.7)	21 (50.0)	86 (52.1)	0.806
Occlusion length ≥ 20 mm, *n* (%)	80 (38.6)	12 (28.6)	68 (41.2)	0.133
Multiple occlusion, *n* (%)	10 (4.8)	1 (2.4)	9 (5.5)	0.670
Proximal reference vessel diameter, mm	3.0 ± 0.7	2.8 ± 0.7	3.0 ± 0.7	0.013
Distal reference vessel diameter, mm	2.2 ± 0.5	2.2 ± 0.5	2.2 ± 0.5	0.755
Blunt stump, *n* (%)	74 (35.7)	9 (21.4)	65 (39.4)	0.030
Side branch, *n* (%)	65 (31.4)	6 (14.3)	59 (35.8)	0.007
Bending > 45°, *n* (%)	42 (20.3)	9 (21.4)	33 (20.0)	0.837
Calcium, any, *n* (%)	80 (38.6)	0 (0)	80 (48.5)	<0.001
Calcium ≥ 50% CSA, *n* (%)	63 (30.4)	0 (0)	63 (38.2)	<0.001

CTO, chronic total occlusion; CSA, cross-sectional area.

TABLE 4 | Predictive assessment of different scoring systems.

	Overall ($n = 207$)	Soft CTO ($n = 42$)	Hard CTO ($n = 165$)	*p*-Value
J-CTO	1.4 ± 1.1	1.1 ± 1.0	1.4 ± 1.1	0.057
PROGRESS-CTO	1.2 ± 0.8	1.1 ± 0.8	1.2 ± 0.8	0.671
CT-RECTOR	1.7 ± 1.2	1.2 ± 0.9	1.8 ± 1.2	0.002
KCCT	2.4 ± 1.8	1.9 ± 1.1	2.5 ± 1.9	0.162
CTA-J CTO	1.5 ± 1.3	0.8 ± 0.9	1.6 ± 1.3	<0.001

previous failed attempt, blunt stump, side branch, bending, and calcification.

For patients with hard CTO, conventional predictive factors established in the J-CTO, PROGRESS-CTO, CT-RECTOR, KCCT, and CTA-J CTO scoring systems, including previous failed attempt [hazard ratio (*HR*) 0.215, 95% *CI* 0.070–0.664, $p = 0.008$], proximal side branch (*HR* 0.250, 95% *CI* 0.110–0.571, $p = 0.001$), bending > 45 degrees (*HR* 0.066, 95% *CI* 0.020–0.218, $p < 0.011$), and calcium ≥ 50% cross-sectional area (*HR* 0.325, 95% *CI* 0.147–0.717, $p = 0.005$) were validated. Additionally, distal reference diameter ≤ 2.5 mm was proved to be associated with GW failure (*HR* 4.748, 95% *CI* 1.698–13.275, $p = 0.003$). For patients with soft CTO, only blunt entry was proved to be an independent predictive factor of GW failure within 30 min (*HR* 0.081, 95% *CI* 0.012–0.563, $p = 0.011$) (**Table 5**).

Development of the HCTO Score

Each independent variable developed in the regression analysis was assigned an integer score. According to the beta coefficients, previous failed attempts (1.536), distal reference diameter ≤ 2.5 mm (1.558), proximal side branch (1.386), and calcium ≥ 50% cross-sectional area (1.124) were assigned an integer score of 1. Bending > 45 degrees (2.720) was assigned 2. For each hard CTO lesion, a total difficulty score for PCI, which is the HCTO score, was determined by summing all points. The area under the ROC curve for the HCTO score was 0.802. **Figure 5** shows the relationship between the HCTO scores and successful GW crossing within 30 min. Then, the patients were categorized into 3 groups with dramatically increase in difficulty: easy (HCTO score of 0–1), intermediate (HCTO score of 2–3), and hard (HCTO score of 4–6). The success rate of CTO recanalization within 30 min for each group was 89.2, 53.5, and 5.6%, respectively.

DISCUSSION

In this study, we innovatively divided CTO lesions into soft and hard ones based on pathological considerations, rather than calcification and non-calcification and further evaluated the impact of plaque composition on the successful GW crossing within 30 min of CTO lesions. Our study revealed that the outcomes and predictive factors in soft CTO that mainly comprised a necrotic core and hard CTO that mainly consisted of fibrous and/or dense calcium are significantly different. The majority lesions with soft CTO could be successfully recanalized, and only proximal entry morphology had an effect on the outcome. The success rate of hard CTO PCI was much lower, which was influenced by several conventional clinical and plaque characteristics. Previous studies usually classify plaques according to the degree of calcification, ignoring the other unfavorable factor for the success, fibrous. In this study, we comprehensively evaluated the compositions of CTO lesions and further established a simpler and more satisfactory classification tool. This is the main innovation of our research.

During the development of CTO therapy and experience accumulation process, numerous scoring systems have been established to predict the successful recanalization of CTO lesions, including J-CTO, CT-RECTOR, CL, PROGRESS-CTO, ORA, KCCT, and CTA-J CTO. Establishing scoring systems could effectively predict the success of CTO recanalization, accurately select appropriate patients for attempting PCI, and ultimately achieve a satisfactory immediate and long-term prognosis. However, these scoring systems exhibited moderate-level performance in predicting the technical outcome of CTO PCI (15) and experienced in our center.

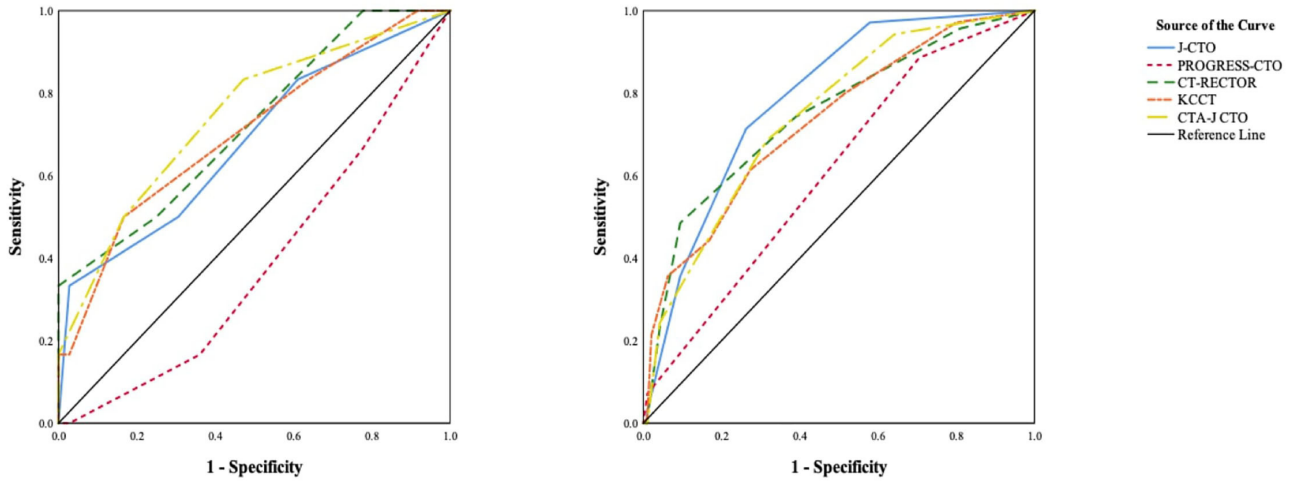

FIGURE 4 | Receiver operating characteristics (ROC) curves of previous scoring systems in patients with soft CTO (left) and hard CTO (right).

TABLE 5 | Independent predictors of 30 min GW crossing CTO.

Variables	Overall			Soft CTO			Hard CTO		
	HR	95%CI	*P*-Value	HR	95%CI	*P*-Value	HR	95%CI	*P*-Value
Blunt entry	0.444	0.216–0.913	0.027	0.081	0.012–0.563	0.011	…	…	…
Failed attempt	0.203	0.077–0.536	0.001	…	…	…	0.215	0.070–0.664	0.008
Distal reference diameter*			…	…	…	…	4.748	1.698–13.275	0.003
Proximal side branch	0.352	0.166–0.748	0.007	…	…	…	0.250	0.110–0.571	0.001
Bending > 45°	0.232	0.100–0.536	0.001	…	…	…	0.066	0.020–0.218	<0.001
Calcium ≥ 50% CSA	0.303	0.149–0.616	0.001	…	…	…	0.325	0.147–0.717	0.005

*Data were analyzed using a Cox regression model. *Distal reference diameter was divided into ≤2.5 and >2.5 mm. CTO, chronic total occlusion; HR, hazard ratio; CI, confidence interval; CSA, cross-sectional area.*

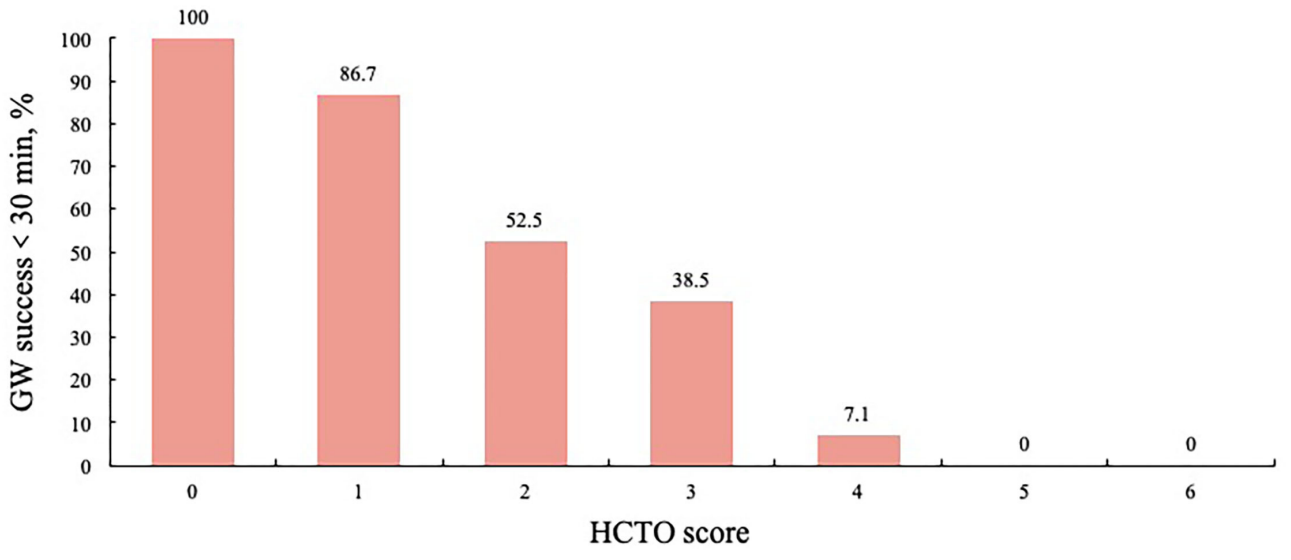

FIGURE 5 | Relationship between HCTO score and GW crossing within 30 min.

A thorough understanding of CTO pathophysiology is critical to explain the phenomenon, optimize predictive models, and further develop newer techniques and technologies. In essence, most CTOs are caused by soft plaque rupture followed by thrombotic coronary occlusion and organization of thrombotic substances, while a minority of CTOs are caused by the progression of atheroma (16). Except for proximal and distal fibrous caps, the occluded segment materials were biologically active with inflammation, neovascularization, and recanalization, giving rise to different CTO compositions. Similar to non-CTO lesions in patients with stable angina, the composition of CTO lesions mainly consists of three types, namely, necrotic core, fibrous, and dense calcium (17). Previous studies exploring GW crossing predictors always focus on the severity of calcification in terms of plaque characteristics, which revealed that calcification is likely to be a predictive factor of failed GW crossing within 30 min. However, these investigations have underestimated the effect of low-density components on the success of CTO PCI, including the other unfavorable factor for the success, fibrous. This may be attributable to the limited ability of CCTA to evaluate.

Intravascular ultrasound (IVUS) is the gold standard for the diagnosis of plaque characteristics, but it is limited due to its high cost and invasive nature (18). Most importantly, IVUS could not be applied in CTO lesions with failed GW crossing. CCTA is a robust non-invasive method to analyze the presence, extent, and severity of coronary atherosclerosis with high accuracy (19, 20). Previous scoring systems, including CT-RECTOR, KCCT, and CTA-J CTO, established grading rules of CTO difficulty using CCTA indexes and provided a more accurate non-invasive tool for predicting the time-efficient GW passaging and final procedure success (21, 22). In our study, J-CTO and PROGRESS-CTO scores were similar between soft CTO and hard CTO groups, whereas CT-RECTOR and CTA-J CTO scores were much higher in the hard CTOs, indicating that CCTA derived scoring systems are more likely to distinguish lesion characteristics, including plaque compositions, compared with ICA derived parameters.

Recent advances in CCTA technology have enabled us to better understand the pathophysiology of coronary atherosclerosis and its association with future CVD risk by providing additional coronary atherosclerosis information, such as plaque characteristics and volumes (23, 24). In our study, non-invasive plaque compositions were analyzed based on the CCTA data using the semi-automated plaque analysis software, which has been used in previous studies (25, 26). We divided the patients into soft and hard CTO groups according to the percentage of the necrotic core. Thus, patients with hard CTO were mainly composed of fibrous and/or calcified plaques. This grouping method fully considered the impact of low-density non-calcified plaques.

According to our analysis, conventional predictive factors, including previous failed attempts, proximal side branch, bending, calcification, and distal reference diameter were confirmed in patients with hard CTO. It is worth mentioning that our study complemented previous observations by introducing a novel predictor distal reference diameter. Yamamoto et al. (27) showed that CTO lesions with positive remodeling apparently have unstable plaques, such as lipid-rich plaque, macrophages, and underlying plaque morphology of plaque rupture or attenuated plaque. This explained why greater distal vessel diameter is associated with an increased GW passage. Even though a blunt stump has been frequently reported as a significant prognostic factor for PCI failure in previous angiographic research, it was not an independent predictor of GW outcome in the hard CTO group. Interestingly, for patients with soft CTO, only entry morphology was proved to be a predictive factor of GW failure within 30 min. The blunt entry was proved to be the single risk factor of failed GW 30 min success. Other characteristics of the CTO segment are irrelevant.

Our study provided a novel approach for the preoperative evaluation of CTO PCI. Based on the above results, further evaluation of CTO lesions should be altered by first analyzing plaque compositions using non-invasive CCTA. Complete assessment of CTO lesion by adding plaque composition analysis to the conventional predictive factors would optimize the treatment strategies of CTO lesions.

Grouping CTO lesions according to the proportion of necrotic core is reasonable and necessary in predicting the GW crossing within 30 min. A soft CTO with a necrotic core is more likely to be recanalized compared with a hard CTO with fibrous and/or dense calcium. Different plaque types have varying predictive factors.

Several limitations of this study need to be addressed. First, the retrospective nature of our study may potentially result in biases. Second, the sample size is small because CCTA was not routinely performed in patients with CTO. Third, we should keep in mind that most of the lesions used an antegrade crossing approach, so the results are more suitable for a certain patient population. Therefore, the findings of our study should be considered as hypothesis-generating, with further large-scale studies warranted to confirm our findings. In addition, this classification method is mainly based on lesion composition recognition, which cannot be realized by the naked eye. This disadvantage might limit its clinical application.

DATA AVAILABILITY STATEMENT

The raw data supporting the conclusions of this article will be made available by the authors, without undue reservation.

ETHICS STATEMENT

The studies involving human participants were reviewed and approved by Beijing Anzhen Hospital Ethics Committee. Written informed consent for participation was not required for this study in accordance with the national legislation and the institutional requirements.

AUTHOR CONTRIBUTIONS

XS and YH contributed substantially to the design of the present study. DZ performed the statistical analyses and drafted the manuscript. All co-authors participated in the interpretation of data and critically revised the manuscript. All authors have approved the final version of the manuscript.

FUNDING

This work was supported by the Capital Health Research and Development of Special of China (Grant Number: 2018-2-2063) and the National Natural Science Foundation of China (Grant Number: 81971569).

REFERENCES

1. Werner GS, Gitt AK, Zeymer U, Juenger C, Towae F, Wienbergen H, et al. Chronic total coronary occlusions in patients with stable angina pectoris: impact on therapy and outcome in present day clinical practice. *Clin Res Cardiol.* (2009) 98:435–41. doi: 10.1007/s00392-009-0013-5
2. Galassi AR, Boukhris M, Toma A, Elhadj Z, Laroussi L, Gaemperli O, et al. Percutaneous coronary intervention of chronic total occlusions in patients with low left ventricular ejection fraction. *JACC Cardiovasc Interv.* (2017) 10:2158–70. doi: 10.1016/j.jcin.2017.06.058
3. Hirai T, Grantham JA, Sapontis J, Cohen DJ, Marso SP, Lombardi W, et al. Quality of life changes after chronic total occlusion angioplasty in patients with baseline refractory angina. *Circ Cardiovasc Interv.* (2019) 12:e007558. doi: 10.1161/CIRCINTERVENTIONS.118.007558
4. Morino Y, Abe M, Morimoto T, Kimura T, Hayashi Y, Muramatsu T, et al. Predicting successful guidewire crossing through chronic total occlusion of native coronary lesions within 30 minutes: the J-CTO (Multicenter CTO Registry in Japan) score as a difficulty grading and time assessment tool. *JACC Cardiovasc Interv.* (2011) 4:213–21. doi: 10.1016/j.jcin.2010.09.024
5. Alessandrino G, Chevalier B, Lefèvre T, Sanguineti F, Garot P, Unterseeh T, et al. A clinical and angiographic scoring system to predict the probability of successful first-attempt percutaneous coronary intervention in patients with total chronic coronary occlusion. *JACC Cardiovasc Interv.* (2015) 8:1540–8. doi: 10.1016/j.jcin.2015.07.009
6. Christopoulos G, Kandzari DE, Yeh RW, Jaffer FA, Karmpaliotis D, Wyman MR, et al. Development and validation of a novel scoring system for predicting technical success of chronic total occlusion percutaneous coronary interventions: the progress CTO (prospective global registry for the study of chronic total occlusion intervention) score. *JACC Cardiovasc Interv.* (2016) 9:1–9. doi: 10.1016/j.jcin.2015.09.022
7. Galassi AR, Boukhris M, Azzarelli S, Castaing M, Marzà F, Tomasello SD. Percutaneous coronary revascularization for chronic total occlusions: a novel predictive score of technical failure using advanced technologies. *JACC Cardiovasc Interv.* (2016) 9:911–22. doi: 10.1016/j.jcin.2016.01.036
8. Opolski MP, Achenbach S, Schuhbäck A, Rolf A, Möllmann H, Nef H, et al. Coronary computed tomographic prediction rule for time-efficient guidewire crossing through chronic total occlusion: insights from the CT-RECTOR multicenter registry (computed tomography registry of chronic total occlusion revascularization). *JACC Cardiovasc Interv.* (2015) 8:257–67. doi: 10.1016/j.jcin.2014.07.031
9. Yu CW, Lee HJ, Suh J, Lee NH, Park SM, Park TK, et al. Coronary computed tomography angiography predicts guidewire crossing and success of percutaneous intervention for chronic total occlusion: Korean multicenter CTO CT registry score as a tool for assessing difficulty in chronic total occlusion percutaneous coronary intervention. *Circ Cardiovasc Imaging.* (2017) 10:e005800. doi: 10.1161/CIRCIMAGING.116.005800
10. Karatasakis A, Danek BA, Karmpaliotis D, Alaswad K, Jaffer FA, Yeh RW, et al. Comparison of various scores for predicting success of chronic total occlusion percutaneous coronary intervention. *Int J Cardiol.* (2016) 224:50–6. doi: 10.1016/j.ijcard.2016.08.317
11. Dalager MG, Bøttcher M, Thygesen J, Andersen G, Bøtker HE. Different plaque composition and progression in patients with stable and unstable coronary syndromes evaluated by cardiac CT. *Biomed Res Int.* (2015) 2015:401357. doi: 10.1155/2015/401357
12. Irving J. CTO pathophysiology: how does this affect management? *Curr Cardiol Rev.* (2014) 10:99–107. doi: 10.2174/1573403X10666140331142349
13. Hoe J. CT coronary angiography of chronic total occlusions of the coronary arteries: how to recognize and evaluate and usefulness for planning percutaneous coronary interventions. *Int J Cardiovasc Imaging.* (2009) 25:43–54. doi: 10.1007/s10554-009-9424-7
14. Brodoefel H, Reimann A, Heuschmid M, Tsiflikas I, Kopp AF, Schroeder S, et al. Characterization of coronary atherosclerosis by dual-source computed tomography and HU-based color mapping: a pilot study. *Eur Radiol.* (2008) 18:2466–74. doi: 10.1007/s00330-008-1019-5
15. Kalnins A, Strele I, Lejnieks A. Comparison among different scoring systems in predicting procedural success and long-term outcomes after percutaneous coronary intervention in patients with chronic total coronary artery occlusions. *Medicina.* (2019) 55:494. doi: 10.3390/medicina55080494
16. Dash D. Coronary chronic total occlusion intervention: a pathophysiological perspective. *Indian Heart J.* (2018) 70:548–55. doi: 10.1016/j.ihj.2018.01.021
17. Park YH, Kim YK, Seo DJ, Seo YH, Lee CS, Song IG, et al. Analysis of plaque composition in coronary chronic total occlusion lesion using virtual histology-intravascular ultrasound. *Korean Circ J.* (2016) 46:33–40. doi: 10.4070/kcj.2016.46.1.33
18. Song FX, Zhou J, Zhou JJ, Shi YX, Zeng MS, Zhang ZY, et al. The diagnosis of coronary plaque stability by multi-slice computed tomography coronary angiography. *J Thorac Dis.* (2018) 10:2365–76. doi: 10.21037/jtd.2018.04.43
19. Budoff MJ, Dowe D, Jollis JG, Gitter M, Sutherland J, Halamert E, et al. Diagnostic performance of 64-multidetector row coronary computed tomographic angiography for evaluation of coronary artery stenosis in individuals without known coronary artery disease: results from the prospective multicenter ACCURACY (assessment by coronary computed tomographic angiography of individuals undergoing invasive coronary angiography) trial. *J Am Coll Cardiol.* (2008) 52:1724–32. doi: 10.1016/j.jacc.2008.07.031
20. Meijboom WB, Meijs MF, Schuijf JD, Cramer MJ, Mollet NR, van Mieghem CA, et al. Diagnostic accuracy of 64-slice computed tomography coronary angiography: a prospective, multicenter, multivendor study. *J Am Coll Cardiol.* (2008) 52:2135–44. doi: 10.1016/j.jacc.2008.08.058
21. Tan Y, Zhou J, Zhang W, Zhou Y, Du L, Tian F, et al. Comparison of CT-RECTOR and J-CTO scores to predict chronic total occlusion difficulty for percutaneous coronary intervention. *Int J Cardiol.* (2017) 235:169–75. doi: 10.1016/j.ijcard.2017.02.008
22. Fujino A, Otsuji S, Hasegawa K, Arita T, Takiuchi S, Fujii K, et al. Accuracy of J-CTO score derived from computed tomography versus angiography to predict successful percutaneous coronary intervention. *JACC Cardiovasc Imaging.* (2018) 11:209–17. doi: 10.1016/j.jcmg.2017.01.028
23. Motoyama S, Ito H, Sarai M, Kondo T, Kawai H, Nagahara Y, et al. Plaque characterization by coronary computed tomography angiography and the likelihood of acute coronary events in mid-term follow-up. *J Am Coll Cardiol.* (2015) 66:337–46. doi: 10.1016/j.jacc.2015.05.069
24. Kristensen TS, Kofoed KF, Kühl JT, Nielsen WB, Nielsen MB, Kelbæk H. Prognostic implications of nonobstructive coronary plaques in patients with non-ST-segment elevation myocardial infarction: a multidetector computed tomography study. *J Am Coll Cardiol.* (2011) 58:502–9. doi: 10.1016/j.jacc.2011.01.058
25. Papadopoulou SL, Neefjes LA, Garcia-Garcia HM, Flu WJ, Rossi A, Dharampal AS, et al. Natural history of coronary atherosclerosis by multislice computed tomography. *JACC*

Cardiovasc Imaging. (2012) 5:S28–37. doi: 10.1016/j.jcmg.2012.01.009

26. Lee SE, Sung JM, Andreini D, Al-Mallah MH, Budoff MJ, Cademartiri F, et al. Differences in progression to obstructive lesions per high-risk plaque features and plaque volumes with CCTA. *JACC Cardiovasc Imaging.* (2020) 13:1409–17. doi: 10.1016/j.jcmg.2019.09.011
27. Yamamoto MH, Maehara A, Poon M, Guo J, Yamashita K, Yakushiji T, et al. Morphological assessment of chronic total occlusions by combined coronary computed tomographic angiography and intravascular ultrasound imaging. *Eur Heart J Cardiovasc Imaging.* (2017) 18:315–22. doi: 10.1093/ehjci/jew077

Conflict of Interest: The authors declare that the research was conducted in the absence of any commercial or financial relationships that could be construed as a potential conflict of interest.

frontiers in Cardiovascular Medicine

ORIGINAL RESEARCH
published: 11 March 2022
doi: 10.3389/fcvm.2022.793067

Indirect Transfer to Catheterization Laboratory for ST Elevation Myocardial Infarction Is Associated With Mortality Independent of System Delays: Insights From the France-PCI Registry

Farzin Beygui[1], Vincent Roule[1], Fabrice Ivanes[2], Thierry Dechery[3], Olivier Bizeau[4], Laurent Roussel[5], Philippe Dequenne[6], Marc-Antoine Arnould[7], Nicolas Combaret[8], Jean Philippe Collet[9], Philippe Commeau[10], Guillaume Cayla[11], Gilles Montalescot[9], Hakim Benamer[12], Pascal Motreff[8], Denis Angoulvant[2], Pierre Marcollet[3], Stephan Chassaing[7], Katrien Blanchart[1], René Koning[13] and Grégoire Rangé[5]*

[1] Cardiology Department, CHU de Caen, Caen, France, [2] Cardiology Department, CHU de Tours, Tours, France, [3] Cardiology Department, Center Hospitalier de Bourges, Bourges, France, [4] Cardiology Department, CHR de Orléans, Orléans, France, [5] Cardiology Department, Les Hôpitaux de Chartres, Chartres, France, [6] Cardiology Department, Clinique Oréliance, Saran, France, [7] Cardiology Department, Nouvelle clinique Tourangelle, Saint-Cyr-sur-Loire, France, [8] Cardiology Department, CHU de Clermont-Ferrand, Clermont-Ferrand, France, [9] Cardiology Department, Groupe hospitalier Pitié-Salpêtrière, Paris, France, [10] Cardiology Department, Polyclinique les fleurs, Ollioules, France, [11] Cardiology Department, CHU Nîmes, Nîmes, France, [12] Cardiology Department, Clinique de la Roseraie, Aubervilliers, France, [13] Cardiology Department, Clinique Saint Hilaire, Saint Hilaire, France

OPEN ACCESS

Edited by:
Tommaso Gori, Johannes Gutenberg University Mainz, Germany

Reviewed by:
Adel Aminian, Center Hospitalier Universitaire de Charleroi, Belgium
Nicola Deluca, University of Naples Federico II, Italy

***Correspondence:**
Farzin Beygui
beygui-f@chu-caen.fr

Specialty section:
This article was submitted to Coronary Artery Disease, a section of the journal Frontiers in Cardiovascular Medicine

Received: *11 October 2021*
Accepted: *09 February 2022*
Published: *11 March 2022*

Citation:
Beygui F, Roule V, Ivanes F, Dechery T, Bizeau O, Roussel L, Dequenne P, Arnould M-A, Combaret N, Collet JP, Commeau P, Cayla G, Montalescot G, Benamer H, Motreff P, Angoulvant D, Marcollet P, Chassaing S, Blanchart K, Koning R and Rangé G (2022) Indirect Transfer to Catheterization Laboratory for ST Elevation Myocardial Infarction Is Associated With Mortality Independent of System Delays: Insights From the France-PCI Registry. Front. Cardiovasc. Med. 9:793067. doi: 10.3389/fcvm.2022.793067

Background: First medical contact (FMC)-to-balloon time is associated with outcome of ST-elevation myocardial infarction (STEMI). We assessed the impact on mortality and the determinants of indirect vs. direct transfer to the cardiac catheterization laboratory (CCL).

Methods: We analyzed data from 2,206 STEMI patients consecutively included in a prospective multiregional percutaneous coronary intervention (PCI) registry. The primary endpoint was 1-year mortality. The impact of indirect admission to CCL on mortality was assessed using Cox models adjusted on FMC-to-balloon time and covariables unequally distributed between groups. A multivariable logistic regression model assessed determinants of indirect transfer.

Results: A total of 359 (16.3%) and 1847 (83.7%) were indirectly and directly admitted for PCI. Indirect admission was associated with higher risk features, different FMCs and suboptimal pre-PCI antithrombotic therapy.

At 1-year follow-up, 51 (14.6%) and 137 (7.7%) were dead in the indirect and direct admission groups, respectively (adjusted-HR 1.73; 95% CI 1.22–2.45). The association of indirect admission with mortality was independent of pre-FMC and FMC characteristics. Older age, paramedics- and private physician-FMCs were independent determinants of indirect admission (adjusted-HRs 1.02 per year, 95% CI 1.003–1.03; 5.94, 95% CI 5.94 3.89–9.01; 3.41; 95% CI 1.86–6.2, respectively).

Conclusions: Our study showed that, indirect admission to PCI for STEMI is associated with 1-year mortality independent of FMC to balloon time and should be considered as an indicator of quality of care. Indirect admission is associated with higher-risk features and suboptimal antithrombotic therapy. Older age, paramedics-FMC and self-presentation to a private physician were independently associated with indirect admission. Our study, supports population education especially targeting elderly, more adequately dispatched FMC and improved pre-CCL management.

Keywords: ST-elevation myocardial infarction, Pre-hospital, percutaneous coronary intervention, mortality, system delays

INTRODUCTION

Primary percutaneous coronary intervention (PCI) is the first-line treatment for ST-elevation myocardial infarction (STEMI) (1). System delays from the first medical contact (FMC) to cardiac catheterization laboratory (CCL) are associated with poor outcome (2–4) and should be reduced to the minimum (1). However, despite improved door to balloon times, within the past decades, rates of mortality seem to be unchanged in the setting of STEMI (5) and further investigations are needed to identify other pre-CCL correlates of outcome and to develop new strategies to improve outcome.

A direct admission to CCL by Pre-hospital emergency medical services (EMS) is recommended in order to reduce system delays (1, 6). Indirect admission to the CCL and the number of contacts, after the FMC, are associated with longer system delays and total ischemic time but their impact on mortality, independent of system delays remains controversial (7, 8).

The objective of our study was to investigate whether indirect admission to CCL impacted mortality independent of FMC to balloon time and other identified co-variables in patients enrolled in a STEMI networks within 24 h following symptom onset and admitted to CCL for primary PCI. We also aimed to assess the determinants of indirect admission.

MATERIALS AND METHODS

Study Design and Population

The France PCI registry is an open, ongoing prospective multicenter registry (clinicaltrials.gov#NCT02778724) including consecutive patients admitted to CCLs for coronary interventions in different French regions as described previously (9, 10). In the setting of STEMI, pre-CCL management, timelines, reperfusion strategies, antithrombotic therapy and intervention characteristics are recorded in patients' medical files and electronically transferred to the registry. In-hospital and 1-year outcomes, derived from source files and/or physical or phone contacts are recorded. The quality of the registry is guaranteed by systematic audits by study coordinators independent of each center.

The current retrospective analysis focused on STEMI patients included within 24 h after symptom onset, undergoing primary PCI between January 1st 2014 and December 31st 2016, excluding patients with out-of-hospital cardiac arrest prior to STEMI, lytic therapy, and no attempt to PCI.

FMC was defined by the first person competent to obtain and interpret the ECG and, to provide initial intervention (1). The standard of care for the management of suspected STEMI in France is the physician-on board ambulance sent to the scene. However, paramedics-on board ambulances and self-presentation to an emergency department (ED) or to a private medical doctor (MD) are other potential pathways. "Door" was defined by the time of admission in the PCI-capable hospital and "balloon" was the time of coronary lesion crossing by the first PCI guidewire or balloon. Successful PCI was defined by a visually assessed coronary diameter stenosis <30% and a thrombolysis in myocardial infarction coronary flow 3. For the purpose of the current study we defined two groups based on the pathway from FMC to CCL: direct admission (guideline-recommended pathway without admission in any other medical facility prior to CCL; e.g., transfer from scene or an ED or ward to CCL) and indirect admission (admission to another medical facility prior to CCL; e.g., private MD or EMS to non-PCI facility then to CCL).

Outcomes

The primary outcome was mortality of any cause at 1-year follow-up. Secondary outcomes included hospital discharge and 1-year mortality, cardiovascular mortality (death related to cardiovascular causes or sudden death), major bleeding defined by the bleeding academic research consortium (BARC) classification $\geq$ 3, Non-fatal myocardial infarction, defined by types 1, 4 and 5 based on the universal definition (11), stroke, definite/probable stent thrombosis based on the academic research consortium criteria (12) and unplanned coronary revascularization.

Statistical Analysis

Baseline data are shown as *n* (%) and mean $\pm$ standard deviation and compared between groups using the $\chi 2$ test and the Student's *t* test for categorical and continuous variables, respectively. The primary outcome and 1-year cardiovascular mortality were compared between the two groups using Kaplan-Meier curves and the log-rank test. The association between the group and the latter outcomes was assessed using un-adjusted and adjusted on FMC to balloon time (primary analysis) cox regression models with calculation of Hazard ratios (HR) and 95% Confidence

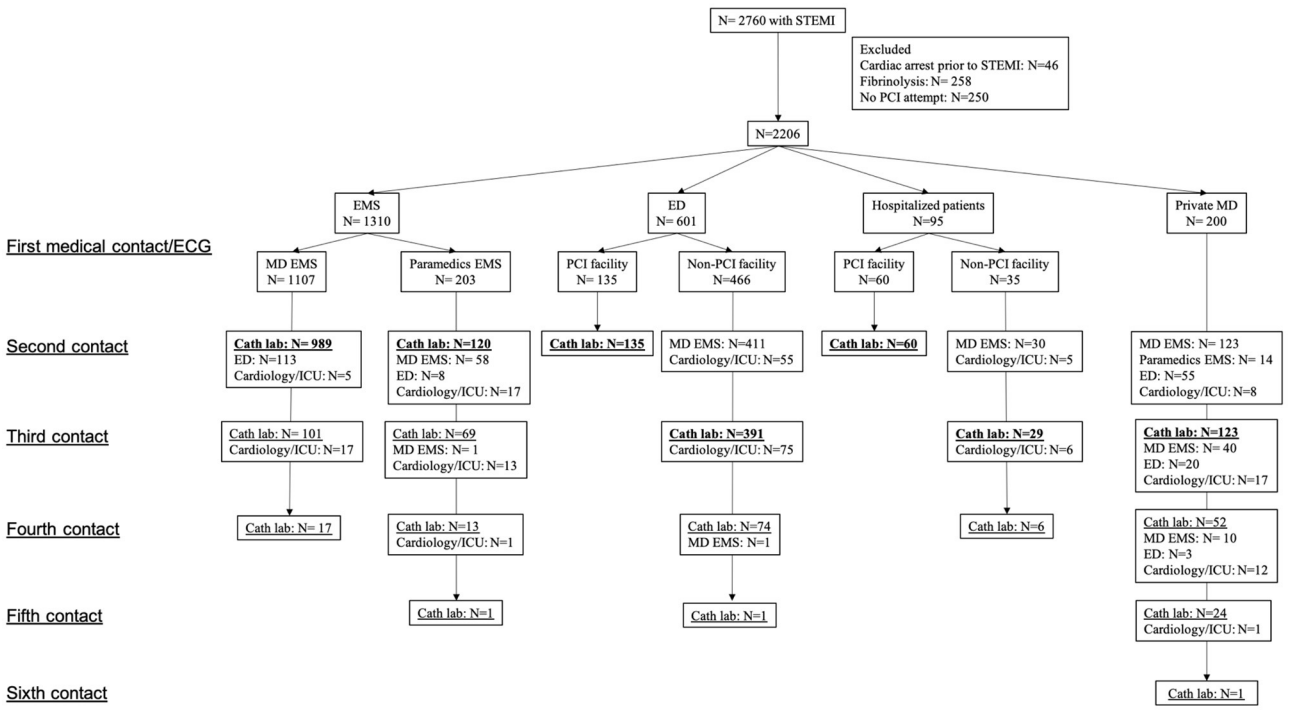

FIGURE 1 | Flow chart and details of first medical contact to cardiac catheterization laboratory pathways. Direct admission to catheterization laboratory appears in bold text. STEMI, ST elevation myocardial infarction; PCI, percutaneous coronary intervention; EMS, emergency medical services; ED, emergency department; MD, medical doctor; ICU, intensive care unit; Cath lab, catheterization laboratory.

intervals (CI). Other 1-year outcomes were assessed by the unadjusted Cox analyses.

Supplementary analyses were performed by adjusting the Cox models on covariables unequally distributed between the two groups with a p value < 0.1 in order to assess: 1. the impact of patient characteristics at the time of FMC; 2. The impact of pre-CCL management; 3. The concomitant impact of all latter variables 4. The impact of all latter variables and in-hospital variables.

Sensitivity analyses were conducted using the number of pre-CCL contacts as a continuous variable (1, 2, $\geq$3) instead of direct vs. indirect admission and total ischemic (symptom-to-balloon) time in replacement of FMC to balloon time in the latter models.

The associations between the groups and in-hospital outcomes were assessed by unadjusted and, in case of significant associations, by adjusted on FMC-to-balloon time logistic regression models with calculation of odds ratios (OR) and 95% CI.

The determinants of indirect admission to CCL were explored using a multivariable logistic regression model including all patient characteristics at the time of FMC unequally distributed between groups ($p < 0.1$) as well as EMS number call, type of FMC and FMC-to-balloon time. Finally, in a final exploratory analysis, we compared data between FMC groups with the MD-EMS group considered as the reference group.

All tests were two sided and a p value < 0.05 was considered as statistically significant.

RESULTS

Population Characteristics

A total of 2,760 consecutive patients were admitted during the analysis period among whom 2,206 fulfilled the inclusion criteria.

Figure 1 depicts the flow chart and pathways from the FMC to CCL. The FMC was an EMS team in 1,310 (59.4%), an ED in 601 (27.2%), a private MD in 200 (9.1%) and a physician in a hospital where patients were already admitted at the time of STEMI in 95 (4.3%) cases. A total of 359 (16.3%) and 1,847 (83.7%) were indirectly and directly admitted to CCL, respectively. The national EMS number was called directly by 1,245 (56%) patients for whom MD- or paramedics-EMS team were sent on scene in 1,090 (88%) and 110 (9%), respectively while others were directed to their MD (0.5%) or an ED (2.5%). Among the 961 (44%) patients who did not call directly the national EMS number, 95 (10%) were already hospitalized for another condition, 601 (62.5%) self-presented to an ED, 200 (20.8%) self-presented to their MD and 65 (6.7%) were referred to the EMS by their MD after a phone call.

Table 1 depicts patient characteristics based on direct vs. indirect admission to CCL. Compared to directly admitted patients, those indirectly transferred were significantly older ($p = 0.0006$) with higher rates of female gender ($p = 0.01$), Killip class $\geq$1 ($p = 0.008$), diabetes ($p = 0.01$), hypertension ($p = 0.02$) and, lower rates of past history of MI ($p = 0.002$) and PCI ($p = 0.0009$). FMC was less often an MD-EMS ($p < 0.0001$), an

TABLE 1 | Patient and procedure characteristics.

	Global population *N* = 2,206	Indirect admission *N* = 359	Direct admission *N* = 1,847	*P* value
Age, years	62.66 ± 13.91	65.07 ± 14.68	62.19 ± 13.71	0.0006
Gender, female	547 (25)	108 (30.1)	439 (23.8)	0.01
BMI, $Kg.m^{-2}$	26.63 ± 4.37	26.87 ± 4.81	26.59 ± 4.27	0.3
Killip class > 1	335 (15)	71 (19.8)	264 (14.3)	0.008
Cradiogenic shock	82 (3.7)	19 (5.3)	64 (3.4)	0.09
Past history				
Diabetes	295 (13)	63 (17.5)	232 (12.6)	0.01
Hyperlipemia	814 (37)	140 (39)	674 (36.5)	0.4
Current smoking	838 (38)	122 (34)	716 (38.8)	0.09
Hypertension	882 (40)	163 (45.4)	719 (38.9)	0.02
PCI	277 (13)	26 (7.2)	251 (13.6)	0.0009
Myocardial infarction	177 (8)	14 (3.9)	163 (8.8)	0.002
Stroke	53 (2)	12 (3.3)	41 (2.2)	0.2
PAD	72 (3)	11 (3.1)	61 (3.3)	0.8
Prehospital data				
EMS number call by patient	1245 (56)	166 (46.2)	1079 (58.4)	<0.0001
FMC				
EMS	1310 (59)	201 (56)	1109 (60)	0.2
MD-EMS	1107 (50)	118 (32.9)	989 (53.5)	<0.0001
Paramedics-EMS	203 (9)	83 (23.1)	120 (6.5)	<0.0001
ED	601 (27)	75 (20.9)	526 (28.5)	0.003
PCI-facility	135 (6)	0 (0)	135 (7.3)	<0.0001
Non-PCI-facility	466 (21)	75 (20.9)	391 (21.2)	0.9
Private MD	200 (9)	77 (21.4)	123 (6.7)	<0.0001
Hospitalized patients	95 (4)	6 (1.7)	89 (4.8)	0.007
PCI-facility	60 (3)	0 (0)	60 (3.2)	<0.0001
Non-PCI-facility	35 (1.6)	6 (1.7)	29 (1.6)	0.9
Times, min				
Symptom to FMC	175 ± 217	228 ± 238	165 ± 212	<0.0001
FMC to door	93 ± 96	176 ± 158	76 ± 67	<0.0001
Door to balloon	56 ± 131	107 ± 262	46 ± 82	<0.0001
FMC to balloon	149 ± 166	283 ± 315	123 ± 98	<0.0001
FMC to balloon <120'	1222 (55)	55 (15.3)	1167 (63.2)	<0.0001
FMC to balloon <90'	745 (34)	20 (5.6)	725 (39.3)	<0.0001
Total ischemic time	324 ± 284	511 ± 397	287 ±240	<0.0001
Pre-catheterization medication				
Aspirin	2098 (95)	344 (95.8)	1754 (95)	0.5
P2Y12 inhibitors	2030 (92)	332 (92.5)	1698 (91.9)	0.7
Clopidogrel	251 (11)	60 (16.5)	191 (10.3)	0.0005
Prasugrel	135 (6)	17 (4.5)	118 (6.4)	0.2
Ticagrelor	1644 (75)	255 (71)	1389 (75.2)	0.1
IV anticoagulation	1968 (89)	306 (85.2)	1662 (90)	0.008
Enoxaparin	845 (38)	146 (40.7)	699 (37.8)	0.3
UFH	1098 (50)	150 (41.8)	948 (51.3)	0.0009
Bivalirudin	22 (1)	5 (1.4)	17 (0.9)	0.4
In-hospital data				
Per-procedure medication				
Aspirin	382 (17)	70 (19.5)	312 (16.9)	0.2
P2Y12 inhibitor	174 (8)	25 (7)	149 (8.1)	0.5

(Continued)

TABLE 1 | Continued

	Global population *N* = 2,206	Indirect admission *N* = 359	Direct admission *N* = 1,847	*P* value
Clopidogrel	24 (1)	4 (1.1)	20 (1.1)	0.96
Prasugrel	11 (0)	3 (0.8)	8 (0.4)	0.3
Ticagrelor	139 (6)	18 (5)	121 (6.6)	0.3
2B3A inhibitor	830 (38)	103 (28.7)	727 (39.4)	0.0001
IV anticogulation	1141 (52)	208 (57.9)	933 (50.5)	0.01
Enoxaparine	19 (1)	3 (0.8)	16 (0.9)	0.95
UFH	1118 (51)	203 (56.5)	915 (49.5)	0.02
Bivalirudin	10 (0)	3 (0.8)	7 (0.4)	0.2
Transradial	1847 (83)	315 (88)	1690 (92)	0.02
Left main disease	4 (0)	1 (0.3)	3 (0.2)	0.6
Single vessel disease	1012 (46)	150 (41.8)	862 (46.7)	0.09
Single vessel PCI	2105 (95)	340 (95)	1765 (96)	0.5
Stents per patient	1.19 ± 0.8	1.24 ± 0.85	1.19 ± 0.79	0.3
Successful PCI	2151 (98)	342 (95.3)	1809 (97.9)	0.003
Medication at discharge	*N* = 2092	*N* = 327	*N* = 1765	
Aspirin[a]	2066 (99)	324 (99)	1742 (99)	0.7
P2Y12 inhibitor	2062 (98.6)	320 (97.9)	1742 (98.7)	0.2
Clopidogrel	282 (13)	61 (18.7)	221 (12.5)	0.003
Prasugrel	181 (9)	23 (7)	158 (9)	0.3
Ticagrelor	1599 (76)	236 (72.2)	1363 (77.2)	0.048
Medication at 1 year[b]	*N* = 1922	*N* = 277	*N* = 1564	
Aspirin	1841 (96)	277 (96)	1564 (96)	1
P2Y12 inhibitor	1006 (53)	156 (54)	850 (52)	0.6
Clopidogrel	255 (13)	44 (15)	211 (13)	0.3
Prasugrel	73 (4)	10 (3.5)	63 (4)	0.7
Ticagrelor	678 (35)	102 (35)	576 (35)	1

[a] *10 patients with missing data.*

[b] *281 and 290 patients with missing data at 1 year with respect to aspirin and P2Y12 inhibitor treatment.*

FMC, first medical contact; BMI, body mass index; ED, emergency department; PCI, percutaneous coronary intervention, PAD, peripheral arterial disease; EMS, emergency medical services; MD, medical doctor; IV, intravenous, UFH, unfractionated heparin.

ED ($p = 0.003$) or a ward MD ($p = 0.007$) and more often a paramedics-EMS ($p < 0.0001$) or a private MD ($p < 0.0001$) in those indirectly transferred.

The rate of patients with a FMC to balloon time <120 min was >3 times lower ($p < 0.0001$) and all delays were longer ($p < 0.0001$) in patients indirectly transferred.

Between FMC and CCL, patients indirectly transferred to the hospital were less likely to receive intravenous anticoagulation ($p = 0.01$) and received more frequently clopidogrel ($p = 0.002$) as compared to newer P2Y12 inhibitors.

During the procedure, 2B3A inhibitors and supplementary doses of intravenous anticoagulation were more frequently used in those indirectly transferred ($p < 0.0001$ and $p = 0.01$, respectively). Angiographic findings and PCI characteristics were similar between the groups but the rates of transradial approach and successful PCI were lower in those indirectly transferred ($p = 0.02$ and $p = 0.003$).

At hospital discharge, patients indirectly transferred were more frequently on clopidogrel ($p = 0.003$) and less frequently on ticagrelor ($p < 0.05$).

Follow-Up and Outcomes

Outcome data (**Table 2**) were complete for all patients at hospital discharge and 2,124 (96.3%) patients at 1-year follow-up.

At hospital discharge 114 (5.2%) patients were reported dead, 32 (8.9%) in the indirect admission and 82 (4.4%) in the direct admission groups, respectively (adjusted-OR 1.84, 95% CI 1.16–2.85, $p = 0.008$). In-hospital cardiovascular death occurred in 26 (7.2%) and 60 (3.2%) patients in the indirect and direct admission groups, respectively (adjusted OR 2.08, 95% CI 1.25–3.36, $p = 0.004$). Other end points were similarly distributed between the two groups.

At 1-year follow-up 188 (9%) were reported dead, 51 (14.6%) in the indirect and 137 (7.7%) in the direct admission groups, respectively (adjusted-HR 1.73, 95% CI 1.22–2.45, $p = 0.002$). Cardiovascular death was reported in 35 (10%) and 83 (4.7%) patients in the indirect and direct admission groups, respectively (adjusted-HR 2.01, 95% CI 1.31–3.07, $p = 0.0003$). **Figure 2** depicts survival and cardiovascular survival Kaplan-Meier curves. Other 1-year end points were similarly distributed between the groups. At 1-year follow-up 96 and 53% of patients

TABLE 2 | Outcomes and their association with indirect vs. direct transfer.

	All	Indirect transfer	Direct transfer	Un-adjusted		Adjusted on FMC-to-balloon time	
In-hospital outcomes	***N = 2,206***	***N = 359***	***N = 1,847***	**OR (95% CI)**	**Wald *p***	**OR (95% CI)**	**Wald *p***
Death	114 (5.2)	32 (8.9)	82 (4.4)	2.11 (1.36–3.19)	0.0006	1.84 (1.16–2.85)	0.008
Cardiovascular death	86 (3.9)	26 (7.2)	60 (3.2)	2.33 (1.43–3.70)	0.0005	2.08 (1.25–3.36)	0.004
Myocardial infarction	25 (1)	7 (1.9)	18 (1)	2.02 (0.78–4.68)	0.1		
Stroke	10 (0)	1 (0.3)	9 (0.5)	0.57 (0.03–3.05)	0.6		
Unplanned revascularization	34 (2)	8 (2.2)	26 (1.4)	1.60 (0.67–3.40)	0.3		
Stent thrombosis	26 (1.1)	4 (1.1)	22 (1.2)	0.94 (0.27–2.60)	0.9		
Major bleeding	48 (2.2)	10 (2.8)	38 (2.1)	1.36 (0.64–2.66)	0.4		
1-*year* outcomes	***N = 2,124***	***N = 347***	***N = 1,777***	**HR (95% CI)**	**Score *p***	**HR (95% CI)**	**Score *p***
Death	188 (9)	51 (14.6)	137 (7.7)	2.02 (1.46–2.78)	<0.0001	1.73 (1.22–2.45)	0.002
Cardiovascular death	118 (5.6)	35 (10)	83 (4.7)	2.28 (1.53–3.38)	<0.0001	2.01 (1.31–3.07)	0.001
Myocardial infarction	52 (2.4)	11 (3.2)	41 (2.3)	1.44 (0.74–2.80)	0.3		
Stroke	20 (0.9)	2 (0.6)	18 (1)	0.59 (0.14–2.56)	0.5		
Unplanned revascularization	128 (6)	19 (5.4)	109 (6.1)	0.95 (0.58–1.54)	0.8		
Stent thrombosis	39 (1.8)	6 (1.7)	33 (1.9)	0.99 (0.41–2.35)	1		
Major bleeding	79 (3.7)	13 (3.7)	66 (3.7)	1.06 (0.94–1.93)	0.8		

FMC, first medical contact.

remained on aspirin and a P2Y12 inhibitor, respectively. Such rates as well as the distribution of different P2Y12 inhibitors were similar between the 2 groups suggesting comparable adherence to treatment.

As shown in **Table 3**, the relationship between the group and, both 1-year mortality and cardiovascular mortality remained significant in models including separately pre-CCL patient (model 1) or intervention characteristics (model 2) both including FMC to balloon time. In model 3 gathering models 1 and 2, and model 4 including in-hospital variables on top of model 3, indirect admission was no more significantly associated with mortality. In the model 4, age, diabetes, Killip class $\geq$2, FMC to balloon time, pre-CCL P2Y12 inhibitor and anticoagulation, transradial access and successful PCI were independently associated with mortality. All such variables except diabetes, were also independently associated with cardiovascular mortality.

Sensitivity analyses (**Supplementary Table 1**) showed consistent results.

Determinants of Indirect Admission

As summerized in **Table 4**, age (OR 1.02 per year, 95% CI 1.003–1.03, $p = 0.01$), paramedics-EMS (OR 5.94 vs. MD-EMS, 95% CI 3.89–9.01, $p < 0.0001$) and private MD (OR 3.41 vs. MD-EMS, 95% CI 1.86–6.21, $p < 0.0001$) were determinants of indirect admission independent of FMC-to-balloon time and other co-variables.

Pre-CCL Pathways

The **Supplementary Table 2** and **Figure 3** depict the analysis based on different pre-CCL pathways and their comparison to the MD-EMS group considered as the reference. The analysis adjusted on FMC to balloon time showed that compared to the MD-EMS group, there was an increased risk of in-hospital (adjusted-OR 1.94, 95% CI 1.10–3.31, $p = 0.02$) and 1 year mortality (adjusted-HR 1.62, 95% CI 1.05–2.48, p = 0.02) and cardiovascular mortality (adjusted OR 2.12, 95% CI 1.11–3.85, $p = 0.02$ and adjusted HR 1.85, 95% CI 1.08–3.15, $p = 0.02$) associated with the paramedic-EMS group.

DISCUSSION

Our study shows that indirect admission of patients to CCL, as defined by guidelines, is associated with more than twice higher risks of both in-hospital and 1-year mortality and cardiovascular mortality. Although indirect admission was associated with increased system delays, its relationship with mortality remained independent of FMC to balloon and total ischemic times. Indirect admission is associated with higher risk features at the time of FMC (older age, female gender, Killip class $\geq$2, diabetes, hypertension, later presentation), different FMC characteristics (lower rates of national EMS number call, higher rates of paramedics-EMS and self-presentation to ED or to a private MD), pre-CCL medication (lower rates of newer P2Y12 inhibitors and anticoagulation) and in-hospital and procedure characteristics (higher rates of GP2B3A inhibitors and anticoagulation and, lower rates of transradial approach and successful PCI). We identified older age, paramedics-EMS and private MD-FMCs as independent determinants of indirect admission. Finally, paramedics-EMS pathway was associated with higher risks of in-hospital and 1 year mortality as compared to MD-EMS.

System delays are associated with increased mortality and heart failure in the setting of primary PCI for STEMI (2, 13, 14). Based on guidelines, STEMI patients should be transferred directly to the CCL bypassing ED and intensive care units in order to shorten the FMC to balloon times (1, 6). Our

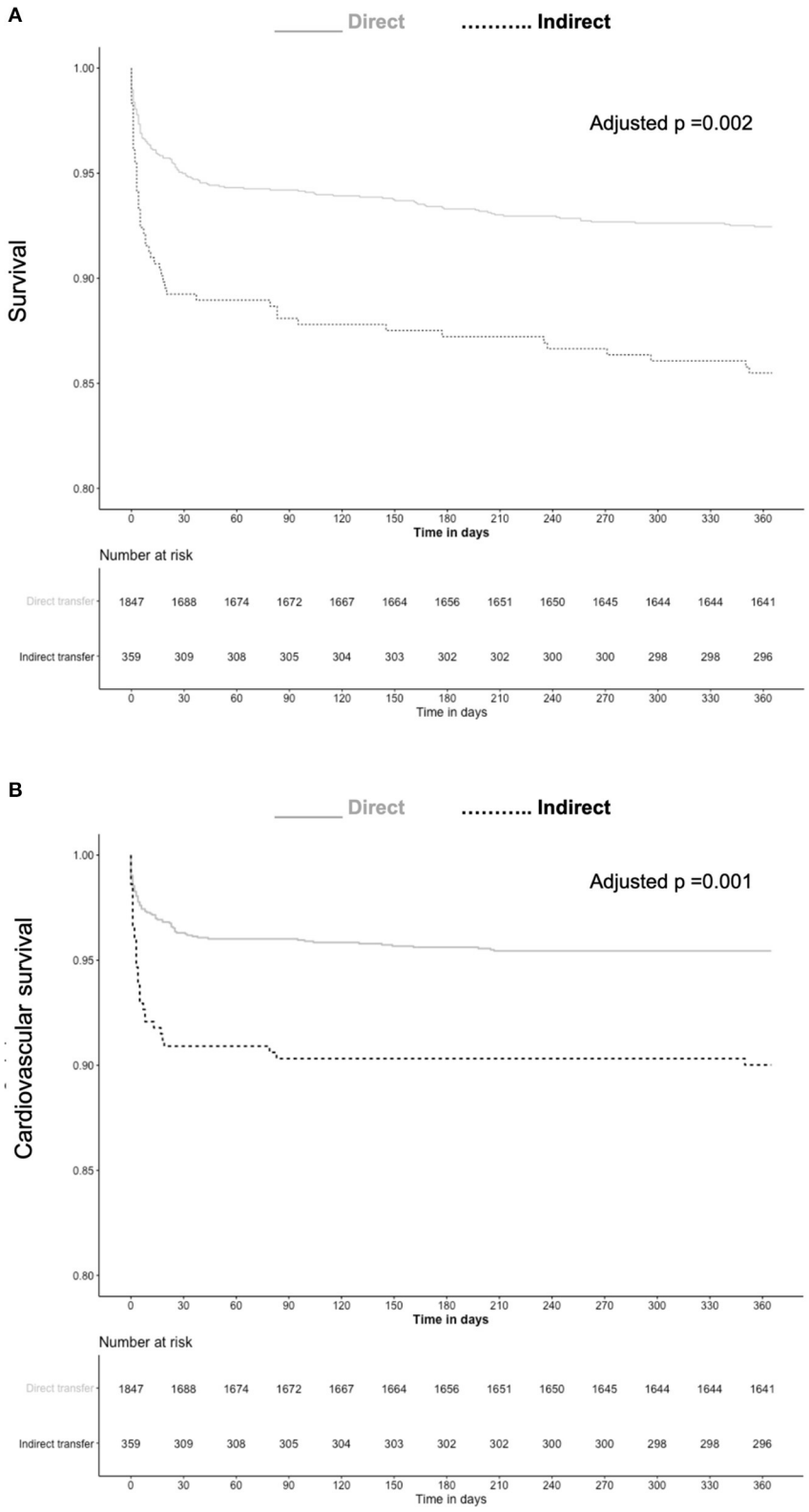

FIGURE 2 | Kaplan-Meier curves for survival **(A)** and cardiovascular survival **(B)** based on direct or indirect admission to catheterization laboratory.

TABLE 3 | Variables significantly associated with 1-year mortality and cardiovascular mortality.

	Model 1		Model 2		Model 3		Model 4	
	HR (95% CI)	***P* value**	**HR (95% CI)**	***P* value**	**HR (95% CI)**	***P* value**	**HR (95% CI)**	***P* value**
Mortality								
Indirect transfer	1.50 (1.08–2.08)	0.02	1.74 (1.20–2.51)	0.003	1.26 (0.86–1.84)	0.2	1.23 (0.83–1.81)	0.3
Age per year	1.06 (1.05–1.08)	<0.0001	–	0.002	1.07 (1.05–1.08)	<0.0001	1.06 (1.05–1.08)	<0.0001
Diabetes	1.88 (1.34–2.64)	0.0003	–	<0.0001	1.88 (1.34–2.65)	0.0003	1.99 (1.41–2.81)	0.0001
Killip class ≥2	7.54 (5.62–10.10)	<0.0001	–	0.001	6.41 (4.73–8.69)	<0.0001	5.81 (4.23–7.98)	<0.0001
FMC to balloon per 10'	–		1.008 (1.003–1.013)		1.007 (1.001–1.01)	0.02	1.007 (1.001–1.01)	0.03
Pre-CCL P2Y12 inhibitor	–		0.28 (0.18–0.42)		0.44 (0.29–0.67)	0.0002	0.55 (0.35–0.86)	0.009
Pre-CCL anticoagulation	–		0.53 (0.37–0.77)		0.60 (0.41–0.88)	0.01	0.66 (0.44–1.01)	0.05
Transradial access	–		–		–		0.66 (0.46–0.94)	0.02
Successful PCI	–		–		–		0.25 (0.16–0.40)	<0.0001
Cardiovascular mortality								
Indirect transfer	1.72 (1.15–2.57)	0.009	1.98 (1.26–3.12)	0.003	1.42 (0.90–2.27)	0.1	1.39 (0.86–2.23)	0.2
Age per year	1.06 (1.04–1.08)	<0.0001	–	0.07	1.07 (1.05–1.08)	<0.0001	1.06 (1.04–1.08)	<0.0001
Killip class ≥2	9.51 (6.49–13.93)	<0.0001	–	<0.0001	8.09 (5.44–11.99)	<0.0001	7.07 (4.68–10.68)	<0.0001
FMC to balloon per 10'	–		1.006 (1–1.01)	0.0009	1.005 (0.997–1.01)	0.2	1.004 (0.996–1.01)	0.3
Pre-CCL P2Y12 inhibitor	–		0.25 (0.15–0.40)		0.39 (0.24–0.65)	0.0003	0.49 (0.29–0.84)	0.01
Pre-CCL anticoagulation	–		0.46 (0.29–0.73)		0.50 (0.31–0.0.79)	0.003	0.56 (0.33–0.93)	0.03
Successful PCI	–		–		–		0.21 (0.12–0.35)	<0.0001

FMC, first medical contact; CCL, cardiac catheterization laboratory; PCI, percutaneous coronary intervention.

Models were adjusted on FMC to balloon time and covariables unequally distributed between groups ($p < 0.1$) at different timepoints: Model 1 included pre-FMC variables: age, gender, diabetes, hypertension, current smoking, Killip class≥ 2, past histories of myocardial infarction and PCI; Model 2 included FMC vraiables: national EMS number call, characteristics of the FMC and, pre-CCL aspirin, P2Y12 inhibitor and intravenous anticoagulation administration; Model 3 included all variables in models 1 and 2; Model 4 included all variables in model 3 and in-hospital variables: transradial access, successful PCI and, per procedure P2Y12 inhibitor, 2B3A inhibitor and intravenous anticoagulation.

study shows that although indirect admission is associated with longer FMC to balloon times, the relationship between indirect admission and mortality remains independent of FMC to balloon time. Such impact of indirect admission on mortality may be explained by several findings in our study. Pre-FMC variables such as older age, female gender, diabetes, hypertension and clinical signs of heart failure (killip class ≥2 and cardiogenic shock), known correlates of mortality were more frequently encountered in the indirect admission group (15–17). Elderly, female and diabetic patients are also more often late presenters, have delayed management and longer total ischemic time and are more likely to have STEMI complicated by heart failure and subsequent mortality (16–18). Concordantly our study shows longer symptom to FMC and total ischemic times in the indirect admission group. However as shown on our multivariable analyses, patient characteristics and longer total ischemic times are not the single explanation to the impact of indirect admission on mortality.

Among FMC-related variables, the pre-CCL medication was different between the groups with higher rates of pretreatment with clopidogrel as compared to newer P2Y12 inhibitors and lower rates of intravenous anticoagulation in those indirectly admitted. Treatment by intravenous anticoagulants and more potent P2Y12 inhibitors rather than clopidogrel is recommended, in the setting of primary PCI based on strong evidence (1). Although the benefit of a pre-CCL administration of ticagrelor as compared to its administration in the CCL on clinical outcome-except in terms of stent thrombosis- or coronary artery flow was not demonstrated in a randomized controlled trial (19), several metanalyses show a benefit of more potent P2Y12 inhibitors over clopidogrel and the benefit of Pre-procedure over per-procedure P2Y12 inhibitors in the setting of STEMI both on clinical endpoints and the quality of coronary flow restoration (20–22). Such discrepancy may be related to the very short time separating the two groups in the latter randomized trial −30′-while in real life, system delays are much longer and allow the P2Y12 inhibitors to be effective at the time of PCI. As a matter of fact a sub-analysis of the above-mentioned trial showed that ticagrelor Pre-treatment was associated with improved reperfusion in those with long transfer delays (23). Pre-CCL anticoagulation has also been

TABLE 4 | Independent correlates of indirect admission to catheterization laboratory.

	OR (95% CI)	Wald *p value*
FMC to balloon per 10′	1.08 (1.06–1.09)	<0.0001
Age per year	1.02 (1.003–1.03)	0.01
Paramedics-EMS vs. MD-EMS	5.94 (3.89–9.01)	<0.0001
Private MD vs. MD-EMS	3.41 (1.86–6.21)	<0.0001

FMC, first medical contact; MD, medical doctor; EMS, emergency medical services. The model included FMC to balloon time, type of FMC (MD EMS, Paramedics EMS, Private MD, PCI-capable hospital, non-PCI-capable hospital) and all pre-FMC characteristics unequally distributed between groups with a p < 0.1 as reported in ***Table 1****.*

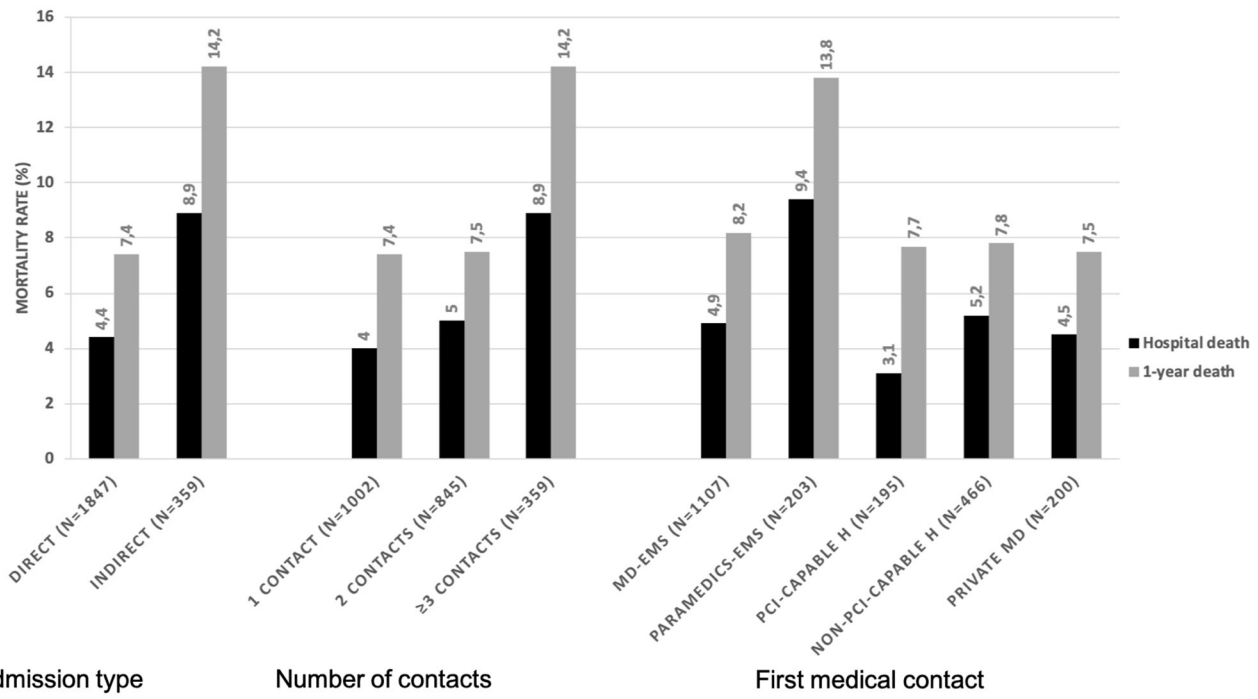

FIGURE 3 | In-hospital and 1-year mortality rates based on different pathways to catheterization laboratory. PCI, percutaneous coronary intervention; EMS, emergency medical services; ED, emergency department; MD, medical doctor; H, hospital.

reported to be associated with improved coronary flow at the time of PCI (24) especially in those with long transfer delays (23) although an effect on clinical endpoints has not been demonstrated to date. In our study both pre-CCL P2Y12 inhibitor use and anticoagulation were associated with lower rates of mortality at 1 year independent of other covariables. The suboptimal pre-CCL antithrombotic management may expose to the risk of higher thrombus burden at the time of PCI, over-exposure to GP2B3A inhibitors in routine or bail-out situations and suboptimal myocardial reperfusion. The impact of pre-CCL administration of such drugs on coronary flow, a correlate of mortality (25), is supported by our findings of lower rates of GP2B3A inhibition and supplementary anticoagulation as well as the higher rates of successful PCI in those directly admitted to the CCL and may be another explanation of the relationship between the groups and mortality.

Another explanation to the differences in pre-CCL management is the diversity of FMCs and pathways. Unlike other FMCs, private MDs and paramedics-EMS, although capable of activating the CCL, did not administer such medication and systematically required another contact. The latter types of FMC, independently associated with indirect admission in our study, are also associated with longer FMC to balloon times and, no or delayed administration of P2Y12 inhibitors and/or intravenous anticoagulation. A poor impact of presentation to a private-MD vs. EMS on system delays and outcome has been previously reported (26).

Our analysis showed that age, paramedics-EMS and private-MD FMCs were associated with indirect admission independent of FMC to balloon time and other pre-FMC variables. The French EMS targeting STEMI patients are based on a dedicated national number and an MD on board organization. However, MD-EMS were the FMC in only half of patients. In almost 10% of patients the FMC was a paramedics-EMS, and mortality rates were almost twice higher in such patients compared to those managed by MD-EMS. Higher patient risk profile (female gender and Killip class >1) and the lack of medical expertise in the paramedics-EMS potentially leading to delayed diagnosis, patient misorientation and suboptimal management may explain such finding. It is likely that in an emergency care organization based on MD-EMS, paramedic-EMS, associated with indirect admission and increased risk of mortality should be avoided. Another 10% of patients self-presented to their private MD or a non-PCI facility ED. Interestingly, compared to MD-EMS, system delays were significantly higher in all such patients but mortality rates were not higher. Such finding may be due, to a selection bias, less severe status being more likely to lead to self-presentation than EMS call.

Direct admission to CCL was also associated with higher rates of transradial approach and successful PCI both known correlates of decreased mortality in the setting of STEMI (15, 27). Although a relationship between indirect admission and lower rates of transradial approach has previously been reported (8), in absence of a plausible mechanistic explanation such finding may be considered as random. Finally, as mentioned above, the relationship between indirect admission and PCI success may be related to more optimal upfront antithrombotic therapy.

Limitations

Our study is a retrospective analysis of a prospective registry and may have several limitations inherent to such design. The impact of several known or unknown variables may have been underestimated or unassessed. The registry focuses on the peri-CCL management and antithrombotic therapy; hence the impact of other evidence-based treatments could not be assessed. Furthermore, compliance to evidence-based medication impacting outcomes was not assessed in our study. However similar 1-year rates of antiplatelet therapy suggest comparable adherence to treatment between groups. The findings are specific to the STEMI networks based on MD-EMS as a reference in mixt rural/urban regions and may not apply to other types of organizations. However, none of the latter limitations is likely to impact the main finding of the study. Finally, the multiple analyses based on different FMCs and pathways, should be considered as only exploratory.

CONCLUSIONS

Our study shows that indirect admission to the CCL for primary PCI in the setting of STEMI is associated with in-hospital and 1-year mortality and cardiovascular mortality independent of system delays. Indirect admission to CCL is not only associated with longer FMC to balloon times but also, with higher rates of high-risk patients, suboptimal pre-CCL antithrombotic therapy and lower rates of successful PCI. Among all assessed variables, older age, Paramedics-EMS and self-presentation to a private MD as FMCs were independently associated with indirect admission to CCL. Such findings in a system based on MD-EMS for the management of STEMI, underscores the potential pitfalls of such organization. Our study, highlights the need for population education especially targeting elderly patients and EMS dispatching and staff training in order to improve pre-CCL management and promote direct admission to CCL. Direct admission and optimal pre-CCL management and not only reduced system delays should be considered as STEMI network quality of care measures.

DATA AVAILABILITY STATEMENT

The data analyzed in this study is subject to the following licenses/restrictions: The data underlying this article were provided by FRANCE-PCI registry. Data will be shared on request to the corresponding author with permission of the FRANCE-PCI registry steering committee. Requests to access these datasets should be directed to FB, beygui-f@chu-caen.r.

ETHICS STATEMENT

The studies involving human participants were reviewed and approved by Commission National Informatique et Libertés-CNIL-, 3 Place de Fontenoy-TSA 80715-75334 PARIS

CEDEX 07. The Ethics Committee waived the requirement of written informed consent for participation.

AUTHOR CONTRIBUTIONS

FB, RK, and GR contributed to conception and design of the study. GR organized the database. FB performed the statistical analysis and wrote the first draft of the manuscript. All authors contributed to manuscript revision, read, and approved the submitted version.

FUNDING

The France-PCI registry's management is funded by the French Regional Health Agencies.

SUPPLEMENTARY MATERIAL

The Supplementary Material for this article can be found online at: https://www.frontiersin.org/articles/10.3389/fcvm.2022.793067/full#supplementary-material

REFERENCES

1. Ibanez B, James S, Agewall S, Antunes MJ, Bucciarelli-Ducci C, Bueno H, et al. 2017 ESC Guidelines for the management of acute myocardial infarction in patients presenting with ST-segment elevation: the task force for the management of acute myocardial infarction in patients presenting with ST-segment elevation of the European Society of Cardiology (ESC). *Eur Heart J.* (2018) 39:119–77. doi: 10.1093/eurheartj/ehx393
2. de Luca G, Suryapranata H, Ottervanger JP, Antman EM. Time delay to treatment and mortality in primary angioplasty for acute myocardial infarction: every minute of delay counts. *Circulation.* (2004) 109:1223–5. doi: 10.1161/01.CIR.0000121424.76486.20
3. Jäger B, Farhan S, Rohla M, Christ G, Podczeck-Schweighofer A, Schreiber W, et al. Clinical predictors of patient related delay in the VIENNA ST-elevation myocardial infarction network and impact on long-term mortality. *Eur Heart J Acute Cardiovasc Care.* (2017) 6:254–61. doi: 10.1177/2048872616633882
4. Terkelsen CJ, Jensen LO, Tilsted H-H, Trautner S, Johnsen SP, Vach W, et al. Health care system delay and heart failure in patients with ST-segment elevation myocardial infarction treated with primary percutaneous coronary intervention: follow-up of population-based medical registry data. *Ann Intern Med.* (2011) 155:361–7. doi: 10.7326/0003-4819-155-6-201109200-00004
5. Menees DS, Peterson ED, Wang Y, Curtis JP, Messenger JC, Rumsfeld JS, et al. Door-to-balloon time and mortality among patients undergoing primary PCI. *N Engl J Med.* (2013) 369:901–9. doi: 10.1056/NEJMoa1208200
6. Beygui F, Castren M, Brunetti ND, Rosell-Ortiz F, Christ M, Zeymer U, et al. Pre-hospital management of patients with chest pain and/or dyspnoea of cardiac origin. A position paper of the Acute Cardiovascular Care Association (ACCA) of the ESC. *Eur Heart J Acute Cardiovasc Care.* (2020) 9:59–81. doi: 10.1177/2048872615604119
7. Ferreira AS, Costa J, Braga CG, Marques J. Impact on mortality of direct admission versus interhospital transfer in patients with ST-segment elevation myocardial infarction undergoing primary percutaneous coronary intervention. *Rev Port Cardiol.* (2019) 38:621–31. doi: 10.1016/j.repce.2019.11.012
8. Rathod KS, Jain AK, Firoozi S, Lim P, Boyle R, Nevett J, et al. Outcome of inter-hospital transfer versus direct admission for primary percutaneous coronary intervention: an observational study of 25,315 patients with ST-elevation myocardial infarction from the London Heart Attack Group. *Eur Heart J Acute Cardiovasc Care.* (2020) 9:948–57.2048872619882340. doi: 10.1177/2048872619882340
9. Rangé G, Chassaing S, Marcollet P, Saint-Étienne C, Dequenne P, Goralski M, et al. The CRAC cohort model: a computerized low cost registry of interventional cardiology with daily update and long-term follow-up. *Rev Epidemiol Sante Publique.* (2018) 66:209–16. doi: 10.1016/j.respe.2018.01.135
10. Hakim R, Revue E, Saint Etienne C, Marcollet P, Chassaing S, Decomis MP, et al. Does helicopter transport delay prehospital transfer for STEMI patients in rural areas? Findings from the CRAC France PCI registry. *Eur Heart J Acute Cardiovasc Care.* (2019) 9:958–65. doi: 10.1177/2048872619848976
11. Thygesen K, Alpert JS, Jaffe AS, Chaitman BR, Bax JJ, Morrow DA, et al. Fourth Universal Definition of Myocardial Infarction (2018). *J Am Coll Cardiol.* (2018) 72:2231–64. doi: 10.1161/CIR.0000000000000617
12. Cutlip DE, Windecker S, Mehran R, Boam A, Cohen DJ, van Es G-A, et al. Clinical end points in coronary stent trials: a case for standardized definitions. *Circulation.* (2007) 115:2344–51. doi: 10.1161/CIRCULATIONAHA.106.685313
13. de Luca G, van't Hof AWJ, de Boer M-J, Ottervanger JP, Hoorntje JCA, Gosselink ATM, et al. Time-to-treatment significantly affects the extent of ST-segment resolution and myocardial blush in patients with acute myocardial infarction treated by primary angioplasty. *Eur Heart J.* (2004) 25:1009–13. doi: 10.1016/j.ehj.2004.03.021
14. Francone M, Bucciarelli-Ducci C, Carbone I, Canali E, Scardala R, Calabrese FA, et al. Impact of primary coronary angioplasty delay on myocardial salvage, infarct size, and microvascular damage in patients with ST-segment elevation myocardial infarction: insight from cardiovascular magnetic resonance. *J Am Coll Cardiol.* (2009) 54:2145–53. doi: 10.1016/j.jacc.2009.08.024
15. Eagle KA, Lim MJ, Dabbous OH, Pieper KS, Goldberg RJ, van de Werf F, et al. A validated prediction model for all forms of acute coronary syndrome: estimating the risk of 6-month postdischarge death in an international registry. *JAMA.* (2004) 291:2727–33. doi: 10.1001/jama.291.22.2727
16. Stehli J, Martin C, Brennan A, Dinh DT, Lefkovits J, Zaman S. Sex differences persist in time to presentation, revascularization, and mortality in myocardial infarction treated with percutaneous coronary intervention. *J Am Heart Assoc.* (2019) 8:e012161. doi: 10.1161/JAHA.119.012161
17. Norhammar A, Lindbäck J, Rydén L, Wallentin L, Stenestrand U, Register of Information and Knowledge about Swedish Heart Intensive Care Admission (RIKS-HIA). Improved but still high short- and long-term mortality rates after myocardial infarction in patients with diabetes mellitus: a time-trend report from the Swedish Register of Information and Knowledge about Swedish Heart Intensive Care Admission. *Heart.* (2007) 93:1577–1583. doi: 10.1136/hrt.2006.097956
18. Margolis G, Letourneau-Shesaf S, Khoury S, Pereg D, Kofman N, Keren G, et al. Trends and predictors of prehospital delay in patients undergoing primary coronary intervention. *Coron Artery Dis.* (2018) 29:373–7. doi: 10.1097/MCA.0000000000000608
19. Montalescot G, van't Hof AW, Lapostolle F, Silvain J, Lassen JF, Bolognese L, et al. Prehospital ticagrelor in ST-segment elevation myocardial infarction. *N Engl J Med.* (2014) 371:1016–27. doi: 10.1056/NEJMoa1407024
20. Bellemain-Appaix A, O'Connor SA, Silvain J, Cucherat M, Beygui F, Barthélémy O, et al. Association of clopidogrel pretreatment with mortality, cardiovascular events, and major bleeding among patients undergoing percutaneous coronary intervention: a systematic review and meta-analysis. *JAMA.* (2012) 308:2507–16. doi: 10.1001/jama.2012.50788
21. Bellemain-Appaix A, Kerneis M, O'Connor SA, Silvain J, Cucherat M, Beygui F, et al. Reappraisal of thienopyridine pretreatment in patients with non-ST elevation acute coronary syndrome: a systematic review and meta-analysis. *BMJ.* (2014) 349:g6269. doi: 10.1136/bmj.g6269
22. Bellemain-Appaix A, Bégué C, Bhatt DL, Ducci K, Harrington RA, Roe M, et al. The efficacy of early versus delayed P2Y12 inhibition in percutaneous coronary intervention for ST-elevation myocardial infarction: a systematic review and meta-analysis. *EuroIntervention.* (2018) 14:78–85. doi: 10.4244/EIJ-D-17-00852
23. Fabris E, van't Hof A, Hamm CW, Lapostolle F, Lassen JF, Goodman SG, et al. Impact of presentation and transfer delays on complete ST-segment resolution before primary percutaneous coronary intervention: insights from the ATLANTIC trial. *EuroIntervention.* (2017) 13:69–77. doi: 10.4244/EIJ-D-16-00965

24. Zijlstra F, Ernst N, de Boer M-J, Nibbering E, Suryapranata H, Hoorntje JCA, et al. Influence of prehospital administration of aspirin and heparin on initial patency of the infarct-related artery in patients with acute ST elevation myocardial infarction. *J Am Coll Cardiol.* (2002) 39:1733–7. doi: 10.1016/S0735-1097(02)01856-9
25. de Luca G, van't Hof AWJ, de Boer M-J, Hoorntje JCA, Gosselink ATM, Dambrink J-HE, et al. Impaired myocardial perfusion is a major explanation of the poor outcome observed in patients undergoing primary angioplasty for ST-segment-elevation myocardial infarction and signs of heart failure. *Circulation.* (2004) 109:958–61. doi: 10.1161/01.CIR.0000120504.31457.28
26. Hafiz AM, Naidu SS, DeLeon J, Islam S, Alkhatib B, Lorenz M, et al. Impact of first contact on symptom onset-to-door time in patients presenting for primary percutaneous coronary intervention. *Am J Emerg Med.* (2013) 31:922–7. doi: 10.1016/j.ajem.2013.03.005
27. Valgimigli M, Frigoli E, Leonardi S, Vranckx P, Rothenbühler M, Tebaldi M, et al. Radial vs. femoral access and bivalirudin vs. unfractionated heparin in invasively managed patients with acute coronary syndrome (MATRIX): final 1-year results of a multicentre, randomised controlled trial. *Lancet.* (2018) 392:835–48. doi: 10.1016/S0140-6736(18)31714-8

Conflict of Interest: The authors declare that the research was conducted in the absence of any commercial or financial relationships that could be construed as a potential conflict of interest.

frontiers in Cardiovascular Medicine

ORIGINAL RESEARCH
published: 16 March 2022
doi: 10.3389/fcvm.2022.790193

Predictive Value of the CHA_2DS_2-VASc Score for Mortality in Hospitalized Acute Coronary Syndrome Patients With Chronic Kidney Disease

Yaxin Wu[1], Yanxiang Gao[2], Qing Li[1], Chao Wu[3,4], Enmin Xie[5], Yimin Tu[5], Ziyu Guo[1], Zixiang Ye[1], Peizhao Li[1], Yike Li[5], Xiaozhai Yu[5], Jingyi Ren[2] and Jingang Zheng[1,2]**

[1] Department of Cardiology, Peking University China-Japan Friendship School of Clinical Medicine, Beijing, China, [2] Department of Cardiology, China-Japan Friendship Hospital, Beijing, China, [3] Department of Cardiology, Guangdong Provincial People's Hospital, Guangdong Academy of Medical Sciences, Guangzhou, China, [4] Guangdong Cardiovascular Institute, Guangzhou, China, [5] Graduate School, Chinese Academy of Medical Sciences and Peking Union Medical College, Beijing, China

OPEN ACCESS

Edited by:
Robert Ekart,
Maribor University Medical Centre, Slovenia

Reviewed by:
Ahmet Öz,
İstanbul Eğitim ve Araştırma Hastanesi, Turkey
Sebastjan Bevc,
Maribor University Medical Centre, Slovenia

***Correspondence:**
Jingang Zheng
mdjingangzheng@163.com
Jingyi Ren
renjingyi1213@163.com

Specialty section:
This article was submitted to Coronary Artery Disease, a section of the journal Frontiers in Cardiovascular Medicine

Received: 06 October 2021
Accepted: 21 February 2022
Published: 16 March 2022

Citation:
Wu Y, Gao Y, Li Q, Wu C, Xie E, Tu Y, Guo Z, Ye Z, Li P, Li Y, Yu X, Ren J and Zheng J (2022) Predictive Value of the CHA_2DS_2-VASc Score for Mortality in Hospitalized Acute Coronary Syndrome Patients With Chronic Kidney Disease. Front. Cardiovasc. Med. 9:790193. doi: 10.3389/fcvm.2022.790193

Background: Chronic kidney disease (CKD) patients have a high prevalence of coronary artery disease and a high risk of cardiovascular events. The present study assessed the value of the CHA_2DS_2-VASc score for predicting mortality among hospitalized acute coronary syndrome (ACS) patients with CKD.

Methods: This was a retrospective cohort study that included CKD patients who were hospitalized for ACS from January 2015 to May 2020. The CHA_2DS_2-VASc score for each eligible patient was determined. Patients were stratified into two groups according to CHA_2DS_2-VASc score: <6 (low) and ≥ 6 (high). The primary endpoint was all-cause mortality.

Results: A total of 313 eligible patients were included in the study, with a mean CHA_2DS_2-VASC score of 4.55 ± 1.68. A total of 220 and 93 patients were assigned to the low and high CHA_2DS_2-VASc score groups, respectively. The most common reason for hospitalization was unstable angina (39.3%), followed by non-ST-elevation myocardial infarction (35.8%) and ST-elevation myocardial infarction (24.9%). A total of 67.7% of the patients (212/313) received coronary reperfusion therapy during hospitalization. The median follow-up time was 23.0 months (interquartile range: 12–38 months). A total of 94 patients (30.0%) died during follow-up. The high score group had a higher mortality rate than the low score group (46.2 vs. 23.2%, respectively; $p < 0.001$). The cumulative incidence of all-cause death was higher in the high score group than in the low score group (Log-rank test, $p < 0.001$). Multivariate Cox regression analysis indicated that CHA_2DS_2-VASc scores were positively associated with all-cause mortality (hazard ratio: 2.02, 95% confidence interval: 1.26–3.27, $p < 0.001$).

Conclusion: The CHA_2DS_2-VASc score is an independent predictive factor for all-cause mortality in CKD patients who are hospitalized with ACS. This simple and practical scoring system may be useful for the early identification of patients with a high risk of death.

Keywords: chronic kidney disease, acute coronary syndrome (ACS), CHA_2DS_2-VASc score, prognosis, mortality

INTRODUCTION

Chronic kidney disease (CKD) is an important contributor to morbidity and mortality from non-communicable diseases and has become a considerable public health issue (1–3). Patients with CKD have a high prevalence of coronary artery disease, and many of these patients die from cardiovascular disease, especially those with acute coronary syndrome (ACS) (4, 5). The early identification of high-risk ACS patients is important for assessing prognosis and guiding treatment. Current international guidelines recommend Global Registry of Acute Coronary Events (GRACE) scores to predict the cumulative risk of death and myocardial infarction (6, 7). However, derivations of GRACE scores are based on unselected and generalizable patients, and the calculation of GRACE scores is relatively complicated (8), which may limit its application in CKD patients, especially those with end-stage renal disease. The CHA_2DS_2-VASc score is used to assess the combination of congestive heart failure, hypertension, diabetes, prior stroke, vascular disease, and age. It is an easily calculated scoring system that can assess the risk of stroke in patients with atrial fibrillation (9, 10). All of these risk factors have been proven to be associated with cardiovascular prognosis. Recent studies also used CHA_2DS_2-VASc scores to predict poor prognosis in patients with cardiovascular disease, regardless of atrial fibrillation (11–13). The risk factors that are included in this scoring system are also common in CKD patients with coronary artery disease (5, 14). The objective of the present study was to evaluate the predictive value of CHA_2DS_2-VASc scores in hospitalized ACS patients with CKD.

METHODS

Study Design and Population

This was a retrospective cohort study that included CKD patients who were hospitalized for ACS from January 2015 to May 2020. We consecutively enrolled patients in the Cardiology Department, China-Japan Friendship Hospital. Cases were identified using International Classification of Diseases-Clinical Modification code 9. All enrolled patients were confirmed to have at least one major coronary artery with more than 50% stenosis, determined by coronary angiography. Data on demographics, medical history, and laboratory tests were abstracted from electronic medical records. The glomerular filtration rate was estimated according to serum creatinine and the Chronic Kidney Disease Epidemiology Collaboration (CKD-EPI). Chronic kidney disease was defined by an estimated glomerular filtration rate <60 ml/min/1.73 m^2, including dialysis. Coronary reperfusion therapy included percutaneous transluminal coronary angioplasty (PTCA) $\pm$ stenting, PTCA alone, or coronary artery bypass grafting. The study conformed to the Declaration of Helsinki and was approved by the Research Ethical Review Committee of China-Japan Friendship Hospital (2020-112-K71).

CHA_2DS_2-VASc Score

For each patient, the CHA_2DS_2-VASc score was calculated at admission based on the following scoring system: (1) point for congestive heart failure, hypertension, 65–74 years of age, diabetes mellitus, vascular disease, and female sex and (2) points for $\geq$75 years of age and prior stroke or transient ischemia attack. We performed a receiver operating characteristic analysis that showed that the best cut-off value of the CHA_2DS_2-VASc score to predict mortality was $\geq$6 with 45.7% sensitivity and 77.2% specificity [area under curve: 0.64; 95% confidence interval (CI): 0.58–0.71, $p < 0.001$; **Supplementary Material**]. Therefore, the CHA_2DS_2-VASc score was classified as $<$6 and $\geq$6. The patients were not further divided into more than these two groups because of the relatively small sample size.

Follow-Up and Outcome

The primary outcome of the study was all-cause mortality, which was the rate of death from any cause from the date of admission until the occurrence of endpoint events or until the latest follow-up date (June 1–July 1, 2021). Clinical events were ascertained by longitudinally tracking patients' medical records or through telephone interviews.

Statistical Analysis

Continuous variables are expressed as the mean $\pm$ standard deviation or median and interquartile range and compared using *t*-tests or the Mann-Whitney *U*-test when appropriate. Categorical variables are expressed as frequencies and percentages and were compared using the χ^2-test or Fisher's exact test. Univariate and multivariate Cox regression analyses were performed to determine risk factors for all-cause death, and the hazard ratio (HR) and 95% CI were calculated. Variables with values of $p < 0.10$ in the univariate analysis were included in the multivariate analysis. Time-dependent survival between groups was evaluated using Kaplan-Meier curves and the Log-rank test. Stratified analyses were performed using the following variables: age ($\geq$65 vs. $<$65 years), sex, hyperlipidemia, diabetes, prior myocardial infarction, hemodialysis, main diagnosis, left ventricular ejection fraction ($\geq$50 vs. $<$50%), and reperfusion therapy. Multiplicative interactions were calculated in each subgroup. All statistical analyses were performed using SPSS 27.0 software (IBM Corp., Armonk, NY, USA). Two-tailed values of $p < 0.05$ were considered statistically significant.

TABLE 1 | Baseline characteristics in CKD patients hospitalized with ACS by CHA2DS2-VASc score.

Characteristic	Total (*N* = 313)	CHA2DS2-VASc score (*N* = 313)		*P*-value
		<6 (*N* = 220)	≥6 (*N* = 93)	
Age, yrs	69.8 ± 11.2	67.7 ± 11.3	74.6 ± 9.2	<0.001
Male sex	128 (40.9)	90 (34.5)	38 (55.9)	<0.001
BMI (kg/m^2)	24.9 ± 4.8	24.7 ± 3.99	25.2 ± 6.3	0.410
Medical history				
Hypertension	274 (87.5)	185 (84.1)	89 (95.7)	0.004
Diabetes mellitus	179 (57.2)	105 (47.7)	74 (79.6)	<0.001
Hyperlipidemia	173 (55.3)	111 (50.5)	62 (66.7)	0.008
Congestive heart failure	164 (52.4)	96 (43.6)	68 (73.1)	<0.001
Prior stroke or TIA	102 (32.6)	35 (15.9)	67 (72.0)	<0.001
Prior MI	85 (27.2)	56 (25.5)	29 (31.2)	0.300
Prior PCI	80 (25.6)	48 (21.8)	32 (34.4)	0.020
Prior CABG	17 (5.4)	10 (4.5)	7 (7.5)	0.290
Peripheral artery disease	57 (18.2)	29 (13.2)	28 (30.1)	<0.001
Stage of CKD				0.690
Stage 3	136 (43.5)	93 (42.6)	43 (46.2)	
Stage 4	47 (15.0)	32 (14.6)	15 (16.1)	
Stage 5	129 (41.2)	94 (42.9)	43 (46.2)	
Clinical presentation				0.820
STEMI	78 (24.9)	57 (25.9)	21 (22.6)	
NSTEMI	112 (35.8)	78 (35.5)	34 (36.6)	
UA	123 (39.3)	85 (38.6)	38 (40.9)	
Laboratory measures				
Hemoglobin, g/dl	112.6 ± 121.6	114.8 ± 21.8	107.2 ± 20.5	0.004
Platelet count, ×10^9/l	194 ± 61	194.3 ± 59.7	189.8 ± 63.1	0.520
LDL, mmol/l	2.5 ± 0.9	2.59 ± 0.88	2.33 ± 0.99	0.005
Serum creatinine, mg/dl	4.33 ± 3.73	4.61 ± 3.94	3.66 ± 3.11	0.110
Uric acid	408 ± 134	404 ± 133	419 ± 136	0.380
Homocysteine, μmol/l	23.6 ± 26.3	24.0 ± 21.4	22.7 ± 35.5	0.007
D-dimer, mg/l	1.30 ± 1.78	1.28 ± 1.93	1.33 ± 1.38	0.060
LVEF	55 ± 12	55 ± 11	55 ± 13	0.450
Reperfusion therapy	212 (67.7)	156 (70.9)	56 (60.2)	0.060
Medical therapy at admission				
Aspirin	301 (96.2)	211 (95.9)	90 (96.8)	0.720
P2Y12 receptor antagonist	297 (94.9)	208 (94.5)	89 (95.7)	0.670
Stain	303 (96.8)	213 (96.8)	90 (96.8)	0.980
β-blockers	286 (91.4)	201 (91.4)	85 (91.4)	0.990

ACEI, angiotensin-converting enzyme inhibitors; ARB, angiotensin receptor blockers; BMI, body mass index; CKD, chronic kidney disease; CABG, coronary artery bypass grafting; LDL, Low-density lipoprotein; LVEF, left ventricular ejection fraction; MI, myocardial infarction; NSTEMI, non-ST-segment elevation myocardial infarction; STEMI, ST-segment elevation myocardial infarction; TIA, transient ischemic attacks; UA, unstable angina.

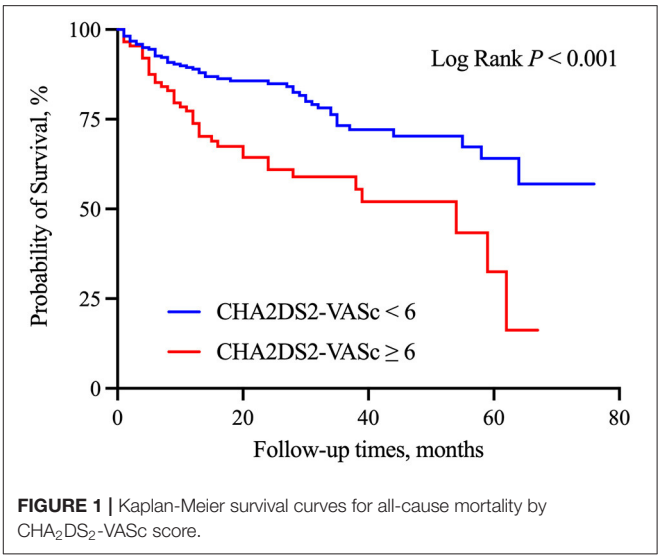

FIGURE 1 | Kaplan-Meier survival curves for all-cause mortality by CHA_2DS_2-VASc score.

RESULTS

A total of 313 eligible patients were recruited in the study. Baseline characteristics are presented in **Table 1**. Among these patients, the mean CHA_2DS_2-VASC score was 4.55 ± 1.68. A total of 220 patients (70.3%) had a low CHA_2DS_2-VASc score (<6 points), and 93 (29.7%) had a high CHA_2DS_2-VASc score (≥6 points). The high CHA_2DS_2-VASC score group included patients who were older and had a higher prevalence of comorbidities, including diabetes mellitus, heart failure, and cerebrovascular disease. Patients who were diagnosed with non-ST-elevation myocardial infarction (35.8%) and unstable angina pectoris (39.3%) were more common than patients who were diagnosed with ST-elevation myocardial infarction (24.9%). Among the 313 patients, 67.7% (212) received coronary reperfusion therapy, including PTCA ± stenting (n = 187), PTCA (n = 15), and coronary artery bypass grafting (n = 10). Accordingly, in-hospital treatment was comparable between the two groups.

The median follow-up time was 23.0 months (interquartile range: 12–38 months). During the follow-up period, a total of 94 patients (30.0%) died. High CHA_2DS_2-VASC scores were associated with a higher risk of mortality (46.2 vs. 23.2%, p < 0.001). Kaplan-Meier curves for patients who were stratified by CHA_2DS_2-VASC scores are presented in **Figure 1**. The cumulative incidence of all-cause mortality (Log-rank test, p < 0.001) was higher in the high CHA_2DS_2-VASC score group than in the low CHA_2DS_2-VASC score group. We performed Cox univariate and multivariate analyses using the low CHA_2DS_2-VASc score group as the reference group. The HR for all-cause mortality was 2.49 (95% CI: 1.66–3.74, p < 0.001). After adjusting for hypertension, diabetes, prior myocardial infarction, and CKD stage, the HR of all-cause mortality was 2.029 (95% CI: 1.33–3.10, p = 0.001). The HR of all-cause mortality was largely unchanged after adding all other variables with p < 0.10 in the univariate analysis (HR: 2.027, 95% CI: 1.26–3.27, p < 0.001). The univariate analysis of factors that were related to all-cause mortality is presented in **Table 2**. The multivariate analyses between the CHA_2DS_2-VASc score group and outcomes are shown in **Table 3**. A significant between-group difference in outcome was found in the subgroup analyses of sex [HR: 2.94 (95% CI: 1.66–5.21) for men; HR: 1.91 (95% CI: 1.00–3.61) for women; p = 0.045]. A similar result was found for death in the subgroup analyses of

TABLE 2 | Cox regression analysis of factors related to all-cause mortality.

Parameter	Univariate (all-cause mortality)	
	HR (95% CI)	*P*-value
Age[a]	1.02 (1.00–1.04)	0.024
Male sex (vs. Female)	0.98 (0.65–1.47)	0.920
BMI[b]	0.79(0.53–1.19)	0.260
Prior PCI	1.13 (0.72–1.78)	0.590
Prior CABG	1.38 (0.60–3.16)	0.470
Stage of CKD		
Stage 3	1 (ref)	..
Stage 4	1.72 (1.11–2.67)	0.015
Stage 5	2.12 (1.14–4.31)	0.019
Diagnosis		
UA	1 (ref)	..
NSTEMI	1.30 (0.76–2.25)	0.340
STEMI	1.80 (1.12–2.89)	0.015
Hemoglobin, g/dl	0.990 (0.981–0.999)	0.027
Platelet count, $\times 10^9$/l	0.998 (0.994–1.000)	0.180
LDL, mmol/l	0.87 (0.69–1.10)	0.250
Uric acid, μmol/l	0.999 (0.998–1.001)	0.360
Serum creatinine, mg/dl	1.04 (0.98–1.09)	0.180
Homocysteine, μmol/l	1.004 (0.999–1.010)	0.100
D-dimer, mg/l	1.08 (1.00–1.164)	0.041
LVEF (≥50 vs. <50)	0.74 (0.48–1.13)	0.160
Reperfusion therapy	0.68 (0.45–1.04)	0.070
Aspirin	1.24 (0.39–3.93)	0.710
P2Y12 receptor antagonist	1.55 (0.49–4.88)	0.460
Stain	1.58 (0.38–6.43)	0.520
β-blockers	1.37 (0.60–3.15)	0.450
ACEI/ARB	1.58 (0.39–6.43)	0.520
CHA2DS2-VASc score[c] ≥ 6	2.48 (1.65–3.73)	<0.001

[a] *Per 1 unit increase.*
[b] *BMI ≥ 24 kg/m^2 vs. BMI< 24 kg/m^2.*
[c] *CHA2DS2-VASc score ≥ 6 score vs. CHA2DS2-VASc score < 6 score.*
ACEI, angiotensin-converting enzyme inhibitors; ARB, angiotensin receptor blockers; BMI, body mass index; CKD, chronic kidney disease; CABG, coronary artery bypass grafting; LDL, Low-density lipoprotein; LVEF, left ventricular ejection fraction; MI, myocardial infarction; NSTEMI, non-ST-segment elevation myocardial infarction; STEMI, ST-segment elevation myocardial infarction; TIA, transient ischemic attacks; UA, unstable angina.

TABLE 3 | Adjusted hazard ratios of all-cause mortality by high CHA2DS2-VASc score (≥6 points) relative to low CHA2DS2-VASc score (<6 points).

Model adjustment	All-cause mortality	
	HR (95% CI)	*P*-value
Unadjusted	2.49 (1.66–3.74)	< 0.001
Model 1	2.49 (1.66–3.74)	< 0.001
Model 2	2.029 (1.33–3.10)	0.001
Model 3	2.027 (1.26–3.27)	0.004

Model 1, adjusted for age, sex; Model 2, adjusted for age, sex, hypertension, diabetes, prior MI, stage of CKD; Model 3, adjusted for age, sex, hypertension, diabetes, Hyperlipidemia, prior MI, stage of CKD, diagnosis, Cr, LVEF, reperfusion therapy and medication therapy at admission.
HR, hazard ratios; CI, confidence interval.

hemodialysis. No significant interactions were found between the other subgroups and CHA_2DS_2-VASC scores for the prediction of all-cause mortality. The results of the subgroup analyses are shown in **Figure 2**.

DISCUSSION

The present study found that CHA_2DS_2-VASC scores were associated with worse clinical outcome in CKD patients with ACS. High scores (≥6) were an independent predictor of all-cause mortality and may be useful for risk stratification. The subgroup analyses indicated that high scores were a slightly better predictor of all-cause mortality in men than in women and in patients who did not undergo hemodialysis. Compared with patients with low scores, patients with high scores were more often older and women and had a higher prevalence of comorbidities. Additionally, patients with high scores were less likely to receive reperfusion therapy in clinical practice.

Acute coronary syndrome is a common critical cardiovascular disease and primary focus of cardiologists. Benefiting from the application of stents, the mortality rate of ACS has gradually decreased over the past decade (15). Patients with coronary disease and CKD, especially end-stage kidney disease, have a very high risk of cardiovascular events (16, 17). The high rate of all-cause mortality in the present study aligns with the high-risk feature of these patients in previous studies. Despite having worse outcomes after a cardiovascular event, patients with CKD are often excluded from the majority of ACS or heart failure cardiovascular outcome trials (18). The reasons for this are likely multifactorial, such as the potential for diminished effects of medical treatment and coronary intervention in trials, complex pathophysiological mechanisms that contribute to cardiovascular disease, safety concerns, and trial recruitment difficulties (19). Therefore, clinical evidence from the general population may not be suitable for this specific patient population. The Framingham risk score is the most well-validated coronary artery disease risk prediction tool, but it has been shown to have poor overall accuracy in predicting cardiac events in individuals with CKD (20). Data from GRACE indicated that the GRACE risk score underestimates the risk of major events in end-stage kidney disease patients who undergo dialysis (21). Moreover, the inclusion of multiple types of variables and relatively complex calculation significantly limit clinical utility of the GRACE risk score (8).

The CHA_2DS_2-VASC score is a validated and extensively used score to estimate thromboembolic risk in patients with atrial fibrillation, consisting of several cardiovascular risk factors (9). Among these factors, old age, hypertension, diabetes, and heart failure have been proven to influence the prognosis of cardiovascular disease (4, 5, 22–24). Prior stroke is also associated with a high risk of major adverse cardiovascular and cerebrovascular events (25). Sex differences in the epidemiology, manifestation, pathophysiology, and outcome of cardiovascular disease have been observed in previous studies (26). Therefore, all

Subgroup	No. of patients	Score≥6 No. of mortality (%)	Score<6 No. of mortality (%)	HR (95%CI)	P for interaction
Age, yrs					0.232
<65	101	5 (45.5)	18 (20.0)	2.51 (0.71-8.90)	
≥65	212	38 (46.3)	33 (25.4)	1.96 (1.22-3.14)	
Sex					0.045
Men	184	22 (53.7)	33 (23.1)	2.94 (1.66-5.21)	
Women	129	21 (40.4)	18 (23.4)	1.91 (1.00-3.62)	
Hyperlipidemia					0.317
No	140	17 (54.8)	30 (27.5)	2.54 (1.40-4.61)	
Yes	173	26 (41.9)	21 (18.9)	1.98 (1.06-3.69)	
Diabetes					0.135
No	134	7 (36.8)	28 (24.3)	2.51 (0.92-6.83)	
Yes	179	36 (48.6)	23 (21.9)	2.15 (1.23-3.74)	
Prior MI					0.404
No	228	29 (45.3)	40 (24.4)	2.45 (1.49-4.01)	
Yes	85	14 (48.3)	11 (19.6)	2.96 (1.28-6.86)	
STEMI					0.103
No	235	37 (51.4)	34 (20.9)	2.96 (1.82-4.79)	
Yes	78	6 (28.6)	17 (29.8)	0.94 (0.26-3.35)	
Hemodialysis					0.029
No	216	36 (49.3)	31 (21.7)	3.50 (2.06-5.95)	
Yes	97	7 (35.0)	20 (26.0)	1.18 (0.41-3.43)	
LVEF					0.086
<50%	92	17 (58.6)	15 (23.8)	3.19 (1.56-6.51)	
≥50%	221	26 (40.6)	36 (22.9)	2.43 (1.45-4.08)	
Reperfusion therapy					0.082
No	101	22 (59.5)	15 (23.4)	3.91 (2.00-7.60)	
Yes	212	21 (37.5)	36 (23.1)	1.86 (0.96-3.63)	

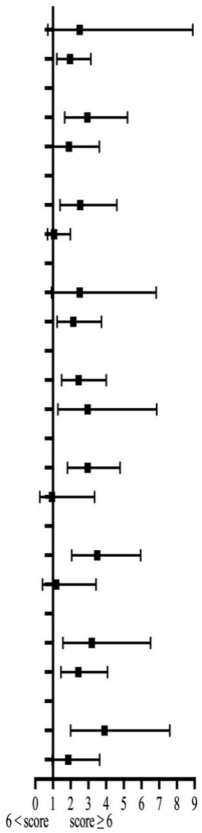

FIGURE 2 | Predictive value of CHA_2DS_2-VASC score for all-cause mortality in different subgroups.

components of the CHA_2DS_2-VASc score have a close association with the prognosis of cardiovascular disease. Tufan Cinar et al. evaluated 267 patients with mechanical mitral valve thrombosis and found that a CHA_2DS_2-VASc score $\geq$ 2.5 was associated with a higher risk of prosthetic valve thrombosis (27). Several recent studies evaluated the predictive value of the CHA_2DS_2-VASc score for clinical outcome. A large real-world cohort study reported that CHA_2DS_2-VASc scores were significantly associated with mortality in heart failure patients (11). Hsu et al. reported the predictive value of CHA_2DS_2-VASc scores for all-cause mortality and cardiovascular mortality in CKD patients without ACS (28). A similar study found that CHA_2DS_2-VASc scores were strongly associated with 1-year mortality and cardiovascular risk in hemodialysis patients (29). Studies that investigated patients with ST-elevation myocardial infarction showed that CHA_2DS_2-VASc scores were an independent predictor of no-reflow and an independent predictor of in-hospital and long-term mortality in patients who underwent primary percutaneous coronary intervention (30–32). Although the association between CHA_2DS_2-VASc score and clinical outcome in ACS patients without CKD or CKD patients without ACS have been estimated, the value of these scores in ACS patients with CKD is unclear. In the present study, we found a significant association between CHA_2DS_2-VASc scores and all-cause mortality in ACS patients with CKD, which may be useful for the risk stratification of these patients. The mean CHA_2DS_2-VASc score in the present study was significantly higher than in patients without CKD in a previous study, which may help explain the high mortality in ACS patients with CKD. Variables that are included in the CHA_2DS_2-VASC score can be readily found in patients' medical histories. Furthermore, CHA_2DS_2-VASC scores may be useful for quickly identifying very high-risk ACS patients with CKD.

The present study has limitations. This was a single-center, retrospective study. We were unable to control the variables that were included in the analyses given the study's observational design. In addition to traditional cardiovascular risk factors (e.g., diabetes and hypertension), non-traditional CKD-related CVD risk factors (e.g., mineral and bone disease abnormalities, vascular calcification, inflammation, and oxidative stress) may also play an important role in the prognosis of cardiovascular disease (4). However, we focused on the prognostic value of the

CHA_2DS_2-VASc scoring system in ACS patients with CKD, based on variables that were readily obtained from the patients' medical records. Another limitation was that the sample size was not sufficiently large to evaluate prognostic value in dialysis and non-dialysis populations separately. Future studies should integrate CHA_2DS_2-VASc scores with non-traditional CKD-related CVD risk factors and develop and validate novel CVD risk prediction scores for the CKD population and dialysis population.

In conclusion, CHA_2DS_2-VASc scores were an independent predictive factor for mortality in ACS patients with CKD. The CHA_2DS_2-VASc scoring system is a simple and practical method for identifying very high-risk ACS patients among the CKD population. Further studies are needed to evaluate whether CHA_2DS_2-VASc scoring can improve the management and outcome of this high-risk population.

DATA AVAILABILITY STATEMENT

The raw data supporting the conclusions of this article will be made available by the authors, without undue reservation.

ETHICS STATEMENT

The studies involving human participants were reviewed and approved by the Research Ethical Review Committee of China-Japan Friendship Hospital. Written informed consent for participation was not required for this study in accordance with the national legislation and the institutional requirements.

AUTHOR CONTRIBUTIONS

YW, JR, and JZ: study design and manuscript preparation. YG, QL, CW, EX, YT, ZG, ZY, PL, YL, and XY: data collection. YW and YG: data analysis and interpretation. All authors contributed to the article and approved the submitted version.

FUNDING

This work was supported by the National Natural Science Foundation of China (No. 91639110), National Key Clinical Specialty Construction Project (No. 2020-QTL-009), Natural Science Foundation of Beijing Municipality (No. 7172195), and Science Foundation of China-Japan Friendship Hospital (No. 2020-HX-40).

ACKNOWLEDGMENTS

The authors acknowledge Zhao Wang from Fuwai Hospital and Xiaoying Gu from China-Japan Friendship Hospital for their support of the study.

SUPPLEMENTARY MATERIAL

The Supplementary Material for this article can be found online at: https://www.frontiersin.org/articles/10.3389/fcvm.2022.790193/full#supplementary-material

REFERENCES

1. Bikbov B, Purcell CA, Levey AS, Smith M, Abdoli A, Abebe M, et al. Global, regional, and national burden of chronic kidney disease, 1990–2017: a systematic analysis for the Global Burden of Disease Study 2017. *Lancet.* (2020) 395:709–33. doi: 10.1016/S0140-6736(20)30045-3
2. Zhang L, Zhao MH, Zuo L, Wang Y, Yu F, Zhang H, et al. China kidney disease network (CK-NET) 2016 annual data report. *Kidney Int Suppl 2011.* (2020) 10:e97–e185. doi: 10.1016/j.kisu.2020.09.001
3. US Renal Data System 2019. Annual data report: epidemiology of kidney disease in the United States. *Am J Kidney Dis.* (2020) 75(1 Suppl. 1):A6–A7. doi: 10.1053/j.ajkd.2019.09.003.
4. Sarnak MJ, Amann K, Bangalore S, Cavalcante JL, Charytan DM, Craig JC, et al. Chronic kidney disease and coronary artery disease: JACC state-of-the-art review. *J Am Coll Cardiol.* (2019) 74:1823–38. doi: 10.1016/j.jacc.2019.08.1017
5. Jankowski J, Floege J, Fliser D, Bohm M, Marx N. Cardiovascular disease in chronic kidney disease: pathophysiological insights and therapeutic options. *Circulation.* (2021) 143:1157–72. doi: 10.1161/CIRCULATIONAHA.120.050686
6. Collet JP, Thiele H, Barbato E, Barthelemy O, Bauersachs J, Bhatt DL, et al. 2020 ESC Guidelines for the management of acute coronary syndromes in patients presenting without persistent ST-segment elevation. *Eur Heart J.* (2021) 42:1289–367. doi: 10.1093/eurheartj/ehab088
7. Ibanez B, James S, Agewall S, Antunes MJ, Bucciarelli-Ducci C, Bueno H, et al. 2017 ESC Guidelines for the management of acute myocardial infarction in patients presenting with ST-segment elevation: the task force for the management of acute myocardial infarction in patients presenting with ST-segment elevation of the European Society of Cardiology (ESC). *Eur Heart J.* (2018) 39:119–77. doi: 10.1093/eurheartj/ehx393
8. Fox KA, Dabbous OH, Goldberg RJ, Pieper KS, Eagle KA, Van de Werf F, et al. Prediction of risk of death and myocardial infarction in the six months after presentation with acute coronary syndrome: prospective multinational observational study (GRACE). *BMJ.* (2006) 333:1091. doi: 10.1136/bmj.38985.646481.55
9. Lip GYH, Nieuwlaat R, Pisters R, Lane DA, Crijns HJGM. Refining clinical risk stratification for predicting stroke and thromboembolism in atrial fibrillation using a novel risk factor-based approach: the euro heart survey on atrial fibrillation. *Chest.* (2010) 137:263–72. doi: 10.1378/chest.09-1584
10. Hindricks G, Potpara T, Dagres N, Arbelo E, Bax JJ, Blomstrom-Lundqvist C, et al. 2020 ESC Guidelines for the diagnosis and management of atrial fibrillation developed in collaboration with the European Association for Cardio-Thoracic Surgery (EACTS): the task force for the diagnosis and management of atrial fibrillation of the European Society of Cardiology (ESC) Developed with the special contribution of the European Heart Rhythm Association (EHRA) of the ESC. *Eur Heart J.* (2021) 42:373–498. doi: 10.1093/eurheartj/ehab648
11. Shuvy M, Zwas DR, Keren A, Gotsman I. Value of the CHA DS -VASc score for predicting outcome in patients with heart failure. *ESC Heart Fail.* (2020) 7:2553–60. doi: 10.1002/ehf2.12831
12. Renda G, Ricci F, Patti G, Aung N, Petersen SE, Gallina S, et al. CHADSVASc score and adverse outcomes in middle-aged individuals without atrial fibrillation. *Eur J Prev Cardiol.* (2019) 26:1987–97. doi: 10.1177/2047487319868320
13. Sanchez Fernandez JJ, Ortiz MR, Ballesteros FM, Luque CO, Penas ER, Ortega MD, et al. CHADS-VASc score as predictor of stroke and all-cause death in stable ischaemic heart disease patients without atrial fibrillation. *J Neurol.* (2020) 267:3061–8. doi: 10.1007/s00415-020-09961-7

14. Di Lullo L, House A, Gorini A, Santoboni A, Russo D, Ronco C. Chronic kidney disease and cardiovascular complications. *Heart Fail Rev.* (2015) 20:259–72. doi: 10.1007/s10741-014-9460-9
15. Widimsky P, Crea F, Binder RK, Lüscher TF. The year in cardiology 2018: acute coronary syndromes. *Eur Heart J.* (2019) 40:271–82. doi: 10.1093/eurheartj/ehy904
16. Go AS, Chertow GM, Fan D, McCulloch CE, Hsu C-y. Chronic kidney disease and the risks of death, cardiovascular events, and hospitalization. *New Engl J Med.* (2004) 351:1296–305. doi: 10.1056/NEJMoa041031
17. Matsushita K, van der Velde M, Astor BC, Woodward M, Levey AS, de Jong PE, et al. Association of estimated glomerular filtration rate and albuminuria with all-cause and cardiovascular mortality in general population cohorts: a collaborative meta-analysis. *Lancet.* (2010) 375:2073–81. doi: 10.1016/S0140-6736(10)60674-5
18. Konstantinidis I, Nadkarni GN, Yacoub R, Saha A, Simoes P, Parikh CR, et al. Representation of patients with kidney disease in trials of cardiovascular interventions: an updated systematic review. *JAMA Intern Med.* (2016) 176:121–4. doi: 10.1001/jamainternmed.2015.6102
19. Zannad F, Rossignol P. Cardiovascular outcome trials in patients with advanced kidney disease: time for action. *Circulation.* (2017) 135:1769–71. doi: 10.1161/CIRCULATIONAHA.117.027338
20. Weiner DE, Tighiouart H, Elsayed EF, Griffith JL, Salem DN, Levey AS, et al. The Framingham predictive instrument in chronic kidney disease. *J Am Coll Cardiol.* (2007) 50:217–24. doi: 10.1016/j.jacc.2007.03.037
21. Gurm HS, Gore JM, Anderson FA, Wyman A, Fox KAA, Steg PG, et al. Comparison of acute coronary syndrome in patients receiving versus not receiving chronic dialysis (from the Global Registry of Acute Coronary Events [GRACE] Registry). *Am J Cardiol.* (2012) 109:19–25. doi: 10.1016/j.amjcard.2011.07.062
22. Flint AC, Conell C, Ren X, Banki NM, Chan SL, Rao VA, et al. Effect of systolic and diastolic blood pressure on cardiovascular outcomes. *N Engl J Med.* (2019) 381:243–51. doi: 10.1056/NEJMoa1803180
23. North BJ, Sinclair DA. The intersection between aging and cardiovascular disease. *Circ Res.* (2012) 110:1097–108. doi: 10.1161/CIRCRESAHA.111.246876
24. Simons LA, Simons J. Diabetes and coronary heart disease. *N Engl J Med.* (1998) 339:2314. doi: 10.1056/NEJM199812033392314
25. Wang H, Ning X, Zhu C, Yin D, Feng L, Xu B, et al. Prognostic significance of prior ischemic stroke in patients with coronary artery disease undergoing percutaneous coronary intervention. *Catheteriz Cardiovasc Interv.* (2019) 93:787–92. doi: 10.1002/ccd.28057
26. Regitz-Zagrosek V, Kararigas G. Mechanistic pathways of sex differences in cardiovascular disease. *Physiol Rev.* (2017) 97:1–37. doi: 10.1152/physrev.00021.2015
27. Cinar T, Hayiroglu MI, Tanik VO, Arugaslan E, Keskin M, Uluganyan M, et al. The predictive value of the CHA2DS2-VASc score in patients with mechanical mitral valve thrombosis. *J Thromb Thrombolysis.* (2018) 45:571–7. doi: 10.1007/s11239-018-1640-3
28. Vodošek Hojs N, Ekart R, Bevc S, Piko N, Hojs R. CHA2DS2-VASc score as a predictor of cardiovascular and all-cause mortality in chronic kidney disease patients. *Am J Nephrol.* (2021) 52:404–11. doi: 10.1159/000516121
29. Schamroth Pravda M, Cohen Hagai K, Topaz G, Schamroth Pravda N, Makhoul N, Shuvy M, et al. Assessment of the CHA2DS2-VASc score in predicting mortality and adverse cardiovascular outcomes of patients on hemodialysis. *Am J Nephrol.* (2020) 51:635–40. doi: 10.1159/000508836
30. Kim KH, Kim W, Hwang SH, Kang WY, Cho SC, Kim W, et al. The CHA2DS2VASc score can be used to stratify the prognosis of acute myocardial infarction patients irrespective of presence of atrial fibrillation. *J Cardiol.* (2015) 65:121–7. doi: 10.1016/j.jjcc.2014.04.011
31. Ipek G, Onuk T, Karatas MB, Gungor B, Osken A, Keskin M, et al. CHA2DS2-VASc score is a predictor of no-reflow in patients with ST-segment elevation myocardial infarction who underwent primary percutaneous intervention. *Angiology.* (2016) 67:840–5. doi: 10.1177/0003319715622844
32. Bozbay M, Uyarel H, Cicek G, Oz A, Keskin M, Murat A, et al. CHA2DS2-VASc score predicts in-hospital and long-term clinical outcomes in patients with st-segment elevation myocardial infarction who were undergoing primary percutaneous coronary intervention. *Clin Appl Thromb Hemost.* (2017) 23:132–8. doi: 10.1177/1076029616646874

Conflict of Interest: The authors declare that the research was conducted in the absence of any commercial or financial relationships that could be construed as a potential conflict of interest.

Advantages of publishing in Frontiers

OPEN ACCESS
Articles are free to read for greatest visibility and readership

FAST PUBLICATION
Around 90 days from submission to decision

HIGH QUALITY PEER-REVIEW
Rigorous, collaborative, and constructive peer-review

TRANSPARENT PEER-REVIEW
Editors and reviewers acknowledged by name on published articles

Frontiers
Avenue du Tribunal-Fédéral 34
1005 Lausanne | Switzerland

Visit us: www.frontiersin.org
Contact us: frontiersin.org/about/contact

REPRODUCIBILITY OF RESEARCH
Support open data and methods to enhance research reproducibility

DIGITAL PUBLISHING
Articles designed for optimal readership across devices

FOLLOW US
@frontiersin

IMPACT METRICS
Advanced article metrics track visibility across digital media

EXTENSIVE PROMOTION
Marketing and promotion of impactful research

LOOP RESEARCH NETWORK
Our network increases your article's readership